

The Pennsylvania State University
The Graduate School
College of Earth and Mineral Sciences

**AN INVESTIGATION OF THE IMPORTANCE OF
SCREENING EFFECTS IN POLYMER SOLUTIONS
AND BLENDS**

A Thesis in
Materials Science and Engineering

by

Lennart P. Berg

© 2005 Lennart P. Berg

Submitted in Partial Fulfillment
of the Requirements
for the Degree of

Doctor of Philosophy

May 2005

The thesis of Lennart P. Berg was reviewed and approved* by the following:

Paul C. Painter
Professor of Polymer Science and Engineering
Thesis Adviser
Chair of Committee

Ronald C. Hedden
Assistant Professor of Materials and Engineering

James P. Runt
Professor of Polymer Science
Associate Head for Graduate Studies

Ramanathan Nagarajan
Professor of Chemical Engineering

Gary L. Messing
Distinguished Professor of Ceramic Science
and Engineering
Head of the Department of Materials and Engineering

*Signatures are on file in the Graduate School.

Abstract

In this work a closer look will be taken at the importance of screening effects in both polymer solutions as well as polymer blends. It is essentially a natural extension of earlier work in this group with functionalized polymer blends, where it was proposed that the number of intramolecular contacts far exceeded what one would expect from the classical mean field theory. Models with varying degrees of complexity were investigated, where intramolecular contacts, in each case, were treated explicitly.

First a very simple modification of the classical Flory-Huggins theory is investigated, and it is shown that it is possible to reproduce the concentration dependence of the interaction parameter in polymer solutions with surprising accuracy. It is also shown that the calculated spinodals were in good agreement with experimentally reported data, especially at higher molecular weights.

Free volume effects are then accounted for through a modification of the Flory-Orwoll-Vrij Equation of State model. The model was tested for a number of systems at θ -conditions as well as non θ -conditions, for its ability to reproduce the concentration dependence of the interaction parameter, using solubility parameters as well as internal pressures, with varying degrees of accuracy.

Another simple modification of the Flory-Huggins theory for polymer blends is presented. It is shown that the model is able to reproduce the very peculiar phenomenon observed in the behavior of the interaction parameters determined from Small Angle Neutron Scattering (SANS) in isotopic polymer blends, by varying the screening factor for one of the components by less than 3 %.

Finally it is shown that a further modification to accommodate copolymer blends, leads to a model which is equally well equipped to describe the strong concentration dependence of the interaction parameter observed experimentally. A few assumptions are made in these calculations, and the most important of these is that the copolymers are treated as homopolymers. Since only isotopic copolymer systems were investigated it is presumably a safe assumption. It was found that a small change of less than 4 % in the screening factor of one of the components was enough to obtain extremely good correspondence with the experimentally observed data.

Table of Contents

List of Figures.....	viii
List of Tables	xiii
Acknowledgements.....	xvi
Chapter 1. Theoretical Background	1
1.1. Introduction.....	1
1.2. Lattice Models	2
1.3. The Interaction Parameter.....	7
1.4. Koningsveld and Kleintjens.....	9
1.5. Outline of Dissertation.....	12
1.6. References.....	14
Chapter 2. Thermodynamics in Polymer Solutions	15
2.1. Introduction.....	15
2.2. Counting Contacts	16
2.3. Packing Effects In Polymer Solutions	23
2.4. The Chemical Potential.....	25
2.5. Calculations and Discussions	33
2.6. Conclusions.....	51
2.7. References.....	54

Chapter 3. Modeling Polymer Solution Thermodynamics	56
3.1. Introduction.....	56
3.2. Theory.....	58
3.2.1. The Flory-Orwoll-Vrij Equation of State	58
3.2.2. The Intramolecular Energy	61
3.2.3. The Combinatorial Term.....	66
3.2.4. The c-parameter	67
3.2.5. Mixing Rules.....	70
3.2.6. Internal Pressure vs. Cohesive Energy Density	70
3.2.7. The Model.....	73
3.3. Results and Discussions.....	77
3.4. Conclusions.....	98
3.5. References.....	100
Chapter 4. Thermodynamics in Isotopic Polymer Blends	102
4.1. Introduction.....	102
4.2. Interaction Parameters In Polymer Blends	105
4.3. Interaction Parameters From SANS	112
4.4. Results and Discussions.....	116
4.5. Conclusions.....	134
4.6. References.....	136

Chapter 5. Thermodynamics in Statistical Copolymer Blends.....	137
5.1. Introduction.....	137
5.2. Interaction Parameters In Copolymer Blends.....	139
5.3. Results and Discussions.....	142
5.4. Conclusions.....	172
5.5. References.....	174
Chapter 6. Summary and Suggestions for Future Work.....	175
6.1. Summary.....	175
6.2. Suggestions for Future Work.....	177
6.3. References.....	178
Appendix.....	179
A. Contact Sites for Stiff or Semiflexible Rods.....	179
B. Contact Sites for Flexible Chains.....	181
C. Guggenheim's Theory of Athermal Mixtures.....	183
D. Determination of Internal Pressures for Various Polymers	193
E. Polymers in Good Solvents	215
F. Interaction Parameters in Copolymer Blends.....	221
G. Effects of Variation of the Screening Factor in Copolymer Blends	230

List of Figures

Figure 1.1	Schematic Illustration of Random Distribution of Polymer Segments on a Lattice.....	3
Figure 1.2	Schematic Illustration of the Distribution of Covalently Bound Polymer Segments on a Lattice.....	5
Figure 1.3	χ versus Composition for PS-Cyclohexane at 34 °C.....	11
Figure 2.1	Local and Long-range Screening Effects.....	18
Figure 2.2	Schematic Representation of a Phase Diagram	28
Figure 2.3	Calculated Values of the Fraction of Intramolecular Contacts.....	38
Figure 2.4	χ^{FH} versus Concentration for Polystyrene-Cyclohexane at 34 °C.....	42
Figure 2.5	Spinodal for Polystyrene ($\overline{M}_w = 51.000$)-Cyclohexane	44
Figure 2.6	Spinodal for Polystyrene ($\overline{M}_w = 163.000$)-Cyclohexane.....	46
Figure 2.7	Spinodal for Polystyrene ($\overline{M}_w = 520.000$)-Cyclohexane	48
Figure 2.8	Spinodal for Polystyrene-Cyclohexane at Various Molecular Weights	49
Figure 2.9	χ^{FH} versus Concentration for Polyisobutylene-Benzene at 25 °C	51
Figure 3.1	Comparison of Experimental data and Calculated Values of χ^{FH} for Polystyrene ($\overline{M}_w = 51.000$)-Cyclohexane at 34 °C using Solubility Parameters.....	79
Figure 3.2	Comparison of Experimental data and Calculated Values of χ^{FH} for Polystyrene ($\overline{M}_w = 51.000$)-Cyclohexane at 34 °C using Internal Pressures	81

Figure 3.3	Comparison of Experimental data and Calculated Values of χ^{FH} for PIB ($M_w = 40.000$)-Benzene at 25 °C using Solubility Parameters.....	82
Figure 3.4	Comparison of Experimental data and Calculated Values of χ^{FH} for PIB ($M_w = 40.000$)-Benzene at 25 °C using Internal Pressures	83
Figure 3.5	Comparison of Experimental data and Calculated Values of χ^{FH} for Polystyrene ($\overline{M}_w = 51.000$)-Ethylbenzene at 35 °C using Solubility Parameters.....	85
Figure 3.6	Comparison of Experimental data and Calculated Values of χ^{FH} for Polystyrene ($\overline{M}_w = 51.000$)-Ethylbenzene at 35 °C using Internal Pressures	86
Figure 3.7	Comparison of Experimental data and Calculated Values of χ^{FH} for Polystyrene ($\overline{M}_w = 51.000$)-MEK at 50 °C using Solubility Parameters.....	87
Figure 3.8	Comparison of Experimental data and Calculated Values of χ^{FH} for Polystyrene ($\overline{M}_w = 51.000$)-MEK at 50 °C using Internal Pressures	88
Figure 3.9	Comparison of Experimental data and Calculated Values of χ^{FH} for Natural Rubber ($M_w = 40.000$)-Benzene at 25 °C using Solubility Parameters.....	89
Figure 3.10	Comparison of Experimental data and Calculated Values of χ^{FH} for Natural Rubber ($M_w = 40.000$)-Benzene at 25 °C using Internal Pressures	90
Figure 3.11	The Screening Factor, γ , as a function of chain expansion, α	94

Figure 3.12	Comparison of Experimental data and Calculated Values of χ^{FH} with an “Elastic Contribution” for Natural Rubber ($M_w = 40.000$)-Benzene at 25 °C using Solubility Parameters	95
Figure 3.13	Comparison of Experimental Data and Calculated Values of χ^{FH} with an “Elastic Contribution” for Natural Rubber ($M_w = 40.000$)-Benzene at 25 °C using Internal Pressures	96
Figure 3.14	Comparison of Experimental Data and Calculated Values of χ^{FH} with an “Elastic Contribution” for PIB ($M_w = 40.000$)-Cyclohexane at 25 °C using Solubility Parameters and Internal Pressures	97
Figure 4.1	Interaction Parameters From SANS For PE/DPE at 155 °C	117
Figure 4.2	Interaction Parameters From SANS For PE/DPE at 155 °C	119
Figure 4.3	Interaction Parameters From SANS For PE/DPE at 155 °C	121
Figure 4.4	Interaction Parameters From SANS For PE/DPE at 155 °C	122
Figure 4.5	Interaction Parameters From SANS For PE/DPE at 155 °C	123
Figure 4.6	Interaction Parameters From SANS For PE/DPE at 155 °C	124
Figure 5.1	Interaction Parameters From SANS For H97/D88 at 27 °C with Identical Screening Factors For the Two Components.....	143
Figure 5.2	Interaction Parameters From SANS For H97/D88 at 27 °C with Varying Screening Factors For the Two Components.....	145
Figure 5.3	Interaction Parameters From SANS For H97/D88 at 27 °C with Varying Screening Factors For the Two Components.....	146
Figure 5.4	Interaction Parameters From SANS For H97/D88 at 51 °C with Varying Screening Factors For the Two Components.....	148
Figure 5.5	Interaction Parameters From SANS For H97/D88 at 83 °C with Varying Screening Factors For the Two Copolymers	149

Figure 5.6	Interaction Parameters From SANS For Various Copolymers at 167 °C with Varying Screening Factors	150
Figure 5.7	Interaction Parameters From SANS For Various Copolymers at 167 °C with Varying Screening Factors	153
Figure 5.8	Interaction Parameters From SANS For Various Copolymers at 167 °C with Varying Screening Factors	155
Figure 5.9	Interaction Parameters From SANS For H97/D88 at Various Temperatures.....	160
Figure 5.10	Interaction Parameters From SANS For H88/D78 at Various Temperatures.....	162
Figure 5.11	Interaction Parameters From SANS For H78/D66 at Various Temperatures.....	164
Figure 5.12	Interaction Parameters From SANS For H66/D52 at Various Temperatures.....	166
Figure 5.13	Interaction Parameters From SANS For H97/D88 at 27 °C	169
Figure 5.14	Interaction Parameters From SANS For H97/D88 at 27 °C	170
Figure D.1	Specific Volume vs. Temperature for PS ($M_w = 110.000$)	194
Figure D.2	Pressure vs. Temperature for PS ($M_w = 110.000$).....	195
Figure D.3	Specific Volume vs. Temperature for Nylon 6/6.....	197
Figure D.4	Pressure vs. Temperature for Nylon 6/6	198
Figure D.5	Specific Volume vs. Temperature for PPO ($M_w = 4000$)	200
Figure D.6	Pressure vs. Temperature for PPO ($M_w = 4000$).....	201
Figure D.7	Specific Volume vs. Temperature for PVDF.....	203

Figure D.8	Pressure vs. Temperature for PVDF	204
Figure D.9	Specific Volume vs. Temperature for PVOH	206
Figure D.10	Pressure vs. Temperature for PVOH	207
Figure D.11	Specific Volume vs. Temperature for PMMA ($M_w = 100.000$)	209
Figure D.12	Pressure vs. Temperature for PMMA ($M_w = 100.000$)	210
Figure D.13	Specific Volume vs. Temperature for PMMA ($M_w = 40.000$)	212
Figure D.14	Pressure vs. Temperature for PMMA ($M_w = 40.000$)	213
Figure E.1	The Chain Expansion Factor as a Function of Concentration for PS	218
Figure G.1	Interaction Parameters From SANS For H97/D88 at 51 °C	231
Figure G.2	Interaction Parameters From SANS For H97/D88 at 51 °C	232
Figure G.3	Interaction Parameters From SANS For H97/D88 at 83 °C	234
Figure G.4	Interaction Parameters From SANS For H97/D88 at 83 °C	235
Figure G.5	Interaction Parameters From SANS For H97/D88 at 121 °C	237
Figure G.6	Interaction Parameters From SANS For H97/D88 at 167 °C	239

List of Tables

Table 2.1	Experimental Critical Data for Polystyrene-Cyclohexane.....	34
Table 2.2	Calculated Values of γ_s and χ_0 for Polystyrene-Cyclohexane at Various Degrees of Polymerization	35
Table 2.3	Selected Experimental Values of the χ Parameter for Polystyrene- Cyclohexane at 34 °C	39
Table 2.4	Calculated Values of χ_H , χ_S and χ^{FH} for Polystyrene-Cyclohexane at 34 °C	41
Table 3.1	Pure Component Parameters for Various Polymer-Solvent Systems	80
Table 4.1	Variations in the Screening Factor of Component A for a=1	125
Table 4.2	Variations in the Screening Factor of Component B for a=1	128
Table 4.3	Variations in the Screening Factor of Component A for b=1	129
Table 4.4	Variations in the Screening Factor of Component B for b=1	130
Table 4.5	Variations in the Screening Factor of Component A for c=1	131
Table 4.6	Variations in the Screening Factor of Component B for c=1	132
Table 5.1	“High” Variations in the “Raw” Screening Factor of Component B for c=1.05 at 167 °C.....	151
Table 5.2	“Low” Variations in the “Raw” Screening Factor of Component B for c=1.05 at 167 °C.....	154

Table 5.3	“High” Variations in the “Raw” Screening Factor of Component B for $c=1.10$ at $167\text{ }^{\circ}\text{C}$	156
Table 5.4	“High” Variations in the “Raw” Screening Factor of Component A for $c=1.05$ at $167\text{ }^{\circ}\text{C}$	157
Table 5.5	“Low” Variations in the “Raw” Screening Factor of Component A for $c=1.05$ at $167\text{ }^{\circ}\text{C}$	158
Table 5.6	“High” Variations in the “Raw” Screening Factor of Component A for $c=1.10$ at $167\text{ }^{\circ}\text{C}$	159
Table 5.7	Variations in the Screening Factor of Component B in the H97/D88 system for $\phi_A=0.249$ and $c=1.05$ at various temperatures	161
Table 5.8	Variations in the Screening Factor of Component B in the H88/D78 system for $\phi_A=0.501$ and $c=1.05$ at various temperatures	163
Table 5.9	Variations in the Screening Factor of Component B in the H78/D66 system for $\phi_A=0.252$ and $c=1.05$ at various temperatures	165
Table 5.10	Variations in the Screening Factor of Component B in the H66/D52 system for $\phi_A=0.238$ and $c=1.05$ at various temperatures	167
Table 5.11	Variations in the Screening Factor of Component B for various c for H97/D88 at $27\text{ }^{\circ}\text{C}$	171
Table D.1	Internal Pressure of PS ($M_w = 110.000$).....	196
Table D.2	Internal Pressure of Nylon 6/6	199
Table D.3	Internal Pressure of Poly Propylene Oxide ($M_w = 4000$).....	202
Table D.4	Internal Pressure of PVDF	205
Table D.5	Internal Pressure of PVOH	208

Table D.6	Internal Pressure of PMMA ($M_w = 100.000$).....	211
Table D.7	Internal Pressure of PMMA ($M_w = 40.000$).....	214
Table E.1	The Radius of Gyration as a Function of Concentration for PS	216
Table G.1	Variations in the Screening Factor of Component B for various c for H97/D88 at 51 °C	233
Table G.2	Variations in the Screening Factor of Component B for various c for H97/D88 at 83 °C	236
Table G.3	Variations in the Screening Factor of Component B for various c for H97/D88 at 121 °C	238
Table G.4	Variations in the Screening Factor of Component B for various c for H97/D88 at 167 °C	240

Acknowledgements

First and foremost I need to express my deepest gratitude to my advisor Professor Paul C. Painter. Throughout my time at the Pennsylvania State University he has been a great support for me in every aspect. He has offered me guidance, encouragement as well as constructive criticism, and for that I will be eternally grateful to him.

I would also like to thank Professor Emeritus Michael M. Coleman, Professor Sanat Kumar and Professor R. Nagarajan, who all contributed in the early stages of this work, and a special thanks to Professor James P. Runt and Professor Ronald Hedden for stepping in to serve in my committee. I also wish to express my gratitude to Professor Ralph Colby, who was always willing to listen and offer constructive ideas related to my research. A special thanks are due to Dr. Boris Veytsman, who was very helpful in offering advice and ideas during his stay at the Pennsylvania State University. Additional thanks goes to my fellow graduate students and post docs in the Polymer Science Program, especially Dr. Maria Sobkoviak, who were always willing to listen whenever I needed someone to talk to.

A very special thanks are reserved for my parents, Kate and Lasse Berg, and my sister, Lizette Paulmann Berg, who have been a tremendous support throughout my stay here at the Pennsylvania State University. Their never ending love and encouragement have been truly inspirational, and if I have learned nothing else, I have learned how important my family is to me. I dedicate this work to them.

Finally I also want to express my gratitude for the financial support from the Office of Chemical Sciences of the US Department of Energy (DE-FG02-86ER13537).

Chapter 1

Theoretical Background

1.1. Introduction

In the past half century, or so, the demands for polymeric materials that can deliver at a higher performance level through improved characteristics, have been ever increasing. A major part in developing these improved products is intrinsically linked to a better understanding of the fundamental theories associated with polymer solution thermodynamics. From an industrial point of view, relatively simple theoretical models have traditionally been preferred, which explains why the so-called Hansen solubility parameters are still used in the paint and coat industry to determine the solubility of organic materials (including polymers). From a scientific point of view there might be a tendency to develop more sophisticated models to explain a range of observed characteristics, but unfortunately, in most cases, with the increased sophistication follows an increase in the models complexity. Although the primary goal in academics might not be to accommodate the industry, there is an undeniable symbiotic connection between the two. A simple model to describe the thermodynamics of polymer solutions is therefore also very appealing in the academic ranks. Numerous attempts have been made to take simple thermodynamic models and improve them through the introduction of various physical or non-physical parameters. One such simple model is derived from the classical Flory-Huggins theory, which despite its inherent errors, manage to explain some of the major features observed in the phase behavior of polymer solutions as well as in blends.

1.2. Lattice Models

The Flory-Huggins theory is a so-called lattice model, which uses a lattice to model the liquid state. The advantage of using a lattice is that it allows for the derivation of explicit expressions, through the application of statistical mechanics. By adopting this approach the number of contacts allowed to a given polymer segment are expressed in terms of the so-called coordination number, z , of the lattice. In the simplest case where the polymer chain is modeled as a stiff rod qz is given by:

$$qz = (z - 2)r + 2 \quad (1)$$

where qz represent the total number of contact sites per chain that neighbor a given polymer segment, excluding the contacts between segments that are covalently bound, and r is the degree of polymerization. Various permutations of equation 1 are given in appendix A, which will be referred to in the subsequent treatment.

In the classical Flory-Huggins theory for polymer solutions, it is assumed that the polymer segments are disconnected and randomly mixed, as illustrated in figure 1.1, when calculating the non-combinatorial part of the free energy, which will be referred to as the excess free energy ($\Delta G_{exc.}$). However, non-random contacts are accounted for when calculating the combinatorial free energy ($\Delta G_{comb.}$). Calculation of the excess free energy involves the probability of finding a polymer segment next to a given solvent molecule:

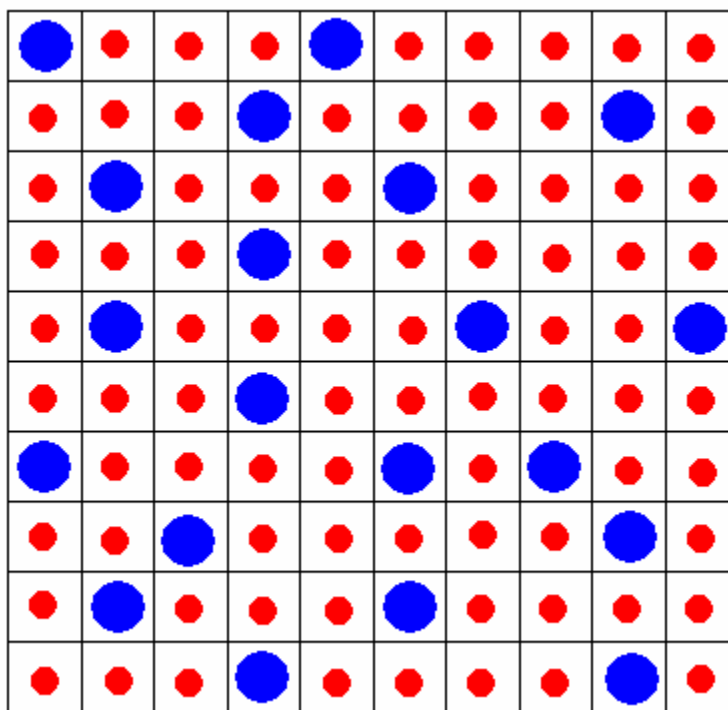


Figure 1.1. Schematic representation of a complete random distribution of polymer segments (blue filled circles) and solvent molecules (red filled circles) on a lattice. (Painter and Coleman¹)

$$\frac{\Delta G_{exc.}}{RT} = n_s p_{ps} \chi \quad (2)$$

where n_s is the number of moles of solvent, p_{ps} represents the probability of finding a polymer segment adjacent to a solvent molecule, χ is an interaction energy parameter, R is the universal gas constant, and T is the temperature.

In the mean field assumption this probability is simply assumed to be given by the volume fraction of the polymer, ϕ_p :

$$\frac{\Delta G_{exc.}}{RT} = n_s \phi_p \chi \quad (3)$$

However, Flory², as well as other workers including Tompa³, recognized that the traditional mean field assumption, where the probability of finding a polymer segment next to a solvent molecule is proportional to the volume fraction of the polymer, is really only valid as the coordination number of the lattice approaches infinity. A better and more "true" representation of the number of polymer contacts available would be to use the so-called surface site fraction of the polymer, θ_p since it takes into account the fact that the segments are connected through covalent bonds, as shown in figure 1.2. The surface site fraction is defined as:

$$\theta_p = \frac{\left(1 - \frac{2}{z} \left(1 - \frac{1}{r}\right)\right) \phi_p}{\left(1 - \frac{2}{z} \left(1 - \frac{1}{r}\right)\right) \phi_p + \phi_s} = \frac{\left(1 - \frac{2}{z} \left(1 - \frac{1}{r}\right)\right) \phi_p}{\left(1 - \frac{2}{z} \left(1 - \frac{1}{r}\right)\right) \phi_p} \quad (4)$$

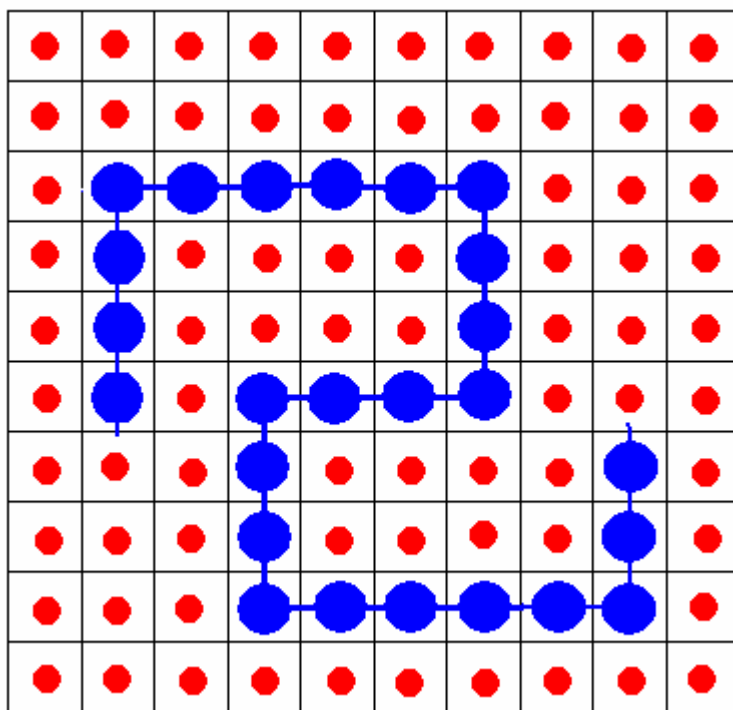


Figure 1.2. Schematic representation of the distribution of covalently bound polymer segments (blue filled circles) and solvent molecules (red filled circles) on a lattice. (Painter and Coleman¹)

It is evident from equation 4 that only as z approaches infinity will the surface site fraction of the polymer, θ_p , equal the volume fraction of the polymer, ϕ_p . The expression for the surface site fraction can be further simplified by introducing the following quantity:

$$\gamma_l = \frac{2}{z} \left(1 - \frac{1}{r} \right) \quad (5)$$

where γ_l effectively represents the fraction of same chain contacts, due to covalent bonds between the polymer segments. The surface site fraction, θ_p , can now be expressed in terms of the γ -factor as:

$$\theta_p = \frac{(1 - \gamma_l)\phi_p}{(1 - \gamma_l\phi_p)} \quad (6)$$

The excess free energy can therefore more appropriately be expressed in terms of the surface site fraction:

$$\frac{\Delta G_{exc.}}{RT} = n_s \theta_p \chi \quad (7)$$

In the classical Flory-Huggins theory, the combinatorial energy, $\Delta G_{comb.}$, is given by:

$$\frac{\Delta G_{comb.}}{RT} = \phi_s \ln \phi_s + \frac{\phi_p}{r} \ln \phi_p \quad (8)$$

but a more refined expression was developed by both Huggins⁴ and Guggenheim⁵. In the latter case the combinatorial entropy is given by:

$$\begin{aligned} \frac{\Delta G_{comb.}}{RT} = & \phi_s \ln \phi_s + \frac{\phi_p}{r} \ln \phi_p \\ & - \left(\frac{r-1}{r} \right) \left(\frac{r}{r-q} - \phi_p \right) \ln \left(1 - \left(\frac{r-q}{r} \right) \phi_p \right) + \phi_p \frac{q(r-1)}{r(r-q)} \ln \left(\frac{q}{r} \right) \end{aligned} \quad (9)$$

The expression that Huggins⁴ proposed was a little more advanced and included a factor, f_0 , but if this factor is set equal to zero, the expression reduces to equation 9.

1.3. The Interaction Parameter

Initially the interaction parameter, χ , was assumed to be independent of concentration. After the solubility parameter concept was introduced by Hildebrand and Scott⁶, it was proposed by Patterson⁷, among others, that the interaction parameter could be calculated as the difference between the solubility parameter of component a, δ_a , and the solubility parameter of component b, δ_b :

$$\chi = \frac{V_r}{RT} (\delta_a - \delta_b)^2 \quad (10)$$

where V_r is a reference volume. It was soon evident that although this form might be relatively successful in describing molecules of similar size, it was less successful in representing systems where large discrepancies in size between the two components of the mixture, such as in polymer solvent mixtures, existed. Instead it was suggested that the addition of a constant to equation 10 would greatly improve its ability to represent the experimental observed values in some of these systems. Many different values of this constant have been reported in the literature⁸, with values ranging between 0.2 and 0.5. The most common accepted value of the constant is 0.34:

$$\chi = 0.34 + \frac{V_r}{RT} (\delta_s - \delta_p)^2 \quad (11)$$

With the introduction of this "fudge" factor, whose origin to this day remains uncertain, although Patterson⁷ attributed it to the inadequacy of Flory's approximation for the combinatorial free energy, a whole new set of models were proposed. Most importantly it was acknowledged that the interaction parameter in many systems exhibited concentration dependence, and it would be necessary to incorporate some kind of concentration dependence for the interaction parameter in order to represent the experimentally observed values. One of the previously mentioned inherent errors in the classic Flory-Huggins theory is precisely its failure to account for the experimentally observed concentration dependence of the interaction parameter, χ .

1.4. Koningsveld and Kleintjens

Koningsveld and Kleintjens⁹ acknowledged the importance of using surface site fractions rather than volume fractions, thereby taking connectivity effects into account, and they defined the term:

$$\gamma = \frac{2}{z} \quad (12)$$

which is an abbreviated form of the following expression:

$$\gamma_l = \frac{2}{z} \left(1 - \frac{1}{r} \right) \quad (5)$$

However, in their treatment the latter part (the $\frac{1}{r}$ -term) was neglected and the physical meaning of this γ -factor was ignored and simply treated as an adjustable parameter.

In this work they preferred a closed form expression for the composition dependence of the pair interaction parameter g :

$$g = \alpha + \frac{\beta_0}{(1 - \gamma\phi_p)} \quad (13)$$

rather than a truncated power series, which is usually derived from the classical lattice theory of polymer solutions. In equation 13 α is an empirical parameter, which accounts

for entropic contributions to the interaction parameter, and β_0 is another parameter defined as:

$$\beta_0 = \beta_{00} + \beta_{01} / T \quad (14)$$

The consequence of equation 14 is that the entire temperature dependence of the interaction parameter is confined to the β_0 parameter.

The pair interaction parameter g is related to the χ parameter through:

$$\chi = g - \phi_s \left(\frac{\partial g}{\partial \phi_p} \right) = \alpha + \frac{\beta_0(1-\gamma)}{(1-\gamma\phi_p)^2} \quad (15)$$

As it can be seen in figure 1.3 the correspondence between experimentally observed data and those calculated with their model is very good up to about $\phi_p=0.5$. Beyond this point the deviations starts to become significant. However, this closed form expression has proven to be a very useful tool in describing polymer solution thermodynamic data, as suggested in the work of Petri et al.¹⁰

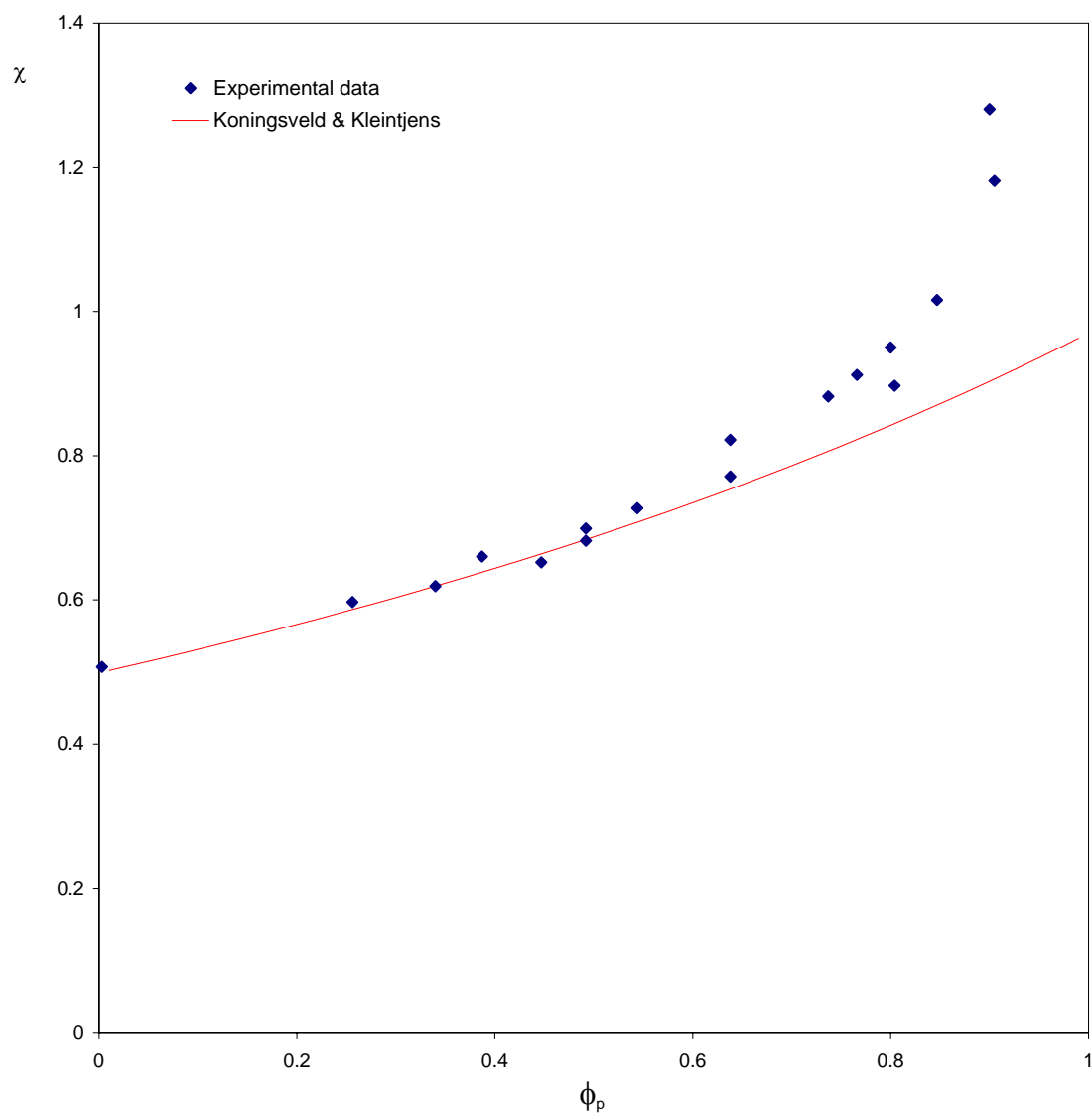


Figure 1.3. χ versus composition for Polystyrene-Cyclohexane at 34 °C. Experimental data by Kriegbaum and Geymer¹¹.

1.5. Outline of Dissertation

Although the initial work of Painter and Coleman¹² were dealing with functionalized polymer blends, where it was discovered that the number of same (polymer) chain contacts far exceeded what would be expected from a classical mean field theory, it was believed that the nature of these findings were of a universal nature. They should therefore not only apply in polymer blends but also in polymer solutions. This was the main inspiration for this work.

In the following it will be investigated whether by making a relatively simple modification of the classical Flory-Huggins theory, in which these intramolecular contacts are treated explicitly, it will be possible to reproduce the composition dependence of the interaction parameter in poor solvent systems at or near the θ -temperature. It will also be investigated whether the model is able to reproduce spinodals curves that are in good agreement with experimental data.

Next a layer of complexity will be added by taking free volume effects into account. This is done through a modification of the Flory-Orwoll-Vrij^{13,14} Equation of State model, where intramolecular screening effects are again accounted for. Special attention is then paid to solubility parameters and internal pressure parameters, to check whether these will be able to provide better agreements with experimental data.

The focus is then directed towards isotopic polymer blends as well as copolymer blends, where the only distinguishing difference between the polymers (or copolymers) is that the hydrogen in some cases has been substituted by deuterium. This allows methods such as *Small Angle Neutron Scattering* (SANS) experiments to determine the concentration dependence of the interaction parameter.

A modified Flory-Huggins model will be tested to see if it is possible to reproduce some of the curious experimentally observed data, such as an apparent strong concentration dependence of the interaction parameter determined from SANS experiments. An attempt to explain these curiosities through the introduction of screening factors will be presented.

1.6. References

1. Painter, P.C.; Coleman, M.M. *Fundamentals of Polymer Science*, CRC Press, Boca Raton, FL, 1997
2. Flory, P.J. *Principles of Polymer Chemistry*, Cornell University Press, Ithaca, N.Y., 1953
3. Tompa, H. *Polymer Solutions*, Butterworths, London, Academic Press, N.Y., 1956
4. Huggins, M.L. *Ann. N.Y. Acad. Sci.*, **43**, 9, 1942
5. Guggenheim, E.A. *Mixtures*, Clarendon, Oxford, 1952
6. Hildebrand, J.H.; Scott, R.L. *The Solubility of Non-Electrolytes*, 3rd Ed., Reinhold Publishing Co., 1950
7. Patterson, D. *Rubber Chem. Technol.*, **40**, 1, 1967
8. Orwoll, R.A. *Rubber Chem. & Tech.*, **50**, 451, 1977
9. Koningsveld, R.; Kleintjens, L.A. *Macromolecules*, **4**, 637, 1971
10. Petri, H.M.; Schuld, N.; Wolf, B.A. *Macromolecules*, **28**, 4975, 1995
11. Kriegbaum, W.R.; Geymer, D.O. *J. Am. Chem. Soc.*, **73**, 1859, 1959
12. Painter, P.C.; Veytsman, B.; Kumar, S.; Shenoy, S.; Graf, J.F.; Xu, Y.; Coleman, M.M. *Macromolecules*, **30**, 932, 1997
13. Flory, P.J.; Orwoll, R.A.; Vrij. A. *J. Am. Chem. Soc.*, **86**, 3507, 1964
14. Flory, P.J.; Orwoll, R.A.; Vrij. A. *J. Am. Chem. Soc.*, **86**, 3515, 1964

Chapter 2

Thermodynamics in Polymer Solutions

2.1. Introduction

In the previous chapter it was discussed how chain connectivity affects the number of contact sites of a given polymer chain segment. The present investigation originated in the work of Coleman and Painter¹, who investigated a number of hydrogen bonding polymer blends. In this work it was found that the number of same-chain contacts far exceeded what would be expected based on the classical mean field models typically applied to these systems. It was suggested that these effects could be of a more universal nature, and therefore should be accounted for not only in non-hydrogen-bonding polymer blends, but might also be very relevant in polymer solutions. In this chapter this effect will be incorporated in a relatively simple manner into the classical Flory-Huggins theory.

In the classical Flory-Huggins theory for polymer solutions it is assumed that the polymer chain segments are disconnected and randomly mixed, when calculating the non-combinatorial part of the free energy, which again will be referred to as the excess free energy, ΔG_{exc} .

$$\frac{\Delta G_{exc}}{RT} = n_s \phi_p \chi \quad (1)$$

However, as mentioned previously it would be more accurate to use the surface site fraction of the polymer, θ_p , to represent the number of polymer contacts, rather than the volume fraction of the polymer, ϕ_p .

$$\frac{\Delta G_{exc}}{RT} = n_s \theta_p \chi \quad (2)$$

This is because the surface site fraction of the polymer, θ_p , actually takes into account that the individual polymer segments are connected through covalent bonds, and not randomly distributed on the lattice as assumed in the classic Flory approximation.

Although using surface site fractions rather than volume fractions does take the covalency of the polymer segments into account, it does not explain the observed excess of polymer contacts in some polymer blends. It was therefore decided to take an in dept look on how these contacts are accounted for.

2.2. Counting Contacts

Traditionally, the number of polymer contact sites in lattice models is given by:

$$qz = (z - 2)r + 2 \quad (3)$$

which can be rewritten to:

$$\frac{q}{r} = 1 - \frac{2}{z} \left(1 - \frac{1}{r} \right) \quad (4)$$

As mentioned in the previous chapter Koningsveld and Kleintjens² acknowledged the importance of taking connectivity effects into account, and they defined the term:

$$\gamma_l = \frac{2}{z} \left(1 - \frac{1}{r} \right) \quad (5)$$

where γ_l effectively represents the fraction of same chain contacts caused by covalent bonds within the polymer chain.

$$\frac{q}{r} = 1 - \gamma_l \quad (6)$$

The remaining contacts for the polymer segments can be divided into two types, those between segments within the same polymer chain, which will be referred to as intramolecular contacts, and those between segments of different polymer chains. This hinges on the assumption that some polymer chains possess enough flexibility to bend back on themselves, and thereby creating opportunities for polymer segment contacts within the same chain. The result of such an interaction could be that some polymer segments are effectively "screened" from interaction with segments from other polymer chains or solvent molecules. Since the "screened" segments are not able to interact with any other polymer segment or solvent molecule, it means that the number of

intermolecular contacts is directly affected, resulting in a fewer number of those intermolecular contacts.

There are two types of intramolecular screening, a local screening which only affects the nearest neighbors of the interacting sites, and a long range screening that affects segments from different parts of the chain. Both are illustrated in figure 2.1. In the following no distinction will be made between these two types of intramolecular screening.

To acknowledge that a number of contacts may not be available to a given polymer chain due to intramolecular screening effects, a screening factor can be introduced. The screening factor, γ_s , is defined as the fraction of same chain contacts in a polymer chain not caused by covalent bonds. Simulations performed by Kumar¹ suggest that the screening factor has the following dependence on the chain length, r :

$$\gamma_s = a + \frac{b}{r^{1/2}} \quad (7)$$

where a and b are constants. An approximate value of 0.38 was reported for a for a polymer blend, but no value has been reported for b yet. Presumably the factor b would be strongly model dependent.

In the following the intramolecular screening factor, γ_s , will be treated as a constant, which essentially means that an average value over the distribution of conformations characteristic of the unperturbed Gaussian state is adopted.

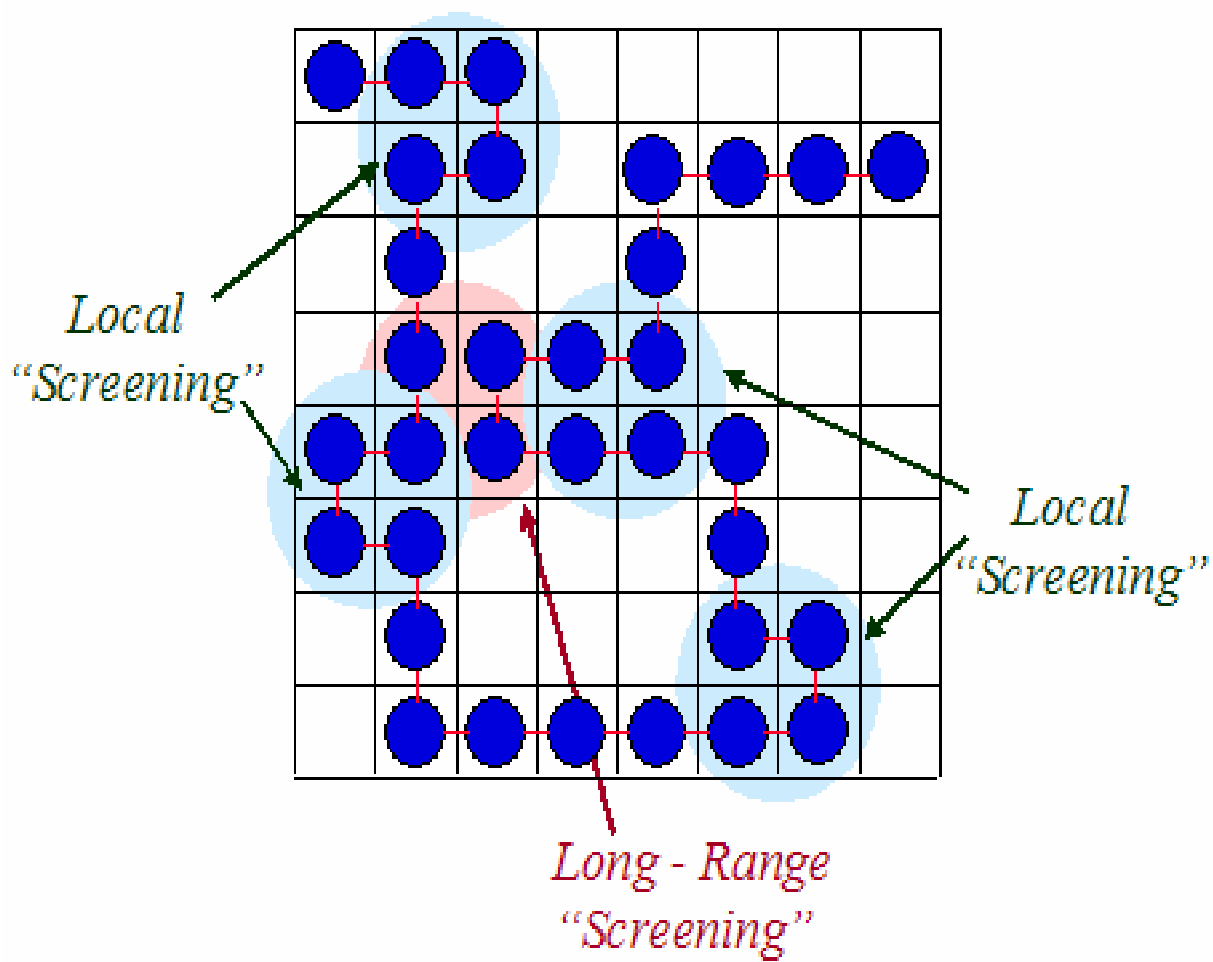


Figure 2.1. Local and long-range screening effects. Painter et al.³

The product qz represents all the polymer segment contacts excluding the contacts between covalently bound segments. A distinction between intramolecular and intermolecular contacts can be made through the introduction of the intramolecular screening factor, γ_s . If γ_s represents the fraction of intramolecular contacts then $\gamma_s qz$ would represent the number of contacts that are intramolecular. The remaining polymer segment contacts, $(1 - \gamma_s)qz$, would then be intermolecular contacts. Using this nomenclature equation 3 can be rewritten to:

$$(1 - \gamma_s)qz + \gamma_s qz = (z - 2)r + 2 \quad (8)$$

Substituting q' for $(1 - \gamma_s)q$ the equation becomes:

$$q'z = (z - 2)r + 2 - \gamma_s qz \quad (9)$$

where $q'z$ is the effective number of intermolecular contacts allowed to a given polymer chain. This equation in turn can be rewritten to:

$$\frac{q'}{r} = (1 - \gamma_l)(1 - \gamma_s) = (1 - \gamma) \quad (10)$$

$$r - q' = r\gamma_l + \gamma_s q \quad (11)$$

$$\frac{r - q'}{r} = \gamma_l + \gamma_s(1 - \gamma_l) \quad (12)$$

where the combined screening factor, γ , is defined as:

$$\gamma = \gamma_l + \gamma_s(1 - \gamma_l) \quad (13)$$

In the previous chapter the excess free energy was defined as:

$$\frac{\Delta G_{exc.}}{RT} = n_s p_{ps} \chi \quad (14)$$

where n_s is the number of moles of solvent, p_{ps} represents the probability of finding a polymer segment adjacent to a solvent molecule, χ is an interaction energy parameter, R is the universal gas constant, and T is the temperature.

The probability of finding a polymer segment next to another polymer segment is given by:

$$P_{pp} = \gamma_s + (1 - \gamma_s) \left[\frac{(1 - \gamma_s) \phi_p}{(1 - \gamma_s) \phi_p + \phi_s} \right] = \gamma_s + \frac{(1 - \gamma_s)^2 \phi_p}{1 - \gamma_s \phi_p} \quad (15)$$

or if expressed in terms of surface site fractions, the equivalent expression is obtained:

$$P_{pp} = \gamma_s + \frac{(1 - \gamma_s)^2 \theta_p}{1 - \gamma_s \theta_p} \quad (16)$$

In either case the first term represents the fraction of intramolecular (same chain) contacts, while the second term represents the fraction of intermolecular contacts between polymer segments from different chains.

The probability that there is a solvent molecule next to a polymer segment would then be:

$$P_{sp} = \frac{(1-\gamma_s)\theta_s}{1-\gamma_s\theta_p} \quad (17)$$

but the more interesting probability is the one that describes the probability of finding a polymer segment next to a solvent molecule, p_{ps} , because this is the one required to calculate the excess free energy (see equation 14). It can be easily shown that:

$$P_{ps} = \frac{\theta_p}{\theta_s} P_{sp} \quad (18)$$

so that:

$$P_{ps} = \frac{(1-\gamma_s)\theta_p}{1-\gamma_s\theta_p} = \frac{(1-\gamma_s)(1-\gamma_l)\phi_p}{(1-\gamma_s\theta_p)(1-\gamma_l\phi_p)} \quad (19)$$

or in terms of the combined screening factor, γ , defined in equation 13 it becomes:

$$P_{ps} = \frac{(1-\gamma)\phi_p}{(1-\gamma\phi_p)} \quad (20)$$

The excess free energy can then be expressed in terms of this probability as:

$$\frac{\Delta G_{exc.}}{RT} = n_s \left(\frac{(1-\gamma)\phi_p}{(1-\gamma\phi_p)} \right) \chi \quad (21)$$

2.3. Packing Effects in Polymer Solutions

In the previous chapter it was briefly mentioned that in the classical Flory-Huggins theory, the combinatorial energy, $\Delta G_{comb.}$, is given by:

$$\frac{\Delta G_{comb.}}{RT} = \phi_s \ln \phi_s + \frac{\phi_p}{r} \ln \phi_p \quad (22)$$

but that a more refined expression was developed by both Huggins⁴ and Guggenheim⁵. In the latter case the combinatorial energy is given by:

$$\begin{aligned} \frac{\Delta G'_{comb.}}{RT} &= \phi_s \ln \phi_s + \frac{\phi_p}{r} \ln \phi_p \\ &- \left(\frac{r-1}{r} \right) \left(\frac{r}{r-q} - \phi_p \right) \ln \left(1 - \left(\frac{r-q}{r} \right) \phi_p \right) + \phi_p \frac{q(r-1)}{r(r-q)} \ln \left(\frac{q}{r} \right) \end{aligned} \quad (23)$$

where the combinatorial Gibbs free energy is expressed on a per mole of lattice sites basis. A thorough derivation of this expression can be found in Appendix C. The expression was originally proposed by Guggenheim⁵ for an athermal polymer solution, where further constraints were imposed on the polymer segments. It was stipulated that each of the polymer segments would be placed on the lattice in such a manner that the polymer chain would not be able to bent back on itself. Essentially this means that intramolecular contacts are disregarded, and only intermolecular contacts are considered. In this case it would be appropriate to replace q by q' , which earlier was defined as the effective number of intermolecular contacts.

$$\begin{aligned} \frac{\Delta G'_{comb.}}{RT} &= \phi_s \ln \phi_s + \frac{\phi_p}{r} \ln \phi_p \\ &- \left(\frac{r-1}{r} \right) \left(\frac{r}{r-q'} - \phi_p \right) \ln \left(1 - \left(\frac{r-q'}{r} \right) \phi_p \right) + \phi_p \frac{q'(r-1)}{r(r-q')} \ln \left(\frac{q'}{r} \right) \end{aligned} \quad (24)$$

by substituting equations 10-12 into equation 24, the combinatorial free energy term can be expressed in terms of the combined screening factor, γ , as:

$$\begin{aligned} \frac{\Delta G'_{comb.}}{RT} &= \phi_s \ln \phi_s + \frac{\phi_p}{r} \ln \phi_p \\ &- \left(\frac{r-1}{r} \right) \left(\frac{1-\gamma\phi_p}{\gamma} \right) \ln(1-\gamma\phi_p) + \phi_p \left(\frac{r-1}{r} \right) \left(\frac{1-\gamma}{\gamma} \right) \ln(1-\gamma) \end{aligned} \quad (25)$$

which for large values of r reduces to:

$$\frac{\Delta G'_{comb.}}{RT} = \phi_s \ln \phi_s + \frac{\phi_p}{r} \ln \phi_p - \left(\frac{1 - \gamma \phi_p}{\gamma} \right) \ln(1 - \gamma \phi_p) + \phi_p \left(\frac{1 - \gamma}{\gamma} \right) \ln(1 - \gamma) \quad (26)$$

2.4. The Chemical Potential

The chemical potential can be determined by taking the derivative of the free energy with respect to the composition:

$$\frac{\Delta \mu_i}{RT} = \left(\frac{\partial \left(\frac{\Delta G}{RT} \right)}{\partial n_i} \right)_{T, P, n_{j \neq i}} \quad (27)$$

From equation 21 it follows that the excess energy contribution to the chemical potential is:

$$\frac{\Delta \mu_s^{exc.}}{RT} = \frac{(1 - \gamma)^2}{(1 - \gamma \phi_p)^2} \phi_p^2 \chi \quad (28)$$

and from equation 26 it then follows that the combinatorial contribution to the chemical potential is:

$$\frac{\Delta \mu_s^{comb.}}{RT} = \ln \phi_s + \left(1 - \frac{1}{r} \right) \phi_p - \frac{1}{\gamma} \ln(1 - \gamma \phi_p) - \phi_p \quad (29)$$

when these two contributions to the chemical potential are combined, the following expression is obtained:

$$\frac{\Delta\mu_s}{RT} = \ln\phi_s + \left(1 - \frac{1}{r}\right)\phi_p - \frac{1}{\gamma}\ln(1 - \gamma\phi_p) - \phi_p + \frac{(1-\gamma)^2}{(1-\gamma\phi_p)^2}\phi_p^2\chi \quad (30)$$

In the traditional Flory theory the chemical potential is expressed as:

$$\frac{\Delta\mu_s}{RT} = \ln\phi_s + \left(1 - \frac{1}{r}\right)\phi_p + \phi_p^2\chi^{FH} \quad (31)$$

where Flory and Höcker⁶ identifies χ^{FH} as the reduced chemical potential:

$$\chi^{FH} = \frac{\left(\frac{\Delta\mu_s}{RT} - \ln\phi_s - \left(1 - \frac{1}{r}\right)\phi_p\right)}{\phi_p^2} \quad (32)$$

If equation 30 is substituted into equation 32 the following expression is obtained:

$$\chi^{FH} = -\left[\frac{1}{\gamma\phi_p^2}\ln(1 - \gamma\phi_p) + \frac{1}{\phi_p}\right] + \frac{(1-\gamma)^2}{(1-\gamma\phi_p)^2}\chi \quad (33)$$

As it can be seen in equation 33, the reduced chemical potential, χ^{FH} , contains a combinatorial term, which is the first term on the right hand side. Traditionally the

combinatorial term is considered an entropic term, and in the following it will be treated as such:

$$\chi_S = - \left[\frac{1}{\gamma\phi_p^2} \ln(1 - \gamma\phi_p) + \frac{1}{\phi_p} \right] \quad (34)$$

The second term on the right hand side of equation 33 contains the interaction parameter χ , which in this treatment will be defined as:

$$\chi = \frac{\chi_0}{T} \quad (35)$$

where χ_0 is a constant having the same dimensions as the temperature, T . Since the second term on the right hand side of equation 33 accounts for the interaction energy, it can appropriately be considered an enthalpic term:

$$\chi_H = \frac{(1 - \gamma)^2}{(1 - \gamma\phi_p)^2} \chi \quad (36)$$

and the reduced chemical potential, χ^{FH} , can therefore be written as:

$$\chi^{FH} = \chi_S + \chi_H \quad (37)$$

In order to obtain chemical equilibrium at a given temperature, T , and pressure, P , the following thermodynamic criteria must be fulfilled:

$$\mu_i^I = \mu_i^{II} \quad (38)$$

where μ_i^I and μ_i^{II} are the chemical potentials of component i in phases I and II, respectively. The chemical potential for the solvent is given in equation 30. By equating the chemical potentials in all the phases for each component, a set of equations is obtained, which can be solved to give the compositions at which a given system is in a single phase at a given temperature. If these calculations are done at varying temperatures, a set of data points are obtained, which can be plotted to obtain the so-called binodal or cloud point curve. This curve defines the transition from a one-phase to a two-phase system, as illustrated in figure 2.2. The temperatures along the binodal curve are commonly referred to as cloud-point temperatures. In the cases where the phase diagram has the appearance similar to that of figure 2.2, where there is an upper boundary for a two phase system, the maximum value of these temperatures is the so-called *Upper Critical Solution Temperature (UCST)*. However, phase diagrams also exist where there is a lower boundary for a two phase system, and in these cases the minimum of these temperatures referred to as the *Lower Critical Solution Temperature (LCST)*. At either extreme of the phase diagram, whether it is a *UCST* or a *LCST*, both the second and third derivatives of the Gibbs free energy of mixing with respect to composition are zero.

The stability of a system is determined by the second derivative of Gibbs free energy of mixing with respect to the composition. By solving the following equation:

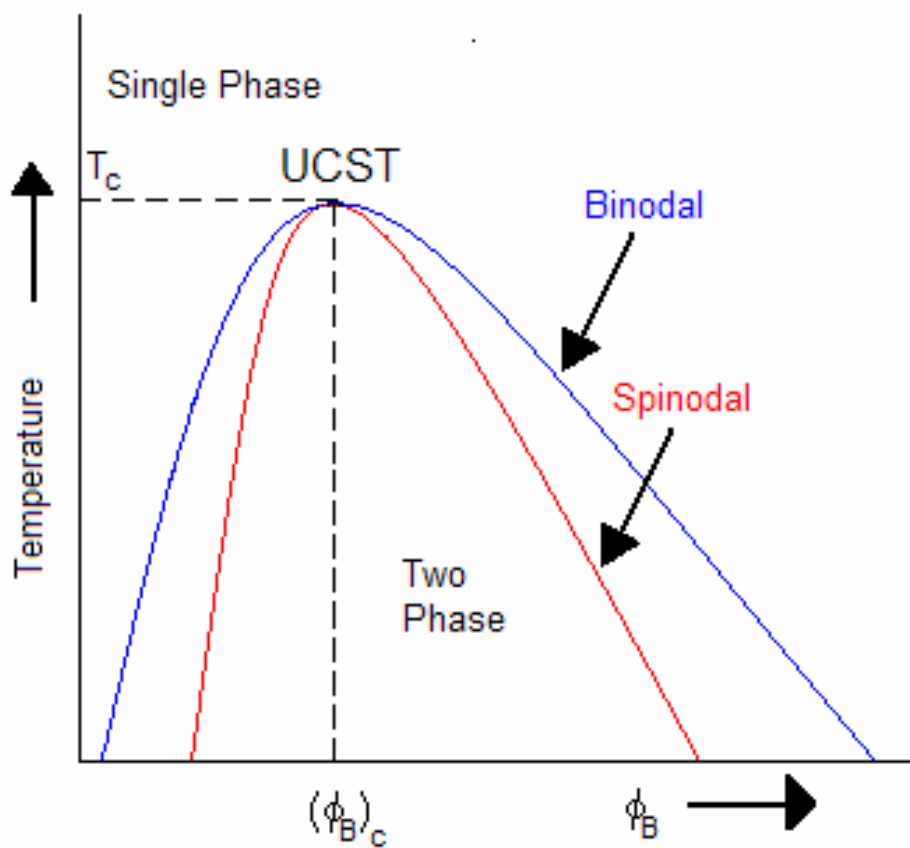


Figure 2.2. Schematic representation of a phase diagram.
Painter and Coleman⁷

$$\left(\frac{\partial^2 \left(\frac{\Delta G}{RT} \right)}{\partial \phi_i^2} \right)_{T,P,\phi_{j \neq i}} = 0 \quad (39)$$

at different temperatures a set of data points is obtained which when connected forms the spinodal curve. The region between the binodal and spinodal curve is called the metastable region. In the metastable region phase separation is thermodynamically preferred, so even though a system in this region might be in a single phase, a small perturbation could trigger a phase separation. As illustrated in figure 2.2, the binodal and spinodal curve meet at the critical point.

The second derivative of equation 21 with respect to the composition will give the excess energy contribution to the spinodal as:

$$\frac{\partial^2 \left(\frac{\Delta G_{exc.}}{RT} \right)}{\partial \phi_s^2} = - \frac{2(1-\gamma)^2}{(1-\gamma\phi_p)^3} \chi \quad (40)$$

and the combinatorial energy contribution to the spinodal can be obtained from the second derivative of equation 26 with respect to the composition:

$$\frac{\partial^2 \left(\frac{\Delta G'_{comb.}}{RT} \right)}{\partial \phi_s^2} = \frac{1}{\phi_s} + \frac{1}{r\phi_p} - \frac{\gamma}{1-\gamma\phi_p} \quad (41)$$

the second derivative of the Gibbs free energy can now be obtained by combining equation 40 and equation 41:

$$\frac{\partial^2 \left(\frac{\Delta G'}{RT} \right)}{\partial \phi_s^2} = \frac{1}{\phi_s} + \frac{1}{r\phi_p} - \frac{\gamma}{1-\gamma\phi_p} - \frac{2(1-\gamma)^2}{(1-\gamma\phi_p)^3} \left(\frac{\chi_0}{T} \right) \quad (42)$$

where the Gibbs free energy is again expressed on a per mole of lattice sites basis. The spinodal is then obtained by equating the right hand side of equation 42 with zero. If this is done the following expression is obtained for the spinodal temperature:

$$T = \frac{\frac{2\chi_0(1-\gamma)^2}{(1-\gamma\phi_p)^3}}{\left(\frac{1}{\phi_s} + \frac{1}{r\phi_p} - \frac{\gamma}{1-\gamma\phi_p} \right)} \quad (43)$$

Following the same procedure the third derivative of the Gibbs free energy is obtained:

$$\frac{\partial^3 \left(\frac{\Delta G'}{RT} \right)}{\partial \phi_s^3} = -\frac{1}{\phi_s^2} + \frac{1}{r\phi_p^2} + \frac{\gamma^2}{(1-\gamma\phi)^2} + \frac{6\gamma(1-\gamma)^2}{(1-\gamma\phi_p)^4} \left(\frac{\chi_0}{T} \right) \quad (44)$$

Since the following criteria:

$$\left(\frac{\partial^3 \left(\frac{\Delta G'}{RT} \right)}{\partial \phi_s^3} \right)_{T,P,\phi_p} = 0 \quad (45)$$

must be met at the critical point, it follows that the temperature at the critical point, T_c , can be expressed in terms of equation 44 as:

$$T_c = - \frac{\frac{6\chi_0\gamma(1-\gamma)^2}{(1-\gamma\phi_p^{crit.})^4}}{\left(-\frac{1}{(1-\phi_p^{crit.})^2} + \frac{1}{r(\phi_p^{crit.})^2} + \frac{\gamma^2}{(1-\gamma\phi_p^{crit.})^2} \right)} \quad (46)$$

Earlier it was mentioned that both the second and third derivative of the Gibbs free energy with respect to composition must be zero at the critical point. Accordingly equation 43 can be expressed in terms of the critical variables:

$$T_c = \frac{\frac{2\chi_0(1-\gamma)^2}{(1-\gamma\phi_p^{crit.})^3}}{\left(\frac{1}{(1-\phi_p^{crit.})} + \frac{1}{r\phi_p^{crit.}} - \frac{\gamma}{1-\gamma\phi_p^{crit.}} \right)} \quad (47)$$

In the literature it is possible to find critical point data ($\phi_p^{crit.}$, T_c) for polymers at various degrees of polymerization. With this data in hand it is possible to solve equations

46 and 47, respectively, for χ_0 and γ , since there are two equations and two unknowns.

2.5. Calculations and Discussion

In principle the model presented above contains three adjustable parameters γ_l , γ_s and χ_0 . Two of them have been combined into a single parameter γ , which was defined earlier as:

$$\gamma = \gamma_l + \gamma_s(1 - \gamma_l) \quad (13)$$

but it follows from equation 5:

$$\gamma_l = \frac{2}{z} \left(1 - \frac{1}{r} \right) \quad (5)$$

that if the lattice coordination number z is fixed, then γ_l approaches a constant value for high degrees of polymerization (large r). Values between 6 and 12 have been reported in the literature⁸ for the lattice coordination number. Koningsveld and Kleintjens² reported a value of 8.5 for the lattice coordination number. In this treatment it was decided to use a lattice coordination number of $z=9$, which is an average value for the random close packing of hard spheres reported by Bernal⁹. By doing so the number of adjustable parameters is reduced to two, because γ_l approaches the constant value of 0.222 for large values of r . Although the two remaining adjustable parameters could be regarded as

purely empirical parameters, it was decided to investigate whether they would have any physical meaning by fitting them to experimental data.

By fitting equations 46 and 47 to experimental data at the critical point, it is possible to extract a set of values for γ_s and χ_0 that gives the best correlation. If the critical data point $(\phi_p^{crit.}, T_c)$ is inserted in both equations, and one of the variables is eliminated by substitution, the following equation is obtained:

$$-\frac{1}{(1-\phi_p^{crit.})^2} + \frac{1}{r(\phi_p^{crit.})^2} - \frac{2\gamma^2}{(1-\gamma\phi_p^{crit.})^2} + \frac{3\gamma}{(1-\gamma\phi_p^{crit.})} \left(\frac{1}{(1-\phi_p^{crit.})} + \frac{1}{r\phi_p^{crit.}} \right) = 0 \quad (48)$$

which can be solved for γ (γ_s). Once the value of γ_s is obtained it can be inserted in either equation 46 or 47 to obtain the value of χ_0 . A set of such calculations were performed for the Polystyrene-Cyclohexane system, using the experimental critical point data reported by Koningsveld et al.¹⁰. The experimental data have been listed in table 2.1, whereas the set of optimized values for the two adjustable parameters γ_s and χ_0 are listed in table 2.2.

The reason why the Polystyrene-Cyclohexane system was chosen to test the proposed models performance was mostly out of necessity. The availability of experimental data of the type needed in this evaluation is very limited. For a given system the following information is required; the critical point data, $(\phi_p^{crit.}, T_c)$, at various degrees of polymerization, the spinodals and the reduced chemical potential, χ^{FH} , as a function of composition. Since all of these data were available for the Polystyrene-Cyclohexane system, it became the system of choice. Another reason why this system was chosen is because Cyclohexane is a poor solvent for Polystyrene at room temperature. This means

Sample no.	r	ϕ_p^{crit}	T_c (°C)
2	490	0.1125	15.7
4	893	0.0895	20.5
5	1594	0.0753	23.45
7	3783	0.0525	27.55
8	5060	0.04825	28.0
9	14402	0.0311	30.05

Table 2.1. Experimental Critical Data ($\phi_p^{crit.}$, T_c) for Polystyrene-Cyclohexane (Koningsveld et al.¹⁰)

r	γ_l	γ_s	γ	χ	χ_0
490	0.222	0.243	0.411	0.893	257.8
893	0.222	0.249	0.416	0.888	260.8
1594	0.222	0.268	0.431	0.901	267.2
3783	0.222	0.272	0.434	0.897	269.8
5060	0.222	0.281	0.441	0.906	272.7
14402	0.222	0.287	0.445	0.908	275.4

Table 2.2. Calculated values of γ_s and χ_0 for Polystyrene-Cyclohexane at various degrees of polymerization.

that the polymer chains prefer to be surrounded by themselves. In a good solvent the polymer chains will expand, thereby opening up for the possibility of more intermolecular contacts. At the so-called θ -temperature, the polymer chains will not be expanded to any great extent, which means one would expect to see the same number of intramolecular contacts in the polymer-solvent mixture as one would expect to see in the pure polymer. It is recalled that the θ -temperature is defined as the temperature at which the residual chemical potential is zero and deviations from ideality vanishes, i.e. it is the temperature at which the intermolecular interactions are exactly cancelled out by volume exclusion effects, and the temperature at which the polymer chains obtain their ideal dimensions. It is also the lowest possible temperature for complete miscibility in the limit of infinite molecular weight.

Since the primary focus in this investigation was to explore the significance of intramolecular contacts or same chain contacts, it made sense to choose a system where such effects would prevail, such as a system where the solvent is poor. As the chains collapses at the θ -temperature, they will be in an environment that is increasingly dominated by polymer-polymer contacts. The θ -temperature of the Polystyrene-Cyclohexane system was reported by Fox and Flory¹¹ as well as several other workers to be 34 °C.

As mentioned earlier this work was inspired by some interesting results obtained in the study of polymer blends, where simulations indicated that the fraction of same-chain contacts had an inverse dependence on the square root of the molecular weight. These simulations were performed on a cubic lattice, using a lattice coordination number of 6 ($z=6$), where the limiting value γ_s of was 0.38 As it can be seen in table 2.2, the

calculated values of γ_s ranges from 0.24 to 0.29, but it should be recalled that these calculations were performed with a different lattice coordination number ($z=9$). However, the same set of calculations was performed for a number of different lattice coordination numbers ranging from 8 to 12 without a significant change in the optimized value of γ_s .

When the optimized values of γ_s are plotted against $r^{-0.5}$, it appears that the relationship is roughly linear, as it can be seen in figure 2.3. Taking the usual errors in experimental data into account, as well as the simplicity of the model, it appears that the correlation between γ_s and the inverse of the square root of the chain length is very good.

From table 2.2 it is also interesting to note that the χ_0 parameter appears to vary with molecular weight. In this investigation the primary idea was to investigate whether screening effects alone could explain some experimentally observed data in the concentrated regime, so it is assumed that the γ -terms can account for the variations in the reduced chemical potential. In principle the χ_0 parameter should therefore be constant, so it could mean that other factors such as free volume or equation of state effects, which were ignored here, are significant.

Kriegbaum and Geymer¹² reported a set of experimental observed values for the interaction parameter as a function of concentration at or near the θ -temperature, which were obtained for three different molecular weight fractions of Polystyrene by a variety of methods. The number average molecular weights were: 25.100 (fraction I), 72.000 (fraction II) and 440.000 (fraction III). These data have been listed in table 2.3.

Once the two adjustable parameters in the model presented in this work, γ_s and χ_0 , have been optimized through critical point data (essentially forcing the model to fit the critical point), it is possible to calculate the reduced chemical potential, χ^{FH} , as a function

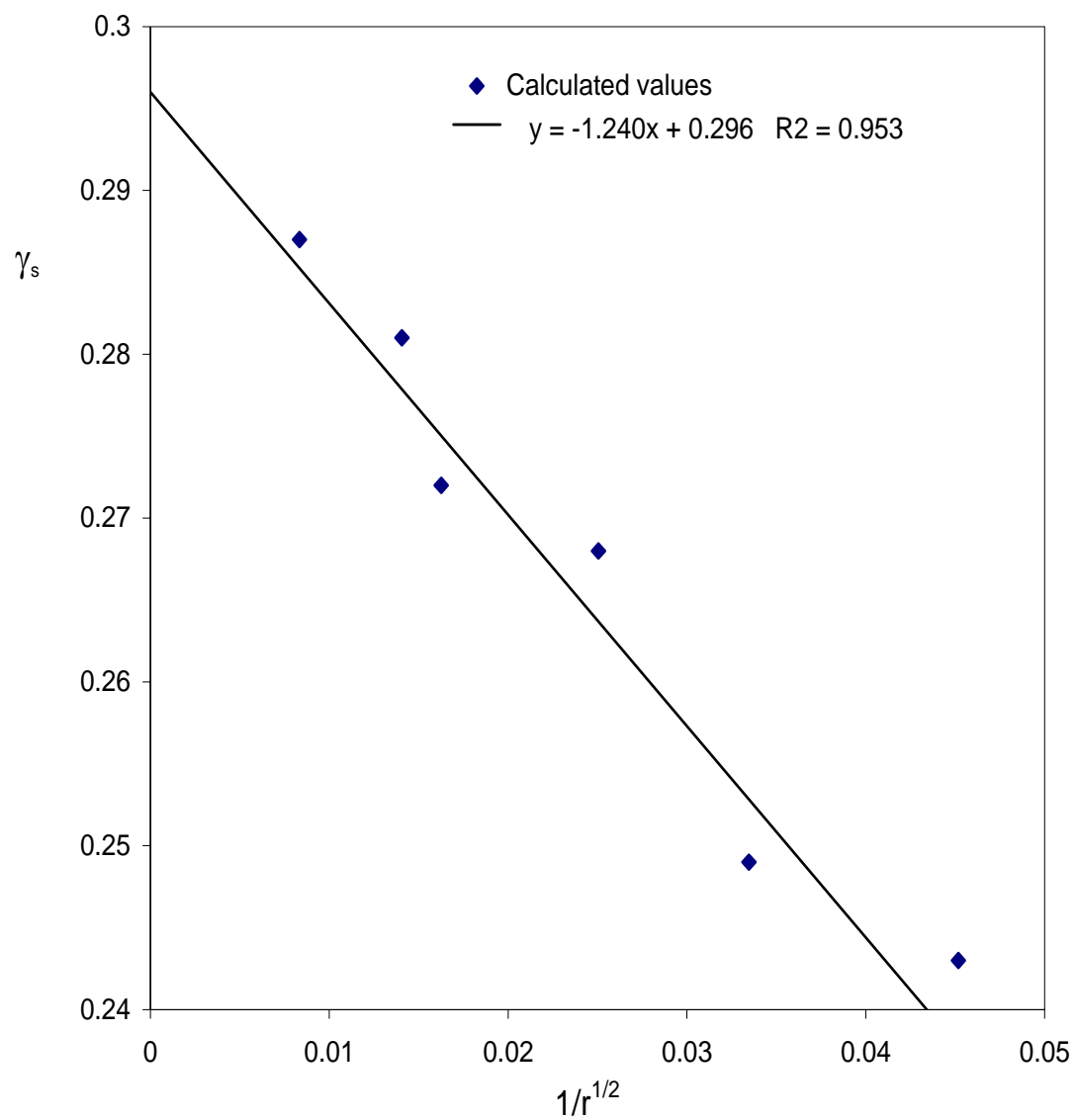


Figure 2.3. Calculated values of the fraction of intramolecular contacts, γ_s , which were optimized using experimental critical point data.

ϕ_p	χ_{exp}
0.003	0.507
0.256	0.597
0.340	0.619
0.387	0.660
0.447	0.652
0.492	0.682
0.492	0.699
0.544	0.727
0.638	0.771
0.638	0.822
0.737	0.882
0.766	0.912
0.800	0.950
0.804	0.897
0.847	1.016
0.900	1.280
0.905	1.182

Table 2.3. Selected experimental values of the χ parameter for Polystyrene-Cyclohexane at 34 °C as a function of concentration of PS. (Kriegbaum and Geymer¹²)

of concentration through equation 33:

$$\chi^{FH} = - \left[\frac{1}{\gamma\phi_p^2} \ln(1 - \gamma\phi_p) + \frac{1}{\phi_p} \right] + \frac{(1 - \gamma)^2}{(1 - \gamma\phi_p)^2} \left(\frac{\chi_0}{T} \right) \quad (33)$$

When the reduced chemical potential, χ^{FH} , is calculated, no additional changes to the two adjustable parameters, γ_s and χ_0 , are allowed once they have been fitted to the critical point. What this means is that a single data point (per molecular weight) is used to extract the values of γ_s and χ_0 that gives the best fit. These values in turn are then used without modification in all subsequent calculations.

The calculated values of χ^{FH} have been listed in table 2.4, along with the individual contributions, χ_s , which is the first term on the right hand side of equation 33, and χ_H , which is the second term on the right hand side of equation 33, to χ^{FH} . From table 2.4, it can be seen that the entropic contribution, χ_s , to χ^{FH} changes in value from 0.22 to 0.31 over the entire concentration range. These values falls well within the range 0.2-0.5 reported in the literature¹³ for the "fudge factor" mentioned in the previous chapter.

When the experimental data listed in table 2.4 are plotted it appears that they all describe in a single curve, as it can be seen in figure 2.4, despite the fact that they represent data from three different molecular weight fractions. With this in mind it was decided to pick an average value for γ_s and χ_0 in the calculations listed in table 2.4. The values chosen were $\gamma_s=0.272$ and $\chi_0=270$, which are the ones for sample # 7 ($r=3783$) listed in table 2.2. This seems reasonable considering that the degree of polymerization for the experimental data ranges from 241 to 4225.

ϕ_p	χ_H	χ_S	χ^{FH}
0.010	0.284	0.218	0.502
0.050	0.294	0.220	0.514
0.100	0.308	0.223	0.531
0.150	0.322	0.227	0.549
0.200	0.338	0.230	0.568
0.250	0.355	0.234	0.589
0.300	0.372	0.238	0.610
0.350	0.392	0.242	0.634
0.400	0.413	0.246	0.659
0.450	0.435	0.250	0.685
0.500	0.460	0.254	0.714
0.550	0.486	0.259	0.745
0.600	0.515	0.264	0.779
0.650	0.547	0.269	0.816
0.700	0.581	0.274	0.855
0.750	0.619	0.280	0.899
0.800	0.661	0.285	0.946
0.850	0.707	0.291	0.998
0.900	0.758	0.298	1.056
0.950	0.815	0.304	1.119
0.980	0.853	0.308	1.161
0.990	0.866	0.310	1.176

Table 2.4. Calculated values of χ_H , χ_S , and χ^{FH} for Polystyrene-Cyclohexane at 34 °C (with $\gamma_s=0.272$, $\gamma_f=0.222$ and $\chi_0=270.0$)

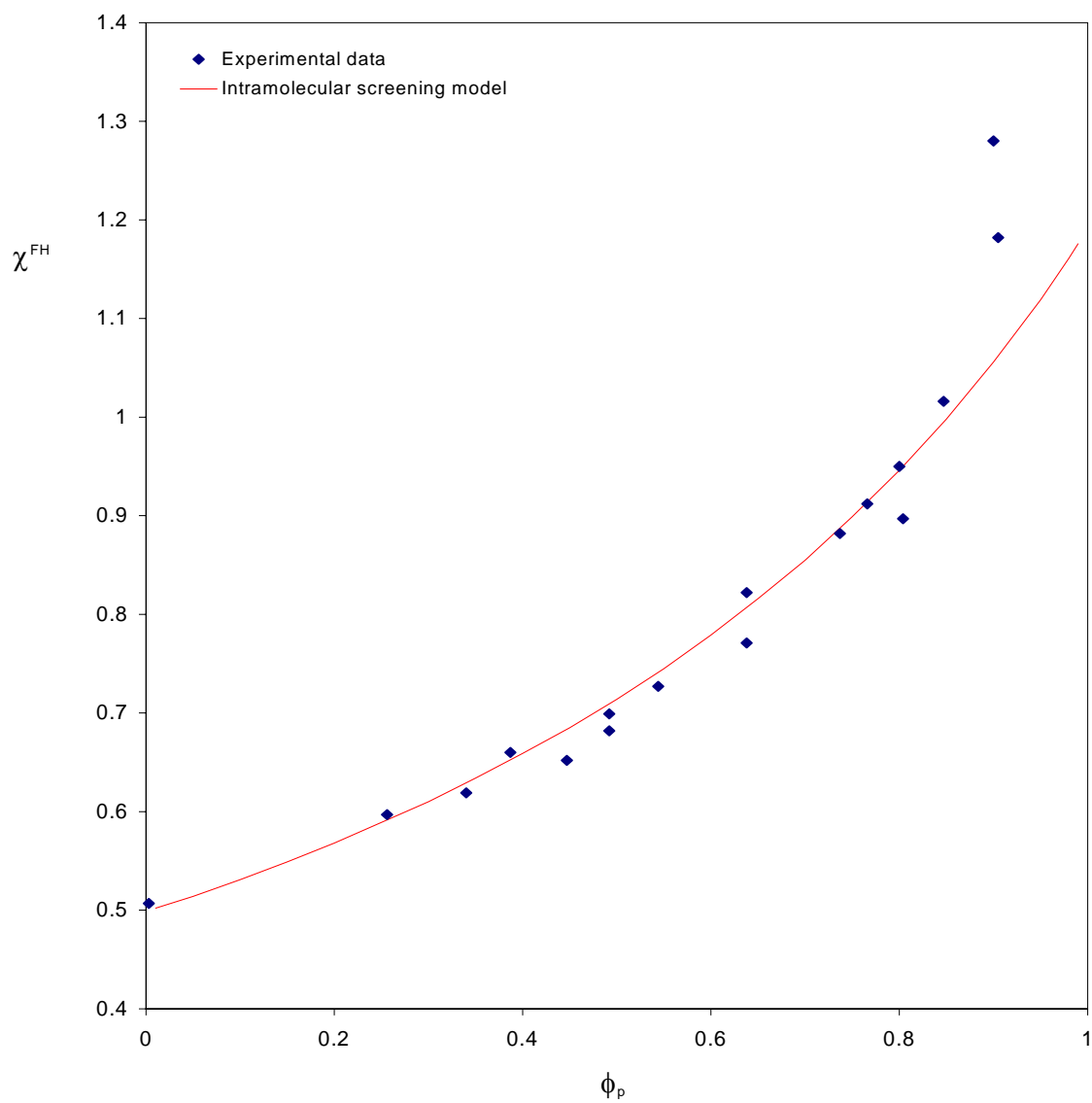


Figure 2.4. χ^{FH} versus composition for Polystyrene-Cyclohexane at 34 °C. Experimental data by Kriegbaum and Geymer¹².

As it can also be seen in figure 2.4, the calculated values of χ^{FH} provide a very good fit to the experimental data across the composition range. At the very high polymer concentration, where there is a noticeable deviation (for $\phi_p > 0.8$) one could question whether the experimentally reported values actually represents the true value of the reduced chemical potential. At these conditions, well below the Glass Transition Temperature of Polystyrene, the polymer will still be a glass. The polymer chains will have very little, if any, mobility, so it is conceivable that the systems at these concentrations were not allowed to reach equilibrium.

In a similar manner it is possible to calculate the spinodal temperature through equation 43, once the values of γ_s and χ_0 are known:

$$T = \frac{\frac{2\chi_0(1-\gamma)^2}{(1-\gamma\phi_p)^3}}{\left(\frac{1}{\phi_s} + \frac{1}{r\phi_p} - \frac{\gamma}{1-\gamma\phi_p}\right)} \quad (43)$$

The spinodals were calculated for three different weight average molecular weights, $\overline{M}_w = 51.000$, $\overline{M}_w = 163.000$ and $\overline{M}_w = 520.000$. These are the molecular weights for which Scholte¹⁴ reported experimentally observed spinodal temperatures as a function of concentration (weight fractions) for the Polystyrene-Cyclohexane system.

In the first system ($\overline{M}_w = 51.000$) the following values $\gamma_s=0.243$ and $\chi_0=258$ were used, which were taken from table 2.2 for sample # 2 ($r=490$). The results of these calculations are shown in figure 2.5 along with the experimental data. For comparison it

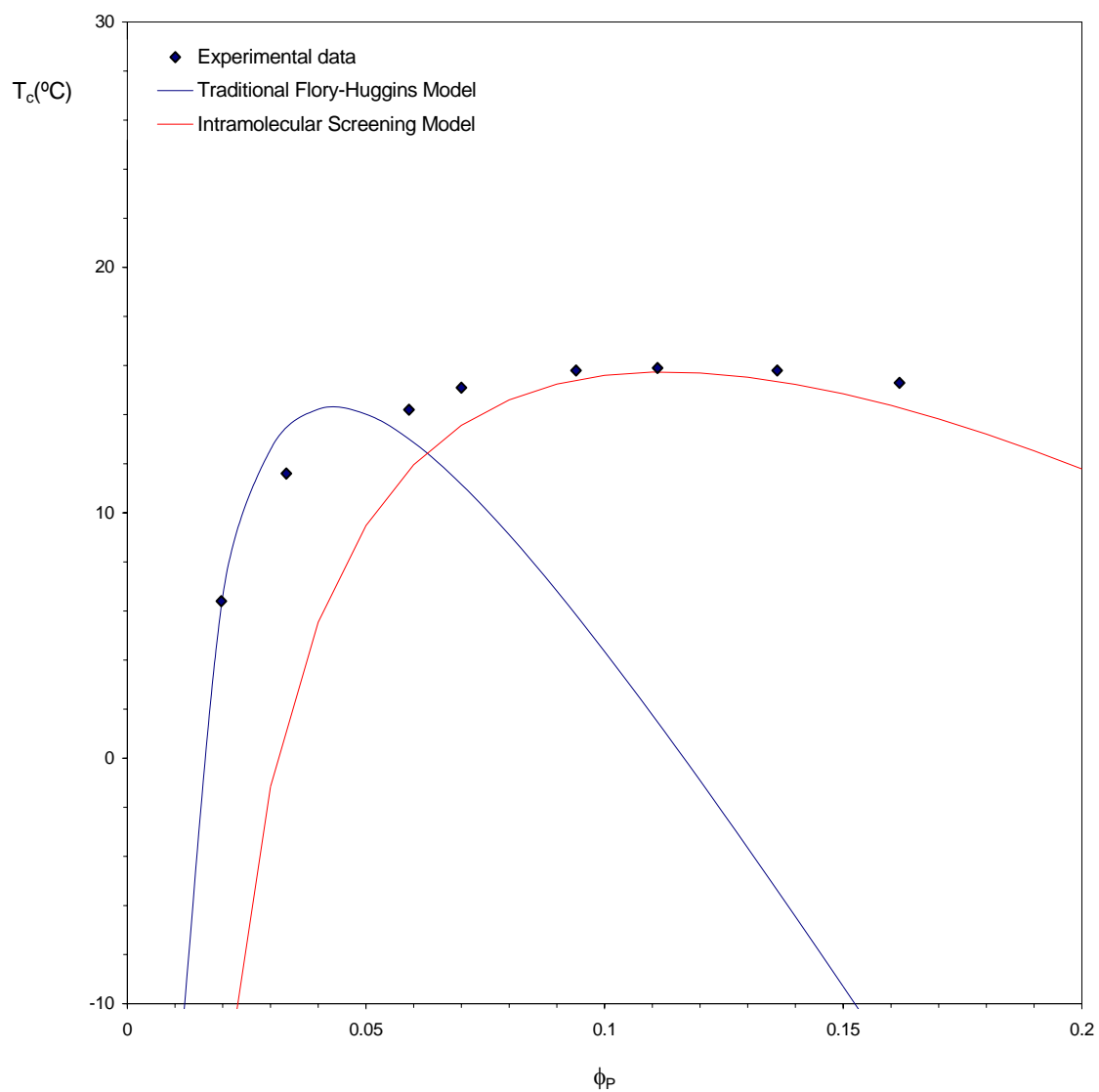


Figure 2.5. Spinodal for Polystyrene($\overline{M}_w = 51.000$)-Cyclohexane. Experimental data by Scholte¹⁴.

was decided also to show how a traditional Flory-Huggins model would perform, where it was optimized to give the best possible fit. However, for the Flory-Huggins model it was not the critical point that was used as a reference point, because that would have led to curves that would not have been comparable to those of the intramolecular screening model. Instead it was decided to use the lowest experimental spinodal temperature in each case.

Figure 2.5 illustrates a well known problem with the traditional Flory-Huggins model, namely its inability to reproduce the experimentally observed spinodals, which in general are much wider than those predicted by the classical theory. Since the model presented in this work is fitted to the critical point data given in table 2.1, it is no surprise that it coincides with this point. However, it appears from figure 2.5 that the model predicts a "wider" spinodal, which is more in line with the experimentally observed data. One could also argue that at the very diluted concentration regime (below $\phi_p^{crit.}$) it is to be expected that the chain dimensions would change. In a good solvent the polymer chains might expand, but in a poor solvent, such as Cyclohexane, it is possible that the Polystyrene chains may collapse. Either way the number of intramolecular contacts would be affected, resulting in a change in the screening factor γ_s .

For the second system ($\overline{M}_w = 163.000$) the following values were used for the two adjustable parameters; $\gamma_s = 0.268$ and $\chi_0 = 267$. These values can again be found in table 2.2 for sample # 5 ($r = 1594$). The results of these calculations are shown in figure 2.6. Although the deviations from experimental data are less pronounced, they are still there, especially below $\phi_p^{crit.}$, which is to be expected following the line of arguments listed above.

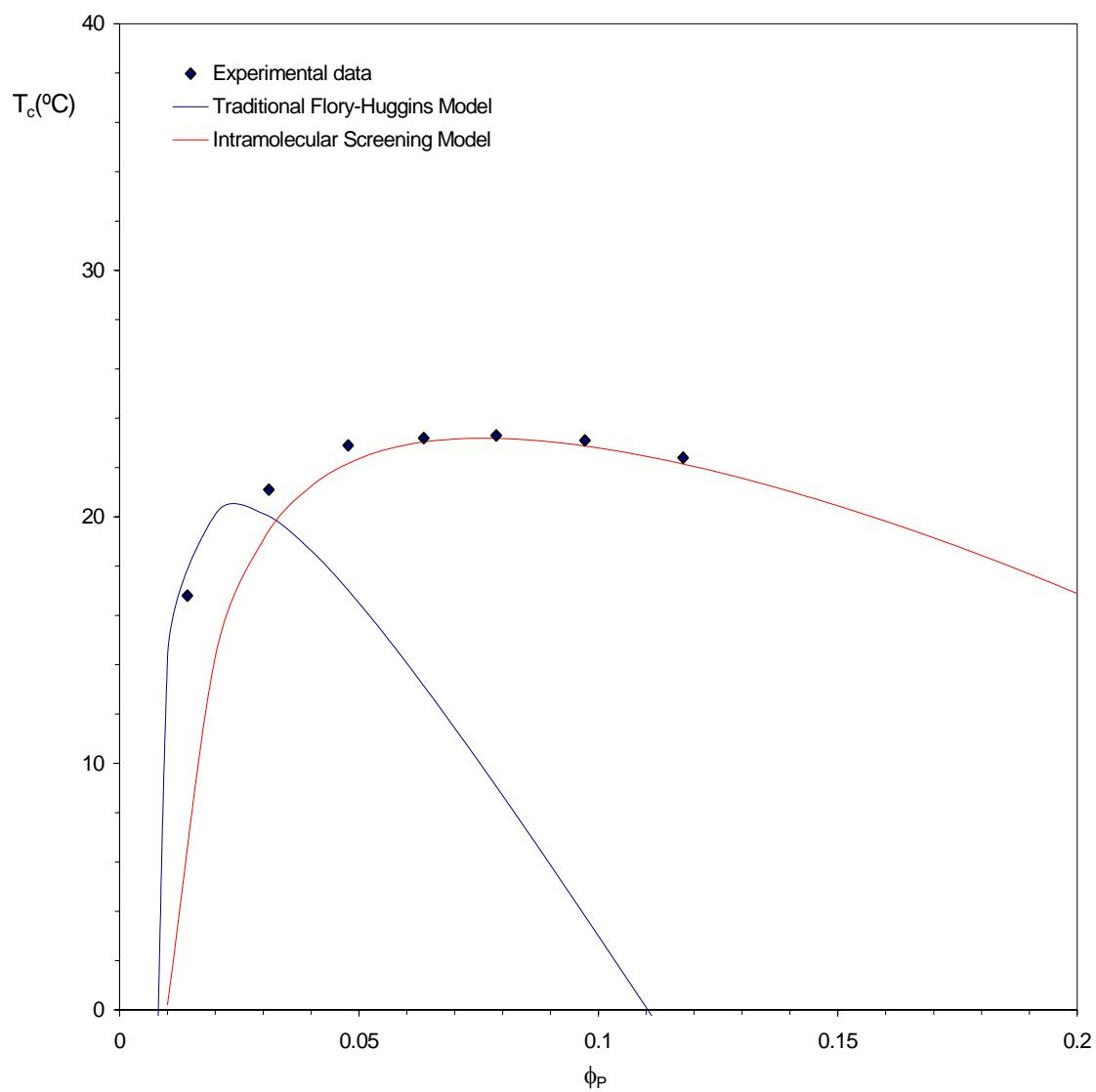


Figure 2.6. Spinodal for Polystyrene($\overline{M}_w = 163.000$)-Cyclohexane. Experimental data by Scholte¹⁴.

For the high molecular weight sample ($\overline{M}_w = 520.000$) the parameters were fixed at the following values; $\gamma_s=0.281$ and $\chi_0=273$. These are the values for sample # 8 ($r=5060$) in table 2.2, which is the sample with a molecular weight closest to that reported by Scholte¹⁴. From figure 2.7 it appears that the correspondence between the experimentally observed spinodal temperatures and those predicted by the relative simple intramolecular screening model presented in this work is very good.

For comparison the spinodals for all three molecular weight samples are shown in figure 2.8. From this figure it appears that as the molecular weight is increased the agreement between the experimentally observed data and the calculated values is improving. This may not be too surprising if it is recalled that the θ -temperature is the limiting value of the *UCST* (or *LCST*) as the molecular weight approaches infinity. As the molecular weight increases with an accompanying increase in the spinodal temperature, the system approaches its θ -temperature, and the chains starts to collapse. At these conditions one would expect intramolecular interactions to have a greater influence on the excess free energy.

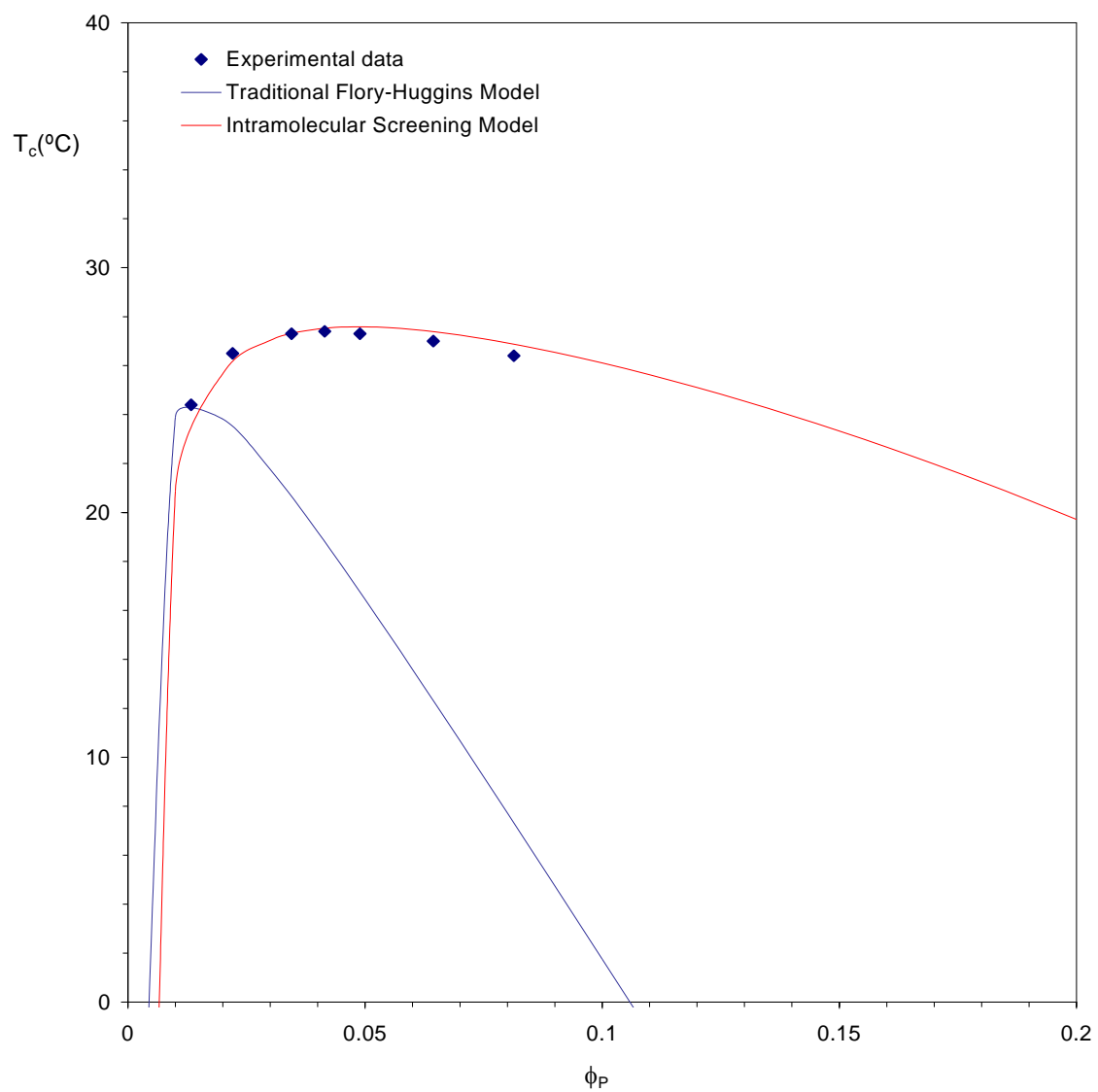


Figure 2.7. Spinodal for Polystyrene($\overline{M}_w = 520.000$)-Cyclohexane. Experimental data by Scholte¹⁴.

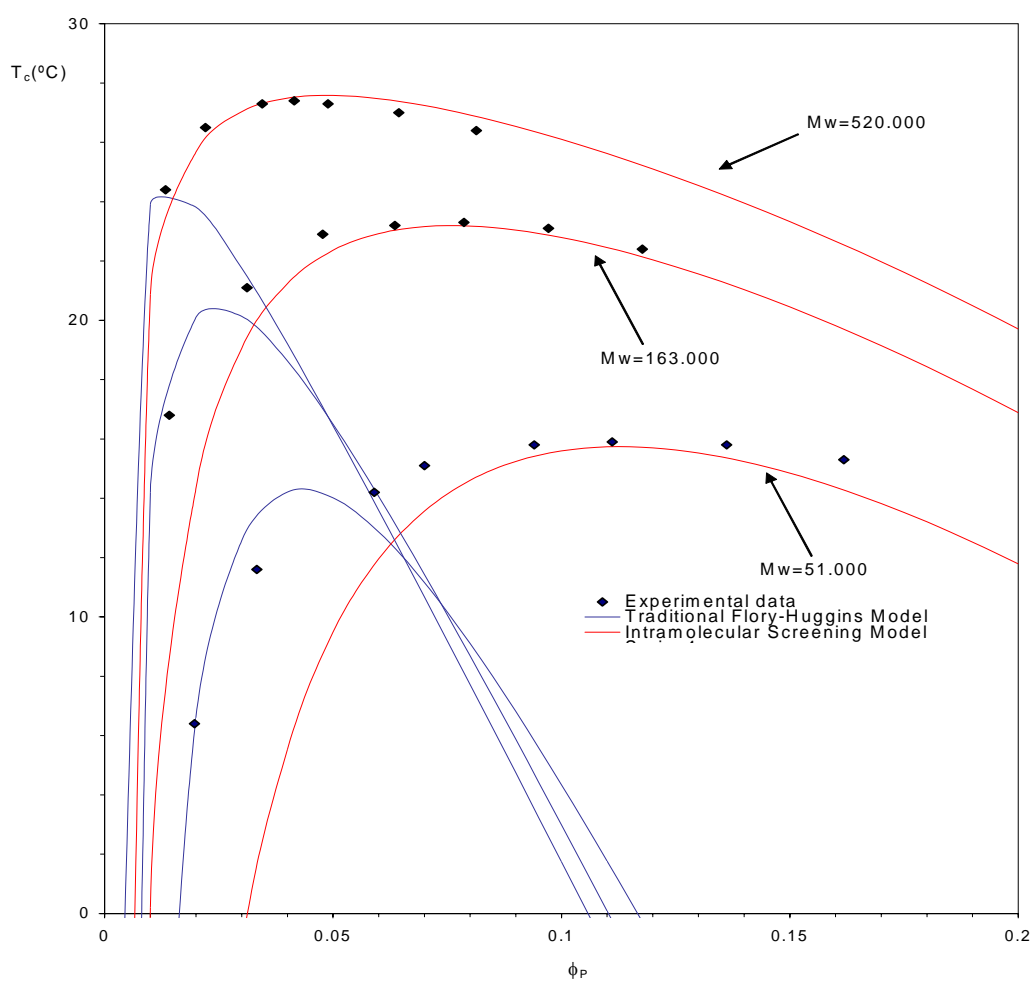


Figure 2.8. Spinodals for Polystyrene-Cyclohexane at various molecular weights. Experimental data by Scholte¹⁴.

2.6. Conclusions

In this work a model was presented, in which intramolecular screening effects were accounted for explicitly. That these types of contacts might be important was acknowledged as early as in the original work of Huggins⁴, in the correlation hole theory of de Gennes¹⁵, and in the work of Szleifer¹⁶ as well as Schweizer and Curro¹⁷. However, the premise of this work was to investigate whether a relatively simple modification of the traditional Flory-Huggins, where intramolecular contacts are accounted for through a so-called screening factor γ_s , would be able to reproduce some of the experimentally observed results in polymer solutions.

It was shown that by correlating the model to a single point, by optimizing two parameters to the critical point, it was possible to reproduce the composition dependence of the reduced chemical potential (the apparent interaction parameter). It was also shown that with the same (unchanged) parameters, it was possible to calculate spinodals that were in very good agreement with the experimental data, especially at high molecular weights.

It is interesting to note that the model presented in this work has the same form as that suggested by Koningsveld and Kleintjens², because this form has been proven to be a very useful way of accounting for the concentration dependence of χ over the years.

Finally, it was decided to see whether the intramolecular screening model presented here would be able to reproduce the composition dependence of the reduced chemical potential in other systems as well. As it can be seen in figure 2.9, where the

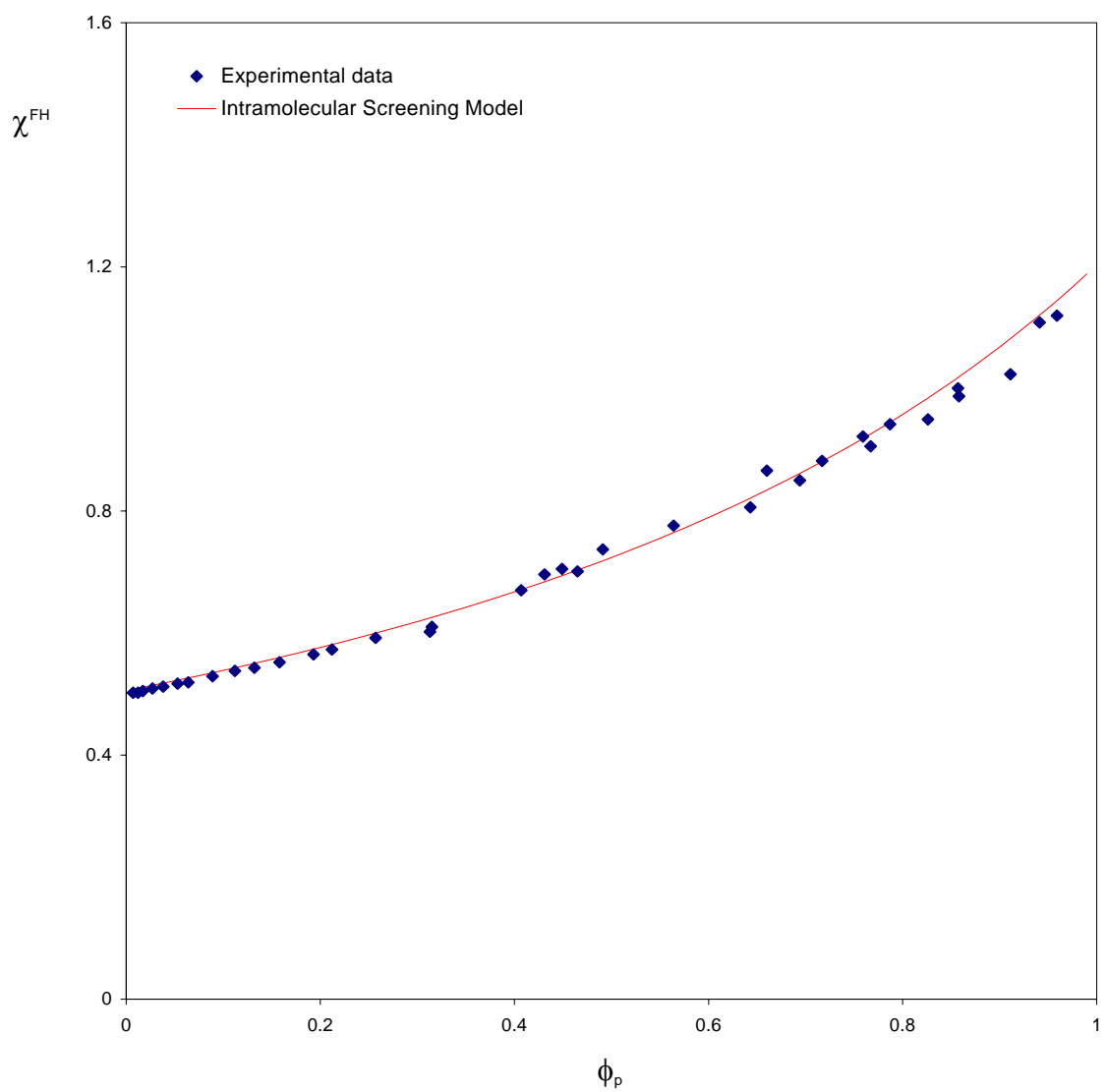


Figure 2.9. χ^{FH} versus composition for Polyisobutylene-Benzene at 25 °C. Experimental data by Eichinger and Flory¹⁸.

calculated values are plotted along with the experimentally observed data reported by Eichinger and Flory¹⁸, the correspondence is excellent. This is another example of a system consisting of a polymer in a poor solvent, where the *UCST* was reported to be 24.5 °C for infinite molecular weight.

In these calculations the following values were used for the two parameters; $\gamma_s=0.268$ and $\chi_0=267$. These values were not optimized to a PIB-Benzene critical point, but were used because sample # 5 ($r=1594$) in table 2.1 has a critical point, which is close to the temperature for which Eichinger and Flory¹⁸ reported the experimentally observed data.

With these encouraging results it would be interesting to see whether adding another layer of complexity, such as free volume effects, would make an even greater improvement.

2.7. References

1. Painter, P.C.; Veytsman, B.; Kumar, S.; Shenoy, S.; Graf, J.F.; Xu, Y.; Coleman, M.M. *Macromolecules*, **30**, 932 (1997)
2. Koningsveld, R.; Kleintjens, L.A. *Macromolecules*, **4**, 637 (1971)
3. Painter, P.C.; Berg, L.P.; Veytsman, B.; Coleman, M.M. *Macromolecules*, **30**, 7529 (1997)
4. Huggins, M.L. *Ann. N.Y. Acad. Sci.*, **43**, 9, 1942
5. Guggenheim, E.A. *Mixtures*, Clarendon, Oxford, 1952
6. Flory, P.J.; Höcker, H. *J. Trans. Faraday Soc.*, **67**, 2258 (1971)
7. Painter, P.C.; Coleman, M.M. *Fundamentals of Polymer Science*, Technomic Publishing Company, Inc., Lancaster, PA (1994)
8. Flory, P.J. *Principles of Polymer Chemistry*, Cornell University Press, Ithaca, N.Y. (1956)
9. Bernal, J.D. In *Liquids: Structure, Properties, Solid Interactions*; Hughel, T.J. Ed., Elsevier, Amsterdam (1965)
10. Koningsveld, R.; Kleintjens, L.A.; Shultz, A.R. *J. Polym. Sci.*, **8**, Part A-2, 1261 (1970)
11. Fox, T.G.; Flory, P.J. *J. Am. Chem. Soc.*, **73**, 1915 (1951)
12. Kriegbaum, W.R.; Geymer, D.O. *J. Am. Chem. Soc.*, **81**, 1859 (1959)
13. Orvoll, R.A. *Rubber Chem. & Tech.*, **50**, 451 (1977)
14. Scholte, T.G. *J. Polym. Sci.*, **9**, Part A-2, 1553 (1971)

15. de Gennes, P.G. *Scaling Concepts in Polymer Physics*, Cornell University Press, Ithaca, N.Y. (1956)
16. Szleifer, I. *J. Chem. Phys.*, **92**, 6940 (1990)
17. Schweizer, K.S.; Curro, J.G. *J. Chem. Phys.*, **149**, 105 (1990)
18. Eichinger, B.; Flory, P.J. *J. Trans. Faraday Soc.*, **64**, 2053 (1968)

Chapter 3

Modeling polymer solution thermodynamics

3.1. Introduction

In the preceding chapter a simple modification of the traditional Flory-Huggins theory, which took intramolecular screening effects (or same chain contacts) into account, was presented. In the following a natural extension to this work, in which free volume effects are also accounted for, through an equation of state model, will be presented.

Because of its simplicity the Flory-Huggins theory remains the starting point for many studies of polymer solutions and blends. The limitations of the model are well understood and are addressed in advanced treatments of the subject. However, this theoretical rigor usually comes with a degree of complexity that makes it inaccessible to those unfamiliar with the chosen mathematical tools. Accordingly, it would be interesting to see what simpler models can accomplish. Along these lines, a relatively simple model was introduced in the previous chapter. It is a modification to the Flory-Huggins theory that reproduces extremely well the composition dependence of χ (in the concentrated regime) and experimental spinodal curves.¹ This modification to the theory grew out of studies of hydrogen bonding in polymer blends, where in well-chosen systems the number of contacts between appropriate functional groups can be “counted” (this work is reviewed in reference 2). As a result, it was found that the fraction of same chain contacts

significantly exceeded that which would be expected on the basis of the usual assumption of a random mixing of segments. It was then assumed that in systems where the chain conformations remain essentially unperturbed (non-swollen) it could, in turn, be assumed that the average fraction of same chain contacts remained constant. In effect, a random mixing of chains is allowed for, but the segments in each of these chains see more of each other than if they were disconnected and randomly distributed through the system. In a hydrogen bonded blend it was determined experimentally that the fraction of same chain contact sites, which are labeled γ_s , is surprisingly large, about 0.27. Furthermore, using data from polystyrene/cyclohexane solutions near the θ -temperature, values of γ_s between 0.25 and 0.3 were determined, with the γ_s varying with molecular weight (M) according to:

$$\gamma_s = a - \frac{b}{M^{0.5}} \quad (1)$$

This latter result is in excellent agreement with simulations performed by Kumar (Painter et. al³), who determined that for chains on a cubic lattice γ_s had this functional form (as a result of both local and long range effects), with γ_s approaching values of about 0.38 for very large M . In real systems, where the coordination number is presumably larger than 6, smaller values of γ_s , would be anticipated, so the experimental values of ~ 0.25 - 0.30 are consistent with these calculations.

In the calculations of γ_s for θ -polymer solutions it was assumed that χ was a constant interaction parameter whose value was determined from a fit to the data. As

such, it must include entropic factors such as those involving free volume differences that are not included in simpler models. It would be interesting to see how the inclusion of what was phrased “screening effects”, the enhanced self-contact introduced by chain connectivity, would improve the agreement between theory and experiment that could be obtained with such models. In addition, it was decided to test whether the use of solubility and internal pressure parameters would now provide a reasonable agreement between theory and experiment. In the following the answers that were found to these questions will be presented.

3.2. Theory

3.2.1. The Flory-Orwoll-Vrij Equation of State

The Flory-Orwoll-Vrij⁴ (FOV) equation of state (EOS) model was chosen in this study. It is by no means the only model, but its simplicity allowed for the introduction of modifications in a very straightforward manner. The FOV-EOS is given by:

$$Z = Z^{comb.} (\gamma_g v^*)^{rN_c} (\tilde{v}^{1/3} - 1)^{3rN_c} \exp(-E_0 / kT) \quad (2)$$

where $Z^{comb.}$ is the combinatorial contribution to the partition function, γ_g is a geometric factor, \tilde{v} is the reduced volume:

$$\tilde{v} = \frac{v}{v^*} \quad (3)$$

where v^* is the reducing volume parameter, or the so-called hard-core volume, rN is the total number of segments, $3c$ is the number of external degrees of freedom per segment, similar to Prigogine's treatment⁵, k is the Boltzman's constant and T is the temperature.

The intermolecular energy, E_0 , is given by:

$$E_0 = -rNs\eta/2v \quad (4)$$

where s is the number of intermolecular contact sites per segment, η is a constant that characterizes the interaction energy between two neighboring sites. As seen above, equation 4 is identical with the expression for the intermolecular energy, E_0 , given by Flory et al.⁴. However, here the interactions will be accounted for in a different manner. This will become evident as the intermolecular energy, E_0 , is dealt with at a later stage.

The reducing parameters for the temperature, T^* , and the pressure, P^* , is introduced as:

$$T^* = s\eta/2ckv^* \quad (5)$$

$$P^* = s\eta/2v^{*2} \quad (6)$$

so that the partition function can be written as:

$$Z = Z^{comb.} (\gamma_g v^*)^{rNc} (\tilde{v}^{1/3} - 1)^{3rNc} \exp(rNc / \tilde{T}\tilde{v}) \quad (7)$$

If it is now assumed that the combinatorial contribution to the partition function is independent of volume, then the equation of state can be easily extracted from the above partition function using the following relationship:

$$-P = \left(\frac{\partial G}{\partial v} \right)_p = -RT \left(\frac{\partial \ln Z}{\partial v} \right)_p = -RT \left(\frac{1}{v^*} \right) \left(\frac{\partial \ln Z}{\partial \tilde{v}} \right)_{\tilde{P}} \quad (8)$$

to yield the following equation of state expressed in reduced variables:

$$\frac{\tilde{P}\tilde{v}}{\tilde{T}} = \frac{\tilde{v}^{1/3}}{\tilde{v}^{1/3} - 1} - \frac{1}{\tilde{T}\tilde{v}} \quad (9)$$

The thermal expansion coefficient, α , the compressibility coefficient, κ , and the thermal pressure coefficient, γ_{tpc} , can be expressed in reduced variables as:

$$\alpha T = \left(\frac{\tilde{T}}{\tilde{v}} \right) \left(\frac{\partial \tilde{v}}{\partial \tilde{T}} \right)_{\tilde{P}} \quad (10)$$

$$\kappa P = - \left(\frac{\tilde{P}}{\tilde{v}} \right) \left(\frac{\partial \tilde{v}}{\partial \tilde{P}} \right)_{\tilde{T}} \quad (11)$$

$$\frac{\gamma_{tpc} T}{P} = \left(\frac{\tilde{T}}{\tilde{P}} \right) \left(\frac{\partial \tilde{P}}{\partial \tilde{T}} \right)_{\tilde{v}} \quad (12)$$

At zero pressure the EOS reduces to:

$$\left(\tilde{v}^{1/3} - 1\right) = \frac{\alpha T}{3(1 + \alpha T)} \quad (13)$$

3.2.2. The Intermolecular Energy

The changes that were made to the FOV theory only involve the interaction energy term, E_0 , and the combinatorial term. The energy term is considered first. For a binary mixture of components 1 and 2 the FOV theory expresses the interaction energy in the following form:

$$E_0 = -\left(\frac{1}{v}\right)(A_{11}\eta_{11} + A_{12}\eta_{12} + A_{22}\eta_{22}) \quad (14)$$

where A_{11} , A_{22} and A_{12} represents the number of contact pairs between the respective species and η_{ij}/v represents the mean interaction energies associated with each of these pairs (η_{ij} is a constant that characterizes the interaction energy between segment i and j).

The number of contacts of species 1 and 2 respectively are given by:

$$2A_{11} + A_{12} = s_1 r_1 N_1 \quad (15)$$

$$2A_{22} + A_{12} = s_2 r_2 N_2 \quad (16)$$

where s_1 and s_2 are the number of intermolecular contact sites per segment for components 1 and 2, respectively, while N_1 and N_2 are the numbers of molecules of each component. When these are inserted in the expression for the intermolecular energy, E_0 , it leads to:

$$E_0 = -\left(\frac{1}{2v}\right)(s_1 r_1 N_1 \eta_{11} + s_2 r_2 N_2 \eta_{22} - A_{12} \Delta \eta) \quad (17)$$

where:

$$\Delta \eta = \eta_{11} + \eta_{22} - 2\eta_{12} \quad (18)$$

Unlike the simple form of the Flory-Huggins theory, the FOV theory accounts for the number of contacts lost through covalent linkages. If the subscripts “ p ” and “ s ” are now used to designate polymer and solvent, respectively, the number of contacts allowed to a chain consisting of r_p segments is given by Flory as:

$$r_p s_p = r_p s_m + s_e \quad (19)$$

where s_p is the mean number of external contacts per segment, s_m is the number of external contacts per internal segment and s_e is the number of external contacts per chain end. To be consistent with previous nomenclature, this equation is written in a different form:

$$r_p s_p' = r_p (s_p - 2s_e) + 2s_e = r_p s_p [1 - \gamma_l] \quad (20)$$

where s_p' are the number of external contacts allowed to a segment, $(s_p - 2s_e)$ describes the number of external contacts for an internal segment (2 chain ends per chain) and $2s_e$ is the number of contacts for chain ends and the parameter γ_l defined as:

$$\gamma_l = \frac{2s_e}{s_p} \left(1 - \frac{1}{r_p} \right) \quad (21)$$

describes the fraction of self contacts, caused by covalent linkage of the segments. A similar approach was also employed by Koningsfeld and Kleintjens⁶, except γ_l was treated as an adjustable parameter. This corresponds to a similar parameter that was introduced in the lattice model used in previous work¹:

$$\gamma_l = \frac{2}{z} \left(1 - \frac{1}{r_p} \right) \quad (22)$$

Here z is the coordination number of the lattice. In this work a coordination number 9 was chosen, based on the average value found for a random close packing of spheres, thereby fixing the value of γ_l (assuming a large r_p).

It is now assumed that the polymer chains bend back on themselves, through both local and long range effects such that additional contacts between other chains and solvent are excluded. This fraction of excluded (screened) polymer contact sites is

designated γ_s (note that each same chain contact excludes two contact sites). A similar factor was included in Huggins⁷ original theory but has been neglected in most subsequent treatments.

The number of external contacts for a chain is then given by:

$$r_p s_p'' = (1 - \gamma_s) r_p s_p' = r_p s_p [1 - \gamma_l][1 - \gamma_s] = r_p s_p [1 - \gamma] \quad (23)$$

where:

$$[1 - \gamma] = [1 - \gamma_l][1 - \gamma_s] \quad (24)$$

In an earlier work¹ it was assumed that γ_s is constant over the entire concentration range. This is only reasonable if the chain dimensions remain relatively unperturbed, so only data obtained from solutions near the Flory θ -temperature were considered. Here initially the same will be done, but then the modifications that would be needed to describe polymers in good solvents will be considered.

With these definitions the number of contact pairs can now be expressed as:

$$2N_{ss} + N_{sp} = N_s r_s s_s = n_s s_s \quad (25)$$

$$2N_{pp} + N_{ps} = N_p r_p s_p' = n_p r_p s_p (1 - \gamma_l) \quad (26)$$

so the expression for the interaction energy, E_0 , becomes:

$$E_0 = -\left(\frac{1}{2\nu}\right)(n_s s_s \eta_{ss} + n_p r_p s_p (1 - \gamma_l) \eta_{pp} - N_{sp} \Delta \eta) \quad (27)$$

where:

$$\Delta \eta = \eta_{ss} + \eta_{pp} - 2\eta_{sp} \quad (28)$$

The number of solvent-polymer contacts, N_{sp} , depends on both γ_l and γ_s through the combined parameter γ , and it was previously shown that:

$$N_{sp} = n_s s_s \frac{(1 - \gamma) \phi_p}{1 - \gamma \phi_p} \quad (29)$$

If a “bare” (concentration independent) interaction parameter, χ_{sp}^0 , is now defined as:

$$\chi_{sp}^0 = \frac{s_s \Delta \eta}{2\nu RT} \quad (30)$$

the interaction energy term, E_0 , becomes:

$$-\frac{E_0}{rN} = \phi_s \varepsilon_{ss} + \phi_p (1 - \gamma_l) \varepsilon_{pp} - \frac{(1 - \gamma) \phi_s \phi_p}{1 - \gamma \phi_p} \chi_{sp}^0 RT \quad (31)$$

where:

$$\varepsilon_{ss} = \left(\frac{s_s \eta_{ss}}{2\nu} \right) \quad (32)$$

$$\varepsilon_{pp} = \left(\frac{s_p \eta_{pp}}{2\nu} \right) \quad (33)$$

It then follows that the energy of mixing, ΔE_{mix} is given by:

$$\Delta E_{mix} = n_s p_s^* \nu^* \left(\frac{1}{\tilde{\nu}} - \frac{1}{\tilde{\nu}_s} \right) + n_p r_p p_p^* \nu^* \left(\frac{1}{\tilde{\nu}} - \frac{1}{\tilde{\nu}_p} \right) - n_s \frac{(1-\gamma)\phi_p}{1-\gamma\phi_p} \chi_{sp}^0 RT \quad (34)$$

3.2.3. The Combinatorial Term

In the FOV model the combinatorial term is taken directly from the Flory-Huggins theory. However, the use of surface site fractions introduces additional terms into the combinatorial entropy, as in the lattice treatments of Huggins⁷ and Guggenheim⁸. The inclusion of an intrachain contact term γ_s is also readily incorporated into lattice models as long as it is assumed that the chains maintain their ideal dimensions. A more rigorous theory would require a relationship between γ_s and chain dimensions, which is not presently available. With the assumption of a constant (average) value of γ_s , the free energy now becomes:

$$\frac{\Delta F_m^{comb.}}{(rN)RT} = \phi_s \ln \phi_s + \frac{\phi_p}{r_p} \ln \phi_p - \frac{1-\gamma\phi_p}{\gamma} \ln(1-\gamma\phi_p) + \frac{(1-\gamma)\phi_p}{\gamma} \ln(1-\gamma) \quad (35)$$

The last two “excess” terms (compared to the Flory-Huggins treatment) result in quite small contributions to the chemical potential over most of the composition range. However, experimental measurements of χ are usually based on fitting osmotic pressure or vapor pressure data to the Flory-Huggins theory. As a result, these terms contribute to the entropic part of the Flory-Huggins interaction parameter, χ_s , through a “connectivity” term:

$$\chi_s^{con} = -\frac{1}{\phi_p^2} \left[\frac{1}{\gamma} \ln(1-\gamma\phi_p) + \phi_p \right] \quad (36)$$

The $\frac{1}{\phi_p^2}$ factor then results in values of χ_s that are of the order of 0.2-0.3, which cannot be neglected.

3.2.4. The c-parameter

By comparing the definition of the reducing parameters T^* and P^* in equation 5 and 6 respectively an expression can be obtained for the c-parameter:

$$c = \frac{P^* v^*}{kT^*} \quad (37)$$

From the definition of the thermal pressure coefficient, γ_{tpc} :

$$\frac{\gamma_{tpc} T}{P} = \left(\frac{\tilde{T}}{\tilde{P}} \right) \left(\frac{\partial \tilde{P}}{\partial \tilde{T}} \right)_{\tilde{v}} \quad (38)$$

it can be deduced that:

$$P^* = \gamma_{tpc} T \tilde{v}^2 \quad (39)$$

which when inserted in equation (37) gives:

$$c = \frac{P^* v^*}{kT^*} = \frac{\gamma_{tpc} T \tilde{v} v}{kT^*} = \left(\frac{\gamma_{tpc} v}{k} \right) \tilde{v} \tilde{T} \quad (40)$$

At zero pressure equation 9 can be rewritten as:

$$\tilde{T} = \frac{(\tilde{v}^{1/3} - 1)}{\tilde{v}^{4/3}} \Leftrightarrow \tilde{T} \tilde{v} = \frac{(\tilde{v}^{1/3} - 1)}{\tilde{v}^{1/3}} \quad (41)$$

with a few manipulations of equation 13 it becomes:

$$\tilde{v}^{1/3} = \left(\frac{3 + 4\alpha T}{3(1 + \alpha T)} \right) \quad (42)$$

so by combining equations 12, 40 and 41 the following expression is obtained:

$$\frac{(\tilde{v}^{1/3} - 1)}{\tilde{v}^{1/3}} = \frac{\frac{\alpha T}{3(1 + \alpha T)}}{\left(\frac{\alpha T + 3(1 + \alpha T)}{3(1 + \alpha T)} \right)} = \frac{\alpha T}{(3 + 4\alpha T)} \quad (43)$$

so that the expression for the c-parameter becomes:

$$c = \left(\frac{\gamma_{ipc} v}{k} \right) \tilde{v} \tilde{T} = \left(\frac{\gamma_{ipc} v}{k} \right) \frac{\alpha T}{(3 + 4\alpha T)} \quad (44)$$

which is identical to the expression in Flory et al.⁴.

3.2.5. Mixing Rules

Several mixing rules were considered for the reduced volume of the mixture, \tilde{v} , and the reduced temperature of the mixture, \tilde{T} , respectively. However, a simple linear mixing rule was chosen:

$$\tilde{v} = \sum_{i=1}^N \theta_i \tilde{v}_i = \theta_s \tilde{v}_s + \theta_p \tilde{v}_p \quad (45)$$

$$\tilde{T} = \sum_{i=1}^N \theta_i \tilde{T}_i = \theta_s \tilde{T}_s + \theta_p \tilde{T}_p \quad (46)$$

where θ_i is the surface site fraction of component i :

$$\theta_s = \frac{\phi_s}{(1 - \gamma_l \phi_p)} \quad \text{and} \quad \theta_p = \frac{(1 - \gamma_l) \phi_p}{(1 - \gamma_l \phi_p)} \quad (47)$$

3.2.6. Internal Pressure vs. Cohesive Energy Density

The internal pressure P^{ip} is a measure of the change in the internal energy when undergoing a very small isothermal expansion:

$$P^{ip} = \left(\frac{\partial U}{\partial V} \right)_T \quad (48)$$

Hildebrand⁹ concluded early on that the solubility of a given solute was determined by the internal pressure of the solvent. The internal pressure, P^{ip} , can be obtained from the thermodynamic equation of state:

$$P^{ip} = \left(\frac{\partial U}{\partial V} \right)_T = T \left(\frac{\partial P}{\partial T} \right)_V - P \quad (49)$$

where $\left(\frac{\partial P}{\partial T} \right)_V$ is the thermal pressure coefficient, γ_{tpc} . In most cases the atmospheric pressure P is negligible compared to $T \left(\frac{\partial P}{\partial T} \right)_V$, so the internal pressure, P^{ip} , can be determined from the thermal pressure coefficient, γ_{tpc} , which in turn can be determined from the coefficient of thermal expansion, α , and the coefficient of isothermal compressibility, κ :

$$\gamma_{tpc} = \left(\frac{\partial P}{\partial T} \right)_V = \frac{\alpha}{\kappa} \quad (50)$$

Difficulties in determining the internal pressure and the lack of such data led Hildebrand¹⁰ to show that the internal pressure for non-polar liquids was related to the cohesive energy density (*c.e.d.*) by:

$$P^{ip} = m(c.e.d.) \quad (51)$$

where the quantity m approaches unity for non-polar liquids, and where the *c.e.d.* is given by:

$$c.e.d. = \left(\frac{\Delta U^v}{v} \right) \quad (52)$$

where ΔU^v is the energy of vaporization:

$$\Delta U^v = \Delta H^v - RT \quad (53)$$

and where ΔH^v is the latent heat of vaporization.

Later on Hildebrand¹¹ introduced the solubility parameter δ , which was defined as:

$$\delta = (c.e.d.)^{1/2} = \left(\frac{\Delta U^v}{v} \right)^{1/2} \quad (54)$$

in recognition of the importance of the *c.e.d.* when determining solubility.

The cohesive energy density, *c.e.d.*, can be determined from the latent heat of vaporization, ΔH^v :

$$c.e.d. = \left(\frac{\Delta U^v}{v} \right) = \frac{\Delta H^v - RT}{M/\rho} \quad (55)$$

where M is the molecular weight and ρ is the density of a liquid at a temperature T .

Although heats of vaporization are relatively easily obtained for smaller molecules from vapor pressure data, that is not the case for high molecular weight polymers for obvious reasons. For polymers one therefore has to make an estimation of the *c.e.d.* based on an indirect measurement such as e.g. a comparative swelling experiment.

Many researchers have assumed that the quantity m in equation 51 equals unity for all liquids, and with this in mind it is easy to see why *c.e.d.'s* have been used interchangeably with the internal pressures when determining the solubility parameter. However, several authors, including Allen et al.^{12,13}, have argued that the use of internal pressures rather than *c.e.d.'s* might be preferable when determining the solubility parameter of a polymer. A few examples of how to obtain internal pressure data for various polymers, when only PVT-data are available, are given in Appendix D.

3.2.7. The Model

The expressions for the contribution of combinatorial and energy terms to the free energy can now be combined with those from free volume, which is labeled $F^{residual}$, to give:

$$\begin{aligned}
\frac{\Delta F_m'}{RT} &= \frac{\Delta F_m^{comb.}}{(rN)RT} + \frac{\Delta F_m^{residual}}{(rN)RT} + \frac{\Delta F_m^{energetic}}{(rN)RT} \\
&= \phi_s \ln \phi_s + \frac{\phi_p}{r_p} \ln \phi_p - \frac{1-\gamma\phi_p}{\gamma} \ln(1-\gamma\phi_p) + \frac{(1-\gamma)\phi_p}{\gamma} \ln(1-\gamma) \\
&\quad + 3\phi_s c_s \ln \left(\frac{\tilde{v}_s^{1/3} - 1}{\tilde{v}^{1/3} - 1} \right) + 3\phi_p c_p \ln \left(\frac{\tilde{v}_p^{1/3} - 1}{\tilde{v}^{1/3} - 1} \right) + \frac{\phi_s p_s^* v^*}{RT} \left(\frac{1}{\tilde{v}_s} - \frac{1}{\tilde{v}} \right) \\
&\quad + \frac{\phi_p p_p^* v^*}{RT} \left(\frac{1}{\tilde{v}_p} - \frac{1}{\tilde{v}} \right) + \frac{(1-\gamma)\phi_s \phi_p}{1-\gamma\phi_p} \chi_{sp}^0
\end{aligned} \tag{56}$$

The chemical potential for species i , $\Delta\mu_i$, can then be found from:

$$\frac{\Delta\mu_i}{RT} = \left(\frac{d(\Delta F_m / RT)}{dn_i} \right)_{T,P,n_{j \neq i}} + \left(\frac{\partial(\Delta F_m / RT)}{\partial \tilde{v}} \right)_{T,P,n_{j \neq i}} \left(\frac{\partial \tilde{v}}{\partial n_i} \right)_{T,P,n_{j \neq i}} \tag{57}$$

As Flory et al.^{4b} point out, the second term only makes a contribution of magnitude $Pv^*(\tilde{v} - \tilde{v}_s)$ and can therefore be neglected at ordinary pressures. For the solvent, equation 57 therefore reduces to:

$$\frac{\Delta\mu_s}{RT} = \left(\frac{d(\Delta F_m / RT)}{dn_s} \right)_{T,P,n_p} \tag{58}$$

And from equations (56) and (58) respectively, one gets:

$$\begin{aligned} \frac{\Delta\mu_s}{RT} &= \ln \phi_s + \phi_p \left(1 - \frac{1}{r_p}\right) + \frac{(1-\gamma)^2 \phi_p^2}{(1-\gamma\phi_p)^2} \chi_{sp}^0 - \frac{1}{\gamma} \ln(1-\gamma\phi_p) - \phi_p \\ &+ 3c_s \ln\left(\frac{\tilde{v}_s^{1/3} - 1}{\tilde{v}^{1/3} - 1}\right) + \frac{p_s^* v^*}{RT} \left(\frac{1}{\tilde{v}_s} - \frac{1}{\tilde{v}}\right) \end{aligned} \quad (59)$$

Now, if this expression is compared to the classical Flory-Huggins expression:

$$\frac{\Delta\mu_s}{RT} = \ln \phi_s + \phi_p \left(1 - \frac{1}{r_p}\right) + \phi_p^2 \chi^{FH} \quad (60)$$

it can be seen that:

$$\begin{aligned} \phi_p^2 \chi^{FH} &= \frac{(1-\gamma)^2 \phi_p^2}{(1-\gamma\phi_p)^2} \chi_{sp}^0 - \frac{1}{\gamma} \ln(1-\gamma\phi_p) - \phi_p \\ &+ 3c_s \ln\left(\frac{\tilde{v}_s^{1/3} - 1}{\tilde{v}^{1/3} - 1}\right) + \frac{p_s^* v^*}{RT} \left(\frac{1}{\tilde{v}_s} - \frac{1}{\tilde{v}}\right) \end{aligned} \quad (61)$$

or:

$$\chi^{FH} = \frac{(1-\gamma)^2}{(1-\gamma\phi_p)^2} \chi_{sp}^0 - \frac{1}{\phi_p^2} \left[\frac{1}{\gamma} \ln(1-\gamma\phi_p) + \phi_p - 3c_s \ln\left(\frac{\tilde{v}_s^{1/3} - 1}{\tilde{v}^{1/3} - 1}\right) - \frac{p_s^* v^*}{RT} \left(\frac{1}{\tilde{v}_s} - \frac{1}{\tilde{v}}\right) \right] \quad (62)$$

The interaction parameter χ^{FH} can now be split into an exchange energy term, χ^E , and an “excess” term, χ^{exc} , to get:

$$\chi^{FH} = \chi^E + \chi^{exc} \quad (63)$$

where the interaction energy contribution, χ^E , to χ^{FH} is defined as:

$$\chi^E = \frac{(1-\gamma)^2}{(1-\gamma\phi_p)^2} \chi_{sp}^0 \quad (64)$$

The parameter χ_{sp}^0 can be calculated in several different ways. If the traditional solubility parameters, determined from cohesive energy densities, are used, the classical expression is obtained:

$$\chi_{sp}^0 = \frac{v}{RT} (\delta_s - \delta_p)^2 \quad (65)$$

where v is the molar volume of the mixture. Alternatively, if the assumption of additivity of internal pressures is adopted, the expression becomes:

$$\chi_{sp}^0 = \frac{v}{RT} \left((P_s^{ip})^{1/2} - (P_p^{ip})^{1/2} \right)^2 \quad (66)$$

where P_i^{ip} is the internal pressure of species i .

The “excess” term, χ^{exc} , to χ^{FH} is defined as:

$$\chi^{exc} = -\frac{1}{\phi_p^2} \left[\frac{1}{\gamma} \ln(1 - \gamma\phi_p) + \phi_p - 3c_s \ln\left(\frac{\tilde{v}_s^{1/3} - 1}{\tilde{v}^{1/3} - 1}\right) - \frac{c_s}{\tilde{T}_s} \left(\frac{1}{\tilde{v}_s} - \frac{1}{\tilde{v}} \right) \right] \quad (67)$$

3.3. Results and Discussion

Initially four systems will be considered; polystyrene-cyclohexane, using the experimental data reported by Kriegbaum and Geymer¹⁴; polystyrene-ethylbenzene, using the experimental data reported by Höcker & Flory¹⁵; polyisobutylene-benzene, using the experimental data reported by Eichinger & Flory¹⁶; and polystyrene-methylethylketone, using the experimental data reported by Flory & Höcker¹⁷. The data for all four polymer solutions were obtained near the θ -temperature, so the assumption of a constant γ_s over the entire composition range would appear to be reasonable. It will also be assumed that the value of γ_s is the same, 0.3, for all four solutions. Simulations indicate that the value of γ_s depends on both local and long range effects^{2,3} and the former should depend upon chemical structure. However, part of the aim here is to see how well the data, with a minimum or even no adjustable parameters, can be reproduced, so this requires that some assumptions are made.

First the polystyrene-cyclohexane system is considered. The values of the Flory-Huggins χ , χ^{FH} , determined by Kriegbaum and Geymer¹⁴, are shown in figure 3.1.

Calculated values of this parameter were obtained using equation 63. The EOS contributions were calculated following Flory et al.⁴ and χ_{sp}^0 was calculated using solubility parameters. The parameters used in these and subsequent calculations are listed in table 3.1. Given the limitations of solubility parameters, the calculated values of χ^{FH} are surprisingly close to, but consistently smaller than, the experimental values across the composition range. As would be expected from the work of Flory and co-workers^{4,15-21}, the major contribution to the calculated value of χ is from the excess term, as also shown in figure 3.1.

If internal pressures are used to calculate χ_{sp} , an excellent agreement between calculated and experimental values of χ^{FH} is obtained over much of the concentration range, as shown in figure 3.2. The deviations at very high polymer concentrations are probably due to the fact that the system is now glassy and the volume parameters used to calculate the EOS terms no longer apply.

If a low T_g polymer is now considered, polyisobutylene, in benzene, the composition dependence of χ is again reasonably well reproduced by solubility parameters across the composition range, as shown in figure 3.3. This time predicting values which are a little higher than those determined by experiments. An opposite effect is seen when internal pressures are used to calculate χ_{sp} , as is shown in figure 3.4, although in this case the deviations from experimental data are far more pronounced, because of the very small difference in internal pressures between the two components.

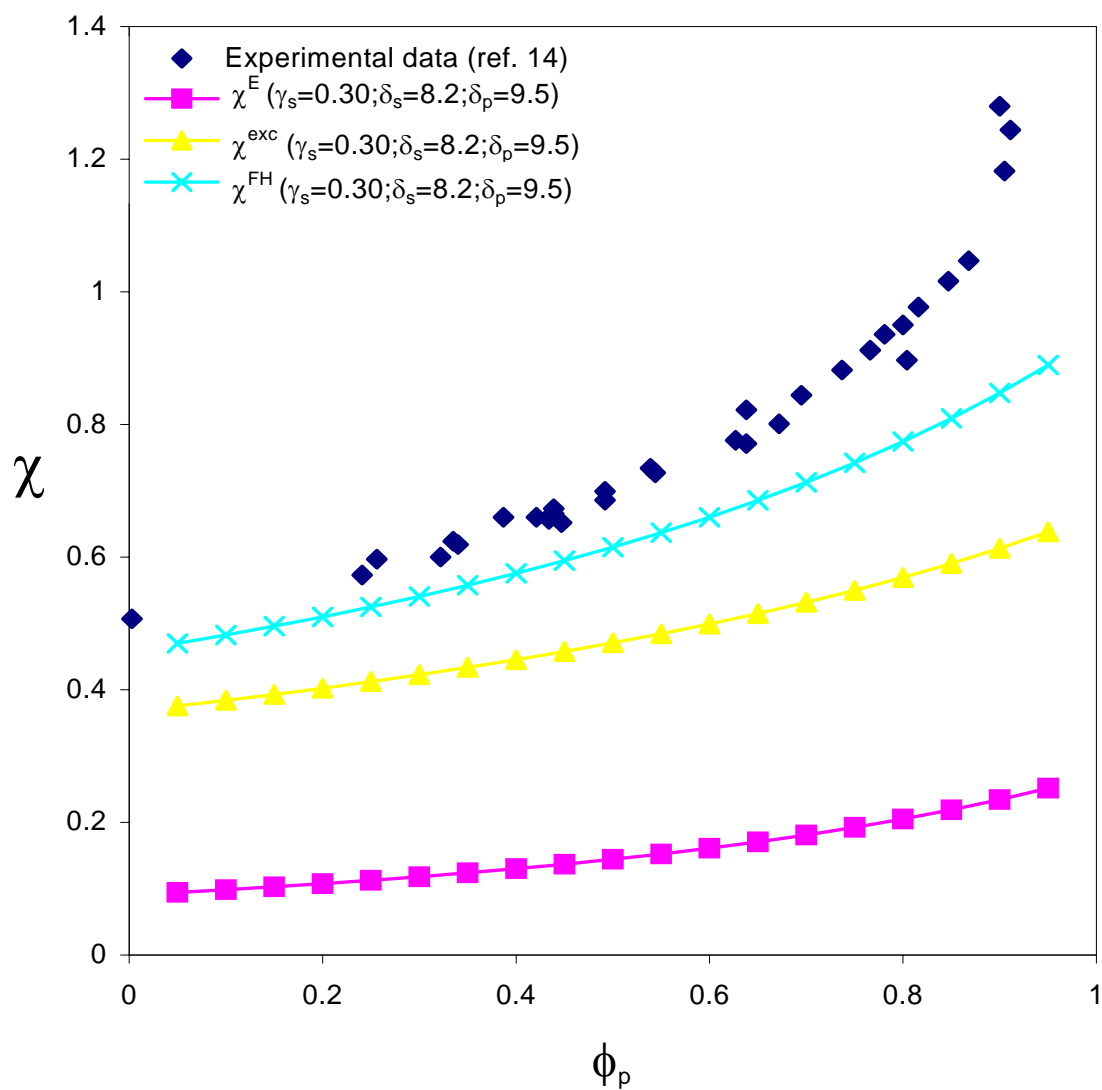


Figure 3.1. Comparison of experimental data and calculated values of χ^{FH} for PS (Mw=51,000)-cyclohexane at 34 °C obtained using solubility parameters in a newly developed model.

Table 3.1. Pure component parameters for various polymer-solvent systems.

System	Temperature (°C)	r_p	α_s deg. ⁻¹	α_p deg. ⁻¹	v_s cm ³ /mole	v_p cm ³ /mole	δ_s (cal/cm ³) ^{1/2}	δ_p (cal/cm ³) ^{1/2}	P_s^{ip} cal/cm ³	P_p^{ip} cal/cm ³
PS-cyclohexane	34	490	1.248*10 ⁻³ ^a	5.73*10 ⁻⁴ ^b	110.1 ^a	97.7 ^b	8.2	9.5	77.8 ^c	110 ^d
PS-MEK	50	490	1.389*10 ⁻³ ^e	5.74*10 ⁻⁴ ^e	93.3 ^e	98.6 ^e	9.14	9.5	81.7 ^c	110 ^d
PIB-benzene	25	713	1.223*10 ⁻³ ^f	5.55*10 ⁻⁴ ^g	89.4 ^f	61.2 ^g	9.2	7.2	90.5 ^c	81.1 ^h
PIB-cyclohexane	25	713	1.217*10 ⁻³ ⁱ	5.55*10 ⁻⁴ ^g	108.7 ⁱ	61.2 ^g	8.2	7.2	77.8 ^c	81.1 ^h
Natural Rubber-benzene	25	587	1.223*10 ⁻³ ^f	6.54*10 ⁻⁴ ^f	89.4 ^f	74.6 ^f	9.2	8	90.5 ^c	88 ^d

(a) linear interpolation from ref. 18, (b) linear interpolation from ref. 17, (c) values at 20 °C from ref. 12, (d) values at 20 °C from ref. 13, (e) from ref. 17, (f) from ref. 21, (g) from ref. 16, (h) calculated from $P_p^{ip} = P^* / \bar{v}^2$ with data from ref. 16, (i) from ref. 20.

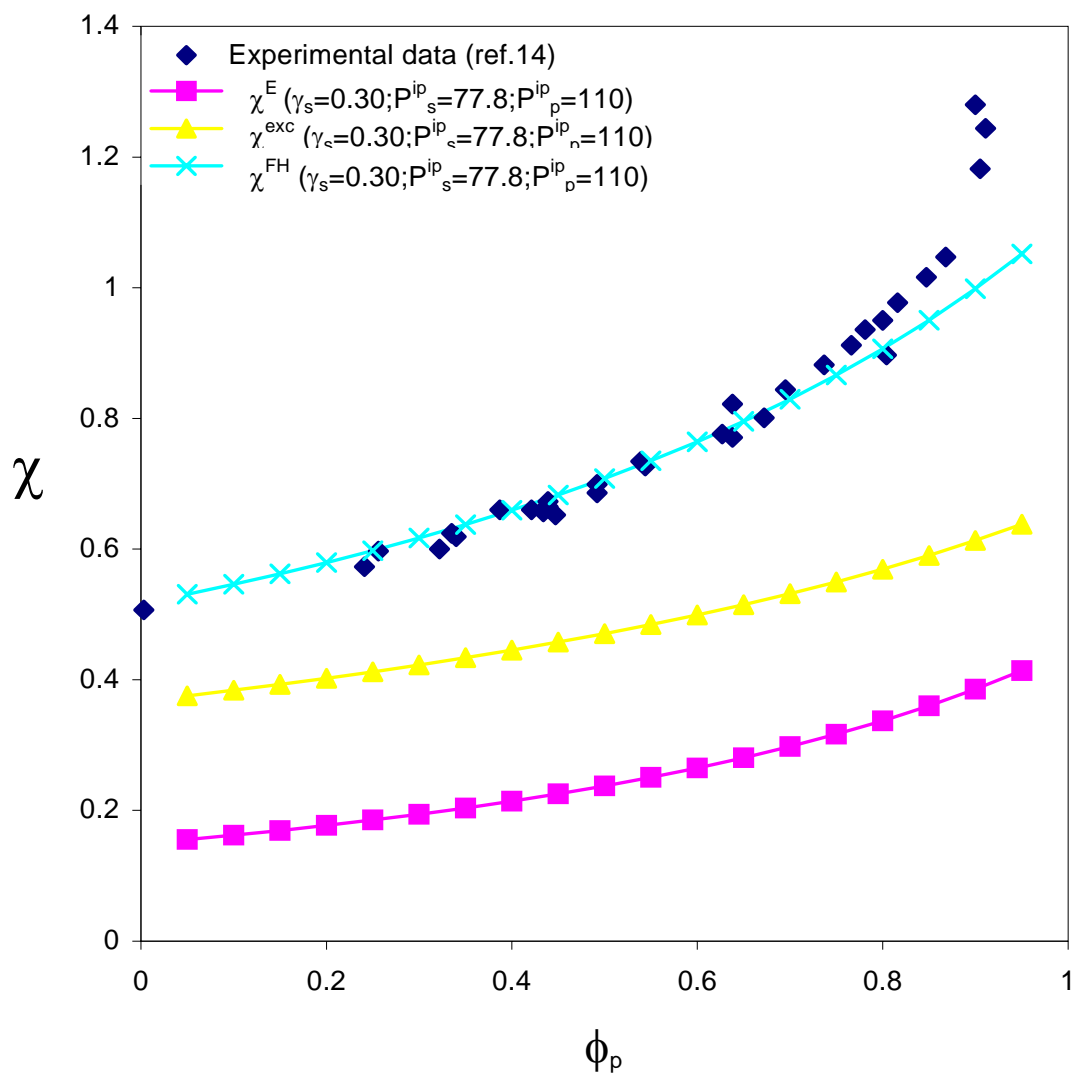


Figure 3.2. Comparison of experimental data and calculated values of χ^{FH} for PS (Mw=51,000)-cyclohexane at 34°C obtained using internal pressures in a newly developed model.

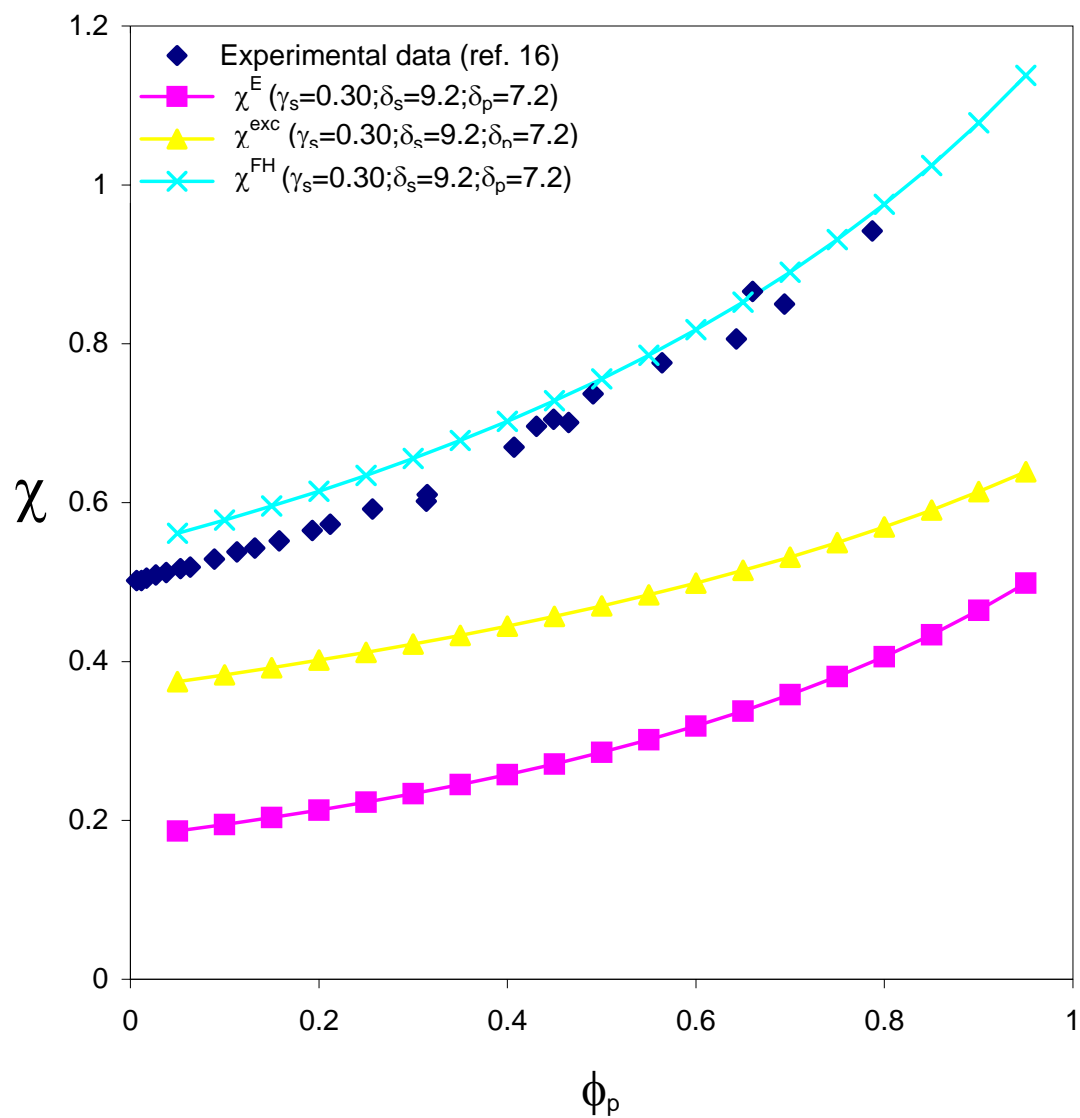


Figure 3.3. Comparison of experimental data and calculated values of χ^m for PIB (Mw=40,000)-benzene at 25°C obtained using solubility parameters in a newly developed model.

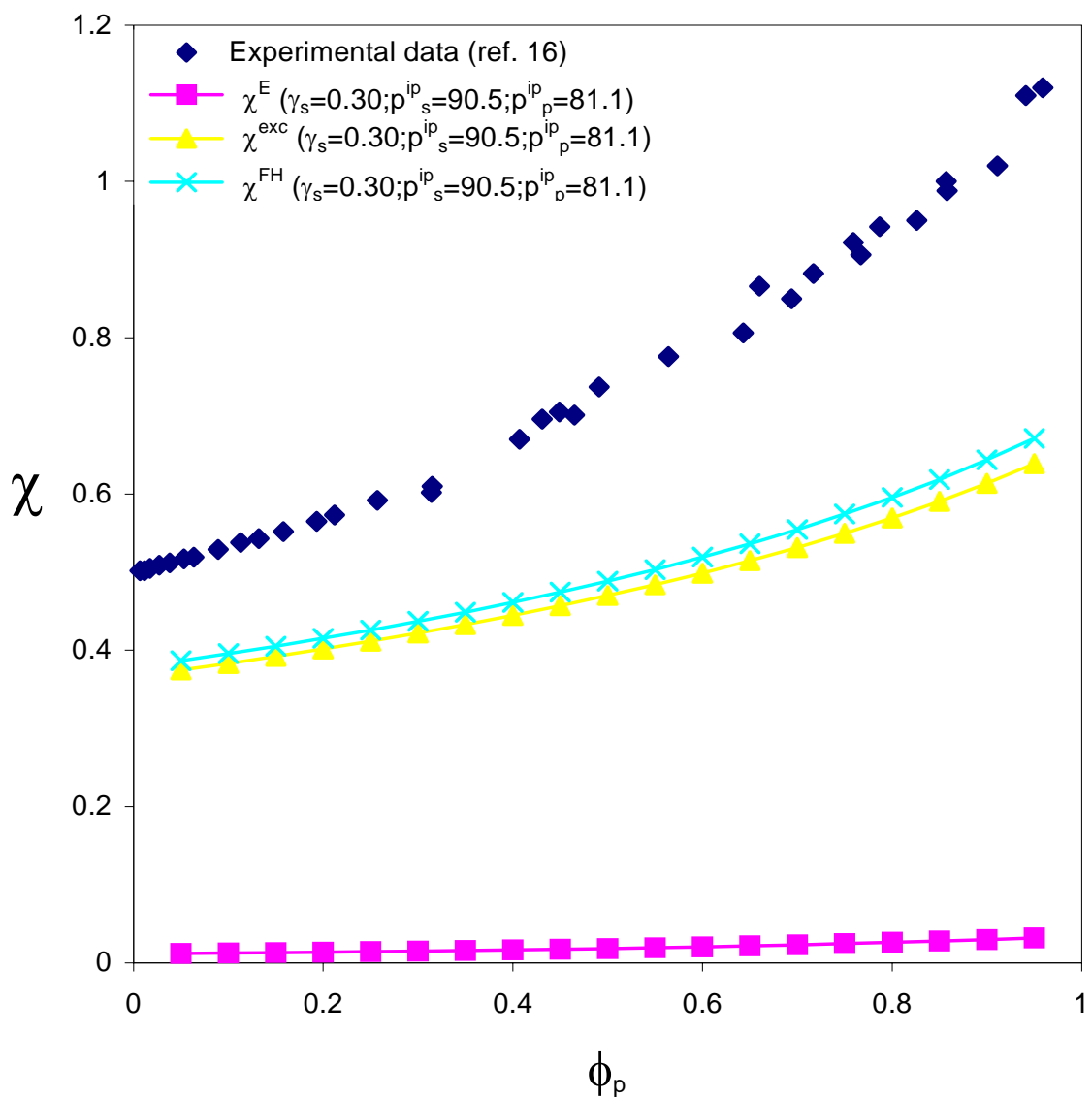


Figure 3.4. Comparison of experimental data and calculated values of χ for PIB (Mw=40,000)-benzene at 25°C obtained using internal pressures in a newly developed model.

Returning the focus to polystyrene, results obtained for the polystyrene-ethylbenzene system are shown in figures 3.5 and 3.6. As in the polystyrene-cyclohexane system, the interaction parameter is underestimated when solubility parameters are used to calculate χ_{sp} , as it can be seen in figure 3.5. However, when internal pressures are used, the predicted values are consistently higher over the entire concentration range.

The results obtained for the system polystyrene-MEK are shown in figures 3.7 and 3.8. Here some significant deviations would be anticipated, because MEK is a polar solvent and this leads to deviations from the geometric mean assumption implicit in using equations 33 and 34. Unsurprisingly, solubility parameters do a poor job of predicting the values of χ_{sp} necessary to obtain an agreement between theory and experiment, as shown in figure 3.7. Furthermore, as in the PIB-benzene system, the internal pressures are so close that the energetic contribution to χ , χ^E , is negligible, and as a consequence a good agreement between the model and experimental data is not obtained, as seen in figure 3.8.

The attention is now directed to polymers in good solvents. Experimental data for the system natural rubber-benzene are shown in figures 3.9 and 3.10, together with the values of χ^{FH} determined from the model. It can be seen that although solubility parameters and internal pressures give a reasonable agreement with experimental values of χ at low and high concentrations, respectively ($\phi_p < 0.2$, $\phi_p > 0.8$), the curvature of the composition dependence is not well reproduced at all.

Data from other polymer/good solvent systems will be presented shortly, but in general what was found when examining data from the literature was that in good solvents χ does not depend as strongly on concentration as it does in theta solvents and the curves are in general “flatter”. This change in composition dependence of χ is most

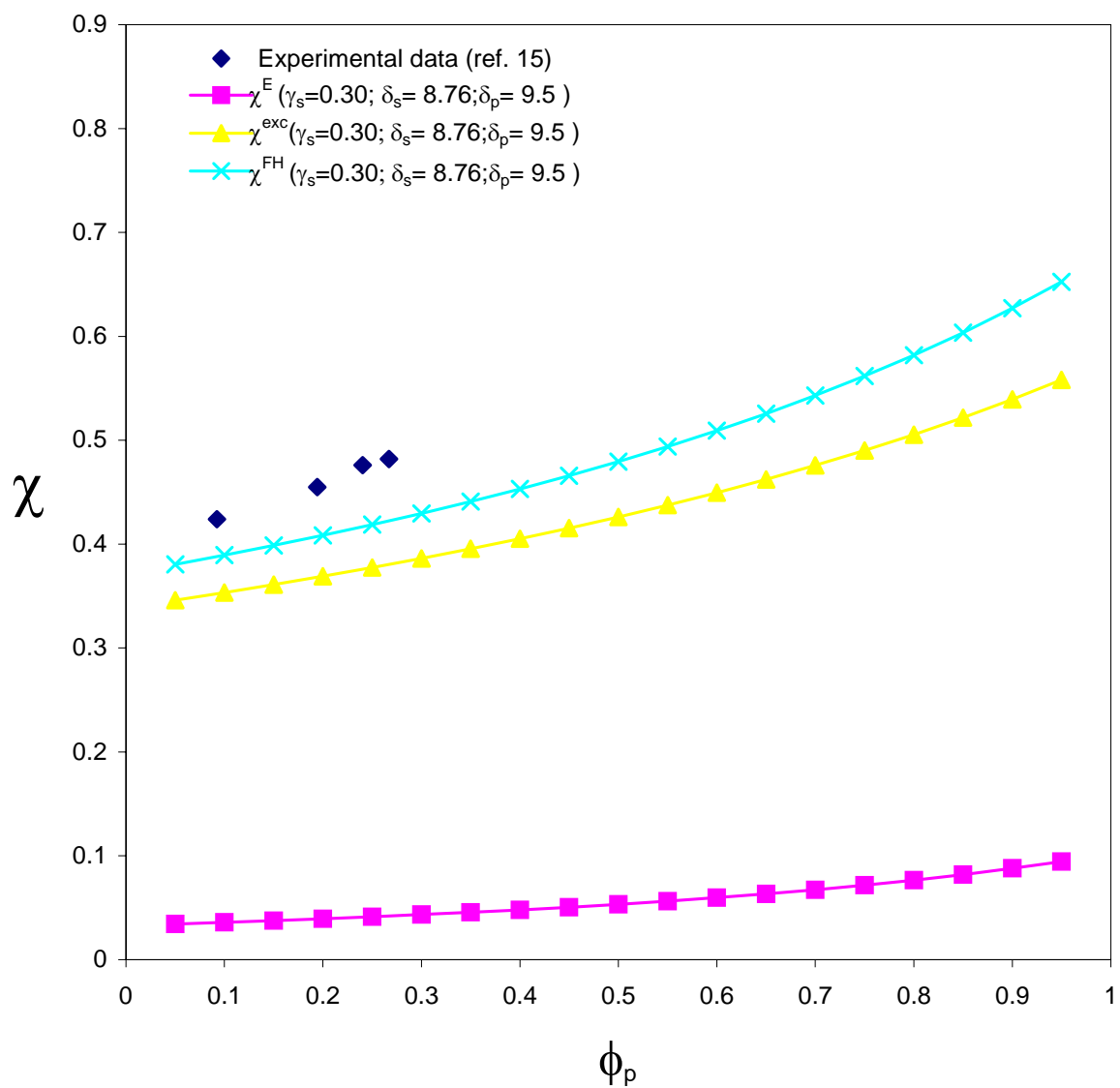


Figure 3.5. Comparison of experimental data and calculated values of χ^{FH} for PS (Mw=51,000)-Ethylbenzene at 35°C obtained using solubility parameters in a newly developed model.

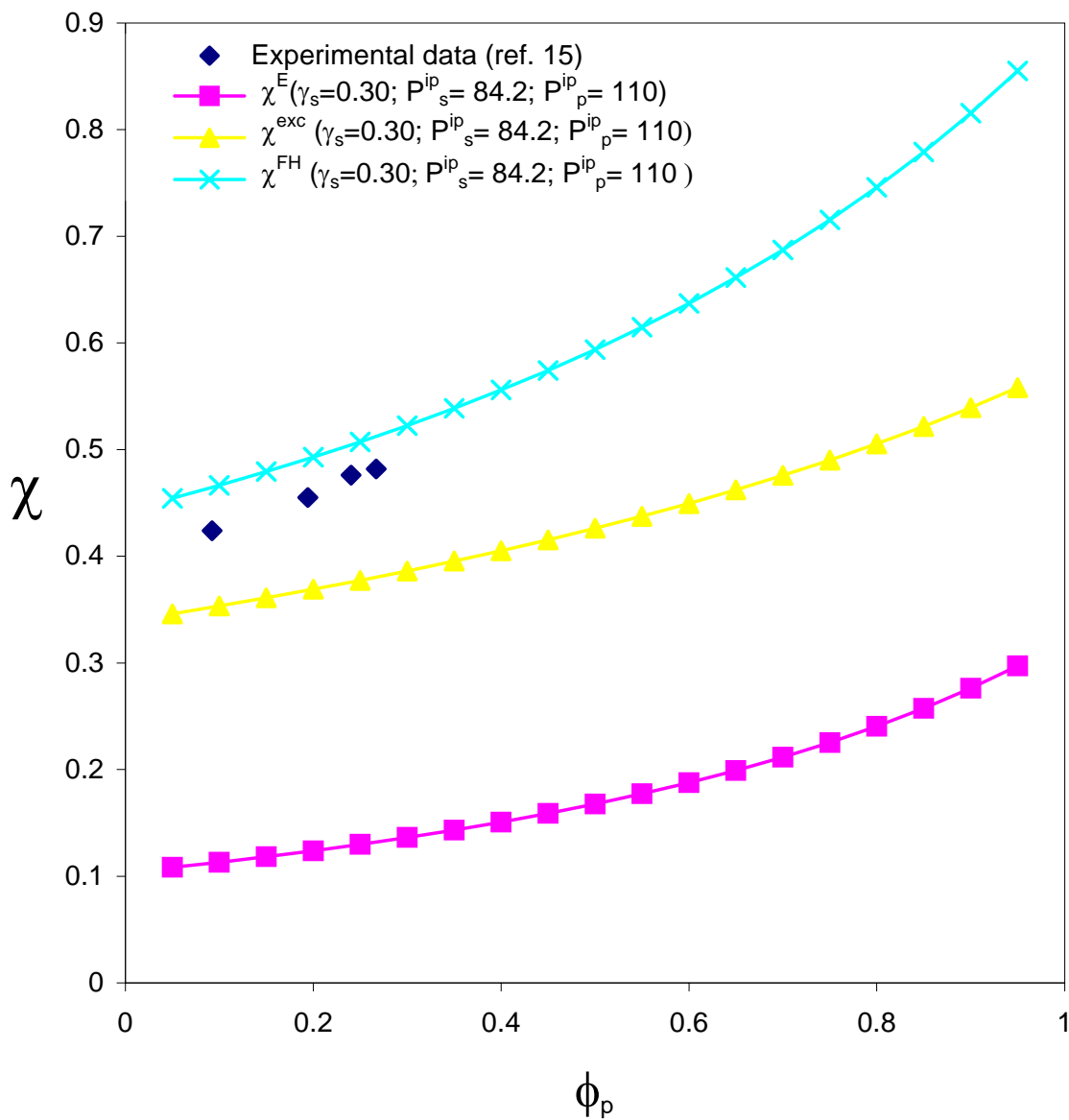


Figure 3.6. Comparison of experimental data and calculated values of χ^{FH} for PS (Mw=51,000)-Ethylbenzene at 35°C obtained using internal pressures in a newly developed model.

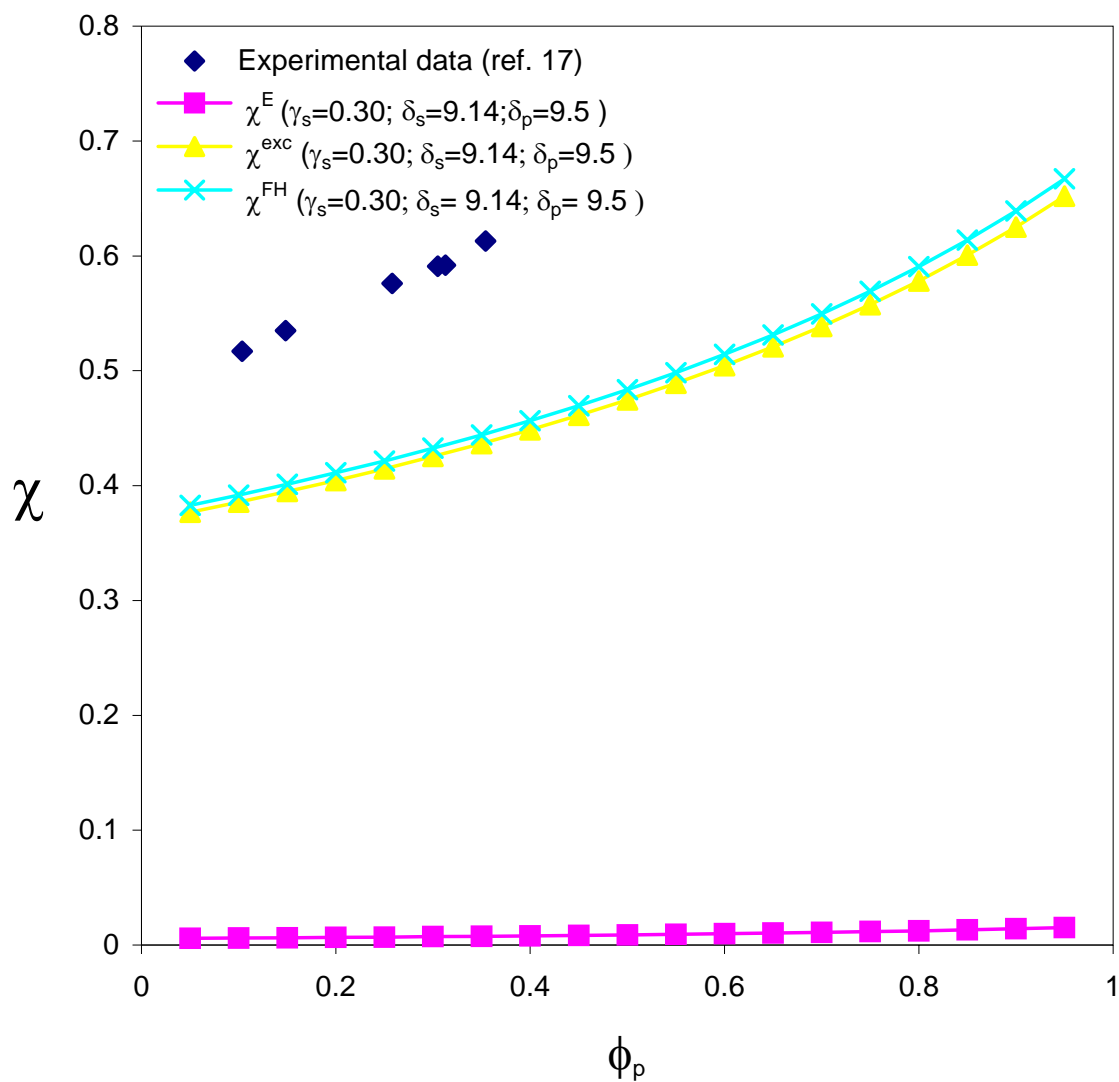


Figure 3.7. Comparison of experimental data and calculated values of χ^m for PS (Mw=51,000)-MEK at 50°C obtained using solubility parameters in a newly developed model.

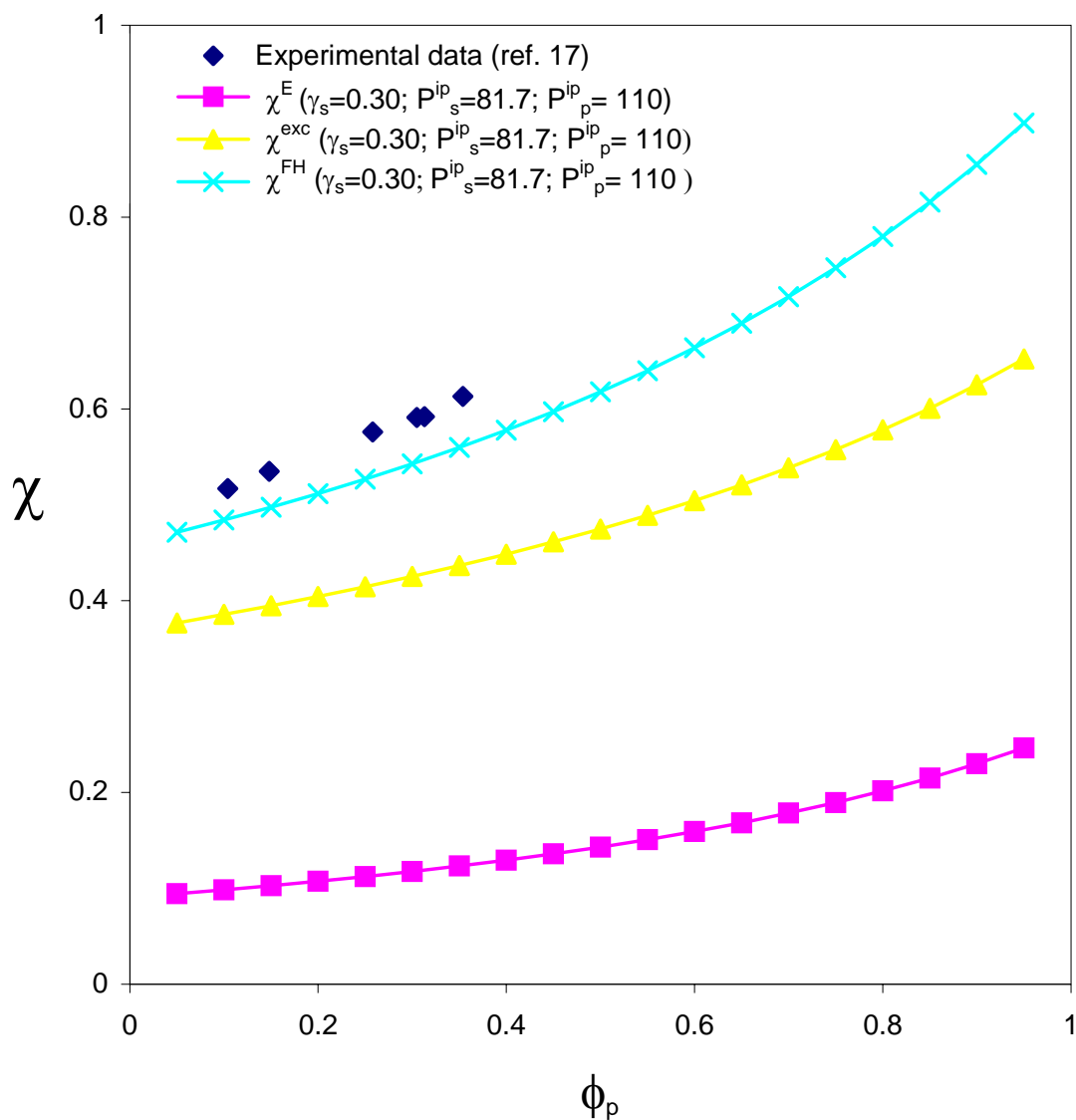


Figure 3.8. Comparison of experimental data and calculated values of χ^m for PS (Mw=51,000)-MEK at 50°C obtained using internal pressures in a newly developed model.

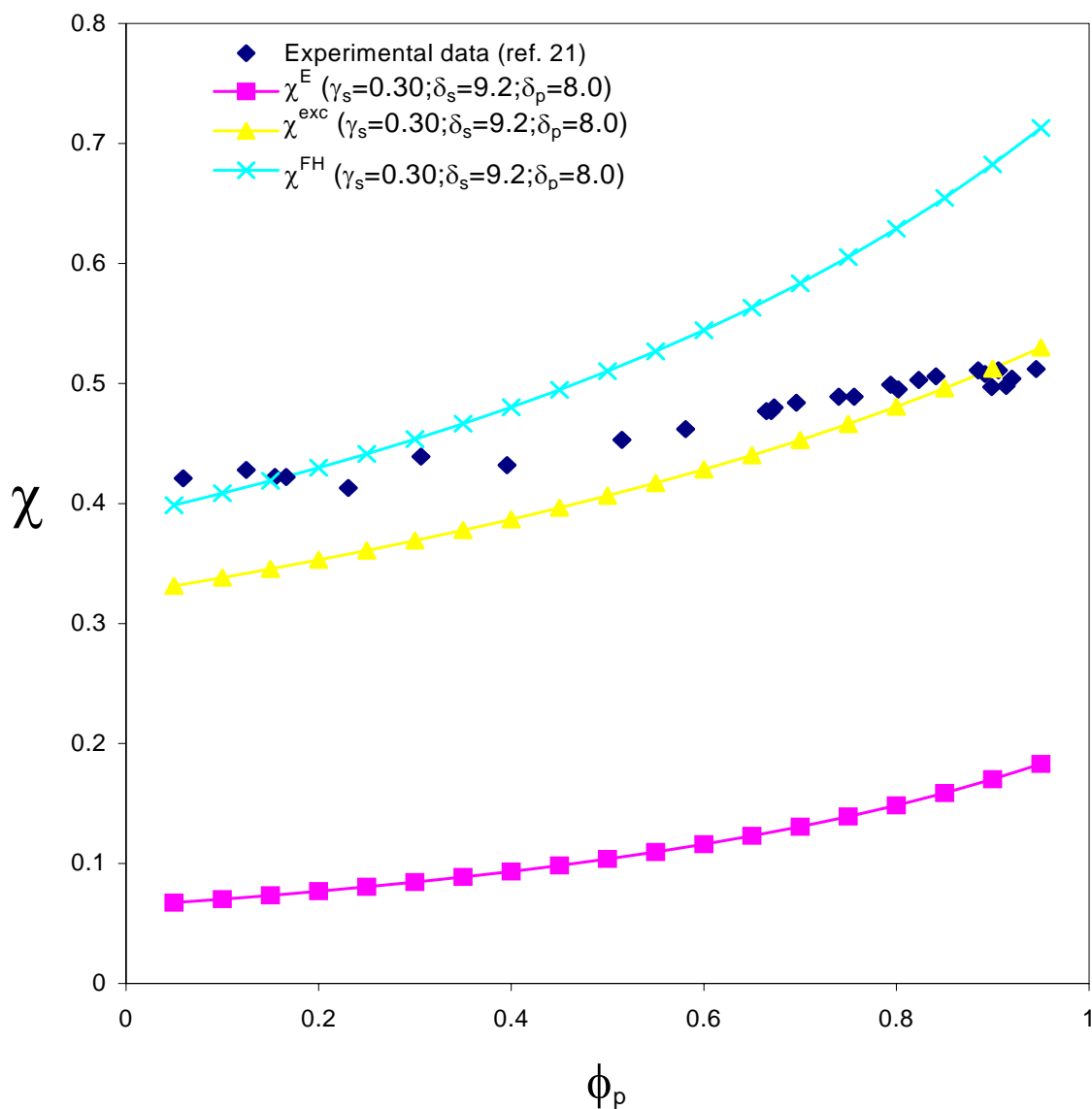


Figure 3.9. Comparison of experimental data and calculated values of χ^m for natural rubber ($M_w=40,000$)-benzene at 25°C obtained using solubility parameters in a newly developed model.

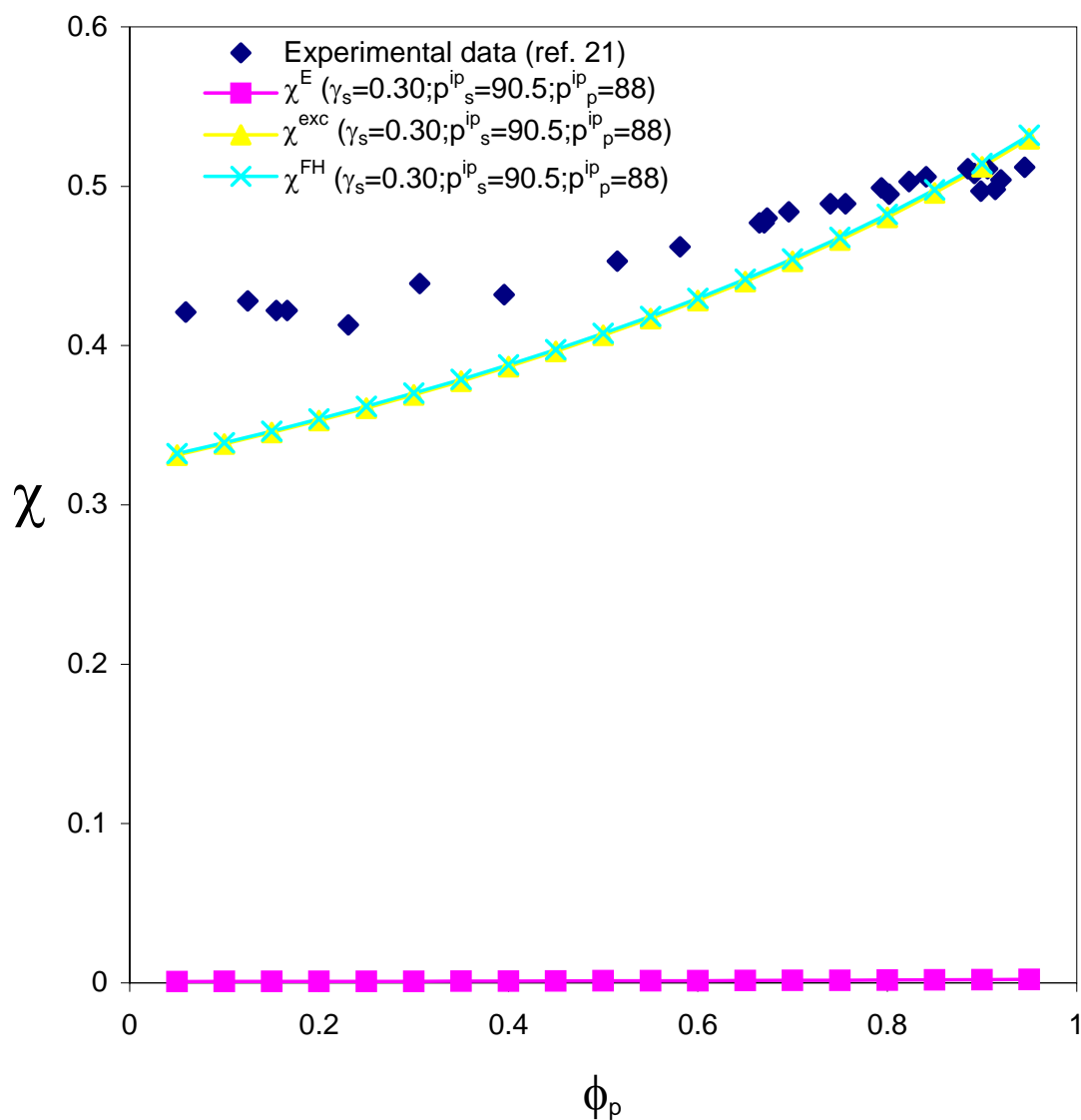


Figure 3.10. Comparison of experimental data and calculated values of χ^m for natural rubber (Mw=40,000) benzene at 25°C obtained using internal pressure in a newly developed model.

likely due to a change in polymer chain dimensions with concentration. Daoud et al.²² showed that even in the concentrated regime, the radius of gyration of chains are expanded considerably from their bulk or theta solvent values (at $\phi_p = 0.5$ polystyrene chains were expanded more than 10 %). This has two possible effects. The first is that an elastic term should be included in the contributions of entropy to the free energy. Intuitively such contributions to the free energy would be expected to be small, but when they are incorporated into the Flory-Huggins χ term they have to be multiplied by $\frac{1}{\phi_p^2}$, thus increasing the magnitude of their contribution significantly at low polymer concentrations.

To account for this, contributions to χ from an elastic term, was calculated using a simple Flory model, where the elastic free energy, ΔF_{el} , and its contributions to the solvent chemical potential are given by:

$$\frac{\Delta F_{el}}{RT} = n_p \left[\frac{3}{2} (\alpha^2 - 1) - \ln \alpha^3 \right] \quad (68)$$

$$\frac{\Delta \mu_{el}}{RT} = - \left[3n_p \left(\alpha - \frac{1}{\alpha} \right) \frac{\phi_p^2}{r_p n_p} \right] \frac{\partial \alpha}{\partial \phi_p} \quad (69)$$

where α is the chain expansion factor. Daoud et al.²² demonstrated that the radius of gyration of a polystyrene chain in a good solvent, $R(\phi)$, follows the de Gennes relationship:

$$R^2(\phi) \cong R_0^2 \phi_p^{-1/4} \quad (70)$$

where R_0 is the radius of gyration found in the melt. It then follows that:

$$\alpha^2 = \frac{R^2(\phi)}{R_0^2} = \phi_p^{-1/4} \quad (71)$$

hence:

$$\frac{\Delta\mu_{el}}{RT} = \frac{3}{8r_p} [\phi_p^{0.75} - \phi_p] \quad (72)$$

A more detailed derivation of equation 72 can be found in Appendix E. In calculating r_p it was assumed that the number of chemical repeat units comprising a Kuhn segment, C_∞ , is seven. The relationship embodied in equations 70 and 71 are only good down to the chain overlap threshold, which experimentally is not well defined. The calculations were therefore limited to values of ϕ_p greater than 0.10. Although the curve describing the composition dependence of χ was flattened slightly by including this factor, the effect was not that significant.

A more important factor in determining the shape of the χ /composition curve is the change in the fraction of same chain contact sites. As the chain expands the number of same chain contacts will decrease drastically. Victor et al.²³ have calculated the

fraction of same chain contacts for a self-avoiding walk on a cubic lattice and from this it was determined that γ_s for high molecular weight polymers should be of the order of 0.1. Unfortunately, there is presently no relationship that allows for the calculation of how γ_s varies with chain expansion, α . Intuitively, the relationship would be expected to be non-linear, with large changes as the chain expands from its initial "ideal" dimensions that get progressively smaller as the chain approaches the dimensions given by self-avoiding walk statistics. Preliminary Monte Carlo simulations performed by Dr. Park²⁴, suggests that this indeed appears to be the case. From figure 3.11 it can be seen that the screening factor changes dramatically from its unperturbed/"relaxed" state ($\alpha=1$) to a state where the chains are stretched by 10 % ($\alpha=1.1$). Even though these are very early stage results, it is probably safe to assume that the screening factor will be changing if the chain is perturbed.

Accordingly, in order to compare theory with experiment two χ /composition curves were calculated, one with values of $\gamma_s = 0.1$ and the second using values of $\gamma_s = 0.3$. The results obtained for the natural rubber/benzene system are shown in figures 3.12 and 3.13, which again shows curves obtained calculated using solubility parameters and internal pressure's, respectively (An elastic contribution to χ , as described earlier, was also included in these calculations). It can be seen that the composition dependence of χ is (unsurprisingly) much more accurately reproduced by values of $\gamma_s = 0.1$, i.e. the curve is "flattened". Also, for this system solubility parameters do a much better job of matching experimental values of χ . Similar results were obtained for the poly(isobutylene)/cyclohexane system, shown in figure 3.14 ($\gamma_s = 0.1$).

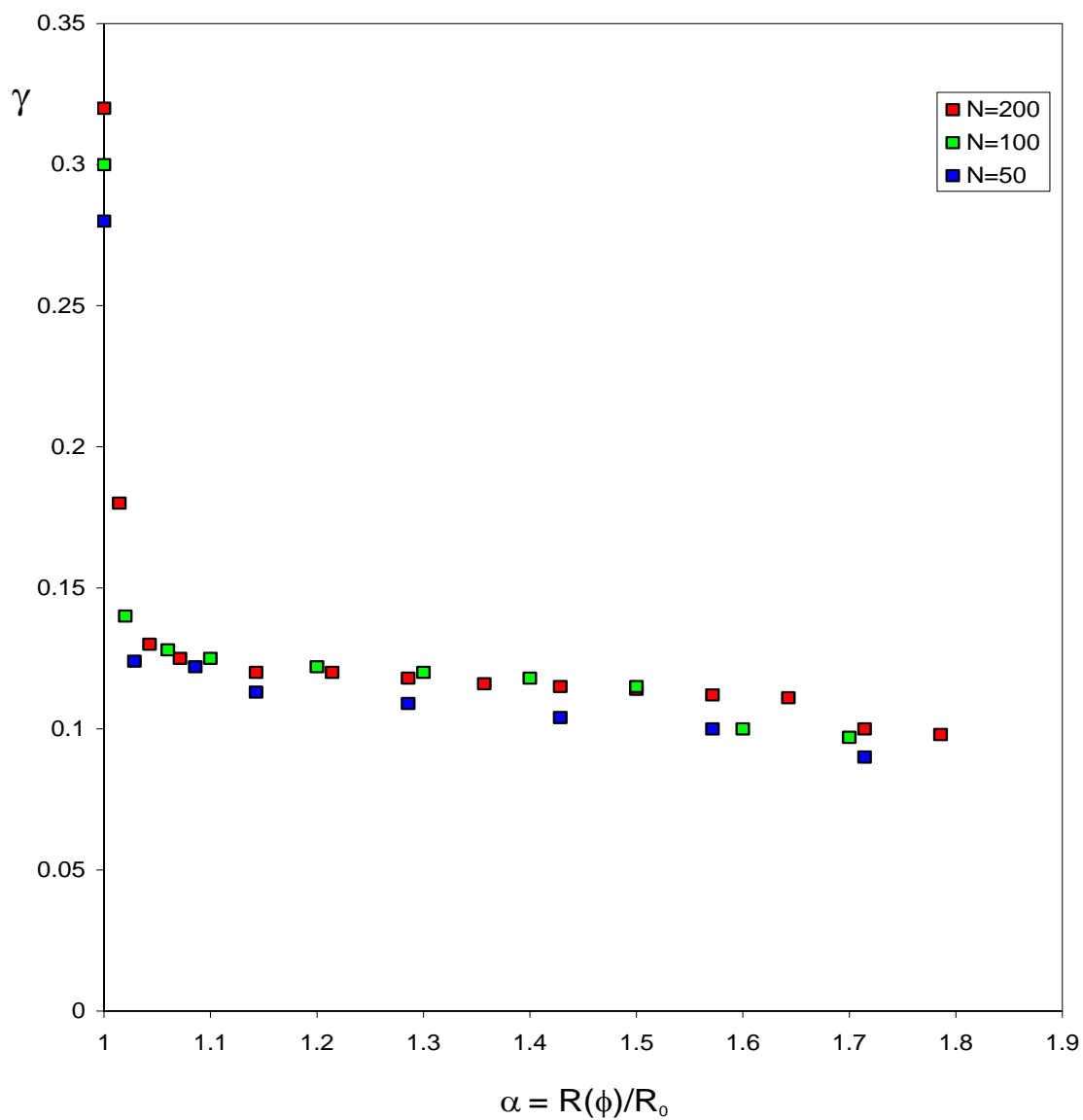


Figure 3.11. The screening factor, γ , as a function of chain expansion, α . Monte Carlo simulations performed by Dr. Park²⁴, where N is the number of steps.

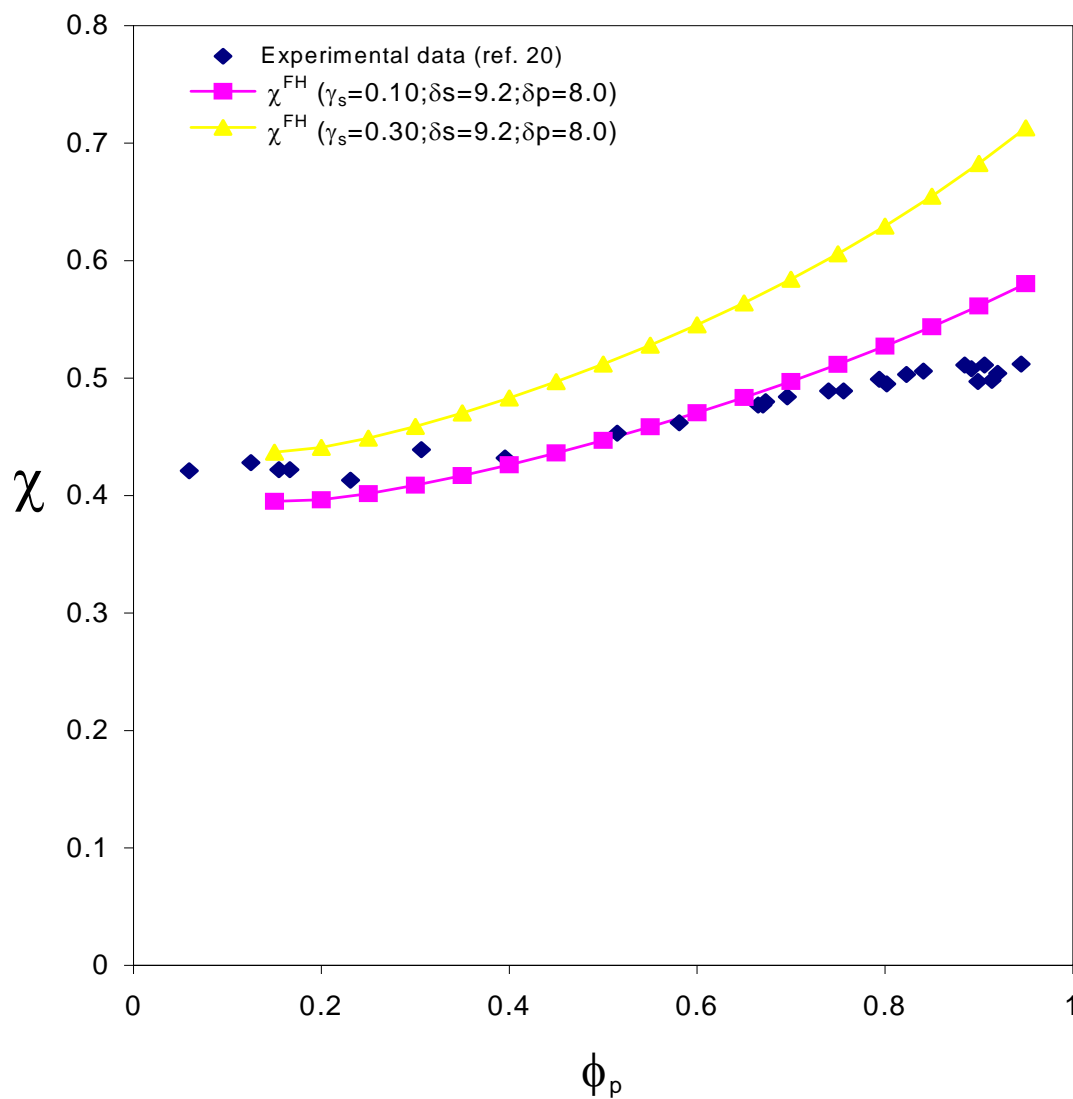


Figure 3.12. Comparison of experimental data and calculated values of χ^{FH} with an "elastic contribution" for natural rubber ($M_w=40,000$)-benzene at 25°C obtained using solubility parameters in a newly developed model for two different values of γ_s .

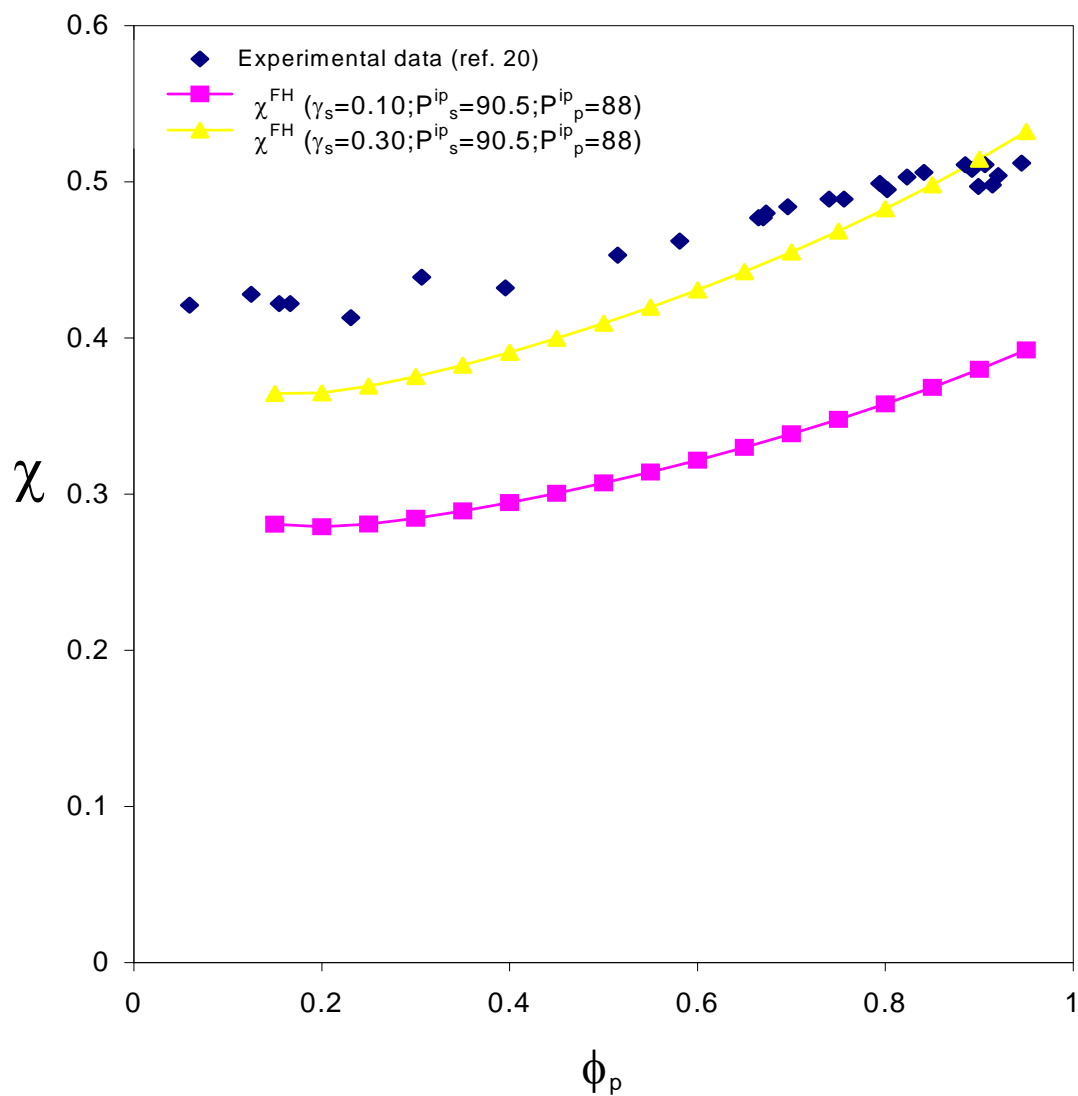


Figure 3.13. Comparison of experimental data and calculated values of χ^{FH} with an "elastic contribution" for natural rubber (Mw=40,000)-benzene at 25°C obtained using internal pressures in a newly developed model for two different values of γ_s .

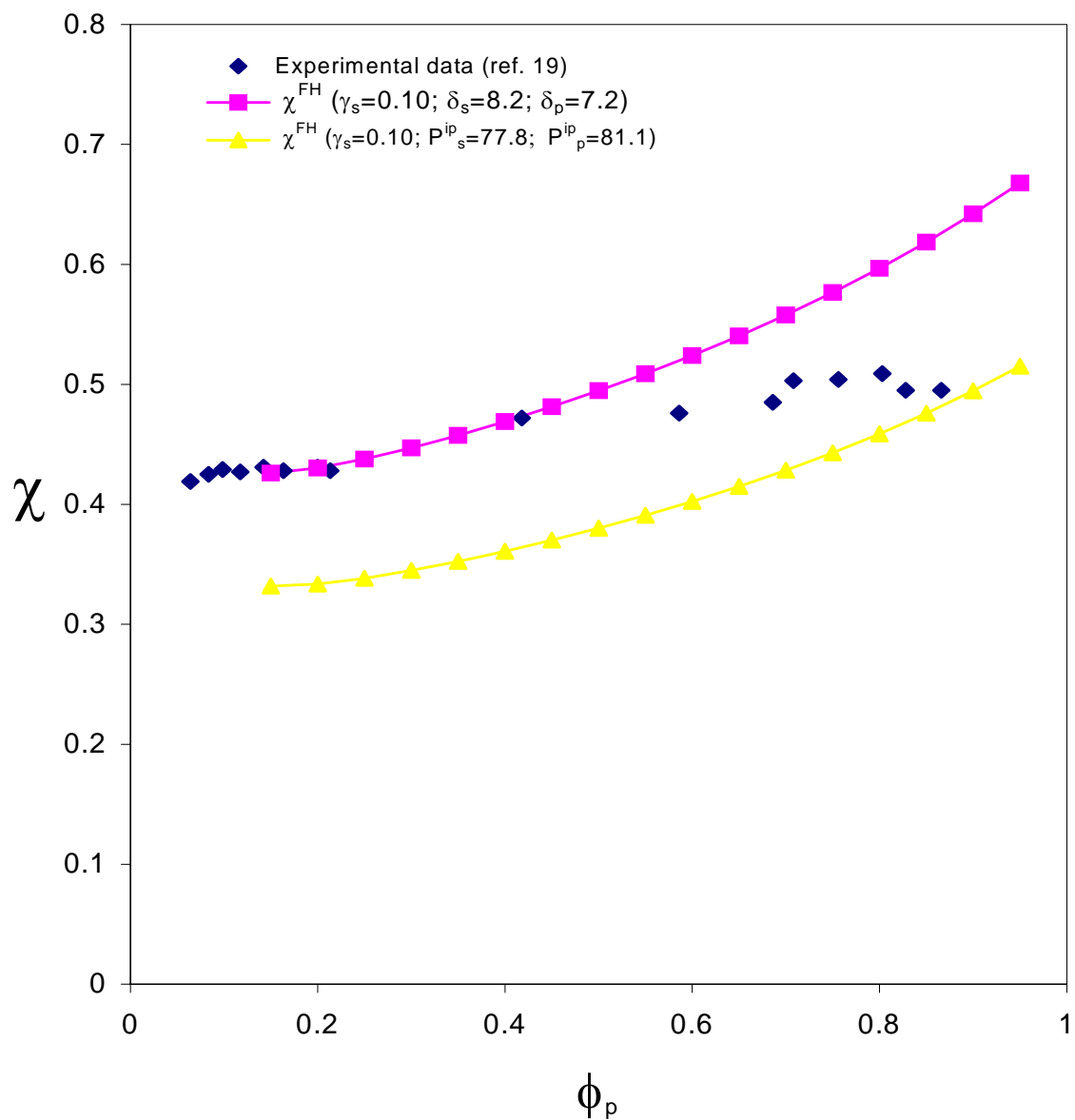


Figure 3.14. Comparison of experimental data and calculated values of χ^{FH} with an "elastic contribution" for PIB(Mw=40,000)-cyclohexane at 25°C obtained using solubility parameters and internal pressures in a newly developed model.

3.4. Conclusions

There are two major conclusions from this study. First, the use of internal pressures and a geometric mean assumption to calculate an exchange energy interaction term gives very inconsistent results in reproducing experimental values of χ for polymers in both theta and non-theta solvents when combined with the FOV equation of state model. Solubility parameters provide a reasonable approximation to both.

In chapter 2 it was found that by letting χ be a simple free energy parameter that has a composition dependence for fitting data related to the chemical potential that is given by:

$$\chi = \frac{(1-\gamma)^2}{(1-\gamma\phi_p)^2} \chi_0$$

then the composition dependence of χ is reproduced with startling accuracy for both polymers in theta solvents and in good solvents. This suggests that the deviations seen here have their origin in the composition dependence of the excess term, given here by the FOV equation.

The equation for the excess energy contribution, χ^E to the interaction parameter χ^{FH} presented here is identical to the one presented in chapter 2 for the enthalpic contribution to the interaction parameter. In the previous chapter it was established that this term greatly contributed to the overall interaction parameter, χ^{FH} , which does not appear to be the case for this model. The contribution from the term above to the overall

interaction parameter, were in the range of 0.28-0.87 over the entire concentration range for the Polystyrene-Cyclohexane system in the previous chapter. For comparison the contribution from the same term when solubility parameters are used to calculate the “bare” interaction parameter in this chapter ranges from about 0.1 to 0.2, and when internal pressures are used it ranges from approximately 0.2 to 0.4 for the same system. It therefore appears that the excess term for the interaction parameter presented in this work is asked to carry more of the “burden” when calculating the overall interaction parameter, χ^{FH} , a task which is not entirely completed with the present model. It would be interesting to see if other approaches, such as the Sanchez-Lacombe model, give a better agreement with experimental data.

It also appears from preliminary simulations performed by Dr. Park²⁴, that the screening factor is very sensitive to even small changes in the chain dimensions. It may therefore not be a good assumption to use a constant value for the screening factor over the entire concentration range. It would be very interesting to pursue the relationship between the screening factor and the chain expansion factor.

3.5. References

1. Painter, P.C.; Berg, L.P.; Veytsman, B.; Coleman, M.M. *Macromolecules*, **30**, 7529 (1997)
2. Painter, P.C.; Coleman, M.M. chapter 4 in "*Polymer Blends Volume 1*", Edited by Paul, D.R.; Bucknall, C.B. John Wiley and Sons, New York, 2000
3. Painter, P.C.; Veytsman, B.; Kumar, S.; Shenoy, S.; Graf, J.F.; Xu, Y.; Coleman, M.M. *Macromolecules*, **30**, 932 (1997)
4. (a) Flory, P.J.; Orwoll, R.A.; Vrij, A. *J. Am. Chem. Soc.*, **86**, 3507 (1964)
(b) Flory, P.J.; Orwoll, R.A.; Vrij, A. *J. Am. Chem. Soc.*, **86**, 3515 (1964)
5. Prigogine, I. *The Molecular Theory of Solutions*, Interscience Publishers Inc., NY, 1957
6. Koningsfeld, R.; Kleintjens, L.A. *Macromolecules*, **4**, 637 (1971)
7. Huggins, M.L. *Ann. N.Y. Acad. Sci.*, **49**, 9 (1942)
8. Guggenheim, E.A. *Mixtures*, Clarendon, Oxford, 1952
9. Hildebrand, J.H. *J. Am. Chem. Soc.*, 1916, **38**, 1452
10. Hildebrand, J.H. *Solubility of Non-electrolytes*, 2nd.Ed., Reinhold Publishing Corporation., NY, 1936
11. Hildebrand, J.H.; Scott, R.L. *The Solubility of Nonelectrolytes*, Revised 3rd. Ed., Dover Publications Inc., NY, 1964
12. Allen, G.; Gee, G.; Wilson, G.J. *Polymer*, **1**, 456 (1960)
13. Allen, G.; Gee, G.; Mangaraj, D.; Sims, D.; Wilson, G.J. *Polymer*, **1**, 467 (1960)
14. Kriegbaum, W.R.; Geymer, D.O. *J. Am. Chem. Soc.*, **81**, 1859 (1959)

15. Höcker, H.; Flory, P.J. *J. Trans. Faraday Soc.*, **67**, 2270 (1971)
16. Eichinger, B.; Flory, P.J. *J. Trans. Faraday Soc.*, **64**, 2053 (1968)
17. Flory, P.J.; Höcker, H. *J. Trans. Faraday Soc.*, **67**, 2258 (1971)
18. Abe, A.; Flory, P.J. *J. Am. Chem. Soc.*, **87**, 1838 (1965)
19. Höcker, H.; Shi, H.; Flory, P.J. *J. Trans. Faraday Soc.*, **67**, 2275 (1971)
20. Eichinger, B.; Flory, P.J. *J. Trans. Faraday Soc.*, **64**, 2061 (1968)
21. Eichinger, B.; Flory, P.J. *J. Trans. Faraday Soc.*, **64**, 2035 (1968)
22. Daoud, M.; Cotton, J.P.; Farnoux, B.; Jannink, G.; Sarma, G.; Benoit, H.; Duplessix, R.; Picot, C.; de Gennes, P.G. *Macromolecules*, **8**, 804 (1975)
23. Victor, J-M.; Imbert, J-B.; Lhuillier, D. *J. Chem. Phys.*, **100**, 5372 (1994)
24. Park, Y.H. Personal Communication, 2005

Chapter 4

Thermodynamics in Isotopic Polymer Blends

4.1. Introduction

Most thermodynamic modeling in polymer blends involves the classical theory of Flory-Huggins in some form or another. However, it has been well documented that this theory has some serious flaws, which are specially pronounced in mixtures of uneven sized molecules (e.g. polymer solutions). Recent experimental results suggest that even in mixtures of even sized (large) and alike molecules, where the expected interaction energy is supposedly minimal, the classical theory is still inadequate. The origin of the concentration dependence of the Flory-Huggins interaction parameter, χ_{NS} , determined from small-angle neutron scattering (SANS) studies of isotope polymer blends remains a perplexing problem. Plotted as a function of composition, χ_{NS} increases significantly at each of the composition extremes for nearly all blend systems studied, the exception being polystyrene isotope blends, where the value of χ_{NS} decreases at the composition extremes. Crist¹ demonstrated that systematic errors lead to such divergences and also the measured inverse dependence of χ_{NS} on N , the degree of polymerization. However, in certain systems, notably the polyethylene isotope blends characterized by Londono et al.², it appears that errors would have to be unreasonably large to account for the measured values of χ_{NS} .

Various attempts have been made to account for the composition dependence of χ_{NS} in these mixtures, succinctly summarized and reviewed in the paper by Melenkevitz et al.³ These authors convincingly demonstrated that compressibility effects and density fluctuations cannot account for the data and concluded that the observed divergences could only be attributable to systematic errors, although, as they pointed out, the degree of divergence in some systems and the fact that the curvature of the χ_{NS} vs. composition plots are with one exception all in the same direction is unsettling.

In this work it will be pointed out that extremely small changes in the fraction of self-contacts in polymer chains can also account for these results. The Flory-Huggins theory assumes a random mixing of the *segments* of the chains in a mixture. Connectivity affects the number of intermolecular contacts allowed to a segment in two ways. First, the number of inter-chain contacts is reduced by the fact that each segment in a linear chain is covalently bonded to two neighbors (neglecting end groups). This factor has been accounted for in the treatments of Huggins⁴ and Guggenheim⁵. Huggins also introduced a second factor for same-chain contacts that are a result of the chain bending back on itself.

As a result of work on hydrogen bonded blends in the Painter/Coleman group, where the number of contacts in well-chosen systems can be “counted”, it was found that the fraction of sites (twice the number of contacts) that are occupied by other segments of the same chain (that are not covalently bonded nearest neighbors) is surprisingly large, about 0.25 – 0.30. Simulations by Kumar (Painter et al.⁶) gave results that are consistent with these values for polymers in the melt.

As an extension to this work it was decided to investigate the probability that at the concentration extremes there could be changes in chain dimensions of the minor

component which could, in turn, change the number of same-chain contacts. Such changes in the radius of gyration of the isotope blends considered by Crist¹ and Melenkevitz et al.³ have not been detected², but it will be shown here that changes in the fraction of same chain contacts of about 2% or less are sufficient to account for the observed concentration dependence of χ_{NS} . Such small changes would presumably be a result of equivalently small changes in chain dimensions and would not be distinguishable from the usual errors involved in SANS measurements.

The effect of same-chain contacts can be readily incorporated into simple lattice models, where the usual assumption of incompressibility and a random mixing of chains (hence no density fluctuations) is maintained. The methodologies of Huggins or Guggenheim can be applied as long as the chains are assumed to maintain their “ideal” dimensions in the concentrated regime. A more rigorous theory requires a relationship between chain expansion and the fraction of same-chain contacts, which has yet to be established. Previously it was shown how a simple model of this type accounts for the composition dependence of χ for polymer solutions at the θ temperature with remarkable accuracy⁷. Equations describing the free energy of mixing blends of, say, polymers A and B, are just as readily obtained, but appear more complex because same chain contacts now have to be accounted for in both components. This is accomplished through a combined factor γ (see references 6 and 7), which accounts for the loss of external contacts to a chain through both covalent linkages and the effect of a chain bending back on itself as a result of both long range and local effects (although in blends of high molecular weight polymers the effect of the former on composition dependence is negligible). This

reduction in the number of AB contacts relative to what is obtained when a random mixing of segments is assumed manifests itself through factors $(1 - \gamma_A)$ and $(1 - \gamma_B)$.

4.2. Interaction Parameters in Polymer Blends

According to Sanchez⁸ there are in general four different interaction parameters for a binary polymer mixture: χ , $\chi_{\mu 1}$, $\chi_{\mu 2}$ and χ_{sc} . One is associated with the free energy (χ), two are associated with the chemical potentials ($\chi_{\mu 1}$ and $\chi_{\mu 2}$; which are related to the first derivative of the free energy), and finally one which can be obtained from scattering experiments (χ_{sc} ; which depends on the second derivative of the free energy). However these parameters are all related via the following equations:

$$\chi_{\mu 1} = \chi + \phi_1 \left(\frac{d\chi}{d\phi_1} \right) \quad (1)$$

$$\chi_{\mu 2} = \chi + \phi_2 \left(\frac{d\chi}{d\phi_2} \right) \quad (2)$$

$$\chi = \phi_2 \chi_{\mu 1} + \phi_1 \chi_{\mu 2} \quad (3)$$

$$\chi_{sc} = \chi + (\phi_1 - \phi_2) \frac{d\chi}{d\phi_1} - \frac{1}{2} \phi_1 \phi_2 \frac{d^2 \chi}{d\phi_1^2} \quad (4)$$

The classical Flory-Huggins expression for the free energy of mixing can be written as:

$$\Delta f = \Delta f_{comb} + \Delta f_{ex} \quad (5)$$

where Δf_{comb} is the traditional combinatorial entropy:

$$\Delta f_{comb}/kT = \left(\frac{\phi_1}{v_1}\right) \ln \phi_1 + \left(\frac{\phi_2}{v_2}\right) \ln \phi_2 \quad (6)$$

and Δf_{ex} is the excess free energy:

$$\Delta f_{ex}/kT = \phi_1 \phi_2 \chi \quad (7)$$

The following term is now considered:

$$n_A q_A \left(\frac{r_A - 1}{r_A - q_A}\right) \ln \left[\left(\frac{q_A}{r_A}\right) \frac{n_0}{n_A q_A + n_B q_B} \right] + n_B q_B \left(\frac{r_B - 1}{r_B - q_B}\right) \ln \left[\left(\frac{q_B}{r_B}\right) \frac{n_0}{n_A q_A + n_B q_B} \right] \quad (8)$$

which if combined with equation 6 yields Guggenheim's expression for the combinatorial entropy. Earlier it was shown that the term above can be reformulated as:

$$\phi_A \left(\frac{r_A - 1}{r_A}\right) \left(\frac{1 - \gamma_A}{\gamma_A}\right) \ln \left[\frac{(1 - \gamma_A)}{1 - \gamma_A \phi_A - \gamma_B \phi_B} \right] + \phi_B \left(\frac{r_B - 1}{r_B}\right) \left(\frac{1 - \gamma_B}{\gamma_B}\right) \ln \left[\frac{(1 - \gamma_B)}{1 - \gamma_A \phi_A - \gamma_B \phi_B} \right] \quad (9)$$

It was also shown that the interaction energy term could be written as:

$$\left(\frac{(1-\gamma_A)(1-\gamma_B)\phi_A\phi_B}{1-\gamma_A\phi_A-\gamma_B\phi_B} \right) (\chi_{bare}) \quad (10)$$

According to equation 5 the excess free energy, Δf_{ex} , is basically the free energy minus the combinatorial entropy. When the modified Guggenheim expression (equation 9) is combined with equation 10, the excess free energy can be expressed as:

$$\begin{aligned} \Delta f_{ex}/kT = & \phi_A \left(\frac{r_A-1}{r_A} \right) \left(\frac{1-\gamma_A}{\gamma_A} \right) \ln \left[\frac{(1-\gamma_A)}{1-\gamma_A\phi_A-\gamma_B\phi_B} \right] \\ & + \phi_B \left(\frac{r_B-1}{r_B} \right) \left(\frac{1-\gamma_B}{\gamma_B} \right) \ln \left[\frac{(1-\gamma_B)}{1-\gamma_A\phi_A-\gamma_B\phi_B} \right] + \left(\frac{(1-\gamma_A)(1-\gamma_B)\phi_A\phi_B}{1-\gamma_A\phi_A-\gamma_B\phi_B} \right) (\chi_{bare}) \end{aligned} \quad (11)$$

By comparison with equation 7 it can be seen that:

$$\begin{aligned} \phi_A\phi_B\chi = & \phi_A \left(\frac{r_A-1}{r_A} \right) \left(\frac{1-\gamma_A}{\gamma_A} \right) \ln \left[\frac{(1-\gamma_A)}{1-\gamma_A\phi_A-\gamma_B\phi_B} \right] \\ & + \phi_B \left(\frac{r_B-1}{r_B} \right) \left(\frac{1-\gamma_B}{\gamma_B} \right) \ln \left[\frac{(1-\gamma_B)}{1-\gamma_A\phi_A-\gamma_B\phi_B} \right] + \left(\frac{(1-\gamma_A)(1-\gamma_B)\phi_A\phi_B}{1-\gamma_A\phi_A-\gamma_B\phi_B} \right) (\chi_{bare}) \end{aligned}$$

or:

$$\begin{aligned} \chi = & \frac{1}{\phi_B} \left(\frac{r_A-1}{r_A} \right) \left(\frac{1-\gamma_A}{\gamma_A} \right) \ln \left[\frac{(1-\gamma_A)}{1-\gamma_A\phi_A-\gamma_B\phi_B} \right] \\ & + \frac{1}{\phi_A} \left(\frac{r_B-1}{r_B} \right) \left(\frac{1-\gamma_B}{\gamma_B} \right) \ln \left[\frac{(1-\gamma_B)}{1-\gamma_A\phi_A-\gamma_B\phi_B} \right] + \left(\frac{(1-\gamma_A)(1-\gamma_B)}{1-\gamma_A\phi_A-\gamma_B\phi_B} \right) (\chi_{bare}) \end{aligned} \quad (12)$$

The derivative of equation 12 with respect to ϕ_A is:

$$\begin{aligned}
\frac{\partial \chi}{\partial \phi_A} = & \left(\frac{r_A - 1}{r_A} \right) \left(\frac{1 - \gamma_A}{\gamma_A} \right) \left[\frac{1}{\phi_B^2} \ln \left[\frac{(1 - \gamma_A)}{1 - \gamma_A \phi_A - \gamma_B \phi_B} \right] + \frac{1}{\phi_B} \left(\frac{\gamma_A - \gamma_B}{1 - \gamma_A \phi_A - \gamma_B \phi_B} \right) \right] \\
& - \left(\frac{r_B - 1}{r_B} \right) \left(\frac{1 - \gamma_B}{\gamma_B} \right) \left[\frac{1}{\phi_A^2} \ln \left[\frac{(1 - \gamma_B)}{1 - \gamma_A \phi_A - \gamma_B \phi_B} \right] - \frac{1}{\phi_A} \left(\frac{\gamma_A - \gamma_B}{1 - \gamma_A \phi_A - \gamma_B \phi_B} \right) \right] \\
& + \left(\frac{(1 - \gamma_A)(1 - \gamma_B)(\gamma_A - \gamma_B)}{(1 - \gamma_A \phi_A - \gamma_B \phi_B)^2} \right) (\chi_{bare})
\end{aligned} \tag{13}$$

and the second derivative is given by:

$$\begin{aligned}
\frac{\partial^2 \chi}{\partial \phi_A^2} = & \left(\frac{r_A - 1}{r_A} \right) \left(\frac{1 - \gamma_A}{\gamma_A} \right) \left[\frac{2}{\phi_B^3} \ln \left(\frac{1 - \gamma_A}{1 - \gamma_A \phi_A - \gamma_B \phi_B} \right) + \frac{2}{\phi_B^2} \frac{(\gamma_A - \gamma_B)}{(1 - \gamma_A \phi_A - \gamma_B \phi_B)} + \frac{1}{\phi_B} \left(\frac{\gamma_A - \gamma_B}{1 - \gamma_A \phi_A - \gamma_B \phi_B} \right)^2 \right] \\
& + \left(\frac{r_B - 1}{r_B} \right) \left(\frac{1 - \gamma_B}{\gamma_B} \right) \left[\frac{2}{\phi_A^3} \ln \left(\frac{1 - \gamma_B}{1 - \gamma_A \phi_A - \gamma_B \phi_B} \right) - \frac{2}{\phi_A^2} \frac{(\gamma_A - \gamma_B)}{(1 - \gamma_A \phi_A - \gamma_B \phi_B)} + \frac{1}{\phi_A} \left(\frac{\gamma_A - \gamma_B}{1 - \gamma_A \phi_A - \gamma_B \phi_B} \right)^2 \right] \\
& + \left(\frac{2(1 - \gamma_A)(1 - \gamma_B)(\gamma_A - \gamma_B)^2}{(1 - \gamma_A \phi_A - \gamma_B \phi_B)^3} \right) (\chi_{bare})
\end{aligned} \tag{14}$$

By inserting equation 12, equation 13 and equation 14 into equation 4 χ_{sc} can be determined.

The energetic part of χ_{sc} is then given by:

$$\chi_{sc}^E = \left(\frac{(1 - \gamma_A)^2 (1 - \gamma_B)^2}{(1 - \gamma_A \phi_A - \gamma_B \phi_B)^3} \right) (\chi_{bare}) \tag{15}$$

whereas the excess part of χ_{sc} is given by:

$$\begin{aligned} \chi_{SC}^{exc} = & \left(\frac{r_B - 1}{r_B} \right) \left(\frac{1 - \gamma_B}{\gamma_B} \right) \left(\frac{\gamma_A - \gamma_B}{1 - \gamma_A \phi_A - \gamma_B \phi_B} \right) \left[1 - \frac{1}{2} \phi_B \left(\frac{\gamma_A - \gamma_B}{1 - \gamma_A \phi_A - \gamma_B \phi_B} \right) \right] \\ & - \left(\frac{r_A - 1}{r_A} \right) \left(\frac{1 - \gamma_A}{\gamma_A} \right) \left(\frac{\gamma_A - \gamma_B}{1 - \gamma_A \phi_A - \gamma_B \phi_B} \right) \left[1 + \frac{1}{2} \phi_A \left(\frac{\gamma_A - \gamma_B}{1 - \gamma_A \phi_A - \gamma_B \phi_B} \right) \right] \end{aligned} \quad (16)$$

However if it is assumed that $r_A \gg 1$ and $r_B \gg 1$ then equation 16 reduces to:

$$\begin{aligned} \chi_{SC}^{exc} = & \left(\frac{1 - \gamma_B}{\gamma_B} \right) \left(\frac{\gamma_A - \gamma_B}{1 - \gamma_A \phi_A - \gamma_B \phi_B} \right) \left[1 - \frac{1}{2} \phi_B \left(\frac{\gamma_A - \gamma_B}{1 - \gamma_A \phi_A - \gamma_B \phi_B} \right) \right] - \left(\frac{1 - \gamma_A}{\gamma_A} \right) \left(\frac{\gamma_A - \gamma_B}{1 - \gamma_A \phi_A - \gamma_B \phi_B} \right) \left[1 + \frac{1}{2} \phi_A \left(\frac{\gamma_A - \gamma_B}{1 - \gamma_A \phi_A - \gamma_B \phi_B} \right) \right] \\ = & \left[\left(\frac{1 - \gamma_B}{\gamma_B} \right) - \left(\frac{1 - \gamma_A}{\gamma_A} \right) \right] \left(\frac{\gamma_A - \gamma_B}{1 - \gamma_A \phi_A - \gamma_B \phi_B} \right) - \left[\frac{1}{2} \phi_B \left(\frac{1 - \gamma_B}{\gamma_B} \right) + \frac{1}{2} \phi_A \left(\frac{1 - \gamma_A}{\gamma_A} \right) \right] \left(\frac{\gamma_A - \gamma_B}{1 - \gamma_A \phi_A - \gamma_B \phi_B} \right)^2 \end{aligned}$$

which again reduces to:

$$\chi_{SC}^{exc} = \frac{1}{2\gamma_A\gamma_B} \left[\frac{(\gamma_A - \gamma_B)^2}{1 - \gamma_A\phi_A - \gamma_B\phi_B} \right] + \frac{1}{2} \left[\frac{(1 - \gamma_A)(1 - \gamma_B)}{\gamma_A\gamma_B} \right] \left[\frac{\gamma_A - \gamma_B}{1 - \gamma_A\phi_A - \gamma_B\phi_B} \right]^2 \quad (17)$$

so a combination of equation 15 and equation 17 leads to:

$$\begin{aligned} \chi_{SC} &= \chi_{SC}^E + \chi_{SC}^{exc} \\ &= \left(\frac{(1 - \gamma_A)^2(1 - \gamma_B)^2}{(1 - \gamma_A\phi_A - \gamma_B\phi_B)^3} \right) (\chi_{bare}) + \frac{1}{2\gamma_A\gamma_B} \left[\frac{(\gamma_A - \gamma_B)^2}{1 - \gamma_A\phi_A - \gamma_B\phi_B} \right] + \frac{1}{2} \left[\frac{(1 - \gamma_A)(1 - \gamma_B)}{\gamma_A\gamma_B} \right] \left[\frac{\gamma_A - \gamma_B}{1 - \gamma_A\phi_A - \gamma_B\phi_B} \right]^2 \end{aligned} \quad (18)$$

4.3. Interaction Parameters from SANS

In Small Angle Neutron Scattering (SANS) experiments on polymer blends, in which one polymer has been deuterium-labeled, an interaction parameter can be obtained, as mentioned earlier. In the literature this parameter is primarily referred to as either χ_{sc} or χ_{NS} , and the two terms are often used interchangeably. This apparent interaction parameter χ_{sc} is related to the thermodynamic interaction parameter, χ , through:

$$\chi_{sc} = \frac{1}{2} \frac{\partial^2(\phi_1\phi_2\chi)}{\partial\phi_1\partial\phi_2} \quad (19)$$

so only when χ is truly concentration independent is $\chi = \chi_{sc}$. The apparent interaction parameter χ_{sc} can be determined from the classical expression for the static structure factor, $S(q)$, which at zero scattering angle ($q=0$) is equal to the second concentration derivative of the free energy.

$$\frac{1}{S(0)} = \frac{1}{N_1\phi_1v_1} + \frac{1}{N_2\phi_2v_2} - \frac{2\chi_{sc}}{v_0} = \frac{\partial^2\left(\frac{\Delta f}{kT}\right)}{\partial\phi_1^2} \quad (20)$$

which can be rewritten to:

$$\chi_{sc} = -\frac{v_0}{2S(0)} + \frac{v_0}{2} \left(\frac{1}{N_1 \phi_1 v_1} + \frac{1}{N_2 \phi_2 v_2} \right) \quad (21)$$

Theoretically the thermodynamic interaction parameter χ could be obtained using this equation, assuming the simple Flory-Huggins theory for blends would apply. This would require an assumption that error free experiments could be performed. If it is also assumed that the differences in molar volumes caused by the deuterium labeling could be disregarded, so that $v_1 = v_2 = v_0 = v$, and the investigation is limited to symmetric blends, where $N_1 = N_2 = N$, equation 21 can be rewritten to:

$$\chi_{sc} = -\frac{v}{2S(0)} + \frac{1}{2N\phi_1\phi_2} \quad (22)$$

The premise of the work of Crist¹ is that systematic errors in the molecular weight, N , and the static structure factor, $S(0)$, can explain the observed results of Londono et al.². Accordingly Crist¹ allows these two factors to differ from their actual values by a factor a :

$$N' = N/a \quad (23)$$

and a factor b respectively:

$$S'(0) = bS(0) \quad (24)$$

Inserting these adjusted values for the molecular weight, N' , and the static structure factor, $S'(0)$, in equation 22 yields:

$$\chi_{NS} \equiv \frac{1}{2N'\phi_1\phi_2} - \frac{\nu}{2S'(0)} \quad (25)$$

Here the symbol χ_{NS} is adopted to distinguish it from χ_{sc} , so that χ_{NS} describes the experimentally obtained interaction parameter, which takes into account systematic errors, whereas χ_{sc} is the parameter one would obtain from theory. Upon substituting the definitions of N' and $S'(0)$ and introducing a combined error factor, c :

$$c = ab \quad (26)$$

equation 25 can be rewritten to:

$$N'\chi_{NS} = \frac{N\chi_{sc}}{c} + \frac{c-1}{c} \frac{1}{2\phi_A\phi_B} \quad (27)$$

In a certain temperature range the interaction parameter determined from SANS, χ_{NS} , will have an inverse temperature dependence:

$$\chi_{NS} = \frac{A}{T} + B \quad (28)$$

By inserting equation 18 and equation 28 into equation 27 the following expression is obtained:

$$N' \left(\frac{A}{T} + B \right) - \frac{c-1}{c} \frac{1}{2\phi_A\phi_B} - \frac{N}{c} \left[\left(\frac{(1-\gamma_A)^2(1-\gamma_B)^2}{(1-\gamma_A\phi_A-\gamma_B\phi_B)^3} \right) (\chi_{bare}) + \frac{1}{2\gamma_A\gamma_B} \left[\frac{(\gamma_A-\gamma_B)^2}{1-\gamma_A\phi_A-\gamma_B\phi_B} \right] \right. \\ \left. + \frac{1}{2} \left[\frac{(1-\gamma_A)(1-\gamma_B)}{\gamma_A\gamma_B} \right] \left[\frac{\gamma_A-\gamma_B}{1-\gamma_A\phi_A-\gamma_B\phi_B} \right]^2 \right] = 0 \quad (29)$$

From experiments the values of N , N' , A , B , ϕ_A , ϕ_B and T are known. So if the values of c , γ_A and χ^0 are fixed, equation 29 can be considered a function of γ_B , which can be solved for a solution(s).

4.4. Results and Discussion

In order to investigate how well the model presented earlier predicts the interaction parameter in blends, it would be wise to start out with a very simple system. Since isotopic polymer blends are structurally similar and generally lacks any strong specific interactions, such a system would be ideal for such an investigation. Londono et al.² reported interaction parameter values determined from SANS for several systems, however here the focus will be on the Polyethylene (PE) and deuterated Polyethylene (DPE) system.

As stated earlier one could choose to solve equation 29 for solution(s) for γ_B , however instead it was decided to investigate how much different γ_B would have to be from γ_A in order to get a good correspondence to experimental data as determined by Londono et al.². In fact two series of calculations were made, one in which the value of γ_A was fixed while the value of γ_B was varied, and one in which the value of γ_B was fixed while the value of γ_A was varied. Considering that the only difference between the two polymers is that one of them is deuterated, it is probably safe to assume that the values of γ_A and γ_B would be almost identical.

Initially the γ -value of each of the components was kept constant over the entire concentration range ($\gamma_A = \gamma_B = 0.25$) for both polymers. The value of χ^0/T was arbitrarily set to be equal to $4 \cdot 10^{-4}$. Initially it was assumed that $N' = N$, which is obviously only true if $a=1$. However, as it can be seen in figure 4.1, the predicted values of the interaction parameter is well above the experimental values reported by

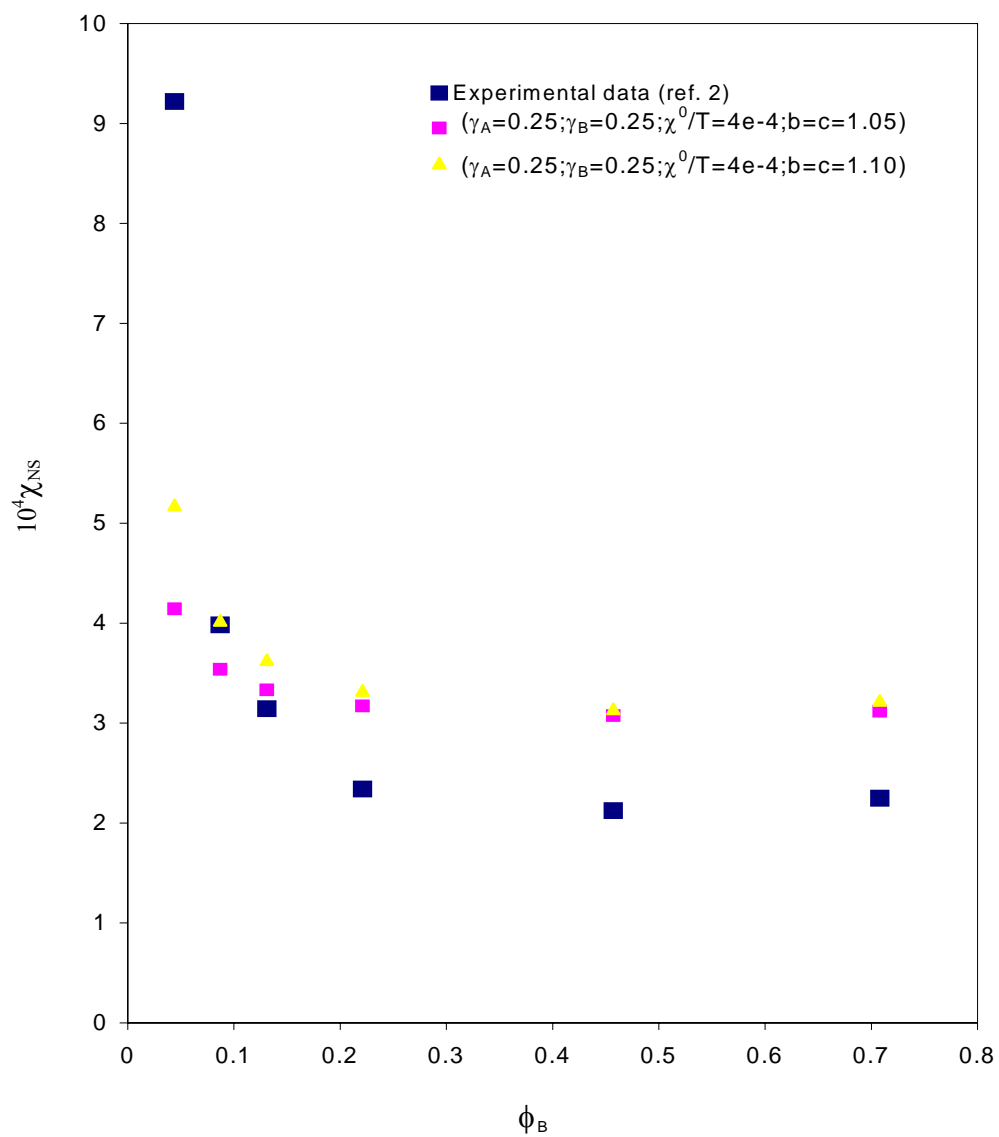


Figure 4.1. Interaction parameters from SANS for PE/DPE at 155 °C.

Londono² at intermediate concentrations ($\phi_B > 0.2$), whereas at very diluted concentrations ($\phi_B < 0.05$) the predicted values of the interaction parameter is severely underestimated. The only point that seems to coincide with the experimental data is at $\phi_B = 0.087$ when the combined error function is 10 % ($c=1.10$).

Clearly the assumption that the screening factor remains constant throughout the entire concentration range is not very good. Intuitively one would expect that the value of the screening factor, γ_i , would have to depend on concentration to some extent, or at the very least it is to be expected that the value at very dilute concentrations would differ from that in the more concentrated regime. Initially $\phi_i = 0.1$ was used as a cutoff, below which a small change to one of the screening factors would be made and the effects would be observed. It was clear early on, that even a small change (less than 5 %) in one of the screening factors, would have a tremendous effect on the results as is evident in figure 4.2. This may not be too surprising since it can be explained by the contribution from the excess energy term (the last two terms on the right hand side of equation 18), which was cancelled out when the two screening factors were identical. A less than 5% change in one of the screening factors, or 4% to be exact, was considered a conservative estimate, and so calculations were done in which one of the screening factors were held constant at 0.25, while the other was set at 0.24 (for $\phi_B < 0.1$) and 0.25 above. Even with this rather conservative change in one of the screening factors, it is evident from figure 4.2, that the predicted values of the interaction parameter are now well above the reported experimental values at very low concentrations ($\phi_B < 0.1$).

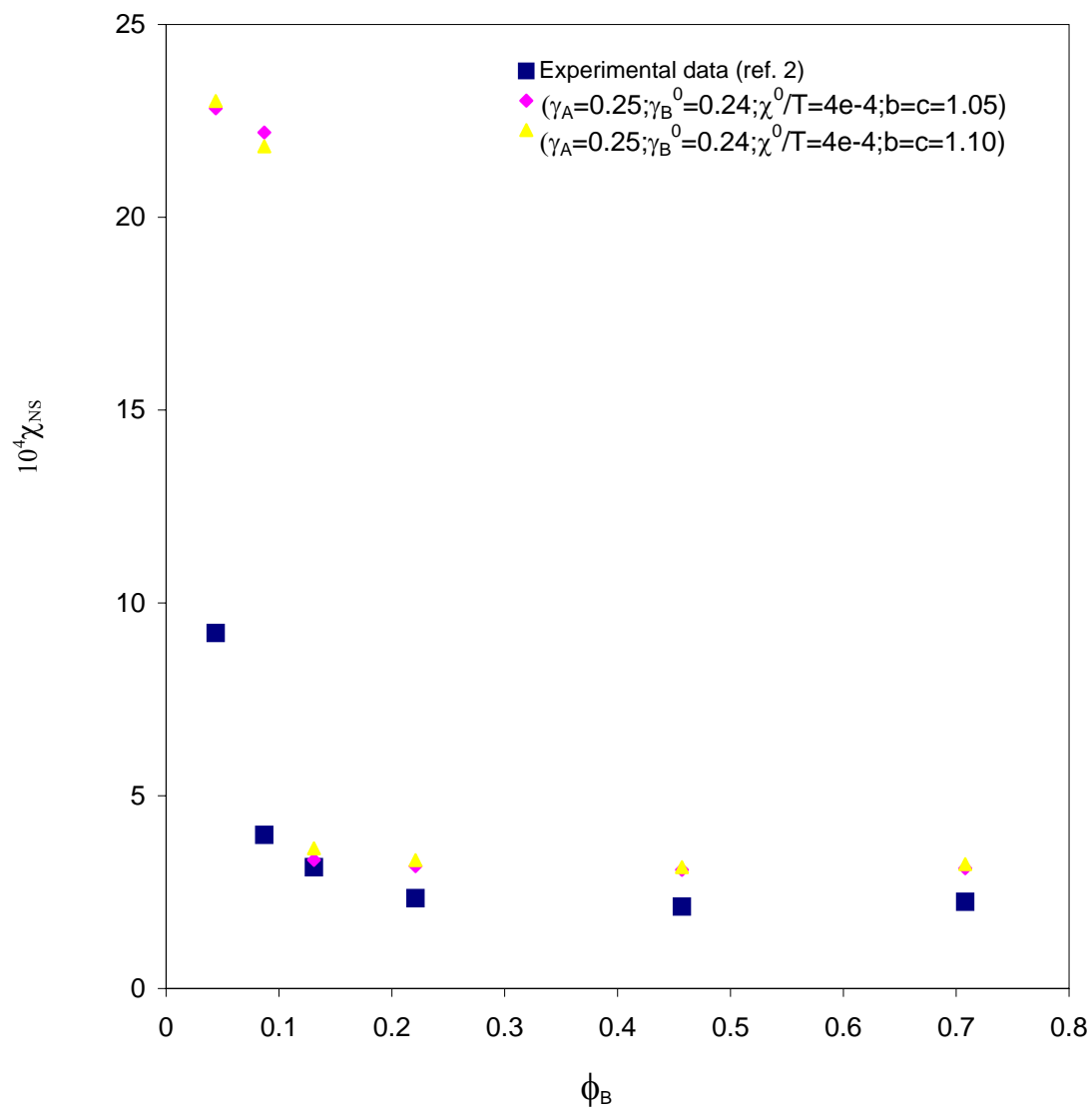


Figure 4.2. Interaction parameters from SANS for PE/DPE at 155 °C.

It seems that an even smaller change is required, so a 2 % change in γ_B was applied instead. As it can be seen in figure 4.3, the predicted value is closer to the experimental value at the very extreme data point ($\phi_B = 0.044$) but is still off at higher concentrations. From figures 4.1-4.3 it can also be seen that the error factor, c , does not seem to have a very big effect in the concentrated regime, but it appears to have more importance in the diluted concentration range as the difference between the two screening factors is lowered. It is also clear that at the intermediate concentration regime all the data points seem to coincide, and each of them are higher than the reported experimental data. It was therefore decided to lower the value of χ^0/T to $2.8 \cdot 10^{-4}$ (for $c=1.00$), $2.7 \cdot 10^{-4}$ (for $c=1.05$) and $2.5 \cdot 10^{-4}$ (for $c=1.10$) respectively, in order to get a good fit to the experimental data. With this adjustment the intermediate data points are now very well accounted for, as it is shown in figure 4.4. However, the lower concentration area ($\phi_B < 0.15$) is still not very well represented, although in this case the excess interaction energy term was disregarded ($\gamma_A = \gamma_B \Rightarrow \chi_{SC}^{exc} = 0$). However, even without this restriction, the discrepancies still exists in the lower concentration area, as is evident from figure 4.5. From the previous figures 4.1-4.5, it was also decided that the previously mentioned cutoff of $\phi_i = 0.1$ was a little low and was reset to $\phi_i = 0.15$.

The next logical step was to allow the screening factor γ_B to vary at low concentrations ($\phi_B < 0.15$), and as it can be seen in figure 4.6 the predicted values now completely coincide with the reported experimental data. The values of γ_B^0 depicted in figure 4.6 are given in table 4.1.

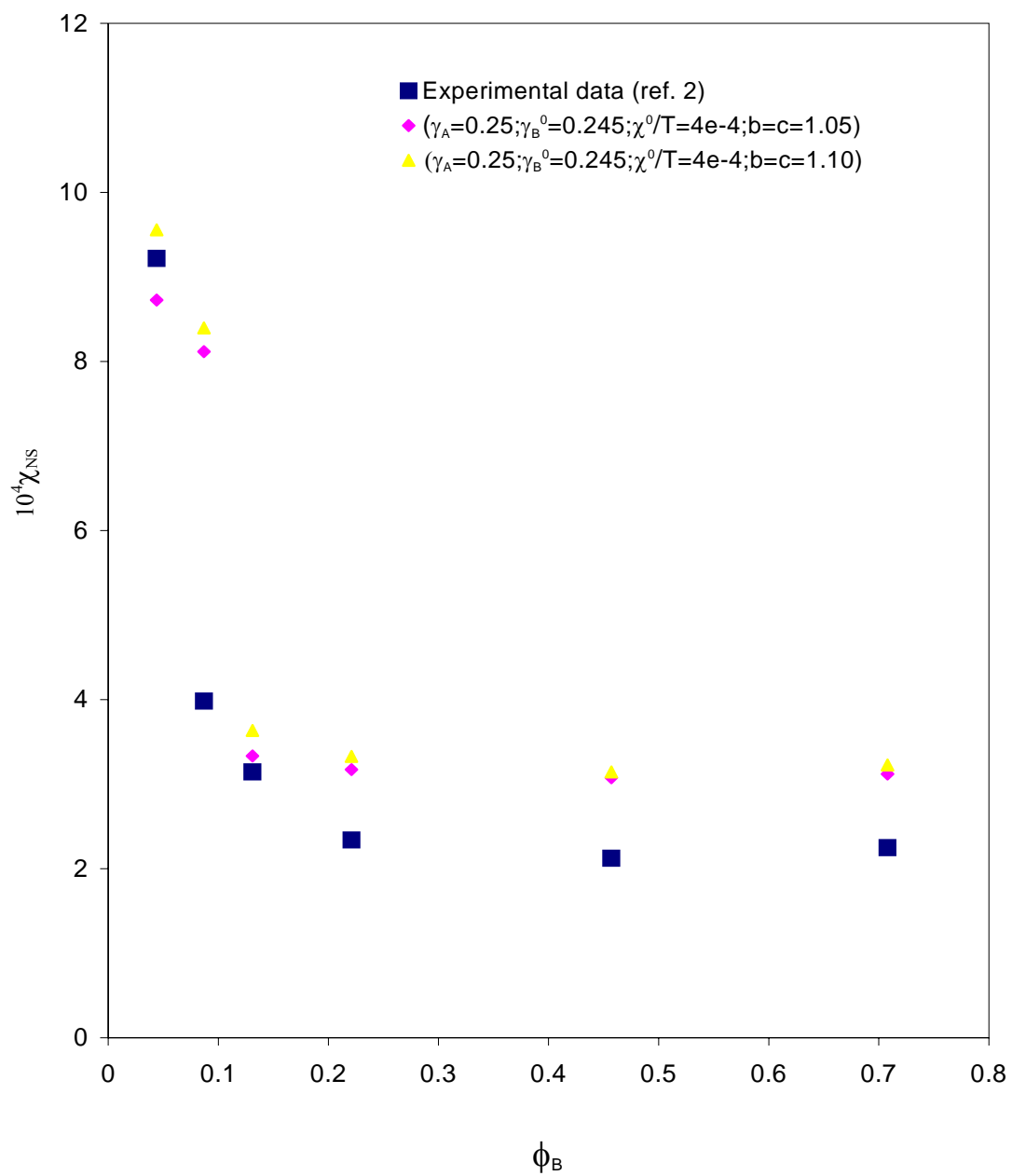


Figure 4.3. Interaction parameters from SANS for PE/DPE at 155 °C.

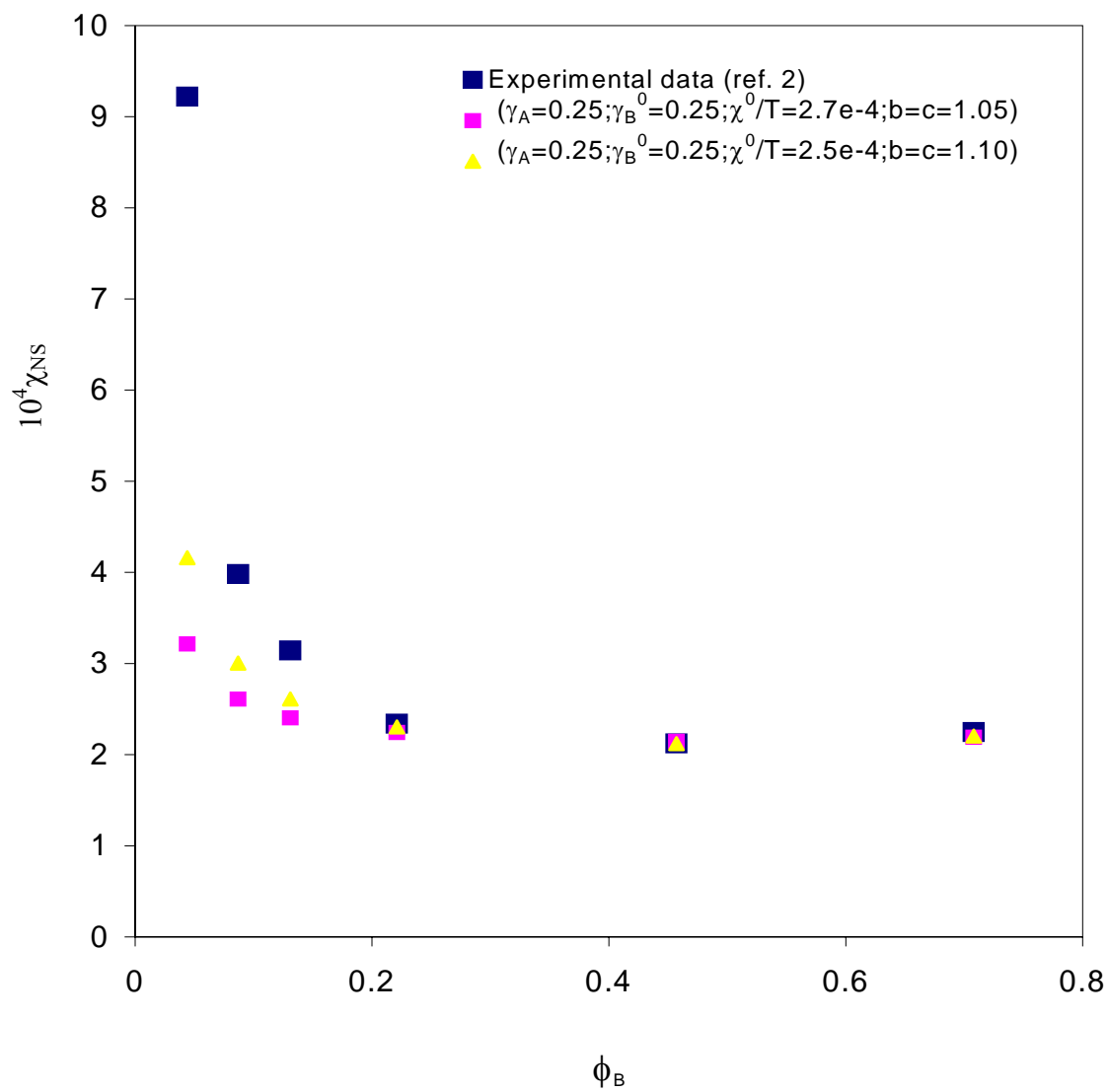


Figure 4.4. Interaction parameters from SANS for PE/DPE at 155 °C.

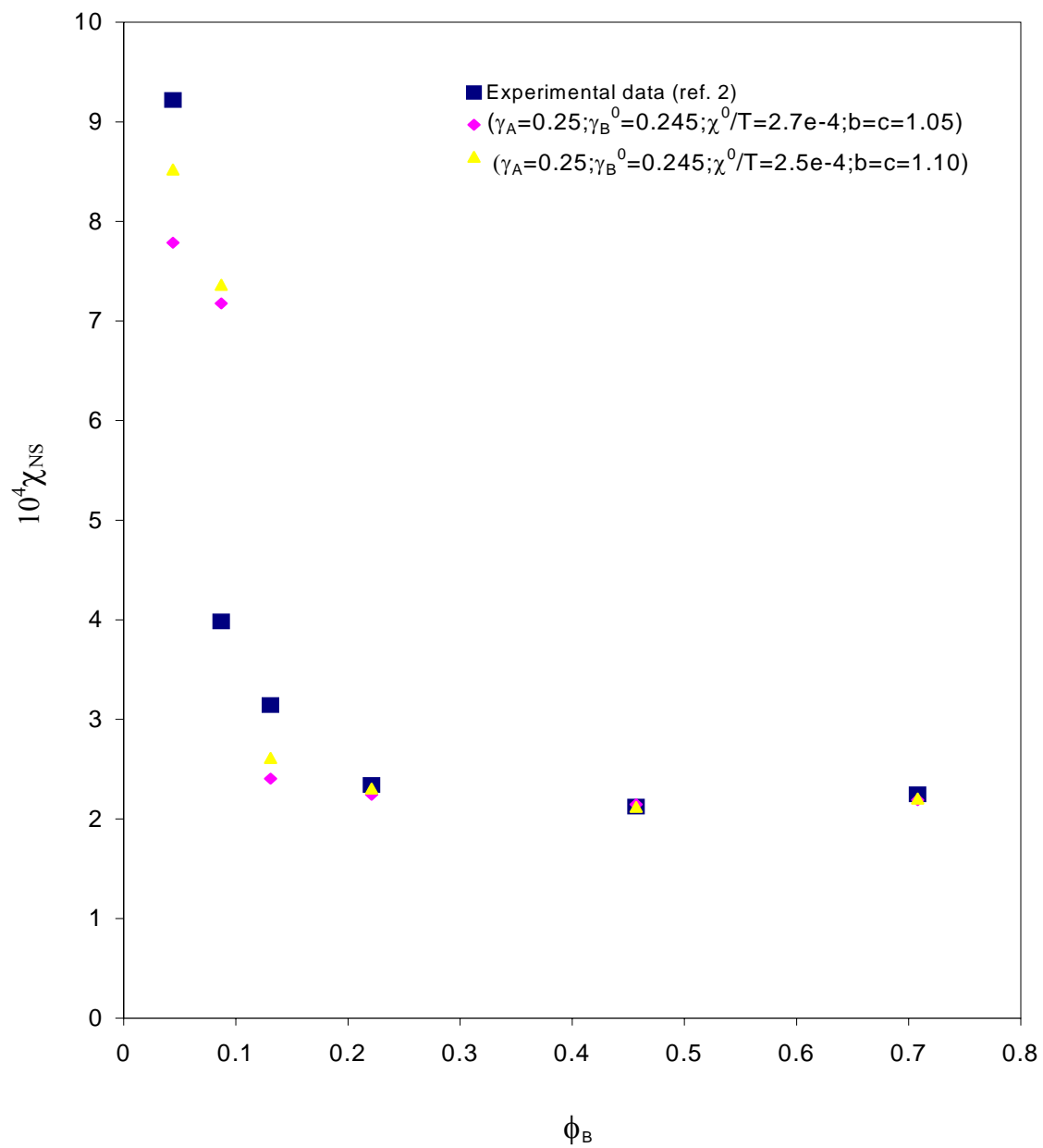


Figure 4.5. Interaction parameters from SANS for PE/DPE at 155 °C.

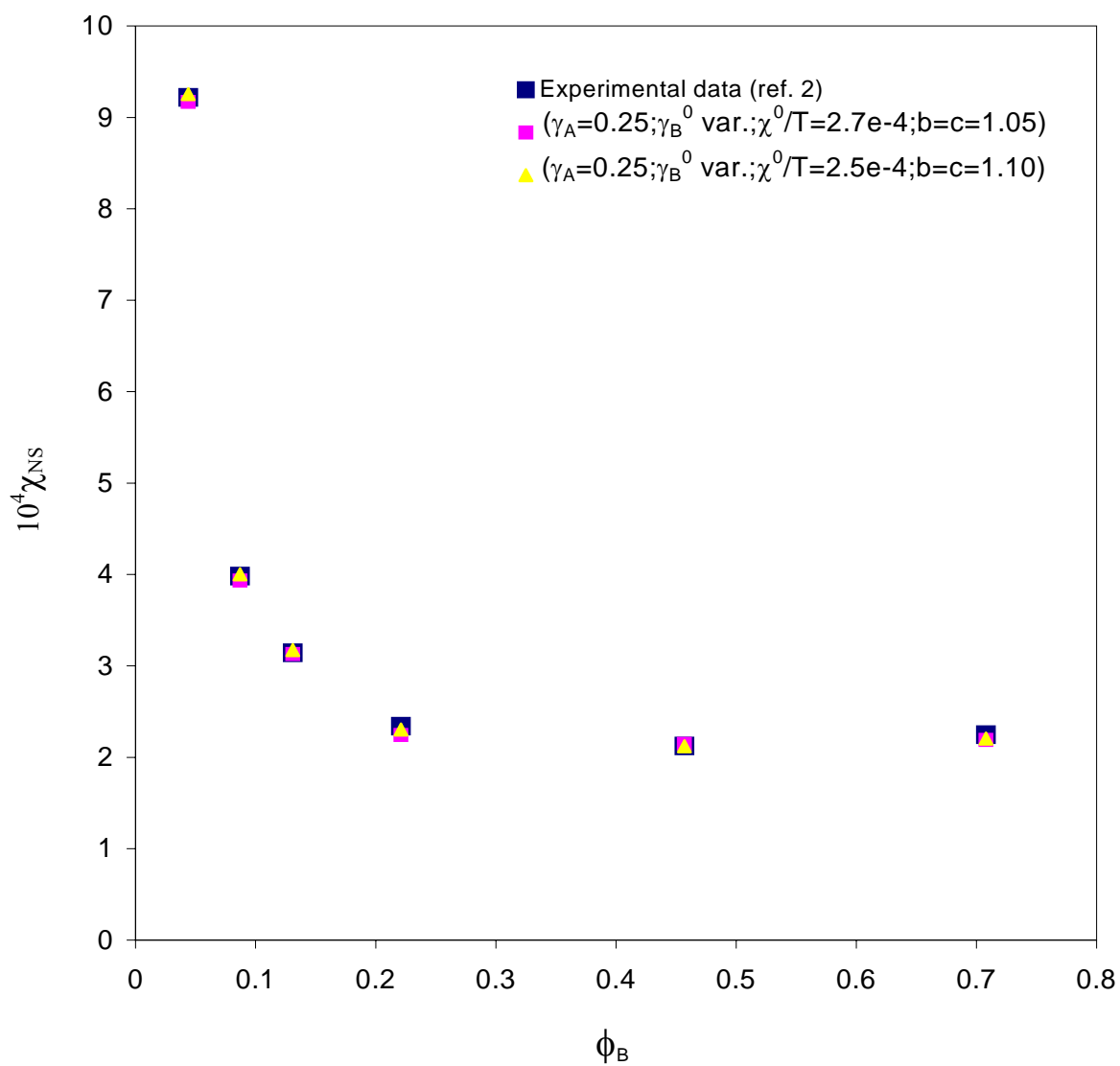


Figure 4.6. Interaction parameters from SANS for PE/DPE at 155 °C.

c	a	b	ϕ_B	γ_A	γ_A^0	γ_B	γ_B^0	% diff.
1.05	1.00	1.05	0.044	0.2500	0.2442	0.2500		-2.32
			0.087		0.2472			-1.12
			0.131		0.2480			-0.80
1.10	1.00	1.10	0.044	0.2500	0.2446	0.2500		-2.16
			0.087		0.2476			-0.96
			0.131		0.2482			-0.72
1.05	1.00	1.05	0.044	0.2500	0.2558	0.2500		2.32
			0.087		0.2528			1.12
			0.131		0.2520			0.80
1.10	1.00	1.10	0.044	0.2500	0.2555	0.2500		2.20
			0.087		0.2524			0.96
			0.131		0.2518			0.72

Table 4.1. Variations in the screening factor of *component A* for $a=1$.

Initially it was only considered lowering the value of one of the screening factors while keeping the other constant, however it soon became clear that there was an almost perfect symmetry around the original starting value (in this case 0.25). Both sets of values are therefore being reported here in table 4.1. The last column of table 4.1 lists the deviation of the screening factor as defined by:

$$\%diff. \equiv \frac{\gamma_i^0 - \gamma_{i,original}}{\gamma_{i,original}} \times 100\% \quad (26)$$

In all of the cases reported the screening factor for *component B* was kept constant ($\gamma_B = 0.25$) over the entire concentration range, whereas the screening factor for *component A* was allowed to vary as needed in the A-rich concentration range ($\phi_B < 0.15$). In the intermediate concentration range ($\phi_B > 0.15$) the screening factor for *component A* is kept constant at 0.25. As it turns out, the changes needed to get an almost perfect fit to the experimental data were very small. As it can be seen in table 4.1, the changes needed to get a perfect fit varies from 2.5 % to less than 1 %. Although the differences are apparently small, there seems to be trend that the changes needed become smaller with increasing error (c). It can also be noted that it takes more of a change in the screening factor, as ϕ_B approaches zero, although it is again small differences. Since they are all alike, it was decided to show just one example of how these results compare with the experimental data, which is depicted in figure 4.6. A similar set of calculations were done where the screening factor of *component A* was kept constant ($\gamma_A = 0.25$) over the entire concentration range, whereas the screening factor for *component B* was allowed to

vary as needed in the A-rich concentration range ($\phi_B < 0.15$). In the intermediate concentration range ($\phi_B > 0.15$) the screening factor for *component B* was kept constant at 0.25. The results are listed in table 4.2, and once again it can be seen that the changes needed to get a good fit to the experimental data are very small. In fact the changes are almost identical with those reported in table 4.1, which might be explained by the symmetry of equation 10.

Similarly it can also be assumed that all the experimental errors stems from the determination of the molecular weight, N . In this case the determination of the structure factor, $S(q)$, is assumed to be perfect, or in other words $a=c$ and $b=1$. As in the previous case where $a=1$, the changes needed to get a perfect fit are very small, ranging between 2.5 % and less than 1 %. It is clear from table 4.3 that there is symmetry around the original starting value for *component A* ($\gamma_A = 0.25$). Now if these results are compared with those in table 4.1, it appears that they are very similar, although the ones in table 4.1 might be a little higher. In the case where the screening factor for *component B* was allowed to vary the differences are again very small, as seen in table 4.4, and almost identical to those in table 4.3.

From the results reported above one could argue that the error function (c) is somewhat mute, which led to the question what would happen if it was ignored (i.e. set $c=1$)? In this case another twist was put into the calculations by allowing one of the screening factor to vary over the entire concentration range, while keeping the other constant. As it can be seen in both table 4.5 and table 4.6, the values are almost identical to those reported in tables 4.1-4.4. These results leads to the conclusion that the model presented earlier is very capable of reproducing the experimental data, by making just a

c	a	b	ϕ_B	γ_A	γ_A^0	γ_B	γ_B^0	% diff.
1.05	1.00	1.05	0.044	0.2500		0.2500	0.2443	-2.28
			0.087				0.2473	-1.08
			0.131				0.2480	-0.80
1.10	1.00	1.10	0.044	0.2500		0.2500	0.2446	-2.16
			0.087				0.2476	-0.96
			0.131				0.2482	-0.72
1.05	1.00	1.05	0.044	0.2500		0.2500	0.2559	2.36
			0.087				0.2528	1.12
			0.131				0.2521	0.84
1.10	1.00	1.10	0.044	0.2500		0.2500	0.2555	2.20
			0.087				0.2524	0.96
			0.131				0.2518	0.72

Table 4.2. Variations in the screening factor of *component B* for $a=1$.

c	a	b	ϕ_B	γ_A	γ_A^0	γ_B	γ_B^0	% diff.
1.05	1.05	1.00	0.044	0.2500	0.2444	0.2500		-2.24
			0.087		0.2473			-1.08
			0.131		0.2480			-0.80
1.10	1.10	1.00	0.044	0.2500	0.2449	0.2500		-2.04
			0.087		0.2478			-0.88
			0.131		0.2484			-0.64
1.05	1.05	1.00	0.044	0.2500	0.2557	0.2500		2.28
			0.087		0.2527			1.08
			0.131		0.2520			0.80
1.10	1.10	1.00	0.044	0.2500	0.2551	0.2500		2.04
			0.087		0.2522			0.88
			0.131		0.2516			0.64

Table 4.3. Variations in the screening factor of *component A* for $b=1$.

c	a	b	ϕ_B	γ_A	γ_A^0	γ_B	γ_B^0	% diff.
1.05	1.05	1.00	0.044	0.2500		0.2500	0.2444	-2.24
			0.087				0.2473	-1.08
			0.131				0.2480	-0.80
1.10	1.10	1.00	0.044	0.2500		0.2500	0.2450	-2.00
			0.087				0.2478	-0.88
			0.131				0.2484	-0.64
1.05	1.05	1.00	0.044	0.2500		0.2500	0.2558	2.32
			0.087				0.2528	1.12
			0.131				0.2521	0.84
1.10	1.10	1.00	0.044	0.2500		0.2500	0.2552	2.08
			0.087				0.2522	0.88
			0.131				0.2516	0.64

Table 4.4. Variations in the screening factor of *component B* for $b=1$.

c	a	b	ϕ_B	γ_A	γ_A^0	γ_B	γ_B^0	% diff.
1.00	1.00	1.00	0.044		0.2439	0.2500		-2.44
			0.087		0.2468			-1.28
			0.131		0.2476			-0.96
			0.221		0.2489			-0.44
			0.457		0.2503			0.12
			0.708		0.2509			0.36
1.00	1.00	1.00	0.044		0.2562	0.2500		2.48
			0.087		0.2532			1.28
			0.131		0.2524			0.96
			0.221		0.2511			0.44
			0.457		0.2503			0.12
			0.708		0.2491			-0.36

Table 4.5. Variations in the screening factor of *component A* for $c=1$.

c	a	b	ϕ_B	γ_A	γ_A^0	γ_B	γ_B^0	% diff.
1.00	1.00	1.00	0.044	0.2500			0.2439	-2.44
			0.087				0.2469	-1.24
			0.131				0.2477	-0.92
			0.221				0.2489	-0.44
			0.457				0.2504	0.16
			0.708				0.2509	0.36
1.00	1.00	1.00	0.044	0.2500			0.2563	2.52
			0.087				0.2532	1.28
			0.131				0.2524	0.96
			0.221				0.2511	0.44
			0.457				0.2504	0.16
			0.708				0.2491	-0.36

Table 4.6. Variations in the screening factor of *component B* for $c=1$.

very little change in one of the screening factors. This is done without introducing an artificial error function, as suggested by Crist et al¹.

4.5. Conclusions

A simple revised form of the traditional Flory-Huggins model was introduced, which among other things accounts for the screening of interaction sites, which presumably occurs when two polymers are mixed. In the reported results the system in question was a mixture of Polyethylene (PE) and deuterated Polyethylene (DPE), for which experimental data were reported by Londono et al.². Although this system (presumably?) lacks any strong specific interactions, it still provides a good insight to the dynamics of a polymer blend.

In theory the model presented here has five "adjustable" parameters. However, two of them (γ_A and γ_B) are component specific and should be constant, or in case they are not, at least their concentration dependence should be known. The third parameter χ^0 is fixed in all the calculations, although it takes on different values depending on the value of the error function c , which is defined by the two final parameters (a and b). Calculations are presented with varying values of the error function (although it was kept constant for each set of calculations).

The results presented, appears to be very symmetrical and almost interchangeable. This may just be a reflection of the system investigated, but it could also be explained by the symmetry of the model. In any case it was shown that minor changes in one of the screening factors alone could explain the curvature of the interaction parameter that has been observed, even in systems where this would not be expected. It is worth noticing that even without the somewhat artificial error function c , the model is still capable of

reproducing the experimental results with changes in one of the screening factors that are less than 3%.

4.6. References

1. Crist, B. *Macromolecules*, **31**, 5853 (1998)
2. Londono, J.D.; Narten, A.H.; Wignall, G.D.; Honnell, K.G.; Hsieh, E.T.; Johnson, T.W.; Bates, F.S. *Macromolecules*, **27**, 2864 (1994)
3. Melenkevitz, J.; Crist, B.; Kumar, S.K. *Macromolecules*, **33**, 6869 (2000)
4. Huggins, M.L. *Ann. N.Y. Acad. Sci.*, **49**, 9 (1942)
5. Guggenheim, E.A. *Mixtures*, Clarendon, Oxford, 1952
6. Painter, P.C.; Veytsman, B.; Kumar, S.; Shenoy, S.; Graf, J.F.; Xu, Y.; Coleman, M.M. *Macromolecules*, **30**, 932 (1997)
7. Painter, P.C.; Berg, L.P.; Veytsman, B.; Coleman, M.M. *Macromolecules*, **30**, 7529 (1997)
8. Sanchez, I.C. *Polymer*, **30**, 471 (1989)

Chapter 5

Thermodynamics in Statistical Copolymer Blends

5.1. Introduction

As mentioned in the previous chapter most polymers are not miscible, so when they are mixed it usually leads to multiphase systems. The properties of such systems are depending on the composition as well as the size and arrangement of these phases among other things. How, why and when the polymers mix in the melt state is essential knowledge when deciding on which polymers to use. Thermodynamics is a valuable tool when looking for answers to most if not all of these questions.

In the pursuit of improving the characteristics of existing polymers as well as developing new high performing polymers, various permutations of polymers have been synthesized, including copolymers.

A copolymer contains two or more different types of components (monomer units), which could vary from isomeric units of the same monomer, such as 1,2 (poly)-isobutylene and 1,4 (poly)-isobutylene, to monomers of differing nature such as (poly) ethyl methacrylate and (poly) 4-vinyl phenol, which has been the subject of much investigation by Coleman and Painter¹.

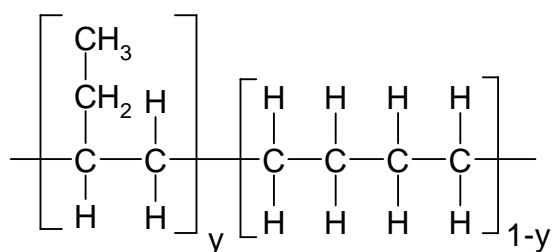
Copolymers can be categorized in one of three major classes. In a block copolymer several segments (or blocks) of the same monomer unit succeed each other followed by several segments of a different type of monomer. In an alternating copolymer, the two monomer components alternate. The final major class of copolymers

is the so-called random copolymers. As the name implies the two monomer components are randomly distributed throughout the copolymer. These are often also referred to as statistical copolymers, and they are also the only ones that will be dealt with in this chapter.

In fact it was results from studies of mixtures containing copolymers such as ethyl methacrylate-*stat*-4-vinylphenol¹ that were the direct inspiration for this as well as the preceding work, as has been mentioned in the past.

Two polymers are said to be "semicompatible" when "their blend has a critical temperature for phase separation, T_c , between the glass transition temperature, T_g , and the thermal degradation temperature, T_d "². Blend systems of the type $P(A_{y_1}B_{1-y_1})/P(A_{y_2}B_{1-y_2})$, where the components are statistical copolymers of the same monomer pair, A and B, always forms semicompatible copolymers, even when the corresponding homopolymers are incompatible.²

In a number of papers Graessley et al.³⁻⁵ investigated a series of copolymer blends. The components investigated were statistical copolymers, A_yB_{1-y} , of hydrogenated polybutadienes, consisting of branched-C₄ and linear-C₄ co-units.



The copolymers were distinguished through deuterium labeling and Small Angle Neutron Scattering (SANS) was used to extract experimental data for the interaction parameter, χ_{NS} . They found that the experimentally determined interaction parameter was not depending on the chain length of the polymer and the component volume fraction in one case. In this study it was also concluded that the interaction parameter was inversely depending on the temperature, obeying the following relationship:

$$\chi = \frac{A}{T} + B \quad (1)$$

where the appropriately chosen values of the coefficients A and B yielded Upper Critical Solution Temperature (UCST) behavior.⁵ In a later study³ with the same copolymers, the concentration dependence of the interaction parameter was revisited. It was noted that there was a significant upturn in χ at the composition extremes, which would diminish with increasing temperature.

5.2. Interaction Parameters in Copolymers

In the previous chapter the following expression was presented for the spinodal condition interaction parameter, χ_{SC} :

$$\begin{aligned}
\chi_{SC} &= \chi_{SC}^E + \chi_{SC}^{exc} \\
&= \left(\frac{(1-\gamma_A)^2(1-\gamma_B)^2}{(1-\gamma_A\phi_A - \gamma_B\phi_B)^3} \right) (\chi_{bare}) \\
&\quad + \frac{1}{2\gamma_A\gamma_B} \left[\frac{(\gamma_A - \gamma_B)^2}{1-\gamma_A\phi_A - \gamma_B\phi_B} \right] + \frac{1}{2} \left[\frac{(1-\gamma_A)(1-\gamma_B)}{\gamma_A\gamma_B} \right] \left[\frac{\gamma_A - \gamma_B}{1-\gamma_A\phi_A - \gamma_B\phi_B} \right]^2
\end{aligned} \tag{2}$$

If the nomenclature of Crist⁶ is adopted, this theoretically determined interaction parameter, χ_{SC} , can be expressed in terms of the experimentally determined interaction parameter from SANS, χ_{NS} , as:

$$N' \chi_{NS} = \frac{N\chi_{sc}}{c} + \frac{c-1}{c} \frac{1}{2\phi_A\phi_B} \tag{3}$$

The premise of this approach is that the discrepancies found between experimentally determined values of the interaction parameter, χ_{NS} , and the so-called thermodynamic interaction parameter, χ_{SC} , which is derived from theory, can be explained through the combined error function parameter, c .

Although these equations strictly speaking were developed for homopolymer blends, they should be equally valid for blends of copolymers. In equation 2, A and B represents homopolymers A and B, respectively. However, if the copolymers initially are treated as homopolymers, for the sake of simplicity, then equations 2 and 3 could be applied for copolymer blends as well, with a few modifications.

Using the terminology of Graessley et al.⁴ the following relationship can be written between the interaction parameter of a binary copolymer blend and the interaction parameter of the corresponding homopolymers:

$$\chi(y_1, y_2) = (y_2 - y_1)^2 \chi_{1/2} \quad (4)$$

where $\chi_{1/2}$ is the interaction parameter of the blends of homopolymer 1 and homopolymer 2. If equation 4 above holds true then it would be expected that $\chi / \Delta y^2$ would “be independent of both the difference in copolymer composition, $\Delta y = y_2 - y_1$, and the composition average, $\bar{y} = (y_1 + y_2) / 2$, for any pair of components investigated”⁴.

This leads to the change in equation 2 that is necessary in order to make it valid for copolymers. By accounting for the various types of interactions that exists in $P(A_x B_{1-x}) / P(C_y D_{1-y})$ copolymer mixtures, of which $P(A_{y_1} B_{1-y_1}) / P(A_{y_2} B_{1-y_2})$ also belongs, it can be shown that the energetic part of the interaction energy in equation 2 be expressed as:

$$\chi_{SC}^E = \left(\frac{(1 - \gamma_A)^2 (1 - \gamma_B)^2}{(1 - \gamma_A \phi_A - \gamma_B \phi_B)^3} \right) (\chi_{bare}) (y_1 - y_2)^2 \quad (5)$$

The derivation of this expression can be found in appendix F.

5.3. Results and Discussion

Once again it was decided to investigate how much different γ_B would have to be from γ_A in order to get a good correspondence to experimental data as determined by Graessley et al.³. In fact two series of calculations were performed in one the value of γ_A was fixed while changing the value of γ_B , and in another the value of γ_B was fixed while the value of γ_A was changed. In Graessley et al.'s work³⁻⁵ the copolymers investigated were so similar that the values of γ_A and γ_B would be expected to be almost identical. The nomenclature used in their work describes the composition of the copolymer, so H97 is a hydrogenated polybutadiene (HPB) in which 97 % of the segments are 1,2-enchainments ($y=0.97$). Similarly D97 is the deuterated version of the corresponding copolymer.

Although these components actually are copolymers, they will initially be treated as homopolymers in this analysis. Initially the γ -value of each of the components was kept constant over the entire concentration range for (at a value of 0.25; $\gamma_A = \gamma_B = 0.25$). The value of χ_{bare} was arbitrarily set to be equal to a minimum value of $4 \cdot 10^{-4}$ at 167 °C, so that:

$$\chi_{bare} = \left(\frac{440.15}{T + 273.15} \right) * (4 \cdot 10^{-4}) \quad (6)$$

But clearly as one can tell from figure 5.1, the predicted values of the interaction parameter is well below the experimental values reported by Graessley³ and without the same curvature.

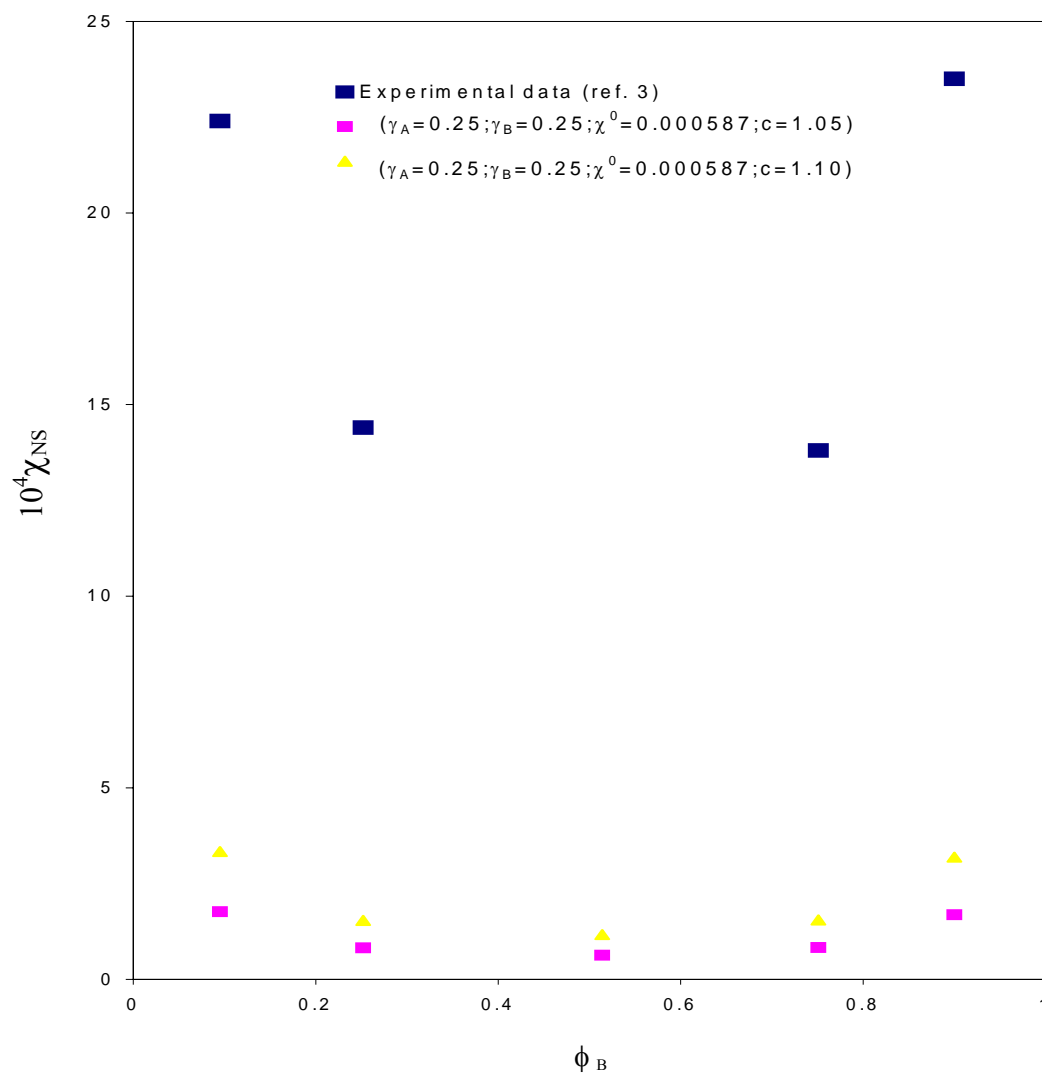


Figure 5.1. Interaction parameters from SANS for H97/D88 at 27 °C, with constant (and identical) screening factors for the two components.

Considering the structural similarity between the two components, it was assumed that the screening factor would be very similar for the two components. However, what would happen if one of the screening factors were altered, while keeping the other constant? This was a question worth investigating, so it was decided to keep one of the γ -values constant while investigating how much the other γ -value would have to be altered to get a good fit. A less than 5% change in one of the screening factors, or 4% to be exact, was considered a conservative estimate, and so calculations were done in which one of the screening factors were held constant at 0.25 while the other was held constant at 0.24. Even with this rather conservative change in one of the screening factors, it is evident from both figure 5.2 and figure 5.3 that the predicted values of the interaction parameter are now above the reported experimental values except at the extremities.

When compared with figure 5.1, the difference is significant. However, it is also clear that the predicted values are "flatter" than the experimental values determined by SANS. So even though the predicted values of the interaction parameter appear to be closer to the reported experimental values, the model can still not reproduce the apparent curvature with the present parameters.

The only difference between the results reported in figure 5.2 and figure 5.3 is that in the former $\gamma_A = 0.25$ and $\gamma_B = 0.24$, while in the latter it is the reverse case ($\gamma_A = 0.24$ and $\gamma_B = 0.25$). From the two figures it can also be deducted that the components are almost "interchangeable", in the sense that there is a very little difference, if any, between the results reported. This again may not be too surprising considering the symmetry of the model.

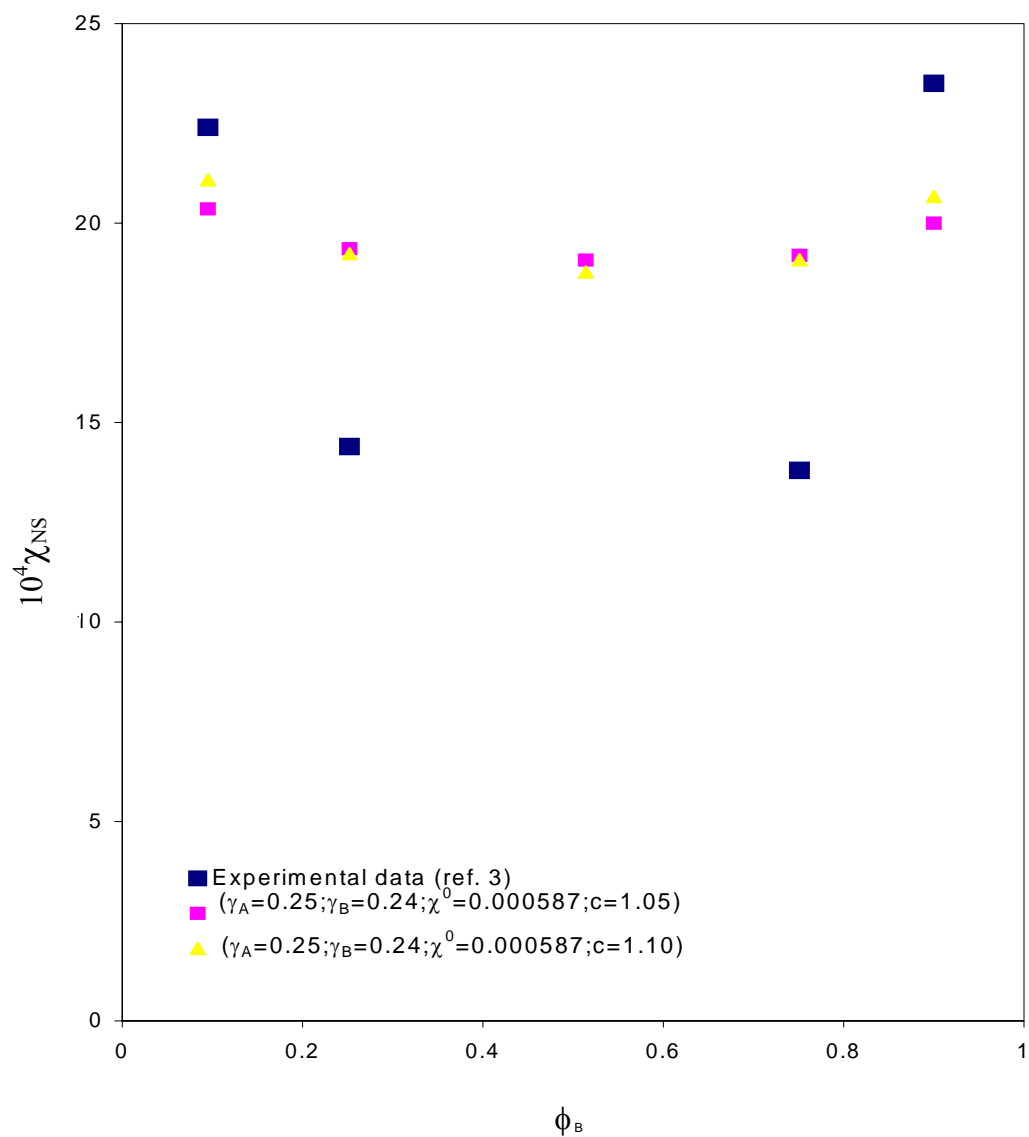


Figure 5.2. Interaction parameters from SANS for H97/D88 at 27 °C, with varying screening factors for the two components.

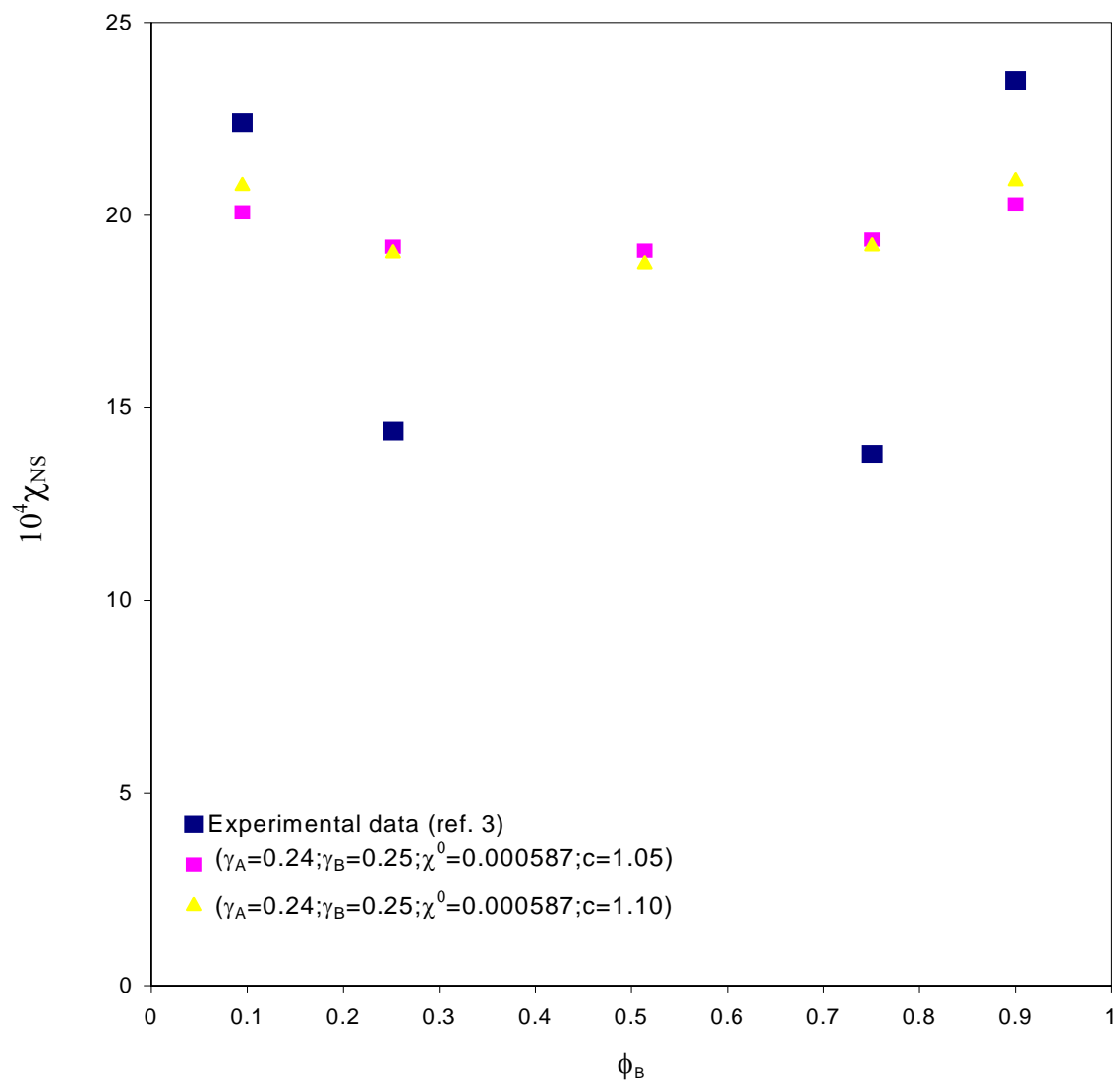


Figure 5.3. Interaction parameters from SANS for H97/D88 at 27 °C, with varying screening factors for the two components.

The same trend is observed for the same system at various temperatures, as is evident from figure 5.4. In this case the discrepancy between the predicted and experimental interaction parameters appears to be much less than at the lower temperature depicted in figures 5.1-5.3.

In figure 5.5 the γ -value was altered from that in figures 5.1-5.4. However, the significance of this change is not overwhelming. Even though the magnitude of the upturn in the value of χ at the composition extremes is supposedly diminished with increasing temperature, that does not appear to apply with this set of data.

It would be expected that the composition of each of the copolymers would influence the value of the screening factor. The composition dependence of γ for the copolymer was accounted for through the following equations:

$$\begin{aligned}\gamma_A &= y_1 \gamma_A^{raw} + (1 - y_1) \gamma_B^{raw} \\ \gamma_B &= y_2 \gamma_A^{raw} + (1 - y_2) \gamma_B^{raw}\end{aligned}\tag{7}$$

As it can be seen from figure 5.6 it is possible to reproduce the experimental data. In figure 5.6 γ_A^{raw} was kept constant, while the value of γ_B^{raw} was allowed to change in order to fit the experimental data. The values of γ_B^{raw} that are needed to get a good agreement with experimental data are given in table 5.1, where the error factor is 5 % ($c=1.05$). Even though there is a bigger difference between the "raw" values, than the 4 % mentioned previously, the resulting values for the two copolymers actually still fall within this range.

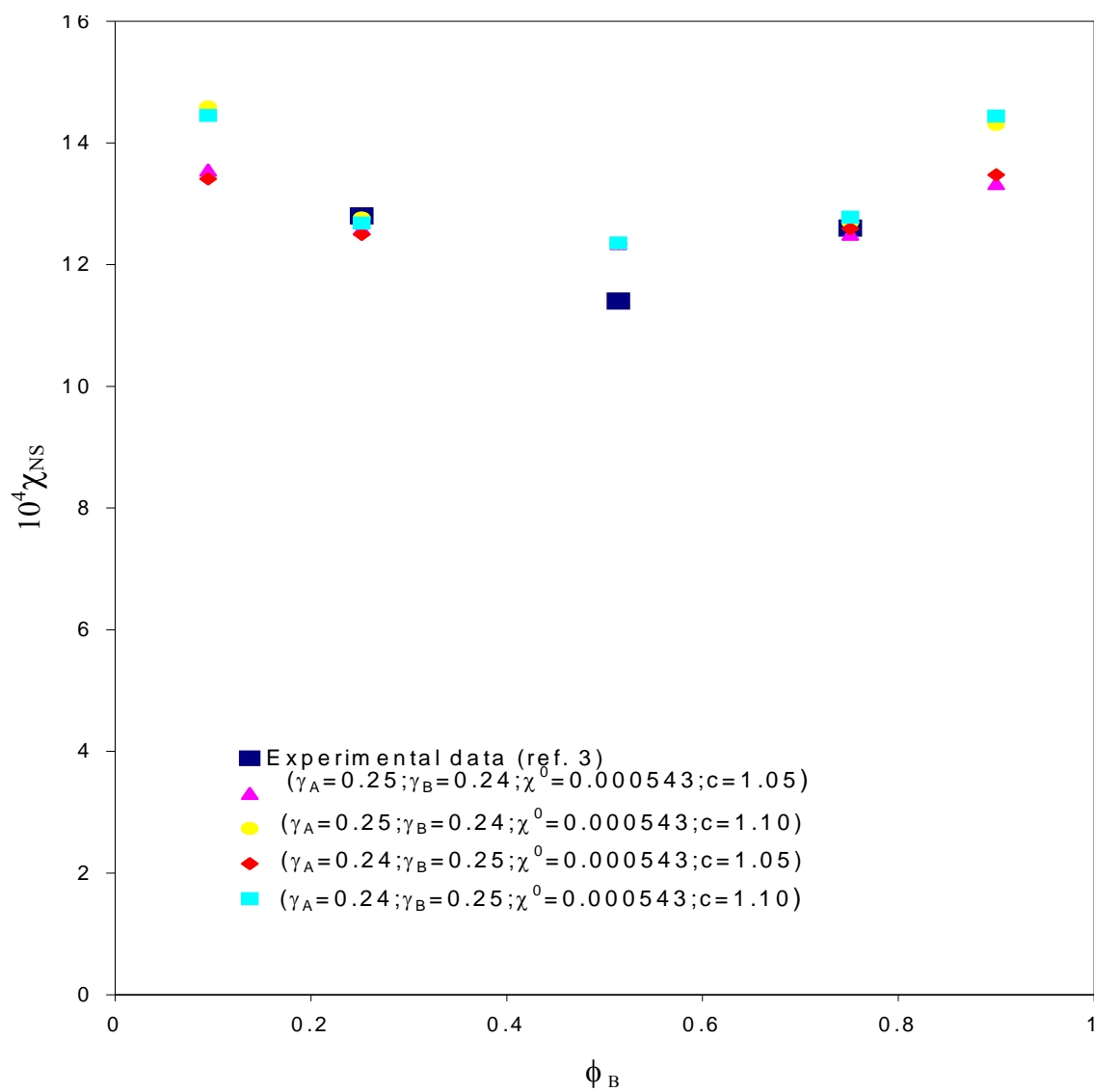


Figure 5.4. Interaction parameters from SANS for H97/D88 at 51 °C, with varying screening factors for the two components.

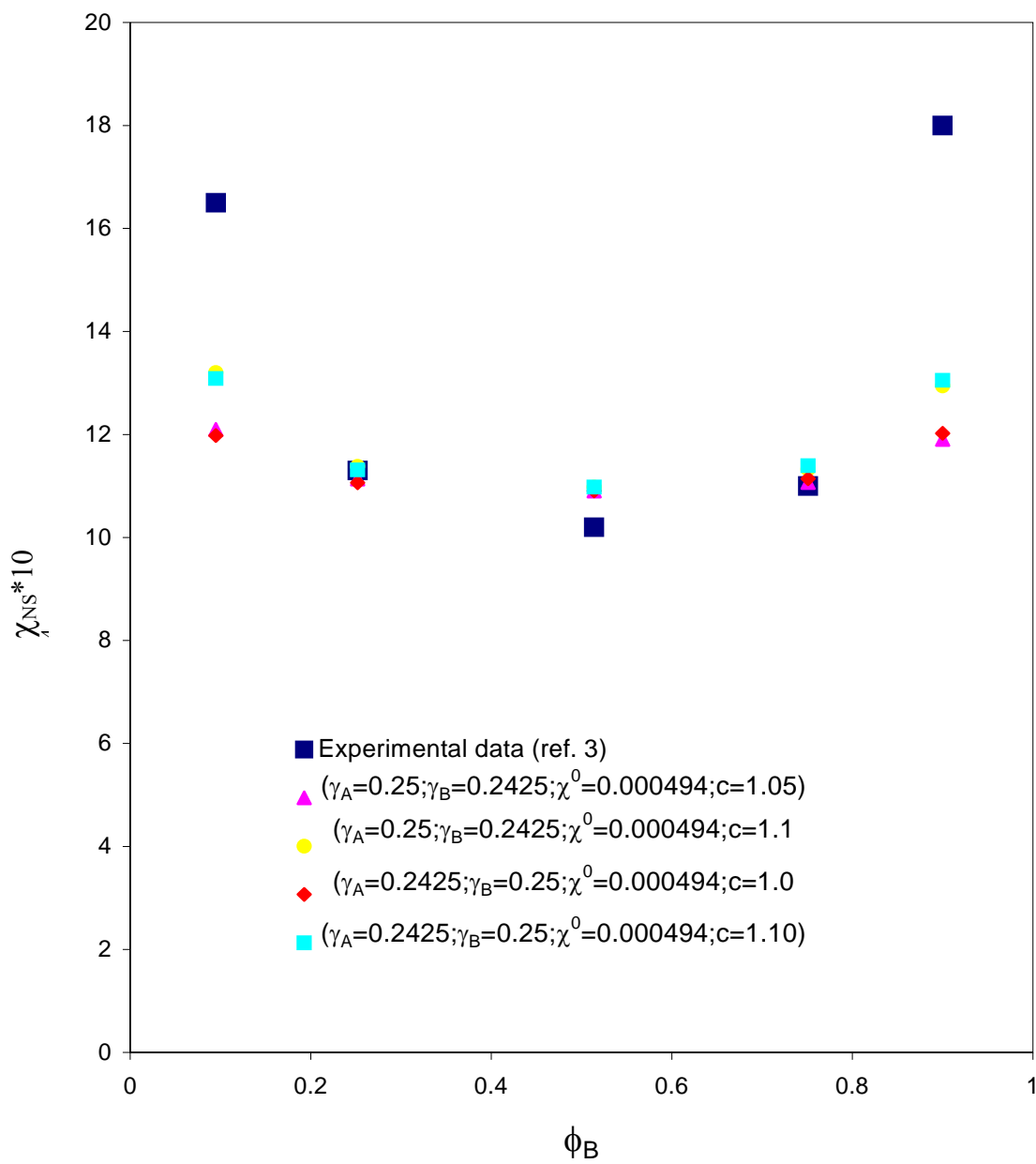


Figure 5.5. Interaction parameters from SANS for H97/D88 at 83 °C, with varying screening factors for the two copolymers.

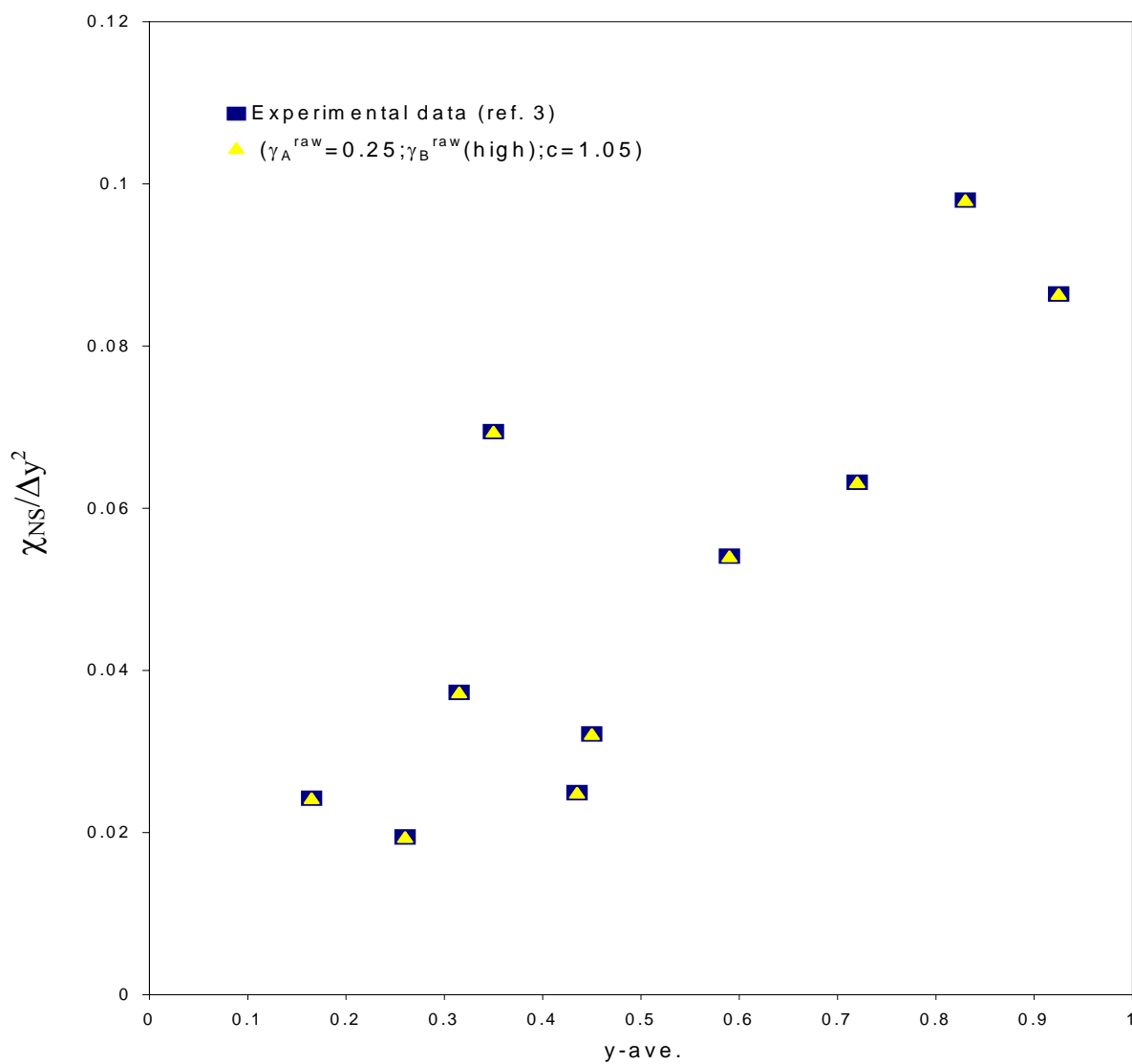


Figure 5.6. Interaction parameters from SANS for various copolymers at 167 °C, with varying screening factors

y_1	y_2	\bar{y}	γ_A^{raw}	γ_B^{raw}	γ_A	γ_B
0.97	0.88	0.925	0.25	0.31779	0.252	0.2581
0.88	0.78	0.83	0.25	0.32514	0.259	0.2665
0.78	0.66	0.72	0.25	0.31103	0.2634	0.2708
0.66	0.52	0.59	0.25	0.30797	0.2697	0.2778
0.52	0.38	0.45	0.25	0.29373	0.271	0.2771
0.52	0.35	0.435	0.25	0.2884	0.2684	0.275
0.38	0.32	0.35	0.25	0.31221	0.2886	0.2923
0.38	0.25	0.315	0.25	0.29853	0.2801	0.2864
0.35	0.17	0.26	0.25	0.28403	0.2721	0.2782
0.25	0.08	0.165	0.25	0.28917	0.2794	0.286

Table 5.1. "High" variations in the "raw" screening factor of component *B* for $c=1.05$ at 167°C .

It was also found that there was a second set of values of γ_B^{rav} that would result in equally good agreement with experimental data, as evident from figure 5.7. This set of values is listed in table 5.2. Once again the resulting values for the fraction of same chain contacts for the two copolymers falls within the 4 % range.

The error factor seems to have little if any affect on the γ -values that were needed to get a good agreement with experimental data. This can be seen in figure 5.8 and table 5.3, respectively. Here the error factor is 10 % ($c=1.10$), but the resulting γ -values of the two copolymers are almost identical with those found when $c=1.05$.

If γ_A^{rav} is now allowed to change, while keeping γ_B^{rav} constant, a similar set of data is obtained. The results are listed in table 5.4-5.6. Although the differences between the resulting γ -value of the two copolymers are still within the 4 % range, it can be seen that the actual values are very different. As anticipated from the beginning, it became clear that the screening factor, γ_i , would have to depend on concentration to some extent, or at the very least it was expected that the value at very dilute concentrations would differ from that in the more concentrated regime. It was clear early on that even a small change (less than 5 %) in one of the screening factors would have a tremendous effect on the results as is evident when comparing figures 5.1-5.5. This may not be too surprising since it can be explained by the contribution from the excess energy term in equation 2 (the second term on the right hand side of equation 2).

It can also be seen in figures 5.9-5.12 that the model can reproduce the temperature dependence of the interaction parameter for various blends, as indicated in equation 1. The screening factors necessary to obtain these figures are given in tables 5.7-5.10.

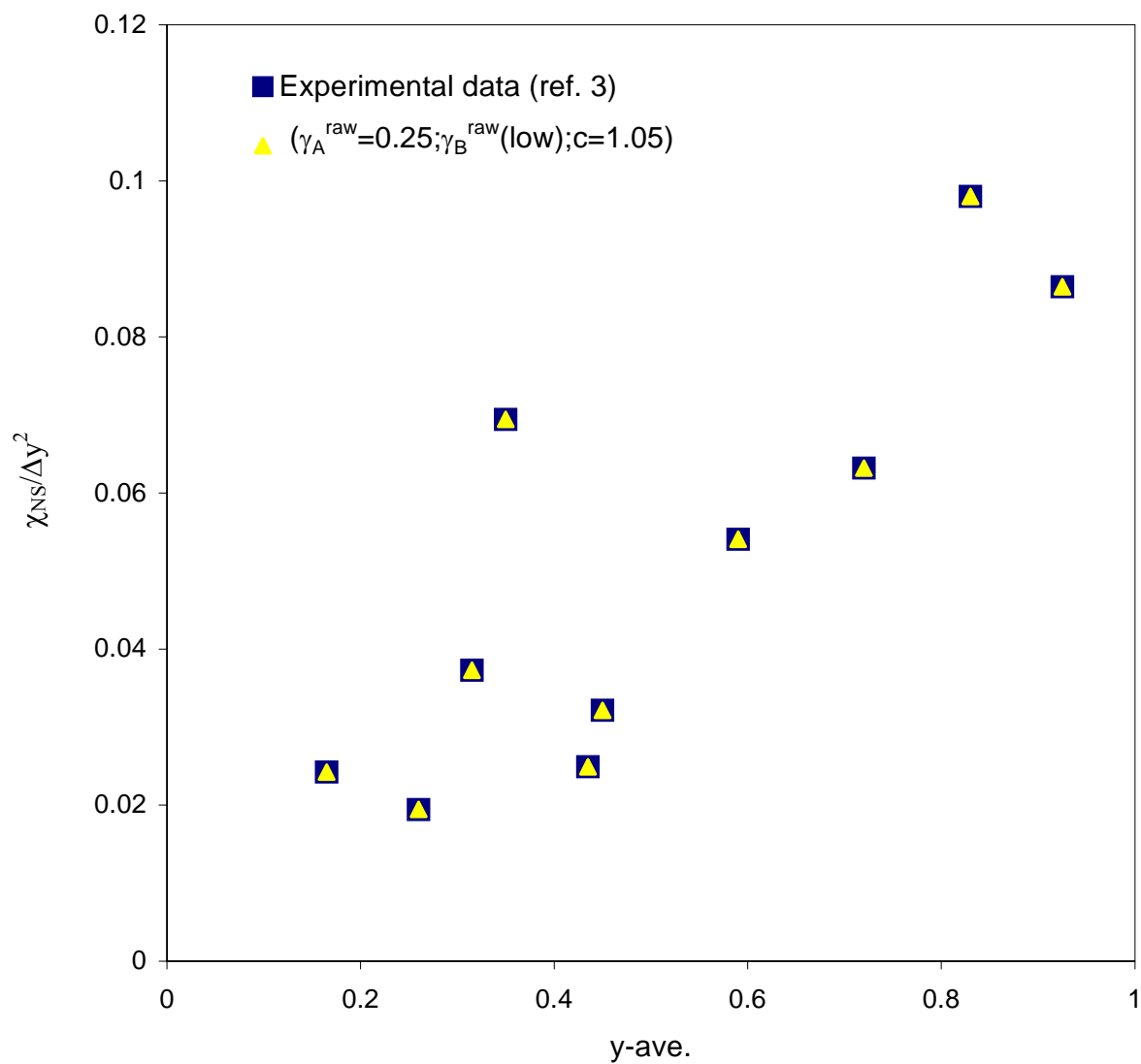


Figure 5.7. Interaction parameters from SANS for various copolymers at 167 °C, with varying screening factors

y_1	y_2	\bar{y}	γ_A^{raw}	γ_B^{raw}	γ_A	γ_B
0.97	0.88	0.925	0.25	0.18462	0.248	0.2422
0.88	0.78	0.83	0.25	0.18122	0.2417	0.2349
0.78	0.66	0.72	0.25	0.1957	0.2381	0.2315
0.66	0.52	0.59	0.25	0.20054	0.2332	0.2263
0.52	0.38	0.45	0.25	0.21276	0.2321	0.2269
0.52	0.35	0.435	0.25	0.21682	0.2341	0.2284
0.38	0.32	0.35	0.25	0.20186	0.2202	0.2173
0.38	0.25	0.315	0.25	0.21088	0.2257	0.2207
0.35	0.17	0.26	0.25	0.22122	0.2313	0.2261
0.25	0.08	0.165	0.25	0.21833	0.2262	0.2209

Table 5.2. "Low" variations in the "raw" screening factor of component B for $c=1.05$ at 167°C .

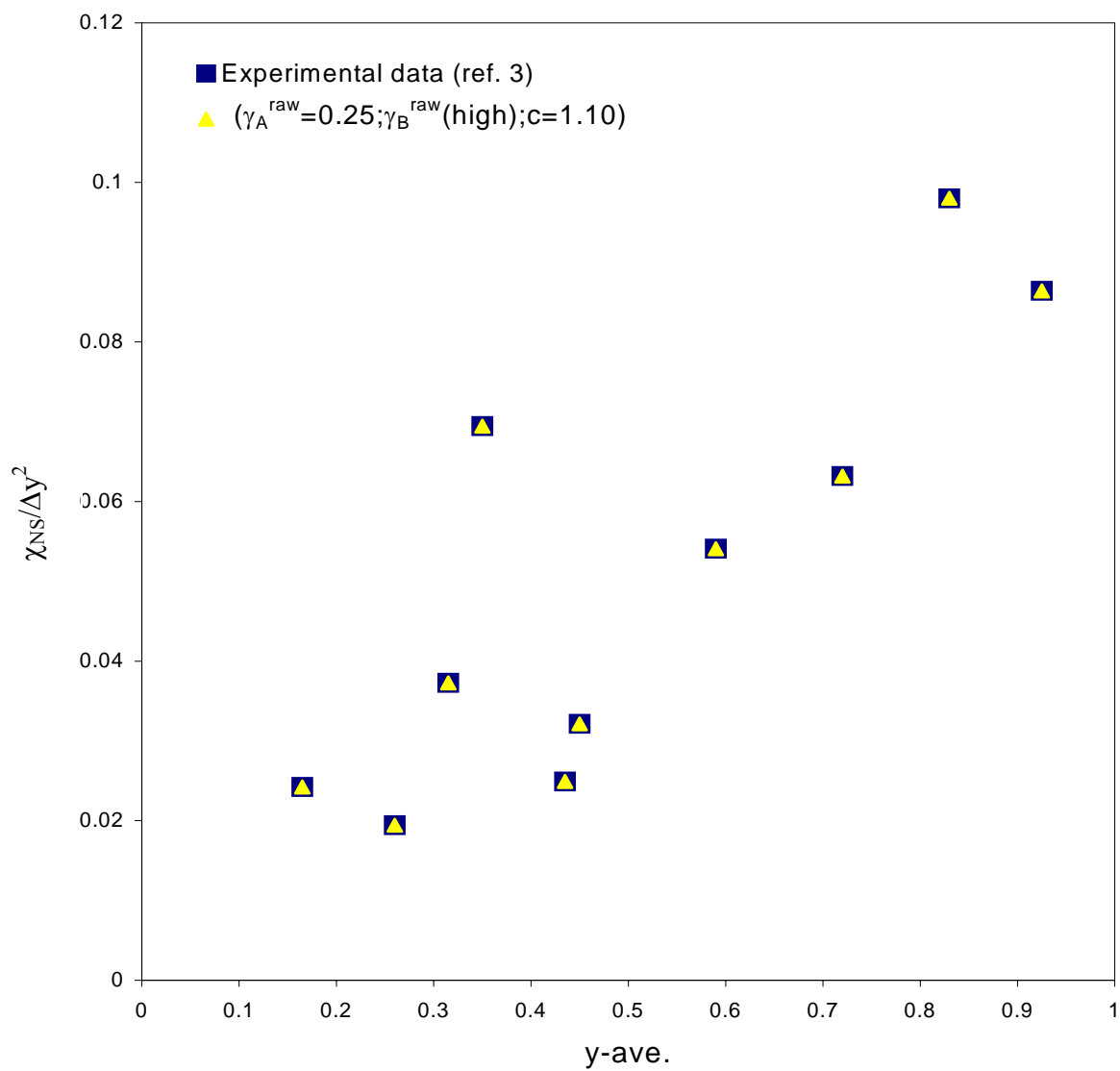


Figure 5.8. Interaction parameters from SANS for various copolymers at 167 °C, with varying screening factors

y_1	y_2	\bar{y}	γ_A^{raw}	γ_B^{raw}	γ_A	γ_B
0.97	0.88	0.925	0.25	0.31635	0.252	0.258
0.88	0.78	0.83	0.25	0.32459	0.259	0.2664
0.78	0.66	0.72	0.25	0.3104	0.2633	0.2705
0.66	0.52	0.59	0.25	0.30769	0.2696	0.2777
0.52	0.38	0.45	0.25	0.29248	0.2704	0.2763
0.52	0.35	0.435	0.25	0.28759	0.268	0.2744
0.38	0.32	0.35	0.25	0.30283	0.2828	0.2859
0.38	0.25	0.315	0.25	0.2971	0.2792	0.2853
0.35	0.17	0.26	0.25	0.28304	0.2715	0.2774
0.25	0.08	0.165	0.25	0.28826	0.2787	0.2852

Table 5.3. "High" variations in the "raw" screening factor of component B for $c=1.10$ at 167°C .

y_1	y_2	\bar{y}	γ_A^{raw}	γ_B^{raw}	γ_A	γ_B
0.97	0.88	0.925	0.3347	0.25	0.3322	0.3245
0.88	0.78	0.83	0.3406	0.25	0.3297	0.3207
0.78	0.66	0.72	0.3173	0.25	0.3025	0.2944
0.66	0.52	0.59	0.3102	0.25	0.2897	0.2813
0.52	0.38	0.45	0.2931	0.25	0.2724	0.2664
0.52	0.35	0.435	0.2877	0.25	0.2696	0.2632
0.38	0.32	0.35	0.3084	0.25	0.2722	0.2687
0.38	0.25	0.315	0.2956	0.25	0.2673	0.2614
0.35	0.17	0.26	0.2822	0.25	0.2613	0.2555
0.25	0.08	0.165	0.2858	0.25	0.259	0.2529

Table 5.4. "High" variations in the "raw" screening factor of component *A* for $c=1.05$ at 167°C .

y_1	y_2	\bar{y}	γ_A^{raw}	γ_B^{raw}	γ_A	γ_B
0.97	0.88	0.925	0.19581	0.25	0.1974	0.2023
0.88	0.78	0.83	0.19116	0.25	0.1982	0.2041
0.78	0.66	0.72	0.20011	0.25	0.2111	0.2171
0.66	0.52	0.59	0.20212	0.25	0.2184	0.2251
0.52	0.38	0.45	0.21224	0.25	0.2304	0.2357
0.52	0.35	0.435	0.21628	0.25	0.2325	0.2382
0.38	0.32	0.35	0.19913	0.25	0.2307	0.2337
0.38	0.25	0.315	0.20867	0.25	0.2343	0.2397
0.35	0.17	0.26	0.21968	0.25	0.2394	0.2448
0.25	0.08	0.165	0.21565	0.25	0.2414	0.2473

Table 5.5. "Low" variations in the "raw" screening factor of component *A* for $c=1.05$ at $167\text{ }^\circ\text{C}$.

y_1	y_2	\bar{y}	γ_A^{raw}	γ_B^{raw}	γ_A	γ_B
0.97	0.88	0.925	0.33247	0.25	0.33	0.3226
0.88	0.78	0.83	0.33983	0.25	0.3291	0.3201
0.78	0.66	0.72	0.31658	0.25	0.3019	0.2939
0.66	0.52	0.59	0.30987	0.25	0.2895	0.2811
0.52	0.38	0.45	0.29185	0.25	0.2718	0.2659
0.52	0.35	0.435	0.28695	0.25	0.2692	0.2629
0.38	0.32	0.35	0.30004	0.25	0.269	0.266
0.38	0.25	0.315	0.29437	0.25	0.2669	0.2611
0.35	0.17	0.26	0.28127	0.25	0.2609	0.2553
0.25	0.08	0.165	0.28506	0.25	0.2588	0.2528

Table 5.6. "High" variations in the "raw" screening factor of component *A* for $c=1.10$ at 167°C .

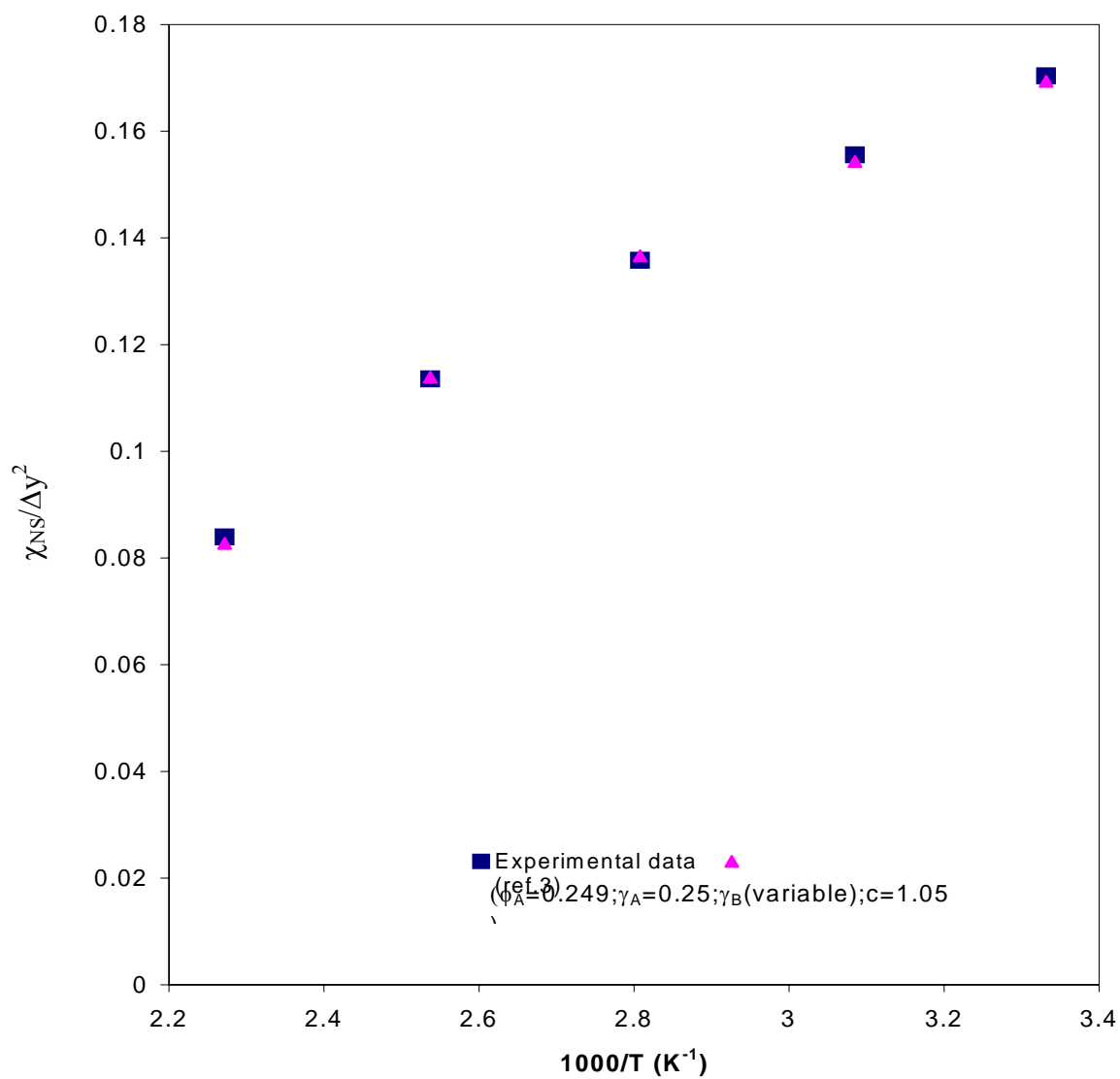


Figure 5.9. Interaction parameters from SANS for H97/D88 at various temperatures.

T (°C)	y ₁	y ₂	$\chi_{\text{bare}} * 10^4$	γ_A	γ_B
27	0.97	0.88	5.87	0.25	0.2416
51	0.97	0.88	5.43	0.25	0.242
83	0.97	0.88	4.94	0.25	0.2425
121	0.97	0.88	4.47	0.25	0.2432
167	0.97	0.88	4.00	0.25	0.2443

Table 5.7. Variations in the screening factor of *component B* in the H97/D88 system for $\phi_A=0.249$ and $c=1.05$ at various temperatures.

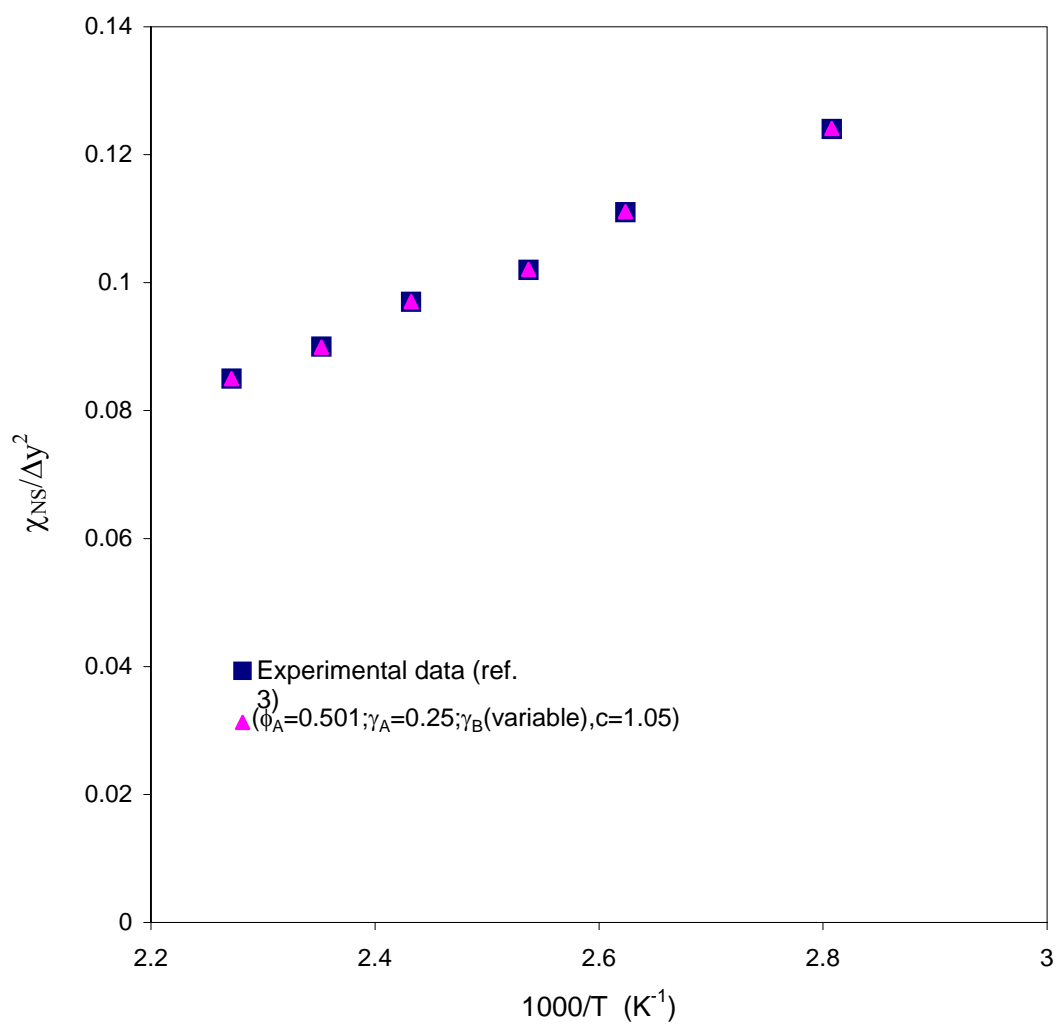


Figure 5.10. Interaction parameters from SANS for H88/D78 at various temperatures.

T (°C)	y ₁	y ₂	$\chi_{\text{bare}} * 10^4$	γ_A	γ_B
83	0.88	0.78	4.94	0.25	0.242
108	0.88	0.78	4.62	0.25	0.24245
121	0.88	0.78	4.47	0.25	0.24278
138	0.88	0.78	4.28	0.25	0.24297
152	0.88	0.78	4.14	0.25	0.24325
167	0.88	0.78	4.00	0.25	0.24345

Table 5.8. Variations in the screening factor of *component B* in the H88/D78 system for $\phi_A=0.501$ and $c=1.05$ at various temperatures.

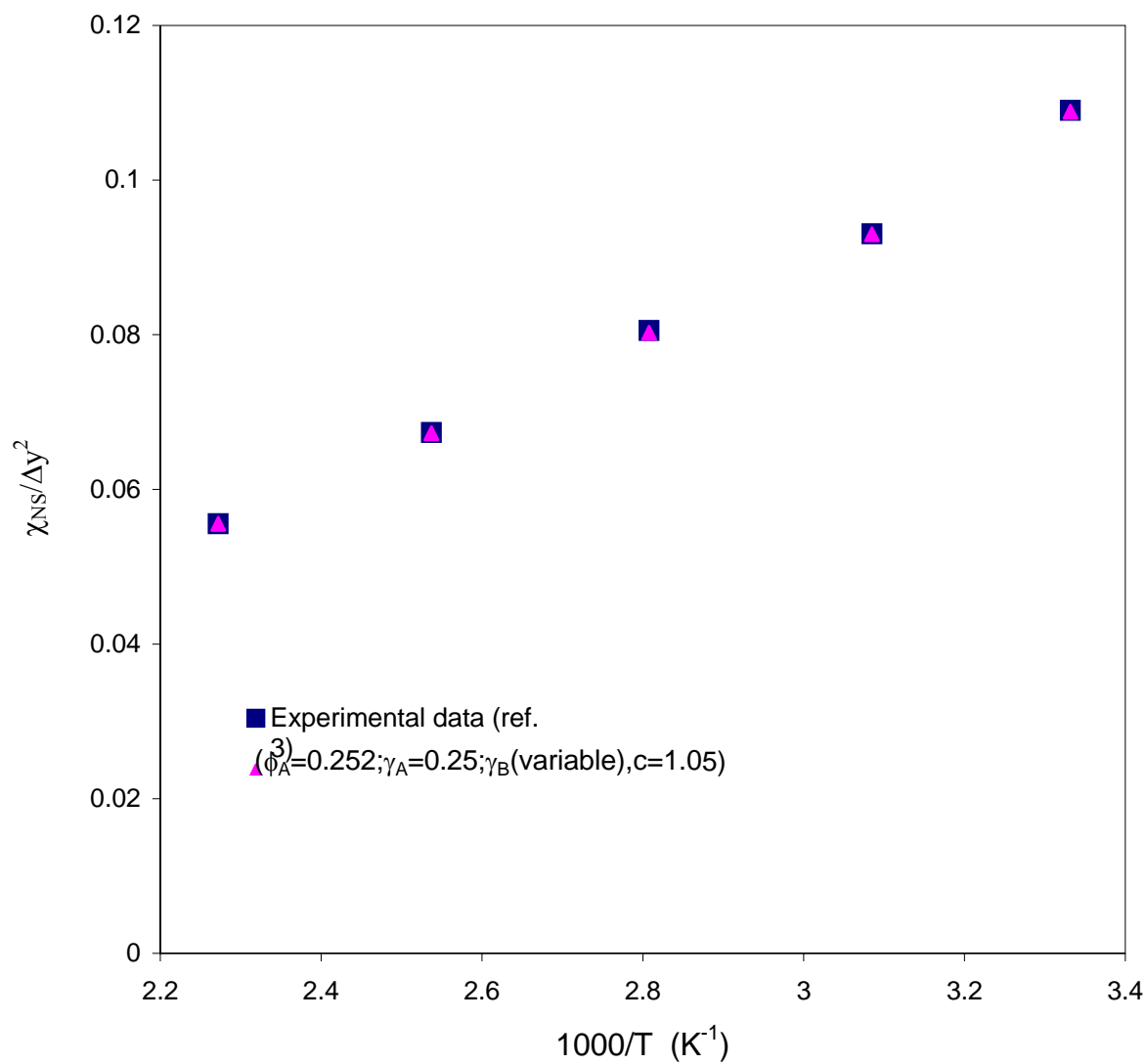


Figure 5.11. Interaction parameters from SANS for H78/D66 at various temperatures.

T (°C)	y ₁	y ₂	$\chi_{\text{bare}} * 10^4$	γ_A	γ_B
27	0.78	0.66	5.87	0.25	0.24099
51	0.78	0.66	5.43	0.25	0.2417
83	0.78	0.66	4.94	0.25	0.24232
121	0.78	0.66	4.47	0.25	0.24301
167	0.78	0.66	4.00	0.25	0.2437

Table 5.9. Variations in the screening factor of *component B* in the H78/D66 system for $\phi_A=0.252$ and $c=1.05$ at various temperatures.

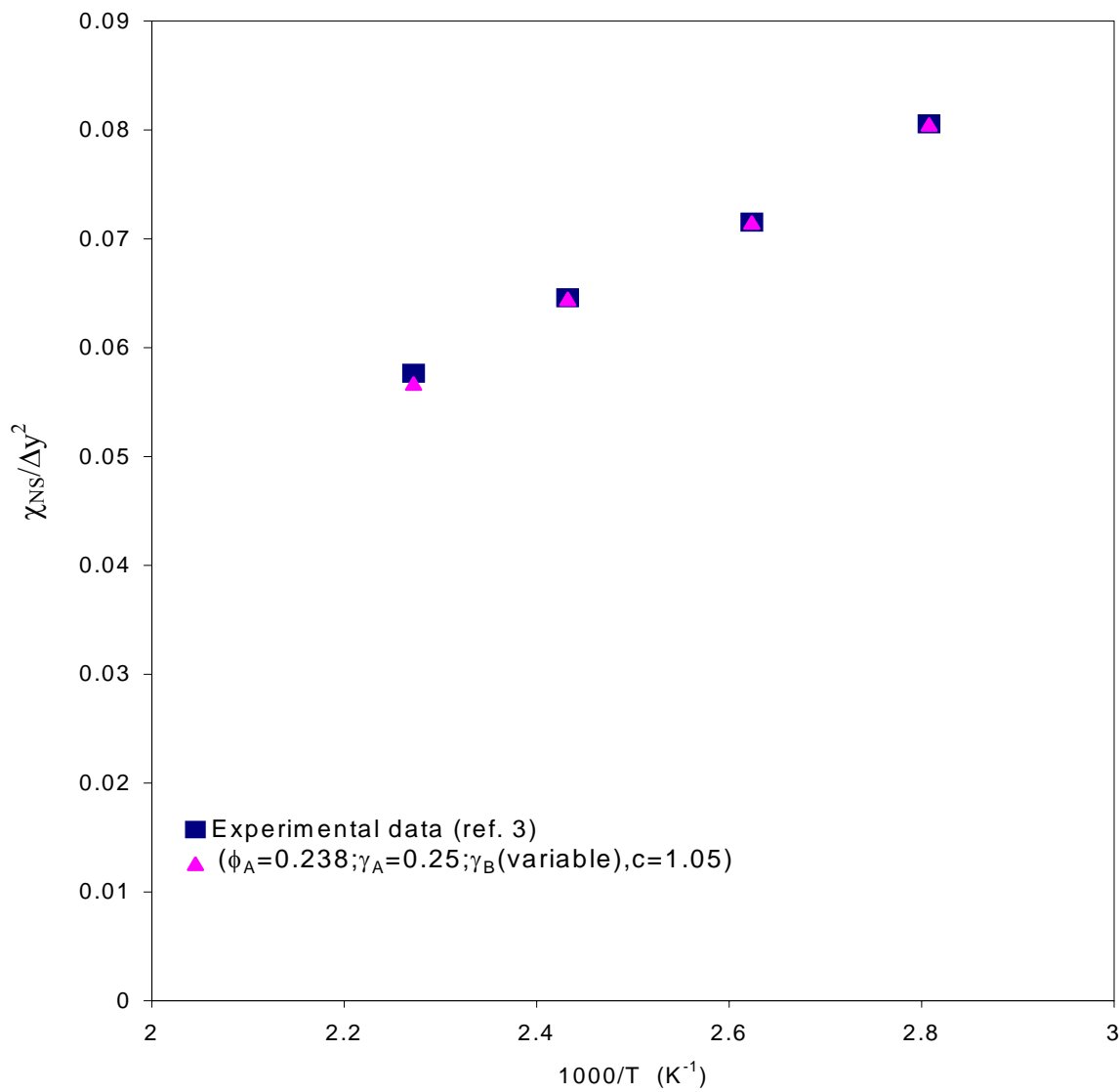


Figure 5.12. Interaction parameters from SANS for H66/D52 at various temperatures.

T (°C)	y ₁	y ₂	$\chi_{\text{bare}} * 10^4$	γ_A	γ_B
83	0.66	0.52	4.94	0.25	0.2423
108	0.66	0.52	4.62	0.25	0.24277
138	0.66	0.52	4.28	0.25	0.24316
167	0.66	0.52	4.00	0.25	0.24362

Table 5.10. Variations in the screening factor of *component B* in the H66/D52 system for $\phi_A=0.238$ and $c=1.05$ at various temperatures.

After having tried various approaches to reconstruct the concentration dependence of the interaction parameter, it was decided to investigate how much one of the screening factors would have to be altered, while keeping the other constant. Rather than keeping the γ -values constant over the entire concentration range, it was decided to let the values change with the composition of the blend. The results of this investigation can be seen in figures 5.13-5.14. The corresponding γ -values can be found in table 5.11. Additional figures and tables from this investigation can be found in Appendix G. Again it appears that the error factor has very little influence, since the values of γ_B does not change significantly. It is interesting to note that the change (from a starting value of 0.25) needed to get a perfect fit all falls within the 4 % that has been mentioned in the past.

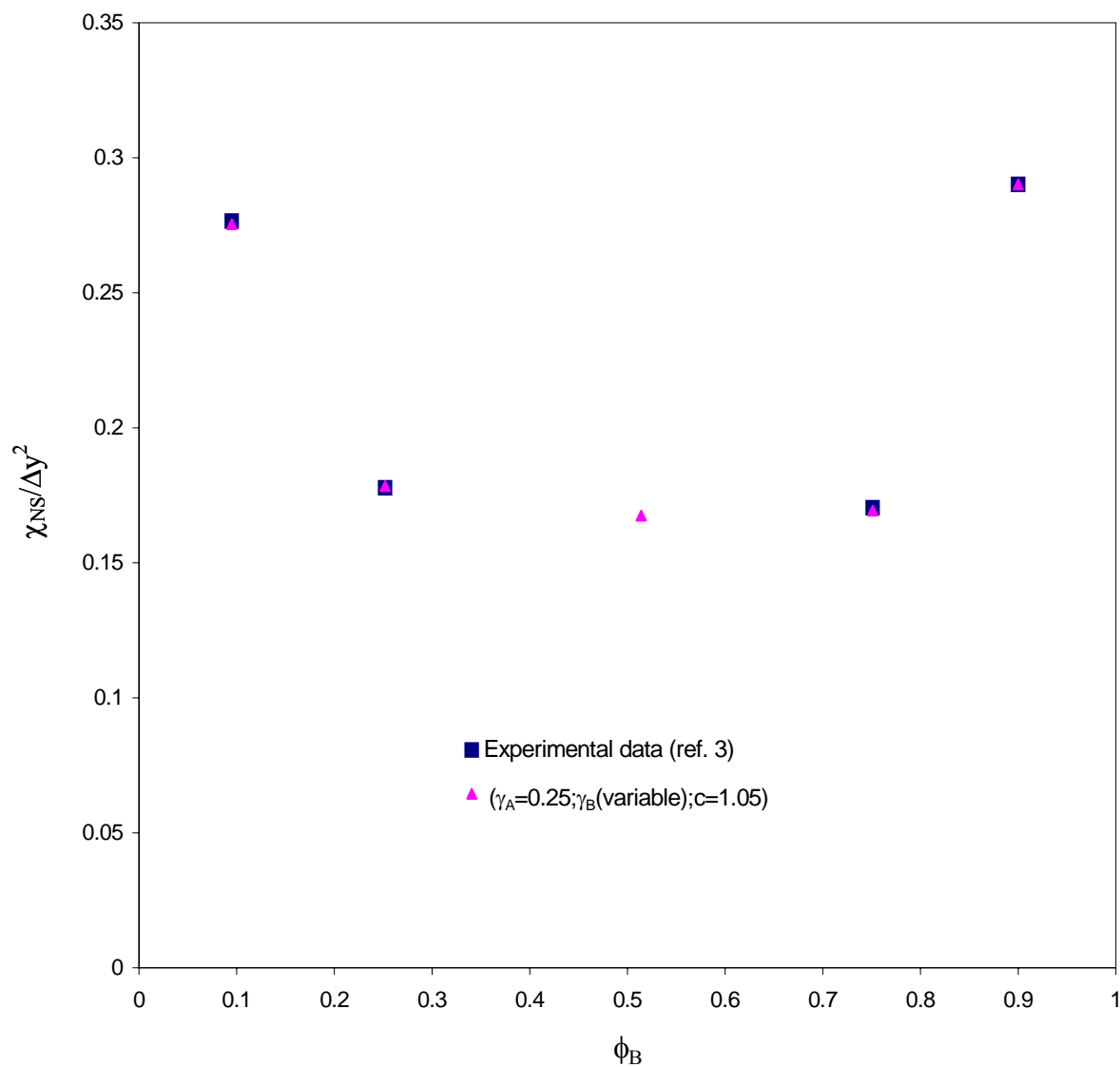


Figure 5.13. Interaction parameters from SANS for H97/D88 at 27 °C.

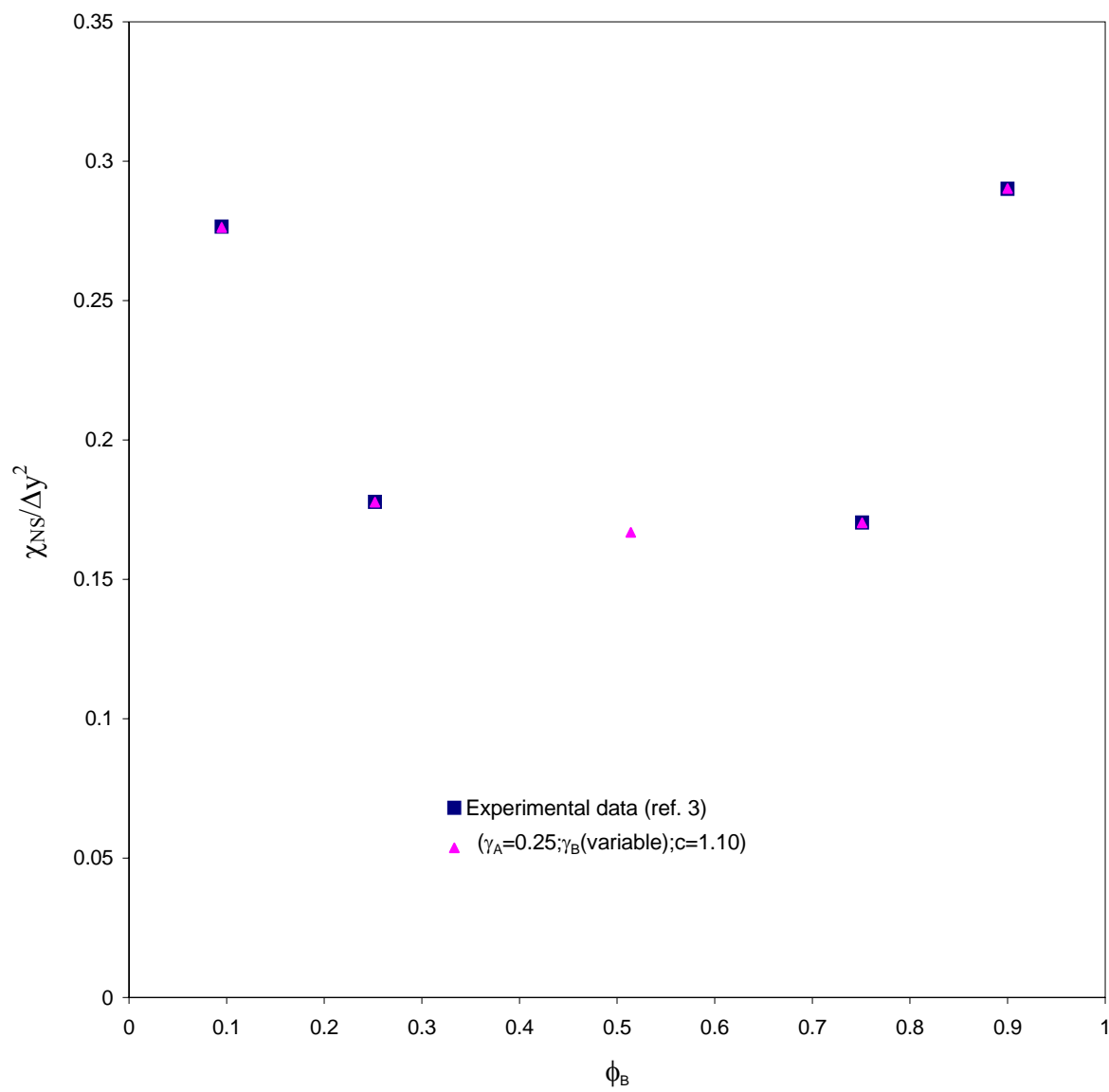


Figure 5.14. Interaction parameters from SANS for H97/D88 at 27 °C.

ϕ_A	ϕ_B	c	$\chi_{\text{bare}} * 10^4$	γ_A	γ_B
0.1	0.9	1.05	5.87	0.25	0.2391
0.249	0.751	1.05	5.87	0.25	0.2416
0.486	0.514	1.05	5.87	0.25	0.2416
0.748	0.252	1.05	5.87	0.25	0.2414
0.905	0.095	1.05	5.87	0.25	0.2395
0.1	0.9	1.10	5.87	0.25	0.23923
0.249	0.751	1.10	5.87	0.25	0.24162
0.486	0.514	1.10	5.87	0.25	0.2416
0.748	0.252	1.10	5.87	0.25	0.24145
0.905	0.095	1.10	5.87	0.25	0.23965

Table 5.11. Variations in the screening factor of *component B* for various c for H97/D88 at 27 °C.

5.4. Conclusions

In nearly all of the polymer blend studies in the literature, where Small Angle Neutron Scattering (SANS) is used to determine the interaction parameter, χ_{NS} , a strong concentration dependence of the interaction parameter, especially at each of the concentration extremes, is reported. At the extremes a strong upturn in χ_{NS} is observed for most systems, however it appears that this concentration dependence becomes less significant with increasing temperature. The origin of this observed concentration dependence, is still not fully understood.

In the previous chapter a fairly simple extension of the Flory-Huggins theory for polymer blends was presented. It was shown that by making a very small change in the fraction of same-chain contacts, it was possible to reproduce experimentally observed values of the interaction parameter. As a natural extension to this work it was decided to adapt the model to blends of copolymers.

A few assumptions were made when adapting the model to copolymers. The most important one being that the copolymers essentially are treated as homopolymers, in the sense that where ϕ_A in the previous chapter represented the volume fraction of homopolymer A, it now represents the volume fraction of copolymer A. The same is true for the fraction of same chain contacts. Since only isotopic copolymer blends are dealt with here, it is presumably a safe assumption. In addition it was initially assumed that the fraction of same chain contacts remained constant over the entire concentration range. Even with a relative small change (less than 4 %) in one of the fractions of same chain contacts, it was clear that the present model was showing some promise. It was also clear

that the model produced almost symmetrical results, whether the fraction of same chain contacts was changed for copolymer A or copolymer B, respectively. Although the model predicts a slight upturn in χ at the concentration extremes, it is not nearly as pronounced as that observed in SANS experiments.

A simple mixing rule was applied to the calculation of the screening factor for the copolymers. The difference between the resulting values of the screening factors all falls within the 4 % range of each other.

As it can be seen in figures 5.6-5.8 the interaction parameter for the copolymer blend $\chi_{NS} / \Delta y^2$ is not truly independent of the average copolymer composition, since it changes with \bar{y} .

With this model it was shown that by taking screening effects into account, it is possible to "match" the experimentally observed upturn in the value of the interaction parameter at the composition extremes. This is accomplished through altering the value of one of the screening factors slightly (less than 4 %).

5.5. References

1. Painter, P.C.; Veytsman, B.; Kumar, S.; Shenoy, S.; Graf, J.F.; Xu, Y.; Coleman, M.M. *Macromolecules*, **30**, 932 (1997)
2. Kohl, P.R.; Seifert, A.M.; Hellmann, G.P. *J. Polym. Sci. Polym. Phys.*, **28**, 1309 (1990)
3. Krishnamoorti, R.; Graessley, W.W.; Balsara, N.P.; Lohse, D.J. *J. Chem. Phys.*, **100**, 3894 (1994)
4. Graessley, W.W.; Krishnamoorti, R.; Balsara, N.P.; Butera, R.J.; Fetters, L.J.; Lohse, D.J.; Schulz, D.N.; Sissano, J.A. *Macromolecules*, **27**, 3896 (1994)
5. Balsara, N.P.; Fetters, L.J.; Hadjichristidis, N.; Lohse, D.J.; Han, C.C.; Graessley, W.W.; Krishnamoorti, R.; *Macromolecules*, **25**, 6137 (1992)
6. Crist, B. *Macromolecules*, **31**, 5853 (1998)

Chapter 6

Summary and Suggestions for Future Work

6.1. Summary

This work was inspired by early findings with functionalized polymer blends, where Painter and Coleman¹ concluded that the number of same (polymer) chain contacts far exceeded what would be expected from a classical mean field theory. By functionalizing the polymers it was possible to design systems where the number of “contacts” could actually be counted.

It was decided to investigate whether these findings of excess same chain contacts, which were believed to be of such a general nature that they would also apply to polymer solutions, could help explain various phenomena in polymer solution thermodynamics as well as polymer blends. In order to do so, it was necessary to distinguish between intermolecular contacts (external) and intramolecular contacts (within the same chain). This was done by introducing a so-called screening factor.

First, a relatively simple modification of the classical Flory-Huggins theory was investigated, in which these intramolecular contacts were treated explicitly. It was shown that it was possible to reproduce the composition dependence of the interaction parameter in poor solvent systems at or near the θ -temperature with amazing accuracy. It was also shown that the model was able to reproduce spinodals curves which were in good agreement with experimental data.

The next natural step was to include free volume effects, which are also often referred to as equation of state effects. This was done through a modification of the Flory-Orwoll-Vrij^{2,3} Equation of State model, where intramolecular screening effects were again accounted for. It was decided to investigate whether using solubility parameters and internal pressure parameters with this new model, would be able to provide better agreements with experimental data. The results were somewhat inconclusive. For some polymer-solvent systems it appeared that the use of solubility parameters provided the best agreement with experimental data, while in other polymer-solvent systems it appeared that the use of internal pressures gave better agreement with experimental data. A number of different approaches were investigated, but only selected elements were presented since none of them gave conclusive results. An elastic energy contribution for systems away from the θ -condition or for polymers in good solvents did not improve the agreement with experimental data greatly. Since there is currently no established relationship between the screening factor and the chain dimensions, all the calculations were performed with one (constant) value for the screening factor over the entire concentration range. Simulations performed by Dr. Park⁴, suggests that this may not be a valid assumption, as these results indicate a very strong dependence of the screening factor on the chain expansion factor.

The focus was then directed towards isotopic polymer blends as well as copolymer blends, where a modified Flory-Huggins model was tested to see if it was possible to reproduce some of the curious experimentally observed data in polymer blends, such as an apparent strong concentration dependence of the interaction parameter determined from *Small Angle Neutron Scattering* (SANS) experiments. It was shown that

by altering the screening factor of one of the components between 2 % (polymers) and 4% (copolymers), it was possible to obtain results that were in almost perfect agreement with the experimental data.

6.2. Suggestions for Future Work

The immediate and perhaps most exciting new avenue to pursue is related to the work done recently by Dr. Park⁴, where Monte Carlo simulations suggests that the relationship between the screening factor and the chain expansion factor may indeed be what was previously anticipated, namely that the fraction of same chain contacts decreases drastically as the chain expands. The limiting value of the number of same chain contacts is approximately 0.1, and this finding is supported by Victor et al.⁵. If a definite relationship between the screening factor and the chain expansion factor, and thereby the concentration (volume fraction), can be established, it would be interesting to revisit the calculations performed in chapter 3 and onwards.

Another approach would be to incorporate a different model, rather than the Flory-Orwoll-Vrij^{2,3} Equation of State model, to account for the free volume effects. In fact an attempt was made to incorporate the Sanchez-Lacombe model, but the resulting equations in this model became a little more complex and cumbersome than desired, so this idea was aborted.

6.3. References

1. Painter, P.C.; Coleman, M.M. chapter 4 in *"Polymer Blends Volume 1"*, Edited by Paul, D.R.; Bucknall, C.B. John Wiley and Sons, New York, 2000
2. Flory, P.J.; Orwoll, R.A.; Vrij, A. *J. Am. Chem. Soc.*, **86**, 3507 (1964)
3. Flory, P.J.; Orwoll, R.A.; Vrij, A. *J. Am. Chem. Soc.*, **86**, 3515 (1964)
4. Park, Y.H. Personal Communication, 2005
5. Victor, J-M.; Imbert, J-B.; Lhuillier, D. *J. Chem. Phys.*, **100**, 5372 (1994)

Appendix

A. Contact Sites for Stiff or Semiflexible Rods

Let the product qz represent the total number of sites per chain that neighbor a given polymer segment excluding the contacts between segments that are covalently bound. In the simplest case of stiff rods qz is given by:

$$qz = (z - 2)r + 2 \quad (\text{A1})$$

where z is the coordination number of the lattice and r is the degree of polymerization.

This equation can be written in a number of equivalent ways:

$$\begin{aligned} q &= \left(1 - \frac{2}{z}\right)r + \frac{2}{z} \\ \Downarrow \\ \frac{q}{r} &= \left(1 - \frac{2}{z}\right) + \frac{2}{zr} \\ \Downarrow \\ \frac{q}{r} &= 1 - \frac{2}{z} \left(1 - \frac{1}{r}\right) \end{aligned} \quad (\text{A2})$$

and:

$$r - q = r - \left(\left(1 - \frac{2}{z} \right) r + \frac{2}{z} \right)$$

$$\Downarrow$$

$$r - q = \frac{2}{z} r - \frac{2}{z} \quad (\text{A3})$$

$$\Downarrow$$

$$r - q = \frac{2}{z} (r - 1)$$

$$\frac{r - q}{r} = \frac{\frac{2}{z} (r - 1)}{r} \quad (\text{A4})$$

$$\Downarrow$$

$$\frac{r - q}{r} = \frac{2}{z} \left(1 - \frac{1}{r} \right)$$

which are the quantities needed in the Guggenheim^{a1} expression for the free energy of mixing.

If the factor γ_l is introduced, which was defined previously by Koningsveld and Kleintjens^{a2} as the fraction of sites on the lattice that are same chain contacts, caused by the chain connectivity of the polymer:

$$\gamma_l = \frac{2}{z} \left(1 - \frac{1}{r} \right) \quad (\text{A5})$$

one gets:

- a1. Guggenheim, E.A. *Mixtures*, Clarendon, Oxford, 1952
 a2. Koningsveld, R.; Kleintjens, L.A. *Macromolecules*, **4**, 637 (1971)

$$\frac{q}{r} = (1 - \gamma_l) \quad (\text{A6})$$

$$r - q = r\gamma_l \quad (\text{A7})$$

$$\frac{r - q}{r} = \gamma_l \quad (\text{A8})$$

B. Contact Sites for Flexible Chains

Since some polymers have chains of a very flexible nature, which enables them to bend back on themselves, one has to distinguish between intramolecular contacts and intermolecular contacts. In order to do that a factor γ_s is introduced, which is defined as the fraction of intramolecular contacts. The sum of intramolecular contacts and intermolecular contacts must equal the total number of contacts:

$$qz = \gamma_s qz + (1 - \gamma_s)qz \quad (\text{B1})$$

which when compared to (A1) gives:

$$(1 - \gamma_s)qz + \gamma_s qz = (z - 2)r + 2 \quad (\text{B2})$$

Substituting q' for the product $(1 - \gamma_s)q$, one gets:

$$q'z = (z - 2)r + 2 - \gamma_s qz \quad (\text{B3})$$

where $q'z$ is the effective number of intermolecular contacts, either between a polymer segment and a solvent molecule or between two polymer segments from different chains.

It will be helpful to remember that:

$$\begin{aligned} q'z &= qz - \gamma_s qz = (1 - \gamma_s)qz \\ \Downarrow \\ q' &= (1 - \gamma_s)q \end{aligned} \tag{B4}$$

which is how q' was defined in the first place. By combining equation A6:

$$\frac{q}{r} = (1 - \gamma_l) \tag{A6}$$

and equation B4 one gets:

$$\frac{q'}{r} = (1 - \gamma_s)(1 - \gamma_l) \tag{B5}$$

Further manipulations of equation B4 leads to:

$$\begin{aligned} r - q' &= r - (1 - \gamma_s)q \\ \Downarrow \\ r - q' &= (r - q) + \gamma_s q \end{aligned} \tag{B6}$$

Previously it was shown that:

$$r - q = r\gamma_l \quad (\text{A7})$$

which when combined with equation B6 leads to:

$$r - q' = r\gamma_l + \gamma_s q \quad (\text{B7})$$

which also can be written as:

$$\begin{aligned} \frac{r - q'}{r} &= \frac{r\gamma_l + \gamma_s q}{r} = \gamma_l + \gamma_s \left(\frac{q}{r} \right) \\ \Downarrow \\ \frac{r - q'}{r} &= \gamma_l + \gamma_s (1 - \gamma_l) \end{aligned} \quad (\text{B8})$$

C. Guggenheim's Theory of Athermal Mixtures

The following paragraph is a brief summary of the theory of athermal mixtures for molecules of different sizes as originally proposed by Guggenheim^{c1}. It was included in the hope that it would clarify the background for proposing this new model. It is also interesting in the sense that it is a more rigorous derivation of the combinatorial entropy term than the one given by Flory^{c2}.

Guggenheim^{c1} introduced a quantity α , which he defined as the ratio of the probability that a group of r sites was fully occupied by a single r -mer to the probability that the group was entirely occupied by monomers. It was defined in terms

c1. Guggenheim, E.A. *Mixtures*, Clarendon, Oxford, 1952

c2. Flory, P.J. *Principles of Polymer Chemistry*, Cornell University Press, Ithaca, N.Y. (1956)

of the grand partition functions q_l and q_r as:

$$\alpha = \frac{\lambda_r q_r}{(\lambda_l q_l)^r} \quad (\text{C1})$$

where the λ 's are the absolute activities.

From basic thermodynamic principles the free energy of mixing N_l monomers and N_r r -mers can be expressed as:

$$dG = \mu_l dN_l + \mu_r dN_r \quad (\text{C2})$$

where the terms in dP and dT have been disregarded, since the primary concern here is the thermodynamics of the non-gaseous phases at ambient pressures and a given temperature.

By substituting the following relationship between the chemical potential μ and the absolute activity λ :

$$\mu = kT \ln \lambda \quad (\text{C3})$$

into equation (C2) one gets:

$$\frac{dG}{kT} = \ln \lambda_l dN_l + \ln \lambda_r dN_r \quad (\text{C4})$$

If N_s represent the total number of sites, and ϕ is the fraction occupied by the r -mer, then:

$$N_s = N_1 + rN_r \quad (\text{C5})$$

$$N_1 = (1 - \phi)N_s \quad (\text{C6})$$

$$N_r = \frac{\phi}{r} N_s \quad (\text{C7})$$

In the framework of a lattice ϕ can be considered the volume fraction of the r -mer. Upon inserting equations (C5)-(C7) in equation (C4) and rewriting it, one gets:

$$\frac{dG}{N_s kT} = \frac{1}{r} \ln \frac{\lambda_r}{(\lambda_1)^r} d\phi \quad (\text{C8})$$

if it is assumed that the total number of lattice sites N_s remains constant. If equation C1 is rewritten to:

$$\frac{\lambda_r}{(\lambda_1)^r} = \frac{\alpha q_1^r}{q_r} \quad (\text{C9})$$

and inserted in equation C8 it leads to:

$$\frac{dG}{N_s kT} = \frac{1}{r} \ln \left(\frac{\alpha q_1^r}{q_r} \right) d\phi \quad (\text{C10})$$

Now by definition the free energy of mixing must be:

$$\Delta G = G - \sum_{i=1}^n G_i \quad (\text{C11})$$

where G is the free energy of the mixture and G_i is the free energy of each of the pure components. If it is assumed that the free energy is a function of N_s and ϕ , equation (C11) becomes:

$$\begin{aligned} \Delta G &= G(N_s, \phi) - (1 - \phi)G(N_s, 0) - \phi G(N_s, 1) \\ &\Downarrow \\ \Delta G &= (G(N_s, \phi) - G(N_s, 0)) - \phi(G(N_s, 1) - G(N_s, 0)) \end{aligned} \quad (\text{C12})$$

When equation C12 is applied to equation C10 one gets:

$$\frac{\Delta G}{N_s kT} = \int_0^\phi \left[\frac{1}{r} \ln \left(\frac{\alpha q_1^r}{q_r} \right) \right] d\phi - \phi \int_0^1 \left[\frac{1}{r} \ln \left(\frac{\alpha q_1^r}{q_r} \right) \right] d\phi$$

which upon rewriting gives:

$$\begin{aligned}
\frac{\Delta G}{N_s kT} &= \frac{1}{r} \int_0^\phi \ln \alpha d\phi + \frac{1}{r} \int_0^\phi r \ln q_1 d\phi - \frac{1}{r} \int_0^\phi \ln q_r d\phi \\
&\quad - \frac{\phi}{r} \left[\int_0^1 \ln \alpha d\phi + \int_0^1 r \ln q_1 d\phi - \int_0^1 \ln q_r d\phi \right] \\
&\quad \Downarrow \\
\frac{\Delta G}{N_s kT} &= \frac{1}{r} \int_0^\phi \ln \alpha d\phi + \ln q_1 (\phi - 0) - \frac{1}{r} \ln q_r (\phi - 0) \\
&\quad - \frac{\phi}{r} \int_0^1 \ln \alpha d\phi - \phi \ln q_1 (1 - 0) + \frac{\phi}{r} \ln q_r (1 - 0)
\end{aligned}$$

which reduces to:

$$\frac{\Delta G}{N_s kT} = \frac{1}{r} \int_0^\phi \ln \alpha d\phi - \frac{\phi}{r} \int_0^1 \ln \alpha d\phi \tag{C13}$$

This is the free energy of mixing expressed in terms of the total number of contact sites. In order to express the free energy in terms of moles of lattice sites one has to divide the left hand side of equation C13 by Avogadro's number. If this is done the following equation is obtained:

$$\frac{\Delta_m G'}{RT} = \frac{1}{r} \int_0^\phi \ln \alpha d\phi - \frac{\phi}{r} \int_0^1 \ln \alpha d\phi \tag{C14}$$

Given equation C14 it would be convenient to express α in terms of ϕ . It is recalled that α was defined as the ratio of the probability that a group of r sites are fully occupied by a single r -mer to the probability that the r sites are fully occupied by monomers.

Before proceeding it is important to notice that Guggenheim^{c1} assumed that all configurations had the same energy, which would result in a completely random distribution of the molecules. He also only considered cases in which the group of r sites were arranged such that an r -mer occupying them would not bent back on itself.

With this in mind, the probability that one particular of the r sites is occupied by any segment of the r -mer must be:

$$\phi = \frac{rN_r}{N_1 + rN_r}$$

and the probability that one particular of the r sites is occupied by a particular segment of the r -mer is:

$$\frac{\phi}{r} = \frac{N_r}{N_1 + rN_r} \quad (\text{C15})$$

If equation C15 is multiplied by the factor (σ_g/ρ) , where ρ was defined "as the number of ways in which the r -mer as a whole can be placed after a particular one of its elements has been placed and σ_g denotes the symmetry number of the group of r sites being considered" (4), the probability that the r sites are fully occupied by a single r -mer is obtained:

$$\frac{\sigma_g}{\rho} \left(\frac{\phi}{r} \right) = \frac{\sigma_g}{\rho} \left(\frac{N_r}{N_1 + rN_r} \right) \quad (\text{C16})$$

If r sites are considered again, the probability that one particular of these sites is occupied by a monomer must be:

$$\frac{N_1}{N_1 + rN_r} \quad (\text{C17})$$

Now if this particular site is occupied by a monomer, then the probability that a neighboring site is also occupied by a monomer must be:

$$\frac{N_1}{N_1 + qN_r} \quad (\text{C18})$$

Since the sought after entity is the probability that a group of r sites is fully occupied by monomers, meaning that $(r-1)$ monomers have to be placed after the first has been placed. The probability that a group of r sites is fully occupied by monomers can therefore be obtained by multiplying equation C17 with $(r-1)$ times equation C18, or:

$$\left(\frac{N_1}{N_1 + rN_r} \right) \left(\frac{N_1}{N_1 + qN_r} \right)^{r-1} \quad (\text{C19})$$

By dividing equation C16 by equation C19 the following equation for α is obtained:

$$\alpha = \frac{\sigma_g}{\rho} \frac{N_r}{N_1} \left(\frac{N_1 + qN_r}{N_1} \right)^{r-1} \quad (\text{C20})$$

which can be rewritten in terms of ϕ to:

$$\alpha = \frac{\sigma_g}{\rho r} \frac{\phi}{1-\phi} \left(\frac{1-(r-q)\phi/r}{1-\phi} \right)^{r-1} \quad (\text{C21})$$

Before equation C21 is substituted into equation C14 it is helpful to note that:

$$\begin{aligned} \ln \alpha &= \ln \sigma_g - \ln \rho r + \ln \phi - \ln(1-\phi) \\ &+ (r-1)[\ln[1-(r-q)\phi/r] - \ln(1-\phi)] \end{aligned} \quad (\text{C22})$$

By inserting equation C22 into equation C14 one gets:

$$\begin{aligned} \frac{\Delta_m G'}{RT} &= \frac{1}{r} \int_0^\phi \left[\ln \sigma_g - \ln \rho r + \ln \phi - \ln(1-\phi) \right. \\ &\quad \left. + (r-1)[\ln[1-(r-q)\phi/r] - \ln(1-\phi)] \right] d\phi \\ &\quad - \frac{\phi}{r} \int_0^1 \left[\ln \sigma_g - \ln \rho r + \ln \phi - \ln(1-\phi) \right. \\ &\quad \left. + (r-1)[\ln[1-(r-q)\phi/r] - \ln(1-\phi)] \right] d\phi \end{aligned}$$

which upon integration gives:

$$\frac{\Delta_m G'}{RT} = \frac{1}{r} \left[\begin{aligned} & \phi \ln \sigma_g - \phi \ln \rho r + [\phi \ln \phi - \phi]_0^\phi + [(1-\phi) \ln(1-\phi) - (1-\phi)]_0^\phi \\ & - \frac{(r-1)r}{(r-q)} \left[\left(1 - \left(\frac{r-q}{r} \right) \phi \right) \ln \left(1 - \left(\frac{r-q}{r} \right) \phi \right) - \left(1 - \left(\frac{r-q}{r} \right) \phi \right) \right]_0^\phi \\ & + (r-1) [(1-\phi) \ln(1-\phi) - (1-\phi)]_0^\phi \end{aligned} \right] \\ - \frac{\phi}{r} \left[\begin{aligned} & \ln \sigma_g - \ln \rho r + [\phi \ln \phi - \phi]_0^1 + [(1-\phi) \ln(1-\phi) - (1-\phi)]_0^1 \\ & - \frac{(r-1)r}{(r-q)} \left[\left(1 - \left(\frac{r-q}{r} \right) \phi \right) \ln \left(1 - \left(\frac{r-q}{r} \right) \phi \right) - \left(1 - \left(\frac{r-q}{r} \right) \phi \right) \right]_0^1 \\ & + (r-1) [(1-\phi) \ln(1-\phi) - (1-\phi)]_0^1 \end{aligned} \right]$$

$$\frac{\Delta_m G'}{RT} = \frac{1}{r} \left[\begin{aligned} & \phi \ln \phi - \phi + (1-\phi) \ln(1-\phi) - (1-\phi) + 1 \\ & - \frac{(r-1)r}{(r-q)} \left[\left(1 - \left(\frac{r-q}{r} \right) \phi \right) \ln \left(1 - \left(\frac{r-q}{r} \right) \phi \right) - \left(1 - \left(\frac{r-q}{r} \right) \phi \right) + 1 \right] \\ & + (r-1) [(1-\phi) \ln(1-\phi) - (1-\phi) + 1] \end{aligned} \right] \\ - \frac{\phi}{r} \left[\begin{aligned} & -1 + 1 \\ & - \frac{(r-1)r}{(r-q)} \left[\left(1 - \left(\frac{r-q}{r} \right) \right) \ln \left(1 - \left(\frac{r-q}{r} \right) \right) - \left(1 - \left(\frac{r-q}{r} \right) \right) + 1 \right] \\ & + (r-1) \end{aligned} \right]$$

$$\frac{\Delta_m G'}{RT} = \frac{\phi}{r} \ln \phi + \frac{1}{r} (1-\phi) \ln(1-\phi) \\ - \frac{(r-1)r}{r(r-q)} \left[\left(1 - \left(\frac{r-q}{r} \right) \phi \right) \ln \left(1 - \left(\frac{r-q}{r} \right) \phi \right) + \left(\frac{r-q}{r} \right) \phi \right] \\ + \frac{(r-1)}{r} [(1-\phi) \ln(1-\phi) + \phi] \\ + \frac{(r-1)\phi r}{r(r-q)} \left[\left(\frac{r-(r-q)}{r} \right) \ln \left(\frac{r-(r-q)}{r} \right) + \left(\frac{r-q}{r} \right) \right] \\ - \frac{(r-1)}{r} \phi$$

$$\begin{aligned}
\frac{\Delta_m G'}{RT} &= \frac{\phi}{r} \ln \phi + \frac{1}{r} (1-\phi) \ln(1-\phi) \\
&\quad - \frac{(r-1)}{r} \left[\left(\frac{r}{(r-q)} - \phi \right) \ln \left(1 - \left(\frac{r-q}{r} \right) \phi \right) + \phi \right] \\
&\quad + (1-\phi) \ln(1-\phi) + \phi - \frac{1}{r} (1-\phi) \ln(1-\phi) - \frac{\phi}{r} \\
&\quad + \frac{(r-1)\phi q}{r(r-q)} \ln \left(\frac{q}{r} \right) + \frac{(r-1)}{r} \phi - \frac{(r-1)}{r} \phi
\end{aligned}$$

$$\begin{aligned}
\frac{\Delta_m G'}{RT} &= \frac{\phi}{r} \ln \phi - \frac{(r-1)}{r} \left(\frac{r}{(r-q)} - \phi \right) \ln \left(1 - \left(\frac{r-q}{r} \right) \phi \right) - \frac{(r-1)}{r} \phi \\
&\quad + (1-\phi) \ln(1-\phi) + \phi \left(1 - \frac{1}{r} \right) + \frac{(r-1)q}{r(r-q)} \phi \ln \left(\frac{q}{r} \right)
\end{aligned}$$

Upon further simplification the final expression for the free energy of mixing, expressed per mole of lattice sites is given by:

$$\begin{aligned}
\frac{\Delta_m G'}{RT} &= \frac{\phi}{r} \ln \phi + (1-\phi) \ln(1-\phi) + \frac{(r-1)q}{r(r-q)} \phi \ln \left(\frac{q}{r} \right) \\
&\quad - \frac{(r-1)}{r} \left(\frac{r}{r-q} - \phi \right) \ln \left(1 - \left(\frac{r-q}{r} \right) \phi \right)
\end{aligned} \tag{C23}$$

The first two terms on the right hand side of equation C23 are usually referred to as the combinatorial entropy. Since Guggenheim^{cl} only considered athermal systems in this study, i.e. systems that involved no energy upon mixing, the other two terms on the right hand side of equation C23 must also be of entropic nature. The two terms combined can therefore be referred to as the non-combinatorial entropy.

D. Determination of Internal Pressures for Various Polymers

In the following it will be explained how to obtain internal pressures from other experimental data in the literature.

The thermodynamic equation of state is given by:

$$P = T \left(\frac{\partial P}{\partial T} \right)_V - P_i \quad (\text{D1})$$

where P is the pressure, V is the volume, T is the temperature and P_i is the internal pressure.

From equation D1 it follows that if (P,T) -data were available for polymers at constant volume, a plot of P vs. T would give P_i as the intercept. Unfortunately most literature does not report data in this form. It is more common to list specific volumes, v , versus temperature. A plot of v versus T at various pressures P , provides a set of (P,T) -data at constant v . If these data are plotted the internal pressures are obtained as the intercepts. All the experimental PVT data were obtained from Zoller and Walsh's compendium^{d1}.

d1. Zoller, P.; Walsh, D.J. *Standard Pressure-Volume-Temperature Data for Polymers*, Technomic Publishing Company, Inc., Lancaster, PA (1995)

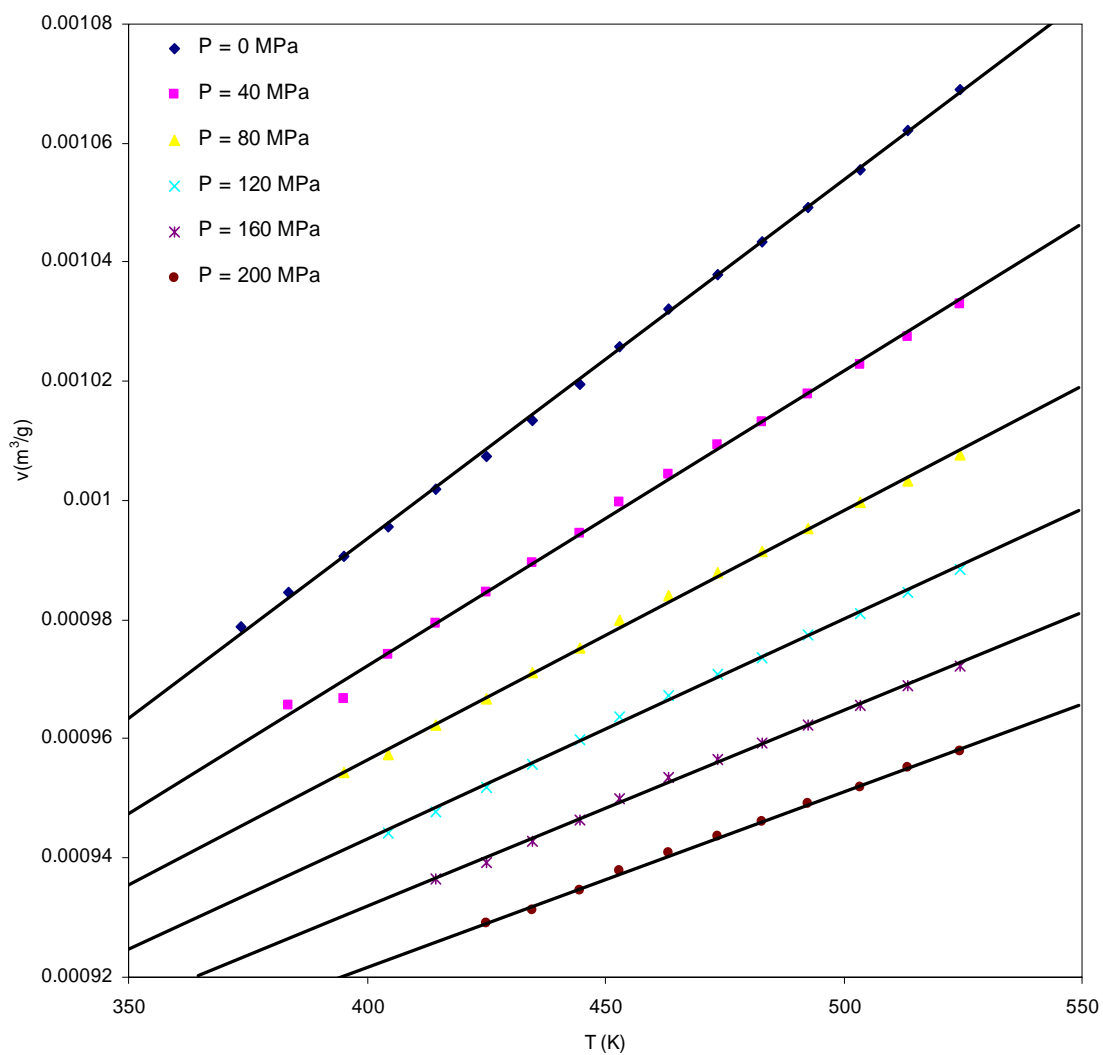


Figure D.1. Specific Volume vs. Temperature
for PS ($M_w=110,000$)

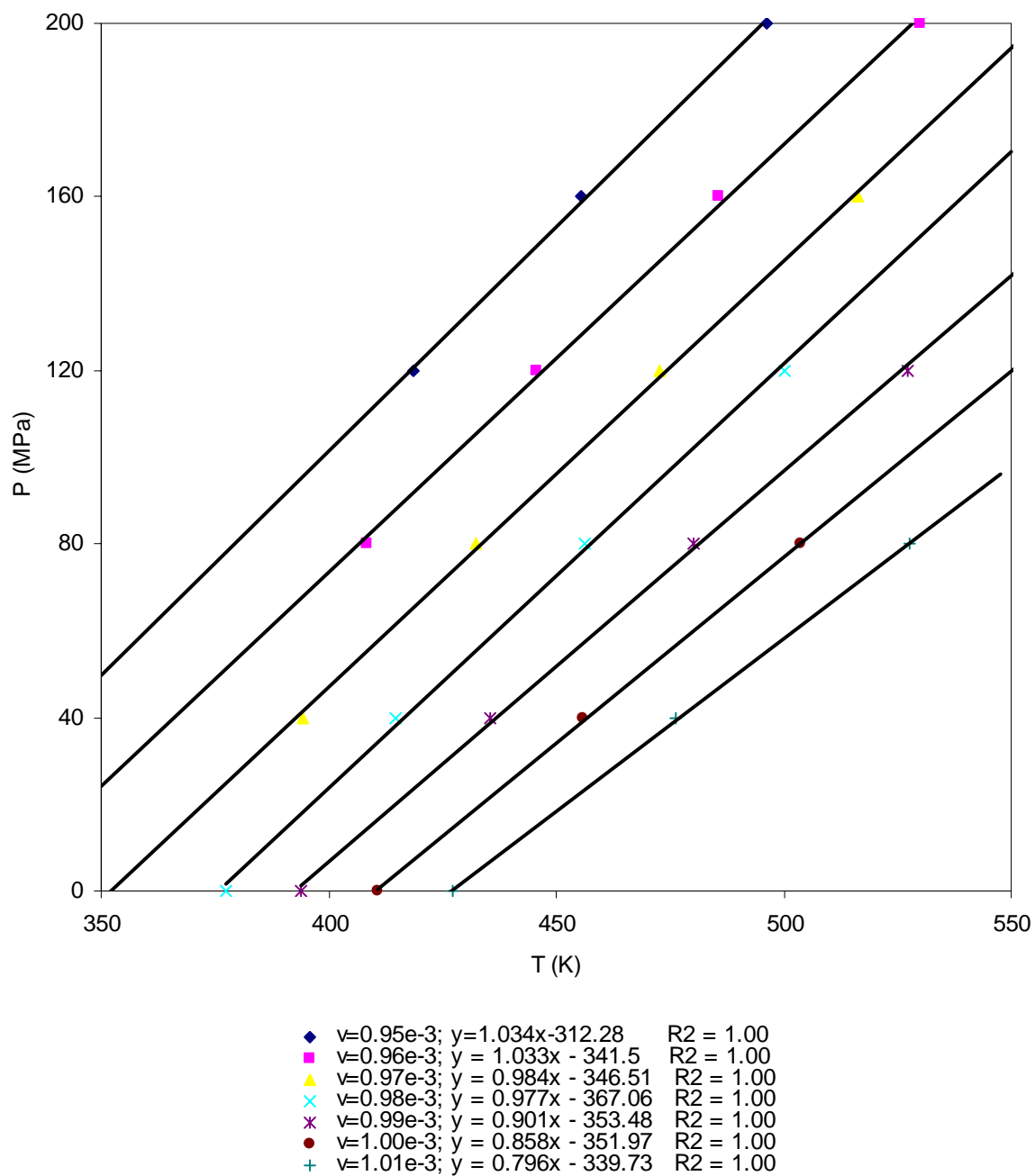


Figure D.2. Pressure vs. Temperature for PS (Mw=110.000)

Specific volume	P_i		$P_i^{1/2}$
(m ³ /kg)	(MPa)	(cal/cm ³)	(cal/cm ³) ^{1/2}
9.5*10 ⁻⁴	312.28	74.6	8.64
9.6*10 ⁻⁴	341.50	81.58	9.03
9.7*10 ⁻⁴	346.51	82.77	9.10
9.8*10 ⁻⁴	367.06	87.69	9.36
9.9*10 ⁻⁴	353.48	84.44	9.19
1.0*10 ⁻³	351.97	84.08	9.17
1.01*10 ⁻³	339.73	81.16	9.01
Average Value	344.65	82.33	9.07

Table D.1. Internal Pressure of PS (Mw=110.000)

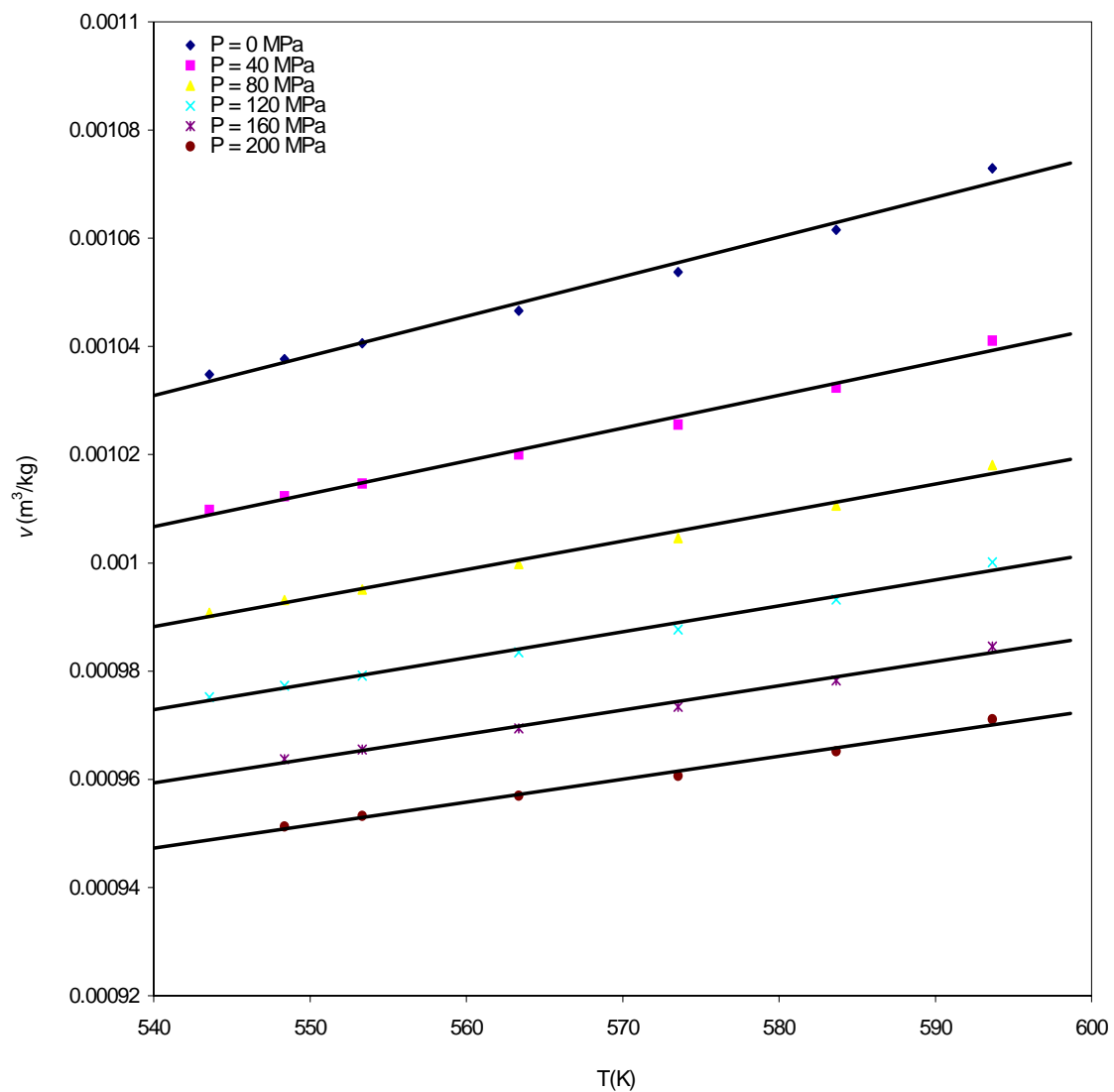


Figure D.3. Specific Volume vs. Temperature for Nylon 6/6

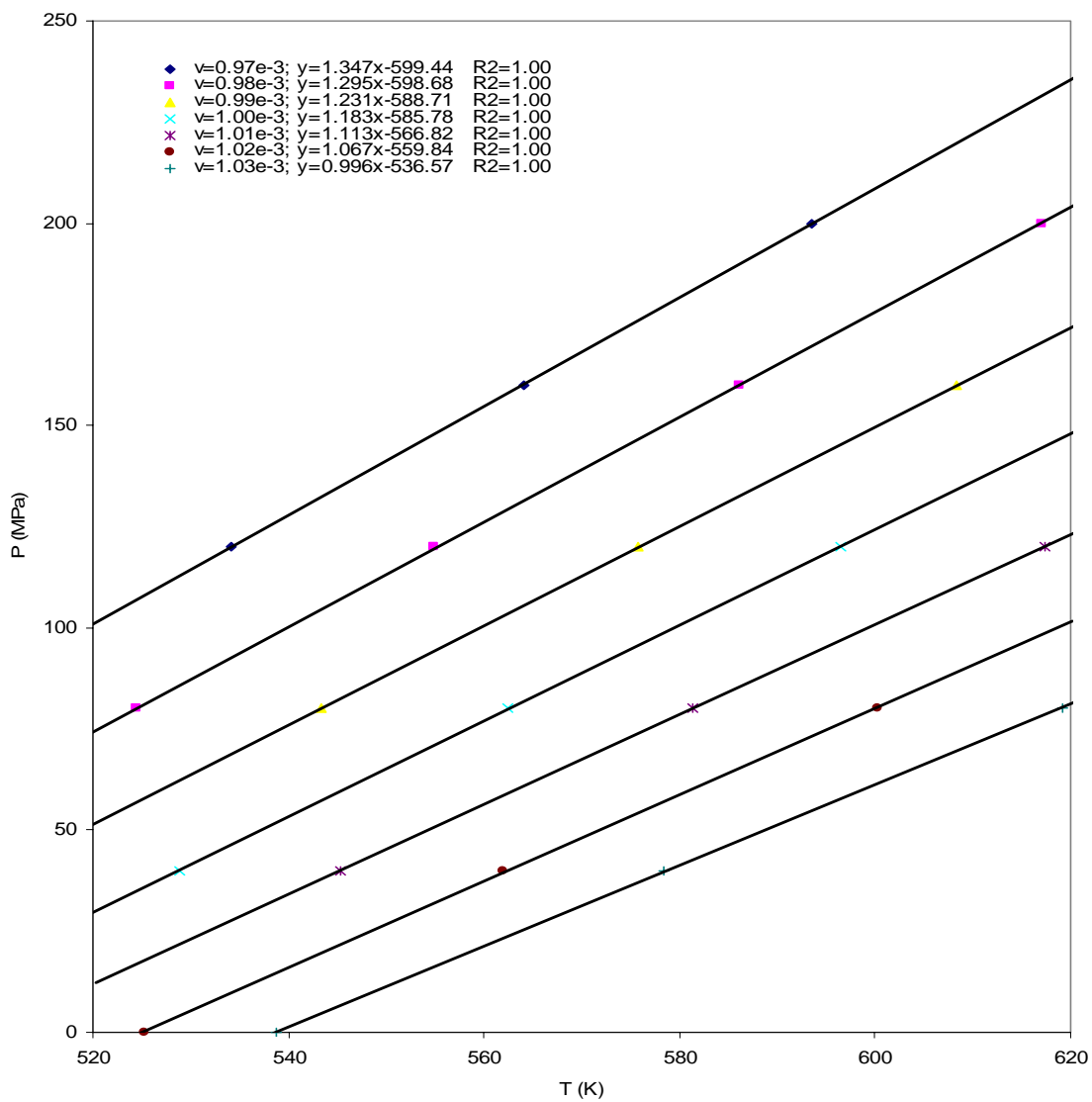


Figure D.4. Pressure vs. Temperature for Nylon 6/6

Specific volume	P_i		$P_i^{1/2}$
(m ³ /kg)	(MPa)	(cal/cm ³)	(cal/cm ³) ^{1/2}
9.7*10 ⁻⁴	599.44	143.20	11.97
9.8*10 ⁻⁴	598.68	143.02	11.96
9.9*10 ⁻⁴	588.71	140.64	11.86
1.0*10 ⁻³	585.78	139.94	11.83
1.01*10 ⁻³	566.82	135.41	11.64
1.02*10 ⁻³	559.82	133.74	11.56
1.03*10 ⁻³	536.57	128.18	11.32
Average Value	576.55	137.73	11.74

Table D.2. Internal Pressure of Nylon 6/6

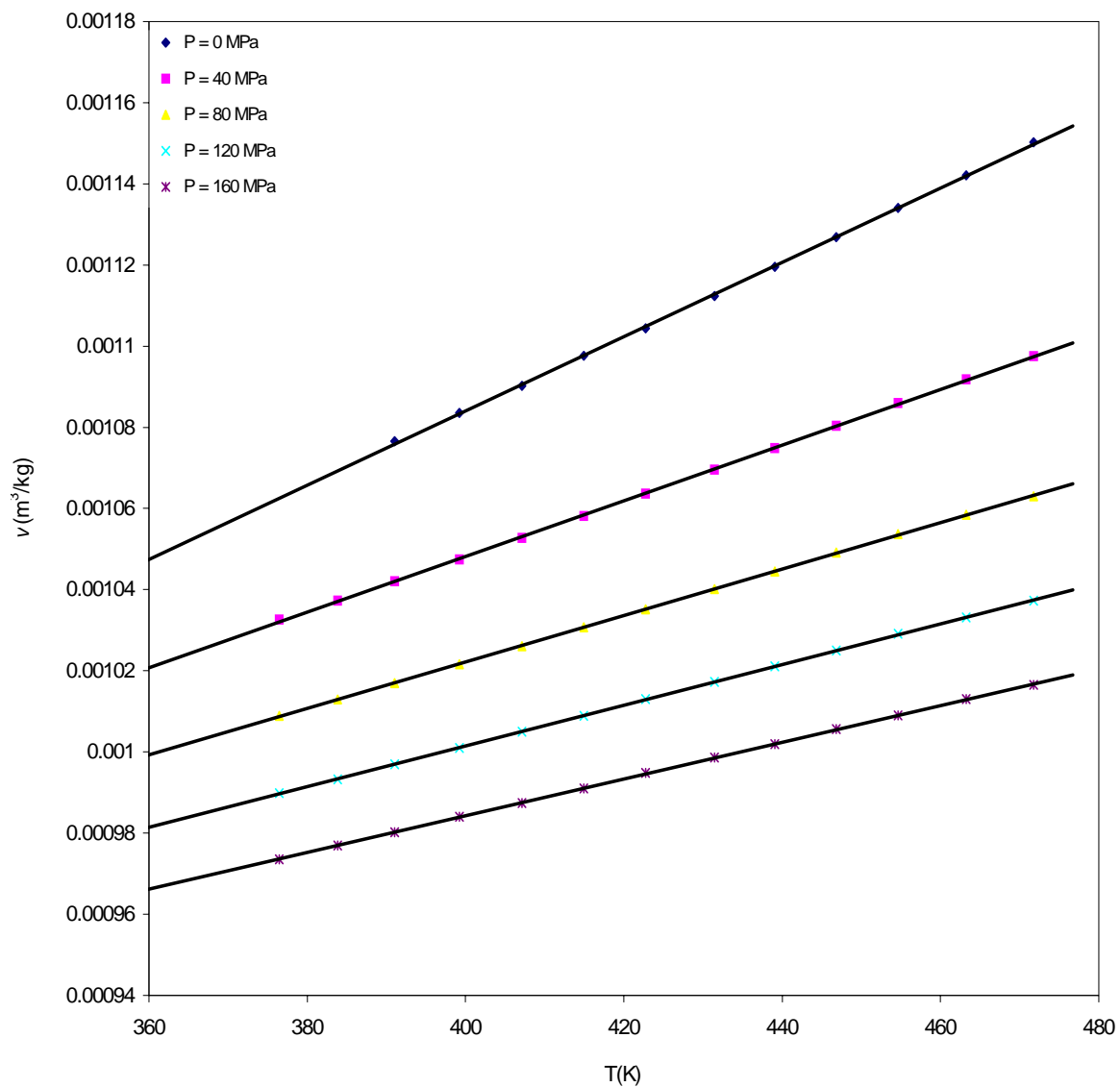


Figure D.5. Specific Volume vs. Temperature for PPO ($M_w=4000$)

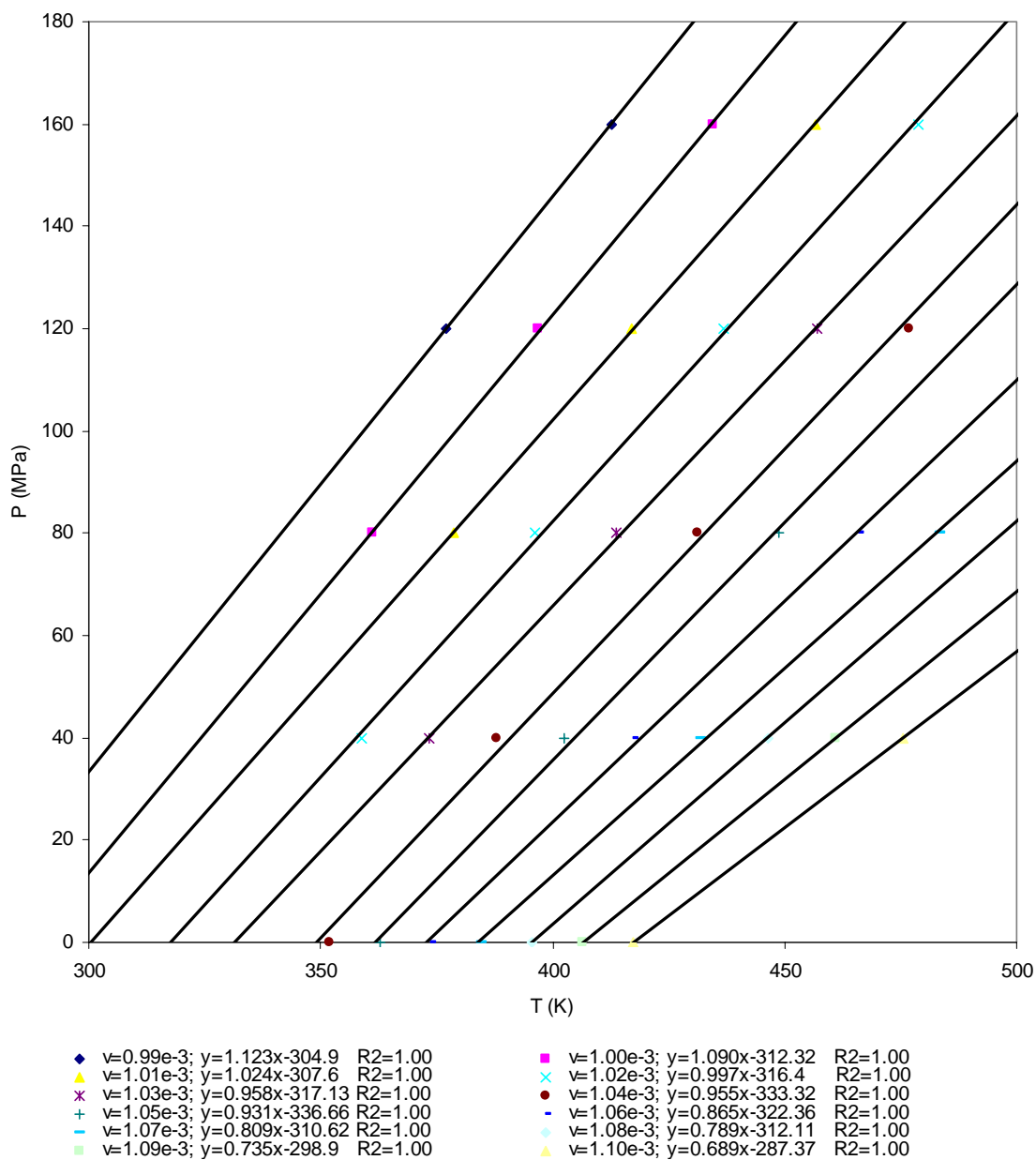


Figure D.6. Pressure vs. Temperature for PPO (Mw=4000)

Specific volume	P_i		$P_i^{1/2}$
(m ³ /kg)	(MPa)	(cal/cm ³)	(cal/cm ³) ^{1/2}
9.9*10 ⁻⁴	304.9	72.84	8.53
1.00*10 ⁻³	312.32	74.61	8.64
1.01*10 ⁻³	307.6	73.48	8.57
1.02*10 ⁻³	316.4	75.59	8.69
1.03*10 ⁻³	317.13	75.76	8.70
1.04*10 ⁻³	333.32	79.63	8.92
1.05*10 ⁻³	336.66	80.43	8.97
1.06*10 ⁻³	322.36	77.01	8.78
1.07*10 ⁻³	310.62	74.20	8.61
1.08*10 ⁻³	312.11	74.56	8.63
1.09*10 ⁻³	298.9	71.40	8.45
1.10*10 ⁻³	287.37	68.65	8.29
Average Value	313.31	74.85	8.65

Table D.3. Internal Pressure of Poly Propylene Oxide (Mw=4000)

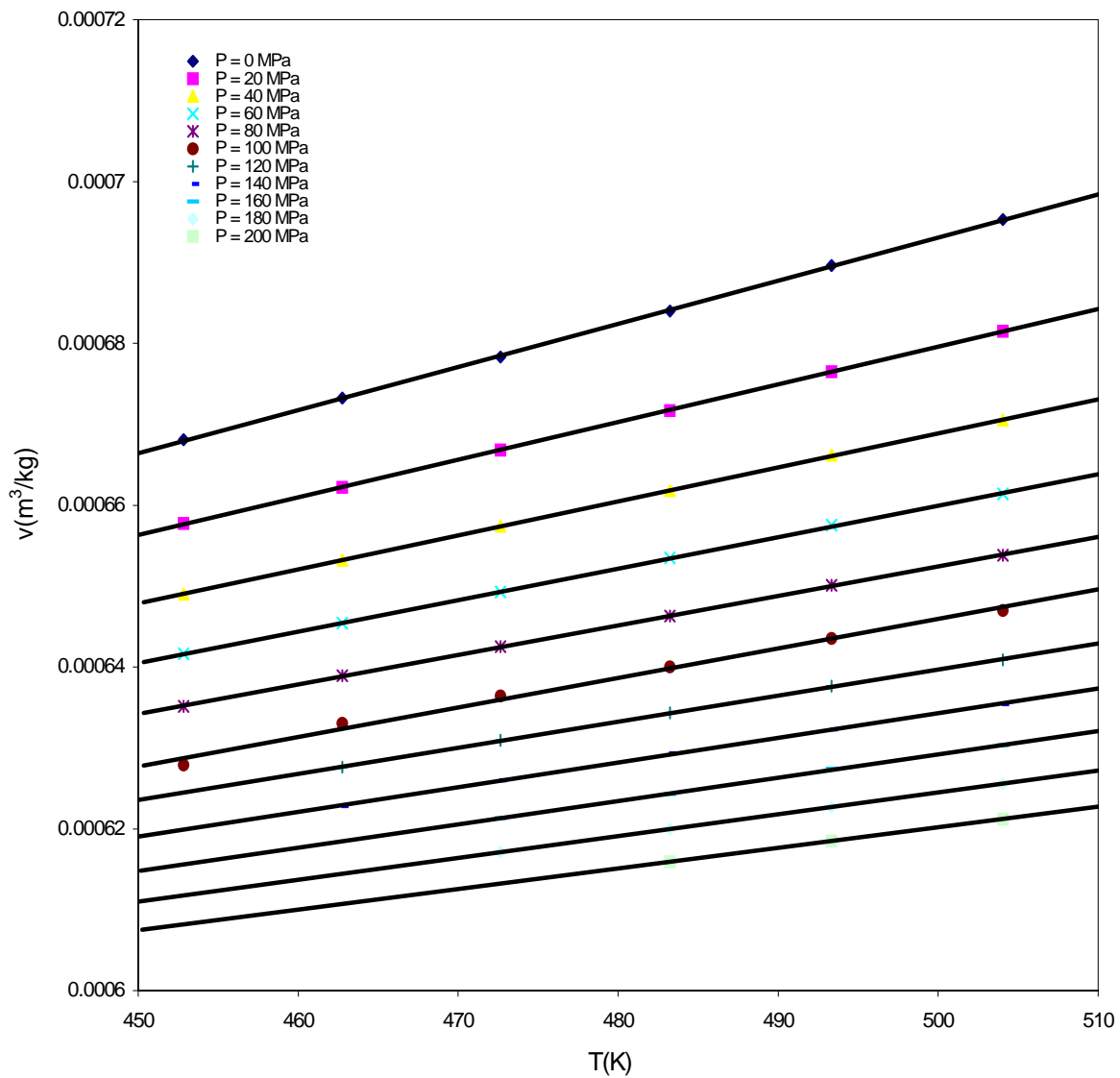


Figure D.7. Specific Volume vs. Temperature for PVDF

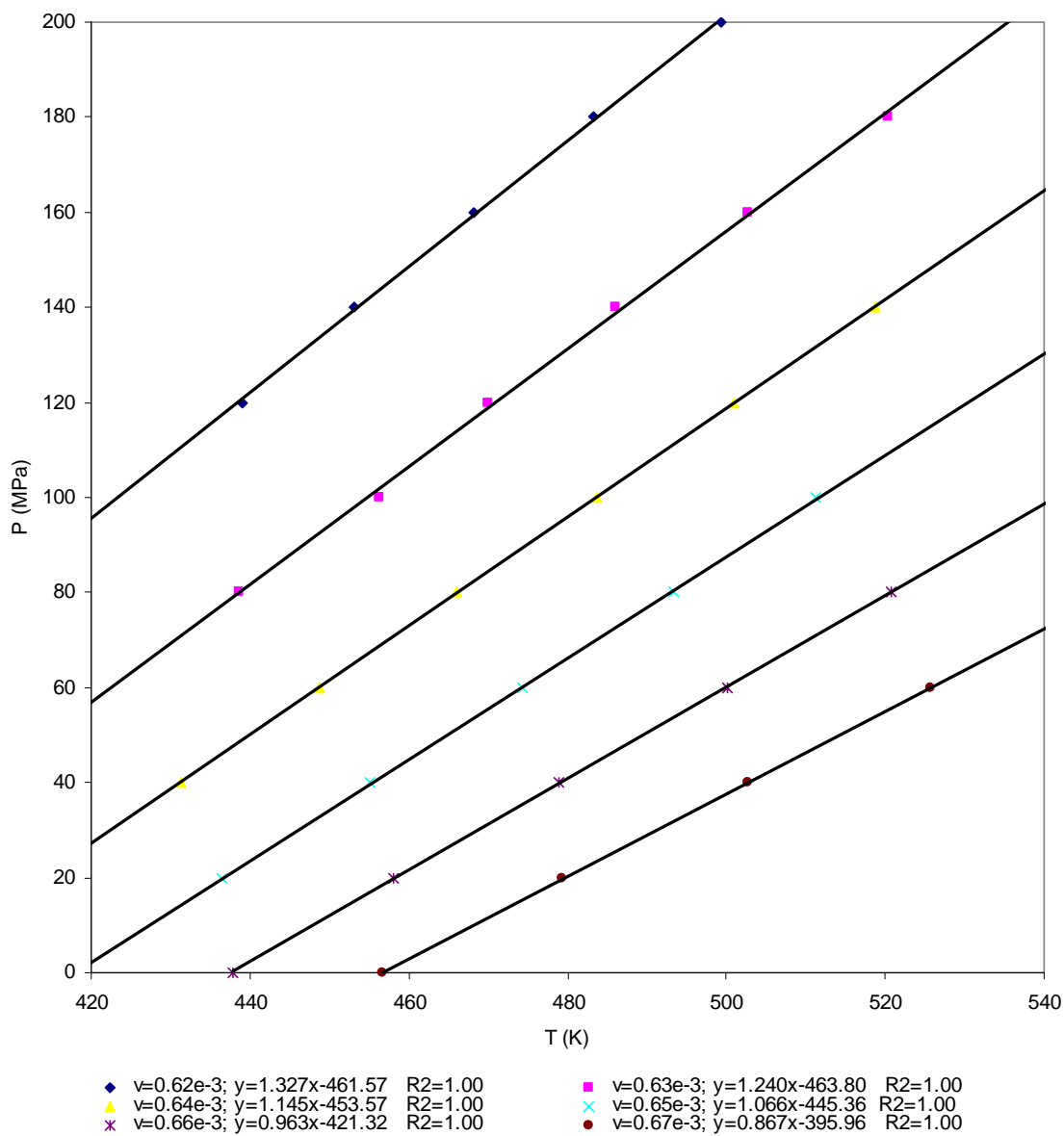


Figure D.8. Pressure vs. Temperature for PVDF

Specific volume	P_i		$P_i^{1/2}$
(m ³ /kg)	(MPa)	(cal/cm ³)	(cal/cm ³) ^{1/2}
6.2*10 ⁻⁴	461.57	110.27	10.50
6.3*10 ⁻⁴	463.80	110.80	10.53
6.4*10 ⁻⁴	453.57	108.35	10.41
6.5*10 ⁻⁴	445.36	106.39	10.31
6.6*10 ⁻⁴	421.32	100.65	10.03
6.7*10 ⁻⁴	395.96	94.59	9.73
Average Value	440.26	105.18	10.26

Table D.4. Internal Pressure of PVDF

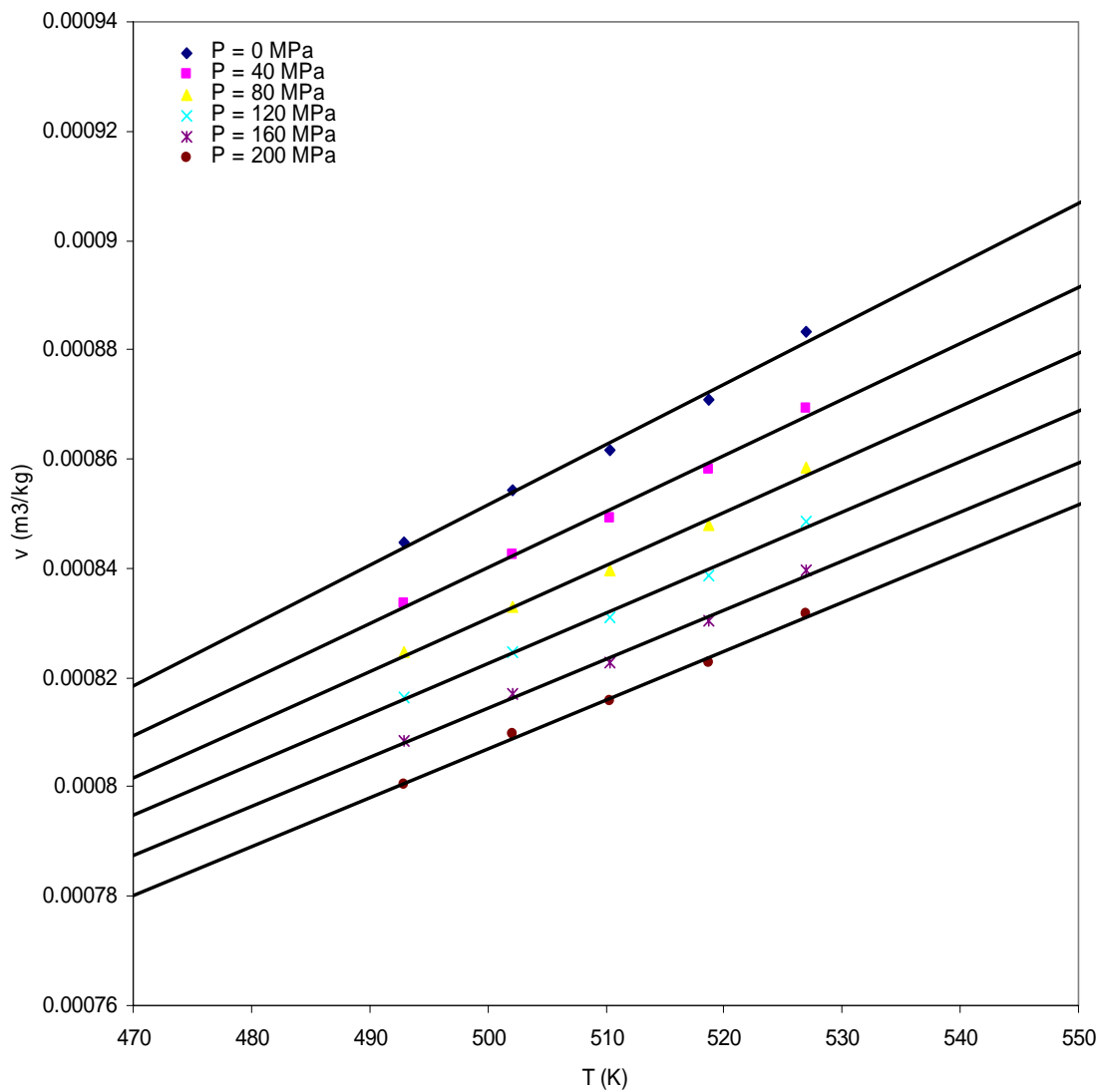


Figure D.9. Specific Volume vs. Temperature for PVOH

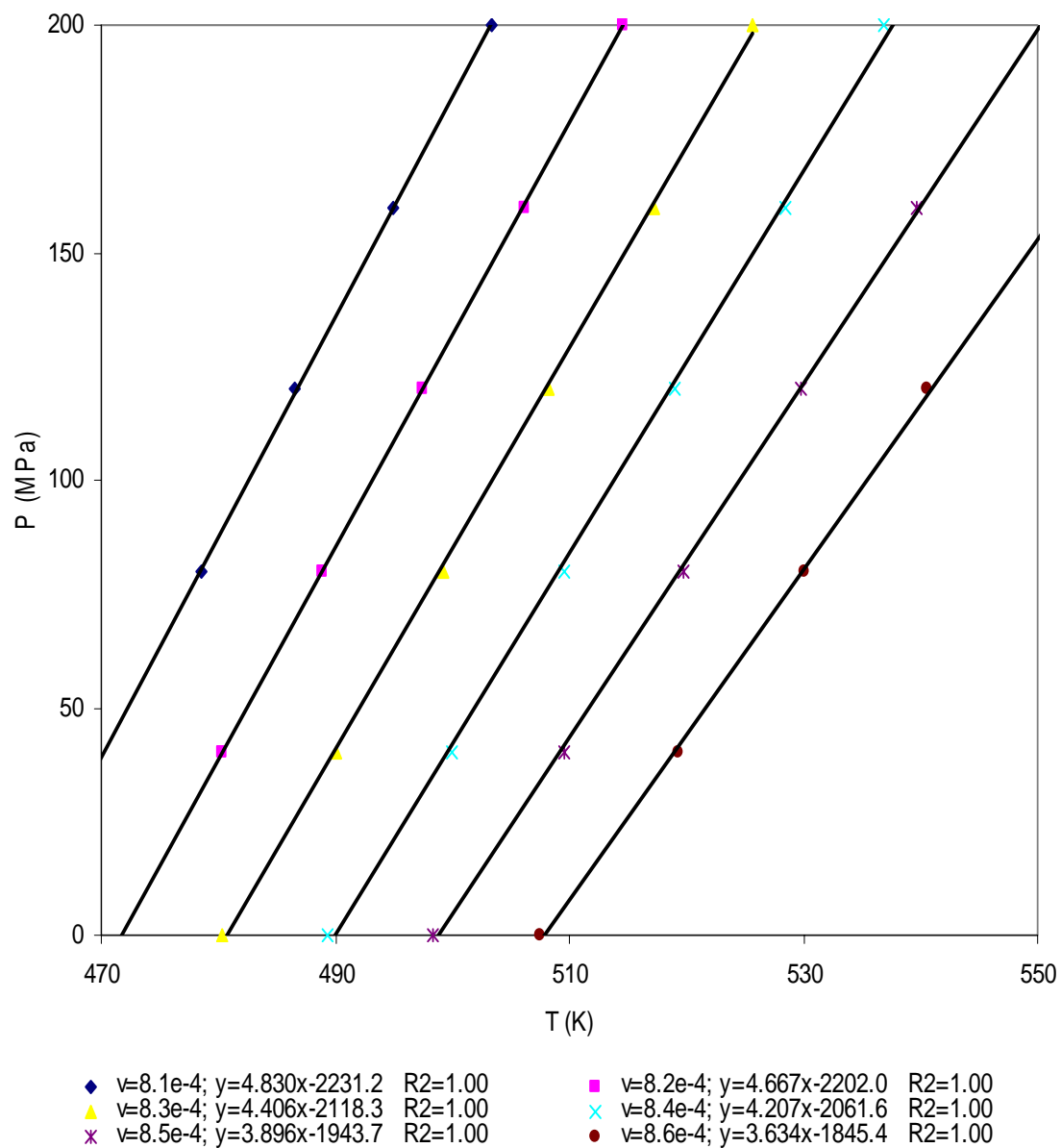


Figure D.10. Pressure vs. Temperature for PVOH

Specific volume	P_i		$P_i^{1/2}$
(m ³ /kg)	(MPa)	(cal/cm ³)	(cal/cm ³) ^{1/2}
8.1*10 ⁻⁴	2231.2	533.01	23.09
8.2*10 ⁻⁴	2202.0	526.04	22.94
8.3*10 ⁻⁴	2118.3	506.04	22.50
8.4*10 ⁻⁴	2061.6	492.50	22.19
8.5*10 ⁻⁴	1943.7	464.33	21.55
8.6*10 ⁻⁴	1845.4	440.85	21.00
Average Value	2067.03	493.80	22.22

Table D.5. Internal Pressure of PVOH

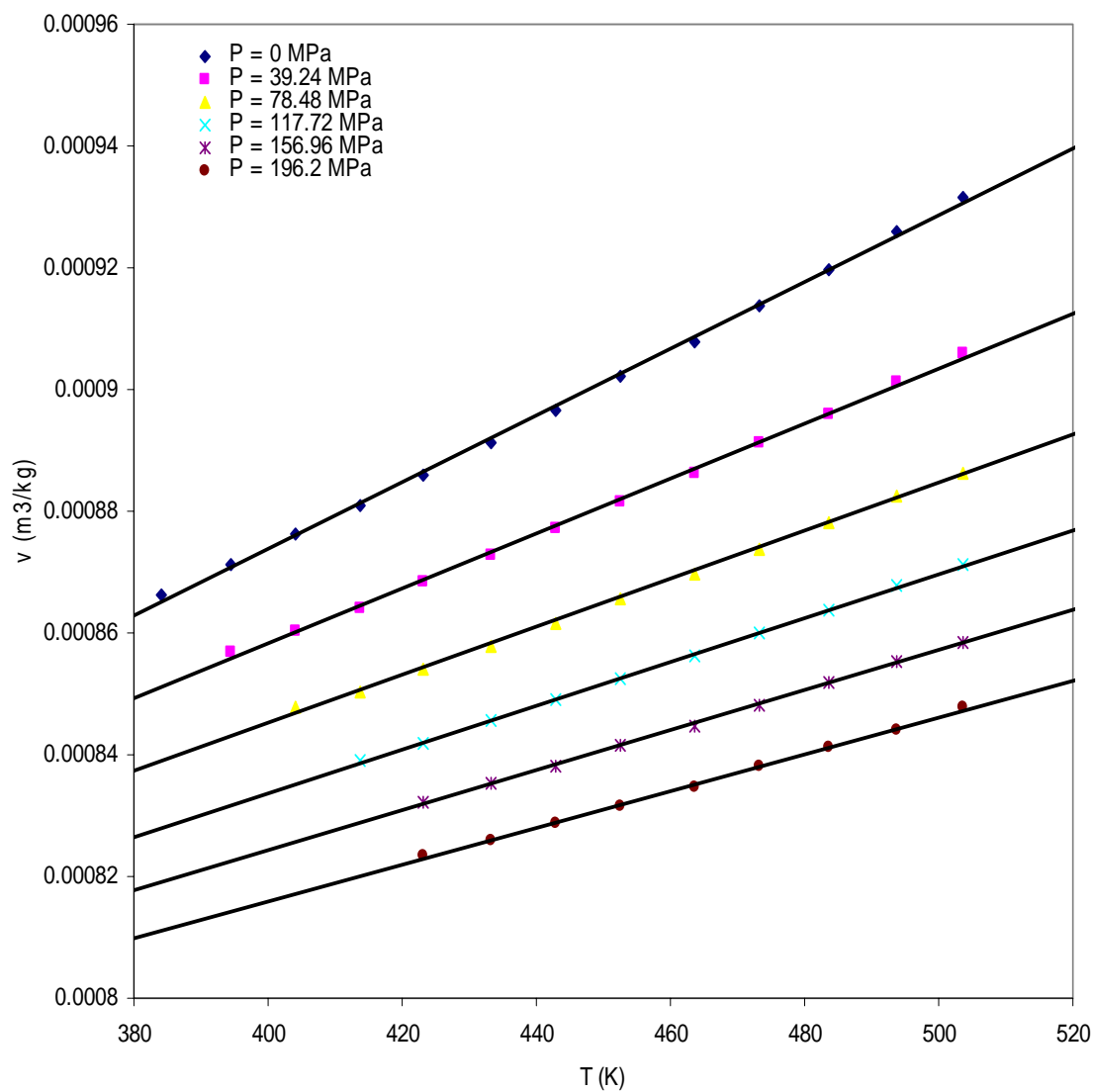


Figure D.11. Specific Volume vs. Temperature for
PMMA ($M_w=100.000$)

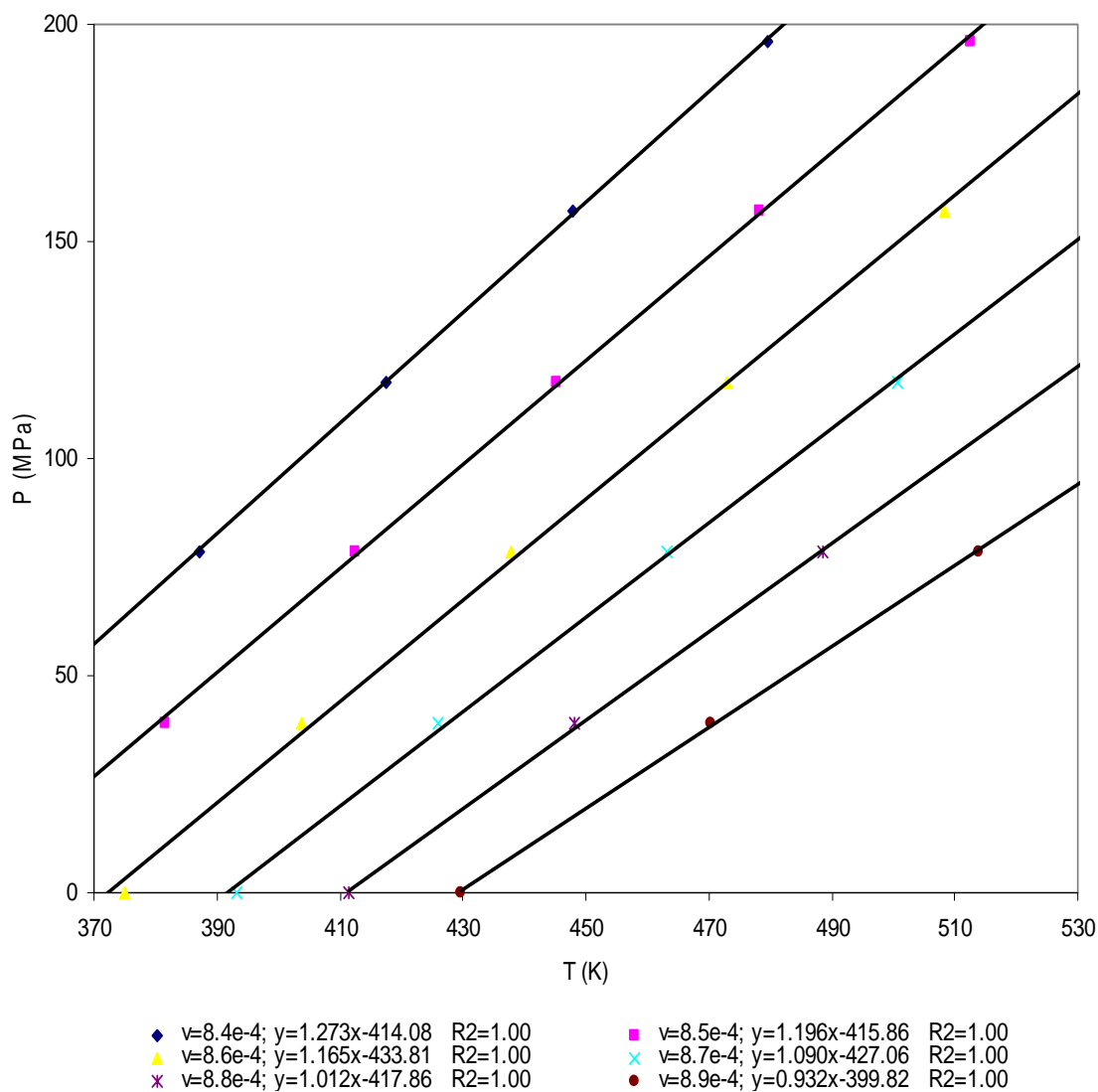


Figure D.12. Pressure vs. Temperature for PMMA

(M_w=100.000)

Specific volume	P_i		$P_i^{1/2}$
(m ³ /kg)	(MPa)	(cal/cm ³)	(cal/cm ³) ^{1/2}
8.4*10 ⁻⁴	414.08	98.92	9.95
8.5*10 ⁻⁴	415.86	99.35	9.97
8.6*10 ⁻⁴	433.81	103.63	10.18
8.7*10 ⁻⁴	427.06	102.02	10.10
8.8*10 ⁻⁴	417.86	99.82	9.99
8.9*10 ⁻⁴	399.82	95.51	9.77
Average Value	418.08	99.88	9.99

Table D.6. Internal Pressure of PMMA (M_w=100.000)

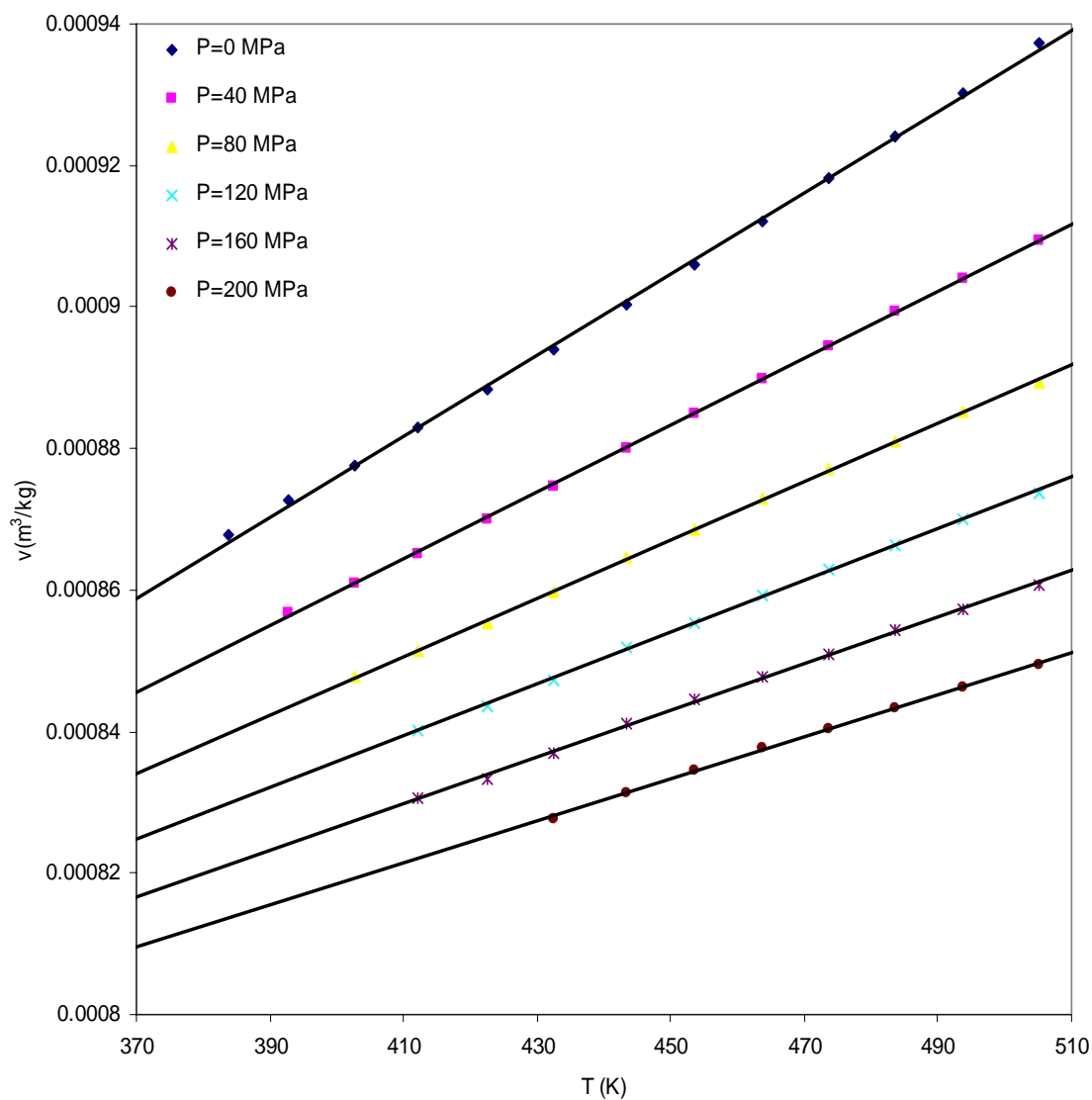


Figure D.13. Specific Volume vs. Temperature for
PMMA ($M_w=40.000$)

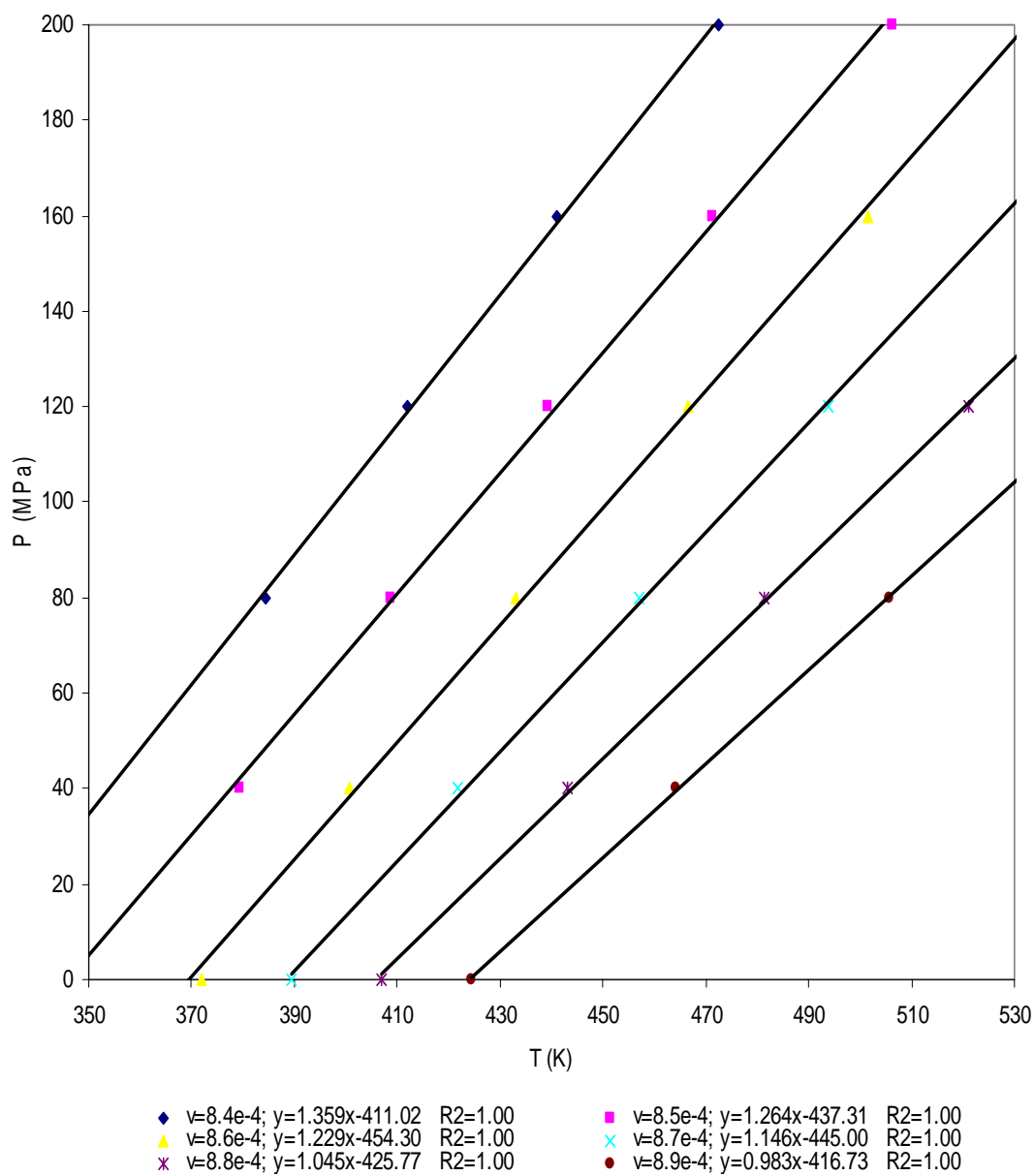


Figure D.14. Pressure vs. Temperature for PMMA ($M_w=40,000$)

Specific volume	P_i		$P_i^{1/2}$
(m ³ /kg)	(MPa)	(cal/cm ³)	(cal/cm ³) ^{1/2}
8.4*10 ⁻⁴	411.02	98.19	9.91
8.5*10 ⁻⁴	437.31	108.53	10.42
8.6*10 ⁻⁴	454.30	108.53	10.42
8.7*10 ⁻⁴	445.00	106.31	10.31
8.8*10 ⁻⁴	425.77	101.71	10.09
8.9*10 ⁻⁴	416.73	99.55	9.98
Average Value	431.69	103.13	10.16

Table D.7. Internal Pressure of PMMA (Mw=40.000)

E. Polymers in Good Solvents

When polymers are dissolved in good solvents, there is a strong thermodynamic driving force for the polymer chains to expand to maximize their ability to interact with solvent molecules. Daoud et. al.^{e1} showed that the radius of gyration, R_G , decreases continuously with increasing polymer concentration, as it can be seen in table E.1. Through Small Angle Neutron Scattering (SANS) experiments they measured the concentration dependence of the radius of gyration for Polystyrene in carbon disulfide (which is a good solvent for PS). They found that R_G^2 is proportional to the molecular weight of the polymer, M , and decreases with concentration as c^{-x} , where $x = 0.25 \pm 0.02$:

$$R_G^2 \propto Mc^{-1/4} \quad (\text{E1})$$

which follows the De Gennes relationship:

$$R^2(\phi) \cong R_0^2 \phi_p^{-1/4} \quad (\text{E2})$$

where R_0 is the radius of gyration in the melt. It then follows that the chain expansion factor can be expressed in terms of the volume fraction of the polymer:

$$\alpha^2 = \frac{R^2(\phi)}{R_0^2} = \phi_p^{-1/4} \quad (\text{E3})$$

e1. Daoud, M.; Cotton, J.P.; Farnoux, B.; Jannink, G.; Sarma, G.; Benoit, H.; Duplessix, R.; Picot, C.; de Gennes, P.G. *Macromolecules*, **8**, 804 (1975)

$c \text{ (g/cm}^3\text{)}$	ϕp	R_G	$\alpha = R_G / R_G^0$
0	0	137	1.67
0.03	0.028	120	1.46
0.06	0.057	117	1.43
0.1	0.094	111	1.35
0.15	0.141	104	1.27
0.2	0.189	101	1.23
0.33	0.311	95	1.16
0.5	0.472	91	1.11
1.06 (bulk)	1	82	1

Table E.1. The Radius of Gyration as a function of concentration for PS. Experimental data from Dauod et. al.^{e1}

This relationship is verified in figure E1, where the experimental data of Dauod et. al.^{e1} listed in table E.1 are plotted.

It appears that even at relatively high polymer concentrations, there is a considerable expansion of the polymer chains. From table E1 it can be seen that it is more than 10 % for $\phi_p \approx 0.5$.

To account for this apparent change in the chain expansion factor, which could possibly contribute to the free energy of mixing (as an entropic contribution), it was decided to use a relatively simple expression originally suggested by Flory^{e2} for the elastic free energy, ΔF_{el} :

$$\frac{\Delta F_{el}}{RT} = n_p \left[\frac{3}{2} (\alpha^2 - 1) - \ln \alpha^3 \right] \quad (E4)$$

The contribution to the chemical potential for this term can be found as:

$$\frac{\Delta \mu_{el}}{RT} = \frac{\partial \left(\frac{\Delta F_{el}}{RT} \right)}{\partial n_s} = \left(\frac{\partial \left(\frac{\Delta F_{el}}{RT} \right)}{\partial \alpha} \right) \left(\frac{\partial \alpha}{\partial \phi_p} \right) \left(\frac{\partial \phi_p}{\partial n_s} \right) \quad (E5)$$

If equation E3 is rewritten to:

$$\alpha = \phi_p^{-1/8} \quad (E6)$$

e2. Flory, P.J. *Principles of Polymer Chemistry*, Cornell University Press, Ithaca, N.Y. (1956)

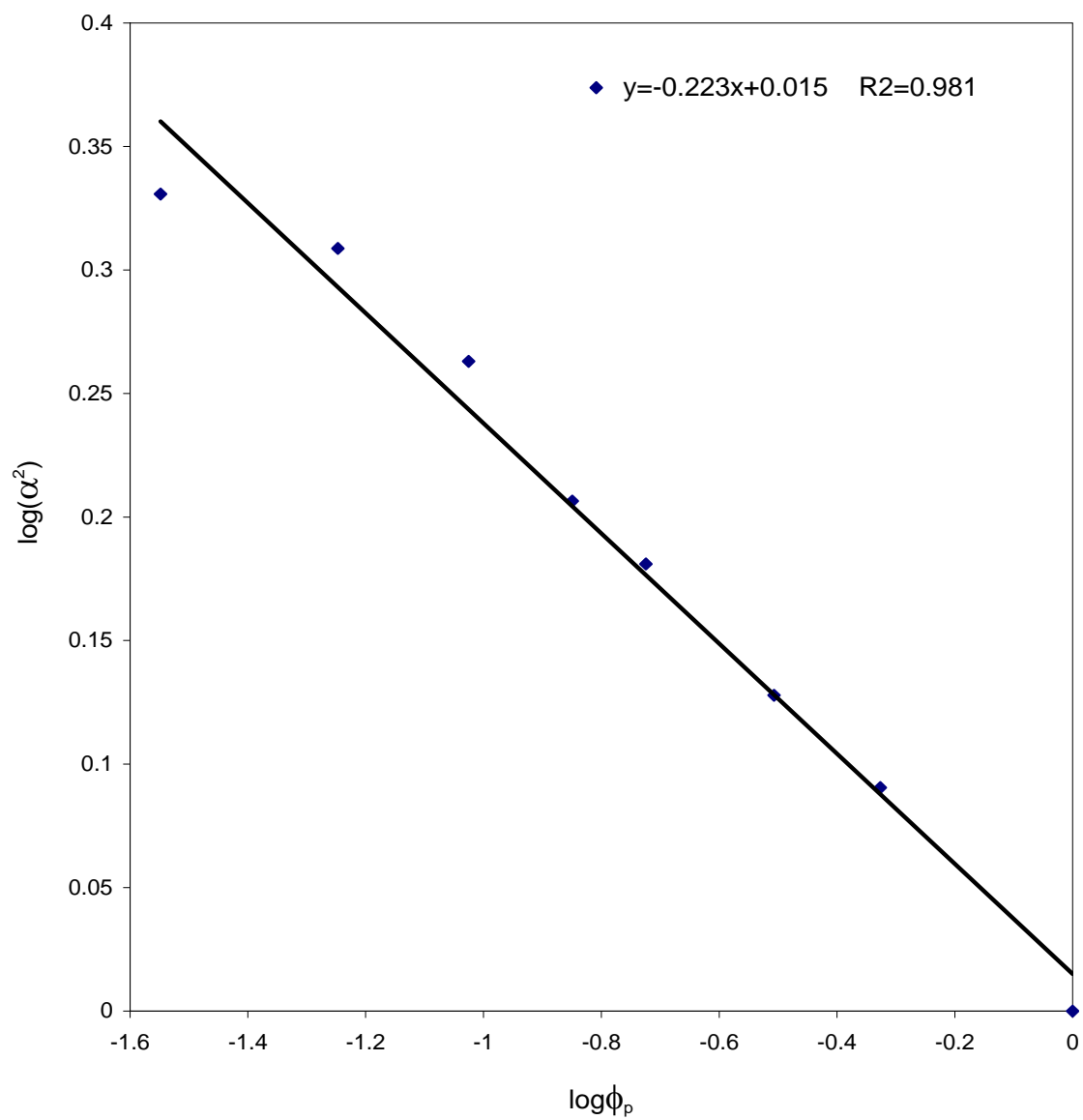


Figure E.1. The Chain Expansion Factor as a function of concentration for PS. Experimental data from Dauod et. al.^{e1}

then it follows that:

$$\frac{\partial \alpha}{\partial \phi_p} = -\frac{1}{8} \phi_p^{-9/8} \quad (\text{E7})$$

From equation E4 it can be shown that:

$$\frac{\partial \left(\frac{\Delta F_{el}}{RT} \right)}{\partial \alpha} = n_p \left[3\alpha - \frac{1}{\alpha^3} 3\alpha^2 \right] = 3n_p \left[\alpha - \frac{1}{\alpha} \right] \quad (\text{E8})$$

And from the definition of the volume fraction of the polymer, ϕ_p :

$$\phi_p = \frac{r_p n_p}{n_s + r_p n_p} \quad (\text{E9})$$

where r_p is the number of polymer segments, and n_i represents the number of moles of component i , it follows that:

$$\frac{\partial \phi_p}{\partial n_s} = -\frac{r n_p}{(n_s + r_p n_p)^2} = -\frac{\phi_p}{(n_s + r_p n_p)} = -\frac{\phi_p^2}{r_p n_p} \quad (\text{E10})$$

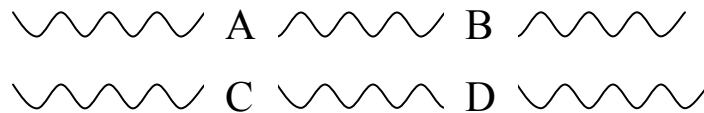
By inserting equation E7, E8 and E10 into equation E5, the following expression is obtained:

$$\begin{aligned}
\frac{\Delta\mu_{el}}{RT} &= 3n_p \left[\alpha - \frac{1}{\alpha} \right] \left(-\frac{1}{8} \phi_p^{-9/8} \right) \left(-\frac{\phi_p^2}{r_p n_p} \right) \\
&= \frac{3}{8r_p} \left[\alpha - \frac{1}{\alpha} \right] \phi_p^{7/8} \\
&= \frac{3}{8r_p} \left[\phi_p^{-1/8} - \phi_p^{1/8} \right] \phi_p^{7/8} \\
&= \frac{3}{8r_p} \left[\phi_p^{3/4} - \phi_p \right]
\end{aligned} \tag{E11}$$

which is the expression used in chapter 3 for the elastic contribution to the chemical potential of the solvent.

F. Interaction Parameters in Copolymer Blends

A generic example of a binary copolymer blend would be a blend of a (A,B)-copolymer and a (C,D)-copolymer, where copolymer 1 consists of A monomer units and B monomer units and copolymer 2 consists of C monomer units and D monomer units, respectively.



If f_i represents the volume fraction of component i , then the probability of finding an A segment next to another A segment is given by:

$$P_{AA} = f_A \gamma_1 + (1 - \gamma_1) \left[\frac{\phi_1 f_A (1 - \gamma_1)}{\phi_1 (1 - \gamma_1) + \phi_2 (1 - \gamma_2)} \right] \quad (\text{F1})$$

and the probability of finding an B segment next to another B segment is given by:

$$P_{BB} = f_B \gamma_1 + (1 - \gamma_1) \left[\frac{\phi_1 f_B (1 - \gamma_1)}{\phi_1 (1 - \gamma_1) + \phi_2 (1 - \gamma_2)} \right] \quad (\text{F2})$$

whereas the probability of finding an B segment next to an A segment is given by:

$$P_{BA} = f_B \gamma_1 + (1 - \gamma_1) \left[\frac{\phi_1 f_B (1 - \gamma_1)}{\phi_1 (1 - \gamma_1) + \phi_2 (1 - \gamma_2)} \right] \quad (\text{F3})$$

Now for contacts between different chains, the probability of finding a C segment next to an A segment is given by:

$$P_{CA} = (1 - \gamma_1) \left[\frac{\phi_2 f_C (1 - \gamma_2)}{\phi_1 (1 - \gamma_1) + \phi_2 (1 - \gamma_2)} \right] \quad (\text{F4})$$

Similar expressions are obtained for the other types of contacts:

$$P_{DA} = (1 - \gamma_1) \left[\frac{\phi_1 f_D (1 - \gamma_2)}{\phi_1 (1 - \gamma_1) + \phi_2 (1 - \gamma_2)} \right] \quad (\text{F5})$$

$$P_{DB} = (1 - \gamma_1) \left[\frac{\phi_1 f_D (1 - \gamma_2)}{\phi_1 (1 - \gamma_1) + \phi_2 (1 - \gamma_2)} \right] \quad (\text{F6})$$

$$P_{CB} = (1 - \gamma_1) \left[\frac{\phi_1 f_C (1 - \gamma_2)}{\phi_1 (1 - \gamma_1) + \phi_2 (1 - \gamma_2)} \right] \quad (\text{F7})$$

The energy interactions in the blend can therefore be written as:

$$\begin{aligned} E_{blend} = & \phi_1 f_A P_{AA} c_{AA} + \phi_1 f_B P_{BB} c_{BB} + \phi_2 f_C P_{CC} c_{CC} + \phi_2 f_D P_{DD} c_{DD} \\ & + 2\phi_1 f_A P_{BA} c_{AB} + 2\phi_1 f_A P_{CA} c_{AC} + 2\phi_1 f_A P_{DA} c_{AD} \\ & + 2\phi_2 f_B P_{CB} c_{BC} + 2\phi_2 f_B P_{DB} c_{BD} + 2\phi_2 f_C P_{DC} c_{CD} \end{aligned} \quad (\text{F8})$$

where c_{ij} is the interaction energy between component i and j , respectively. In the pure states the interaction energy is given by:

$$E_1 = \phi_1 (f_A^2 c_{AA} + f_B^2 c_{BB} + 2f_A f_B c_{AB}) \quad (\text{F9})$$

$$E_2 = \phi_2 (f_C^2 c_{CC} + f_D^2 c_{DD} + 2f_C f_D c_{CD}) \quad (\text{F10})$$

It then follows that the combined interaction energy is given by:

$$\Delta E = E_{blend} - \sum E_i \quad (\text{F11})$$

It is now possible to look at the individual terms. For contacts between two A segments the interaction energy term is:

$$\begin{aligned} \Delta E_{AA} &= \phi_1 f_A p_{AA} c_{AA} - \phi_1 f_A^2 c_{AA} \\ &= \phi_1 f_A c_{AA} \left[f_A \gamma_1 + \left[\frac{\phi_1 f_A (1-\gamma_1)^2}{\phi_1 (1-\gamma_1) + \phi_2 (1-\gamma_2)} \right] - f_A \right] \\ &= -\phi_1 f_A c_{AA} \left[f_A (1-\gamma_1) - \left[\frac{\phi_1 f_A (1-\gamma_1)^2}{\phi_1 (1-\gamma_1) + \phi_2 (1-\gamma_2)} \right] \right] \\ &= -\phi_1 f_A^2 (1-\gamma_1) c_{AA} \left[1 - \left[\frac{\phi_1 (1-\gamma_1)}{\phi_1 (1-\gamma_1) + \phi_2 (1-\gamma_2)} \right] \right] \\ &= -\phi_1 \phi_2 f_A^2 \left[\frac{(1-\gamma_1)(1-\gamma_2)}{\phi_1 (1-\gamma_1) + \phi_2 (1-\gamma_2)} \right] c_{AA} \end{aligned} \quad (\text{F12})$$

In the same manner it is possible to express the interaction energy between two B segments as:

$$\begin{aligned}
\Delta E_{BB} &= \phi_1 f_B P_{BB} c_{BB} - \phi_1 f_B^2 c_{BB} \\
&= \phi_1 f_B c_{BB} \left[f_B \gamma_1 + \left[\frac{\phi_1 f_B (1-\gamma_1)^2}{\phi_1 (1-\gamma_1) + \phi_2 (1-\gamma_2)} \right] - f_B \right] \\
&= -\phi_1 f_B c_{BB} \left[f_B (1-\gamma_1) - \left[\frac{\phi_1 f_B (1-\gamma_1)^2}{\phi_1 (1-\gamma_1) + \phi_2 (1-\gamma_2)} \right] \right] \\
&= -\phi_1 f_B^2 (1-\gamma_1) c_{BB} \left[1 - \left[\frac{\phi_1 (1-\gamma_1)}{\phi_1 (1-\gamma_1) + \phi_2 (1-\gamma_2)} \right] \right] \\
&= -\phi_1 \phi_2 f_B^2 \left[\frac{(1-\gamma_1)(1-\gamma_2)}{\phi_1 (1-\gamma_1) + \phi_2 (1-\gamma_2)} \right] c_{BB}
\end{aligned} \tag{F13}$$

and the interaction energy between A and B segments can be expressed as:

$$\begin{aligned}
\Delta E_{AB} &= 2\phi_1 f_A P_{BA} c_{AB} - 2\phi_1 f_A f_B c_{AB} \\
&= 2\phi_1 f_A c_{AB} \left[f_B \gamma_1 + \left[\frac{\phi_1 f_B (1-\gamma_1)^2}{\phi_1 (1-\gamma_1) + \phi_2 (1-\gamma_2)} \right] - f_B \right] \\
&= -2\phi_1 f_A c_{AB} \left[f_B (1-\gamma_1) - \left[\frac{\phi_1 f_B (1-\gamma_1)^2}{\phi_1 (1-\gamma_1) + \phi_2 (1-\gamma_2)} \right] \right] \\
&= -2\phi_1 f_A f_B (1-\gamma_1) c_{AB} \left[1 - \left[\frac{\phi_1 (1-\gamma_1)}{\phi_1 (1-\gamma_1) + \phi_2 (1-\gamma_2)} \right] \right] \\
&= -2\phi_1 \phi_2 f_A f_B \left[\frac{(1-\gamma_1)(1-\gamma_2)}{\phi_1 (1-\gamma_1) + \phi_2 (1-\gamma_2)} \right] c_{AB}
\end{aligned} \tag{F14}$$

Similar expressions can be written for interactions involving C and D segments as well:

$$\Delta E_{CC} = -\phi_1 \phi_2 f_C^2 \left[\frac{(1-\gamma_1)(1-\gamma_2)}{\phi_1(1-\gamma_1) + \phi_2(1-\gamma_2)} \right] c_{CC} \quad (\text{F15})$$

$$\Delta E_{DD} = -\phi_1 \phi_2 f_D^2 \left[\frac{(1-\gamma_1)(1-\gamma_2)}{\phi_1(1-\gamma_1) + \phi_2(1-\gamma_2)} \right] c_{DD} \quad (\text{F16})$$

$$\Delta E_{CD} = -2\phi_1 \phi_2 f_C f_D \left[\frac{(1-\gamma_1)(1-\gamma_2)}{\phi_1(1-\gamma_1) + \phi_2(1-\gamma_2)} \right] c_{CD} \quad (\text{F17})$$

as well as the cross interaction terms:

$$\Delta E_{AC} = 2\phi_1 \phi_2 f_A f_C \left[\frac{(1-\gamma_1)(1-\gamma_2)}{\phi_1(1-\gamma_1) + \phi_2(1-\gamma_2)} \right] c_{AC} \quad (\text{F18})$$

$$\Delta E_{AD} = 2\phi_1 \phi_2 f_A f_D \left[\frac{(1-\gamma_1)(1-\gamma_2)}{\phi_1(1-\gamma_1) + \phi_2(1-\gamma_2)} \right] c_{AD} \quad (\text{F19})$$

$$\Delta E_{BC} = 2\phi_1 \phi_2 f_B f_C \left[\frac{(1-\gamma_1)(1-\gamma_2)}{\phi_1(1-\gamma_1) + \phi_2(1-\gamma_2)} \right] c_{BC} \quad (\text{F20})$$

$$\Delta E_{BD} = 2\phi_1 \phi_2 f_B f_D \left[\frac{(1-\gamma_1)(1-\gamma_2)}{\phi_1(1-\gamma_1) + \phi_2(1-\gamma_2)} \right] c_{BD} \quad (\text{F21})$$

By combining equation F12 through equation F21, the following expression is obtained:

$$\Delta E = \phi_1 \phi_2 \left(\frac{(1-\gamma_1)(1-\gamma_2)}{\phi_1(1-\gamma_1) + \phi_2(1-\gamma_2)} \right) \begin{bmatrix} 2f_A f_C c_{AC} + 2f_A f_D c_{AD} + 2f_B f_C c_{BC} \\ + 2f_B f_D c_{BD} - f_A^2 c_{AA} - f_B^2 c_{BB} \\ - 2f_A f_B c_{AB} - f_C^2 c_{CC} - f_D^2 c_{DD} - 2f_C f_D c_{CD} \end{bmatrix} \quad (\text{F22})$$

Since the interaction parameter can be defined as:

$$\chi_{ij} = 2c_{ij} - c_{ii} - c_{jj} \quad (\text{F23})$$

Equation F22 can be expressed as:

$$\begin{aligned} \Delta E &= \phi_1 \phi_2 \left(\frac{(1-\gamma_1)(1-\gamma_2)}{\phi_1(1-\gamma_1) + \phi_2(1-\gamma_2)} \right) \begin{bmatrix} f_A f_C (\chi_{AC} + c_{AA} + c_{CC}) + f_A f_D (\chi_{AD} + c_{AA} + c_{DD}) \\ + f_B f_C (\chi_{BC} + c_{BB} + c_{CC}) + f_B f_D (\chi_{BD} + c_{BB} + c_{DD}) \\ - f_A f_B (\chi_{AB} + c_{AA} + c_{BB}) - f_C f_D (\chi_{CD} + c_{CC} + c_{DD}) \\ - f_A^2 c_{AA} - f_B^2 c_{BB} - f_C^2 c_{CC} - f_D^2 c_{DD} \end{bmatrix} \\ &= \phi_1 \phi_2 \left(\frac{(1-\gamma_1)(1-\gamma_2)}{\phi_1(1-\gamma_1) + \phi_2(1-\gamma_2)} \right) \begin{bmatrix} f_A f_C \chi_{AC} + f_A f_D \chi_{AD} + f_B f_C \chi_{BC} + f_B f_D \chi_{BD} \\ - f_A f_B \chi_{AB} - f_C f_D \chi_{CD} + f_A c_{AA} (f_C + f_D - f_A - f_B) \\ + f_B c_{BB} (f_C + f_D - f_A - f_B) + f_C c_{CC} (f_A + f_B - f_C - f_D) \\ + f_D c_{DD} (f_A + f_B - f_C - f_D) \end{bmatrix} \end{aligned} \quad (\text{F24})$$

Since $f_A + f_B = 1$ and $f_C + f_D = 1$ the equation further reduces to:

$$\Delta E = \phi_1 \phi_2 \left(\frac{(1-\gamma_1)(1-\gamma_2)}{\phi_1(1-\gamma_1) + \phi_2(1-\gamma_2)} \right) \begin{bmatrix} f_A f_C \chi_{AC} + f_A f_D \chi_{AD} + f_B f_C \chi_{BC} \\ + f_B f_D \chi_{BD} - f_A f_B \chi_{AB} - f_C f_D \chi_{CD} \end{bmatrix} \quad (\text{F25})$$

When this term is compared to the energetic interaction term in the traditional Flory-Huggins theory:

$$\phi_1\phi_2\chi^{FH} \quad (F26)$$

it can be seen that:

$$\chi_E^{FH} = \left(\frac{(1-\gamma_1)(1-\gamma_2)}{1-\gamma_1\phi_1-\gamma_2\phi_2} \right) \left[\begin{aligned} &f_A f_C \chi_{AC} + f_A f_D \chi_{AD} + f_B f_C \chi_{BC} \\ &+ f_B f_D \chi_{BD} - f_A f_B \chi_{AB} - f_C f_D \chi_{CD} \end{aligned} \right] \quad (F27)$$

Using the relationship from chapter 4 (equation 4):

$$\chi_{SC}^E = \chi_E^{FH} + (\phi_1 - \phi_2) \frac{d\chi_E^{FH}}{d\phi_1} - \frac{1}{2} \phi_1 \phi_2 \frac{d^2 \chi_E^{FH}}{d\phi_1^2} \quad (F28)$$

and:

$$\frac{\partial \chi_E^{FH}}{\partial \phi_1} = - \frac{(1-\gamma_1)(1-\gamma_2)(\gamma_2-\gamma_1)}{(1-\gamma_1\phi_1-\gamma_2\phi_2)^2} \left[\begin{aligned} &f_A f_C \chi_{AC} + f_A f_D \chi_{AD} + f_B f_C \chi_{BC} \\ &+ f_B f_D \chi_{BD} - f_A f_B \chi_{AB} - f_C f_D \chi_{CD} \end{aligned} \right] \quad (F29)$$

$$\frac{\partial^2 \chi_E^{FH}}{\partial \phi_1^2} = \frac{2(1-\gamma_1)(1-\gamma_2)(\gamma_2-\gamma_1)^2}{(1-\gamma_1\phi_1-\gamma_2\phi_2)^3} \left[\begin{aligned} &f_A f_C \chi_{AC} + f_A f_D \chi_{AD} + f_B f_C \chi_{BC} \\ &+ f_B f_D \chi_{BD} - f_A f_B \chi_{AB} - f_C f_D \chi_{CD} \end{aligned} \right] \quad (F30)$$

it then follows that:

$$\begin{aligned} \chi_{SC}^E = & \left[\left(\frac{(1-\gamma_1)(1-\gamma_2)}{1-\gamma_1\phi_1-\gamma_2\phi_2} \right) - (\phi_1-\phi_2) \frac{(1-\gamma_1)(1-\gamma_2)(\gamma_2-\gamma_1)}{(1-\gamma_1\phi_1-\gamma_2\phi_2)^2} - \frac{1}{2}\phi_1\phi_2 \frac{2(1-\gamma_1)(1-\gamma_2)(\gamma_2-\gamma_1)^2}{(1-\gamma_1\phi_1-\gamma_2\phi_2)^3} \right] \times \\ & \left[\begin{aligned} & f_A f_C \chi_{AC} + f_A f_D \chi_{AD} + f_B f_C \chi_{BC} \\ & + f_B f_D \chi_{BD} - f_A f_B \chi_{AB} - f_C f_D \chi_{CD} \end{aligned} \right] \end{aligned} \quad (\text{F31})$$

which reduces to:

$$\begin{aligned} \chi_{SC}^E = & \left[\left(\frac{(1-\gamma_1)(1-\gamma_2)}{1-\gamma_1\phi_1-\gamma_2\phi_2} \right) - (\phi_1-\phi_2) \frac{(1-\gamma_1)(1-\gamma_2)(\gamma_2-\gamma_1)}{(1-\gamma_1\phi_1-\gamma_2\phi_2)^2} - \frac{1}{2}\phi_1\phi_2 \frac{2(1-\gamma_1)(1-\gamma_2)(\gamma_2-\gamma_1)^2}{(1-\gamma_1\phi_1-\gamma_2\phi_2)^3} \right] \times \\ & \left[\begin{aligned} & f_A f_C \chi_{AC} + f_A f_D \chi_{AD} + f_B f_C \chi_{BC} \\ & + f_B f_D \chi_{BD} - f_A f_B \chi_{AB} - f_C f_D \chi_{CD} \end{aligned} \right] \\ = & \frac{(1-\gamma_1)(1-\gamma_2)}{(1-\gamma_1\phi_1-\gamma_2\phi_2)^3} \left[(1-\gamma_1\phi_1-\gamma_2\phi_2)^2 - (\phi_1-\phi_2)(\gamma_2-\gamma_1)(1-\gamma_1\phi_1-\gamma_2\phi_2) - \phi_1\phi_2(\gamma_2-\gamma_1)^2 \right] \times \\ & \left[\begin{aligned} & f_A f_C \chi_{AC} + f_A f_D \chi_{AD} + f_B f_C \chi_{BC} \\ & + f_B f_D \chi_{BD} - f_A f_B \chi_{AB} - f_C f_D \chi_{CD} \end{aligned} \right] \\ = & \frac{(1-\gamma_1)(1-\gamma_2)}{(1-\gamma_1\phi_1-\gamma_2\phi_2)^3} [(1-\gamma_1)(1-\gamma_2)] \times \left[\begin{aligned} & f_A f_C \chi_{AC} + f_A f_D \chi_{AD} + f_B f_C \chi_{BC} \\ & + f_B f_D \chi_{BD} - f_A f_B \chi_{AB} - f_C f_D \chi_{CD} \end{aligned} \right] \\ = & \frac{(1-\gamma_1)^2(1-\gamma_2)^2}{(1-\gamma_1\phi_1-\gamma_2\phi_2)^3} \times \left[\begin{aligned} & f_A f_C \chi_{AC} + f_A f_D \chi_{AD} + f_B f_C \chi_{BC} \\ & + f_B f_D \chi_{BD} - f_A f_B \chi_{AB} - f_C f_D \chi_{CD} \end{aligned} \right] \end{aligned} \quad (\text{F32})$$

If the local volume fractions are now redefined as:

$$f_A = y_1; f_B = 1 - y_1; f_C = y_2; f_D = 1 - y_2 \quad (\text{F33})$$

and if it is observed that for isotopic blends (*where* $A \equiv C$ and $B \equiv D$):

$$\chi_{AC} = \chi_{BD} = 0 \quad \text{and} \quad \chi_{AB} = \chi_{AD} = \chi_{CD} = \chi_{BC} \quad (\text{F34})$$

then equation F32 can be rewritten as:

$$\begin{aligned} \chi_{SC}^E &= \frac{(1-\gamma_1)^2(1-\gamma_2)^2}{(1-\gamma_1\phi_1-\gamma_2\phi_2)^3} \times \left[\begin{aligned} &f_A f_C \chi_{AC} + f_A f_D \chi_{AD} + f_B f_C \chi_{BC} \\ &+ f_B f_D \chi_{BD} - f_A f_B \chi_{AB} - f_C f_D \chi_{CD} \end{aligned} \right] \\ &= \frac{(1-\gamma_1)^2(1-\gamma_2)^2}{(1-\gamma_1\phi_1-\gamma_2\phi_2)^3} \times \left[\begin{aligned} &y_1(1-y_2)\chi_{AB} + (1-y_1)y_2\chi_{AB} \\ &-y_1(1-y_1)\chi_{AB} - y_2(1-y_2)\chi_{AB} \end{aligned} \right] \\ &= \frac{(1-\gamma_1)^2(1-\gamma_2)^2}{(1-\gamma_1\phi_1-\gamma_2\phi_2)^3} \times [(y_1 - y_2)(1 - y_2) + (1 - y_1)(y_2 - y_1)]\chi_{AB} \\ &= \frac{(1-\gamma_1)^2(1-\gamma_2)^2}{(1-\gamma_1\phi_1-\gamma_2\phi_2)^3} (y_1 - y_2)[(1 - y_2) - (1 - y_1)]\chi_{AB} \\ &= \frac{(1-\gamma_1)^2(1-\gamma_2)^2(y_1 - y_2)^2}{(1-\gamma_1\phi_1-\gamma_2\phi_2)^3} \chi_{AB} \end{aligned} \quad (\text{F35})$$

which is the expression used in chapter 5.

G. Effects of Variation of the Screening Factor in Copolymer Blends

In the following, additional figures and tables stemming from calculations described in chapter 5 are given, where the screening factor of one of the copolymers are allowed to vary over the entire concentration range. In all these calculations, the screening factor of one of the copolymers is allowed to change to obtain the closest possible match to the experimental data reported by Graessley et al.^{g1}

As it can be seen in table G.1, where the number of significant digits for the screening factor, γ_B , has been extended to illustrate how small a change is needed in order to obtain a perfect fit with the experimental data. It can also be observed from table G.1, that the error function, c , seems to have very little influence on the resulting values of the screening factor, which will give the optimal fit. This observation seems to be true for all the temperatures studied here, as illustrated in tables G.2-G.4, respectively.

g1. Krishnamoorti, R.; Graessley, W.W.; Balsara, N.P.; Lohse, D.J. *J. Chem. Phys.*, **100**, 3894 (1994)

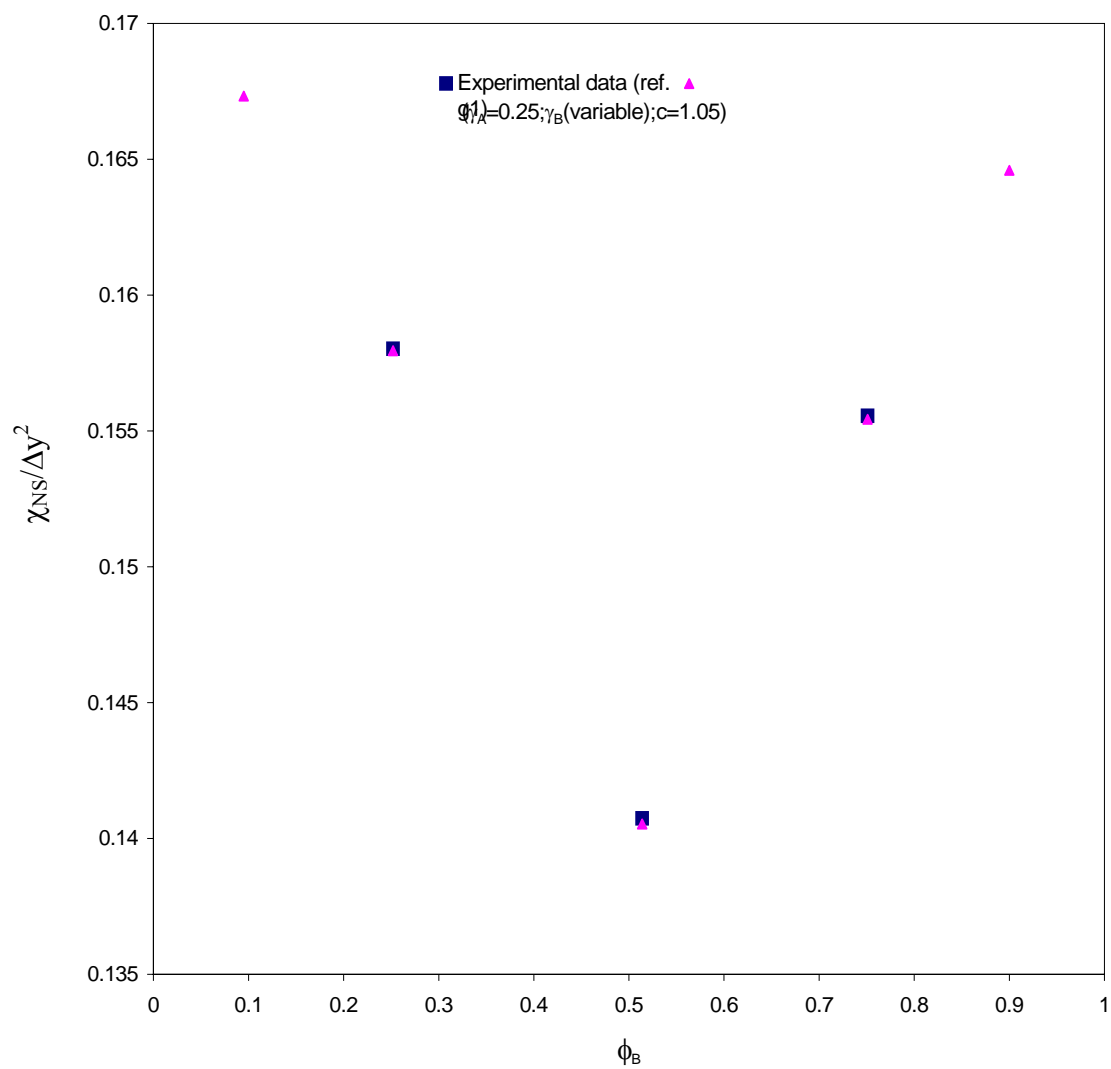


Figure G.1. Interaction parameters from SANS for H97/D88 at 51 °C.

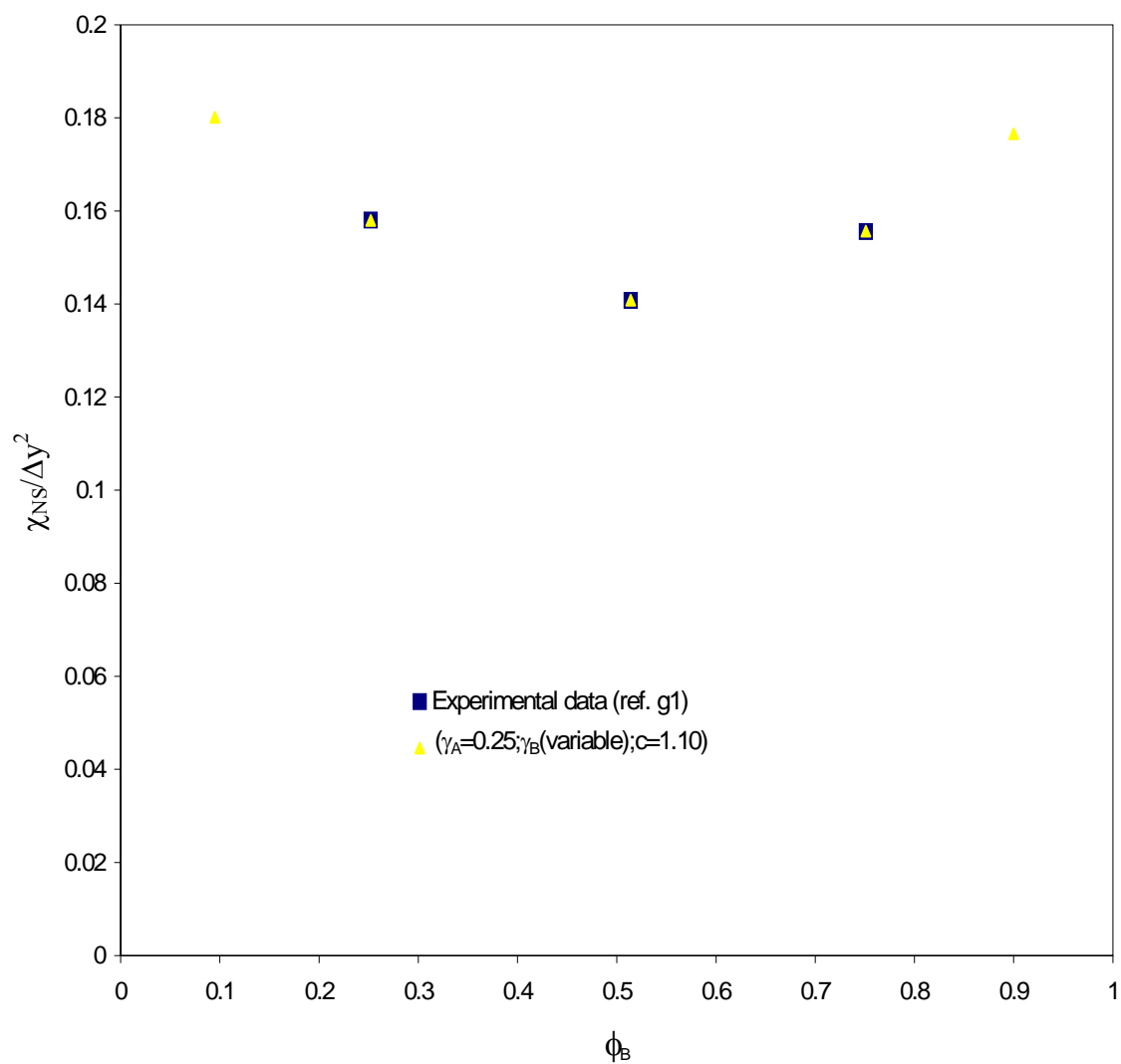


Figure G.2. Interaction parameters from SANS for H97/D88 at 51 °C.

ϕ_A	ϕ_B	c	$\chi_{\text{bare}} * 10^4$	γ_A	γ_B
0.1	0.9	1.05	5.43	0.25	0.242
0.249	0.751	1.05	5.43	0.25	0.24197
0.486	0.514	1.05	5.43	0.25	0.24233
0.748	0.252	1.05	5.43	0.25	0.24193
0.905	0.095	1.05	5.43	0.25	0.242
0.1	0.9	1.10	5.43	0.25	0.242
0.249	0.751	1.10	5.43	0.25	0.24203
0.486	0.514	1.10	5.43	0.25	0.24234
0.748	0.252	1.10	5.43	0.25	0.24199
0.905	0.095	1.10	5.43	0.25	0.242

Table G.1. Variations in the screening factor of *component B* for various c for H97/D88 at 51 °C.

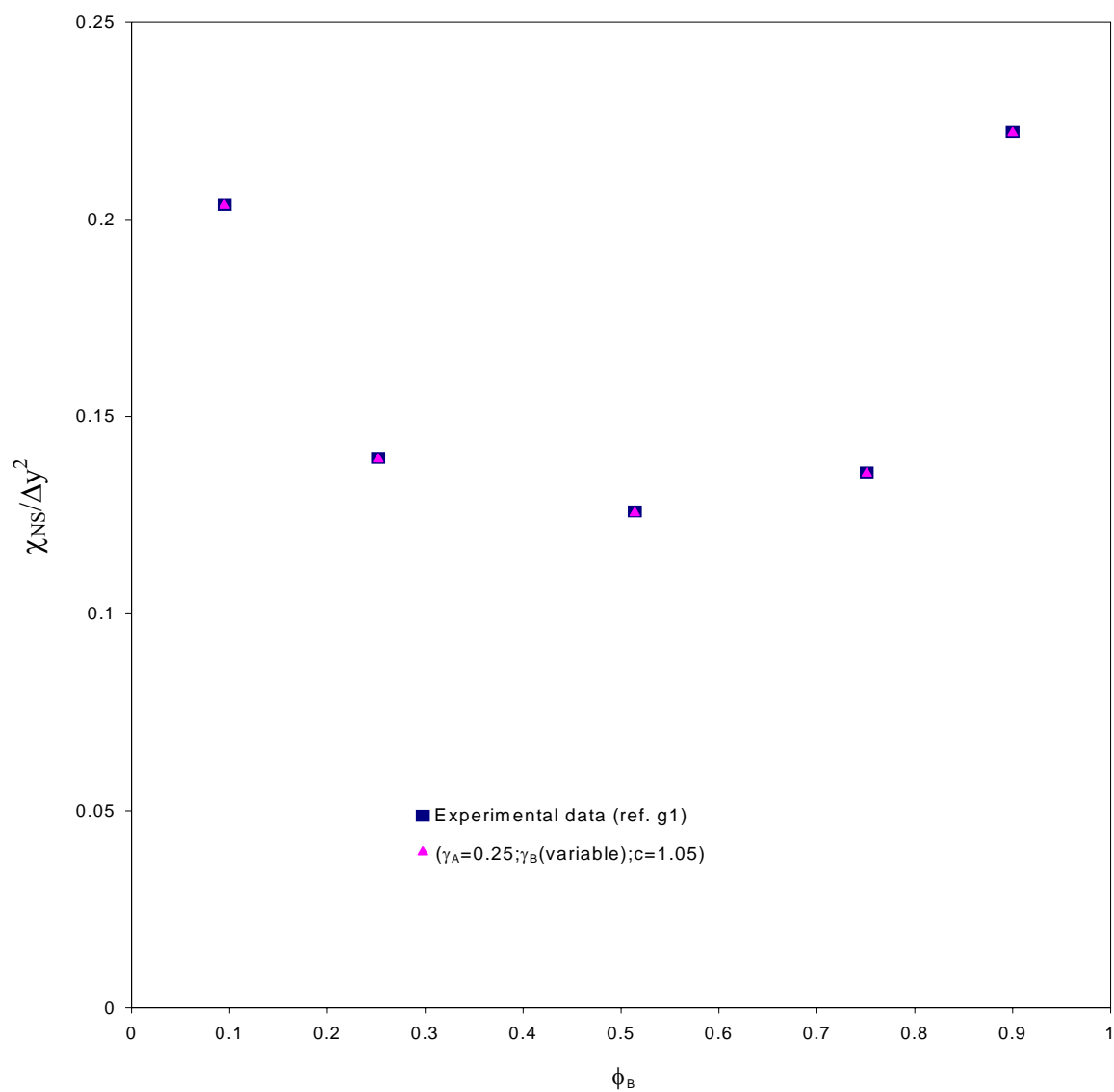


Figure G.3. Interaction parameters from SANS for H97/D88 at 83 °C.

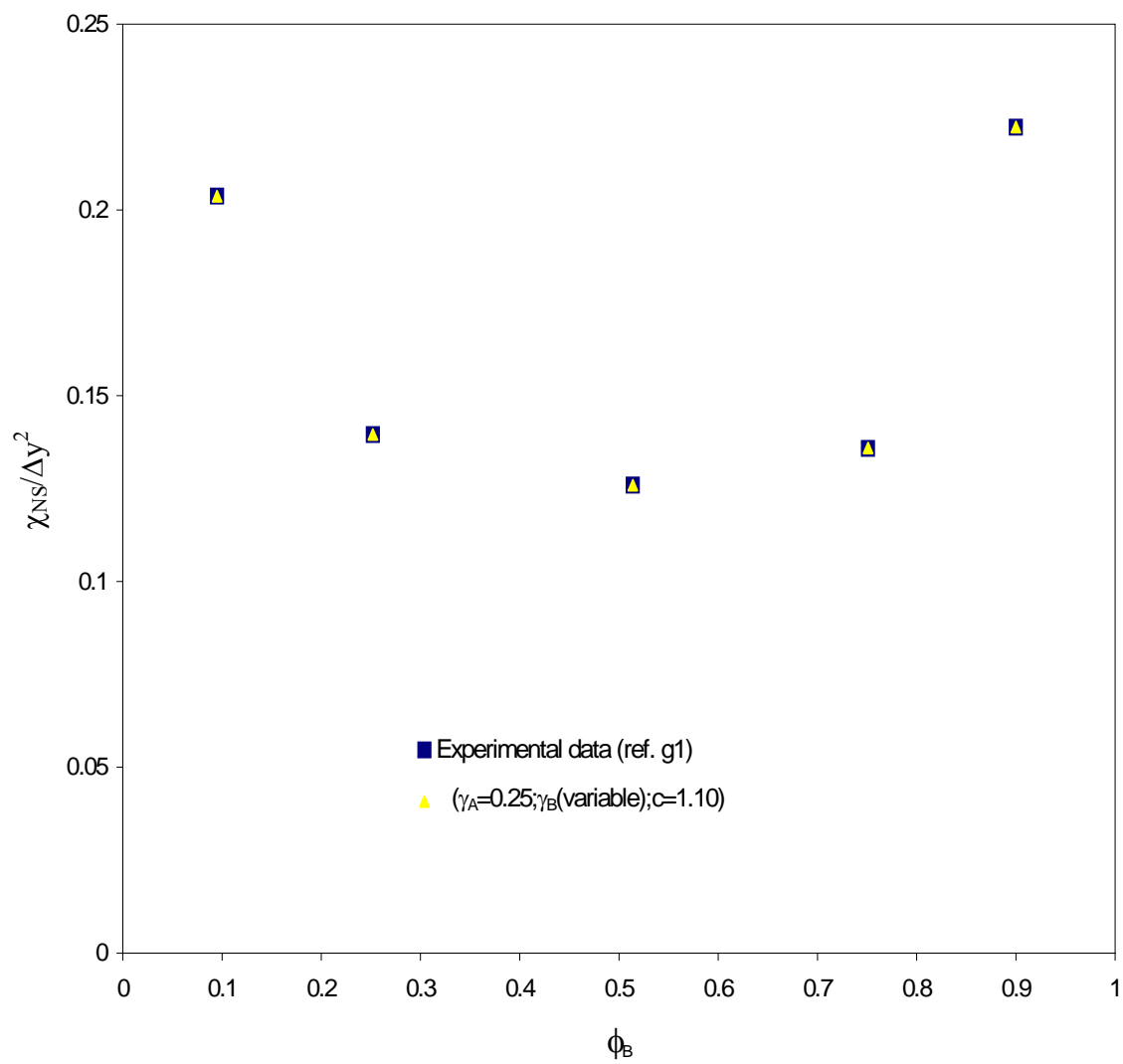


Figure G.4. Interaction parameters from SANS for H97/D88 at 83 °C.

ϕ_A	ϕ_B	c	$\chi_{bare} * 10^4$	γ_A	γ_B
0.1	0.9	1.05	4.94	0.25	0.24055
0.249	0.751	1.05	4.94	0.25	0.24252
0.486	0.514	1.05	4.94	0.25	0.24276
0.748	0.252	1.05	4.94	0.25	0.24244
0.905	0.095	1.05	4.94	0.25	0.24107
0.1	0.9	1.10	4.94	0.25	0.24078
0.249	0.751	1.10	4.94	0.25	0.24262
0.486	0.514	1.10	4.94	0.25	0.2428
0.748	0.252	1.10	4.94	0.25	0.24253
0.905	0.095	1.10	4.94	0.25	0.24136

Table G.2. Variations in the screening factor of *component B* for various c for H97/D88 at 83 °C.

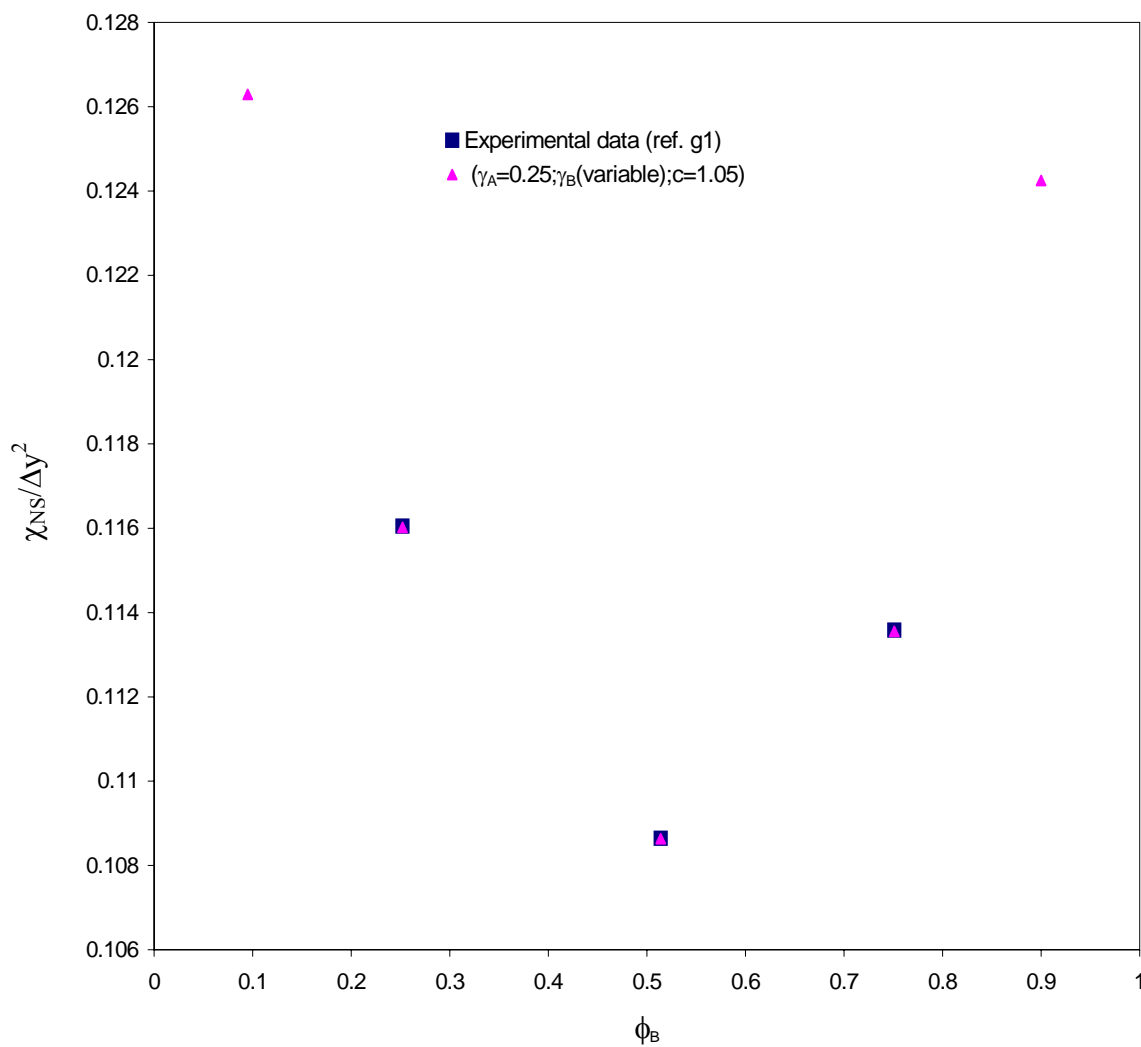


Figure G.5. Interaction parameters from SANS for H97/D88 at 121 °C.

ϕ_A	ϕ_B	c	$\chi_{bare} * 10^4$	γ_A	γ_B
0.1	0.9	1.05	4.47	0.25	0.2432
0.249	0.751	1.05	4.47	0.25	0.24321
0.486	0.514	1.05	4.47	0.25	0.2433
0.748	0.252	1.05	4.47	0.25	0.24315
0.905	0.095	1.05	4.47	0.25	0.2432
0.1	0.9	1.10	4.47	0.25	0.2432
0.249	0.751	1.10	4.47	0.25	0.24335
0.486	0.514	1.10	4.47	0.25	0.24337
0.748	0.252	1.10	4.47	0.25	0.24329
0.905	0.095	1.10	4.47	0.25	0.2432

Table G.3. Variations in the screening factor of *component B* for various c for H97/D88 at 121 °C.

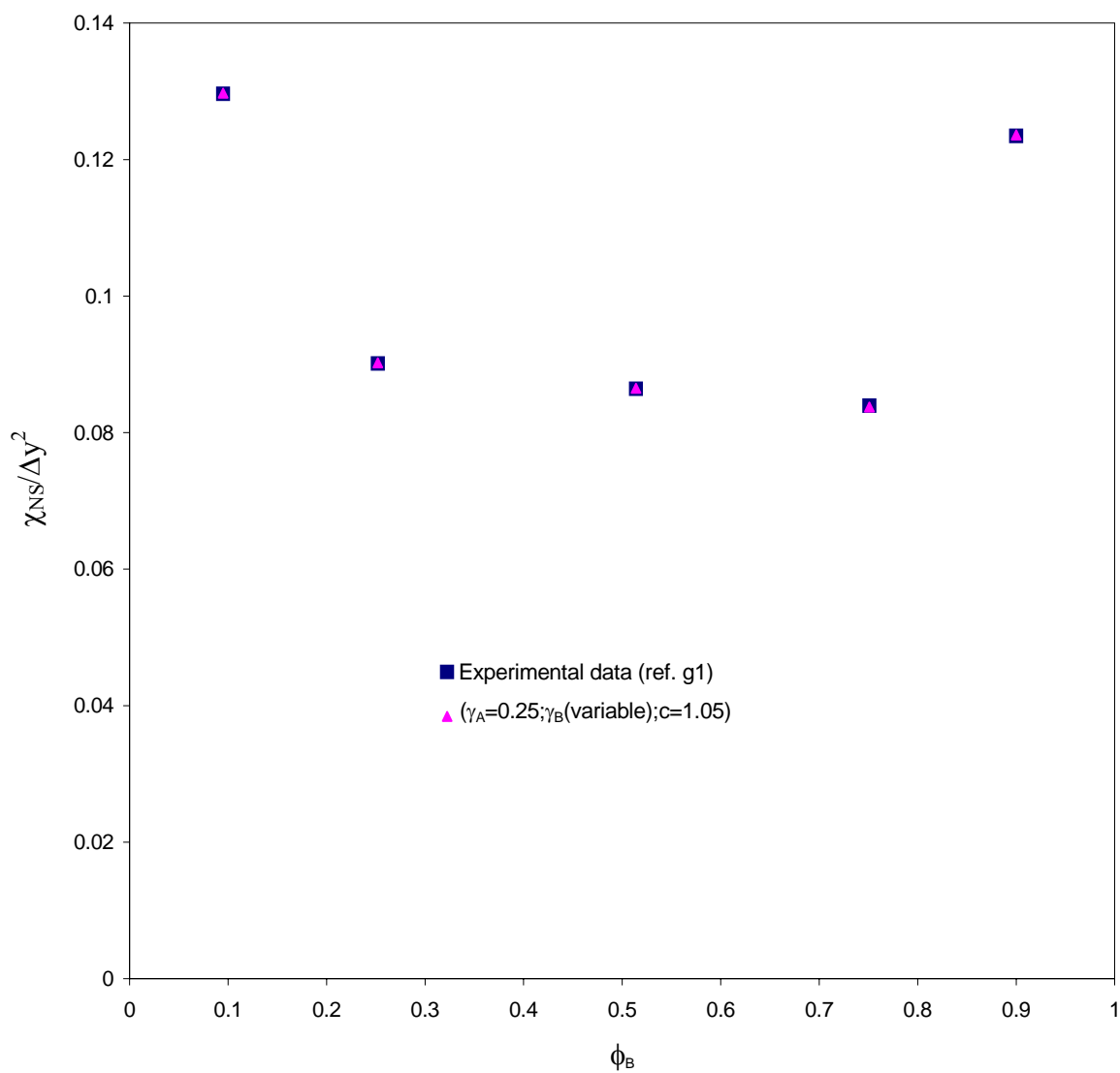


Figure G.6. Interaction parameters from SANS for H97/D88 at 167 °C.

ϕ_A	ϕ_B	c	$\chi_{\text{bare}} * 10^4$	γ_A	γ_B
0.1	0.9	1.05	4.00	0.25	0.24322
0.249	0.751	1.05	4.00	0.25	0.24426
0.486	0.514	1.05	4.00	0.25	0.24407
0.748	0.252	1.05	4.00	0.25	0.24403
0.905	0.095	1.05	4.00	0.25	0.24309
0.1	0.9	1.10	4.00	0.25	0.24372
0.249	0.751	1.10	4.00	0.25	0.2445
0.486	0.514	1.10	4.00	0.25	0.2442
0.748	0.252	1.10	4.00	0.25	0.24424
0.905	0.095	1.10	4.00	0.25	0.24359

Table G.4. Variations in the screening factor of *component B* for various c for H97/D88 at 167 °C.

Vita

Lennart Paulmann Berg

Lennart Paulmann Berg was born in Søborggård (just outside Copenhagen), Denmark on September 5, 1965. He attended the Technical University of Denmark, where he received a Masters degree in Chemical Engineering in 1992. During his work on his Master thesis he was invited to apply for Graduate School at the Pennsylvania State University, and was subsequently accepted for admission.

After working for a short spell as a research associate at the Technical University of Denmark and completing his draft obligations at the Civil Defense of Denmark, he accepted a position as a graduate assistant at the Pennsylvania State University, to pursue his dream of obtaining a doctoral degree in the United States. To that end he was awarded a research stipend from the Danish National Academy of Science.

While working towards his Ph.D, he served as both the President as well as the Vice President of the European Student Club, where he was involved in many events trying to promote a better understanding of foreign cultures in the local community. He also volunteered in many other events involving grade school as well as high school students, predominantly through serving as a judge in the Pennsylvania Junior Academy of Science for a number of years. During this spell he was invited to join an honor society for his efforts. He is currently a member of the Danish Civil Engineering Society and the Danish Chemical Engineering Society.